

**ANALYSIS OF PLANAR CURVES :
A NEW APPROACH TO THE ANALYSIS OF
FACIAL PROFILES**

JOÃO CARLOS FANELLI de ALMEIDA CAMPOS

UNIVERSITY COLLEGE LONDON

Submitted for the Degree of Doctor of Philosophy

University of London

JUNE 1996

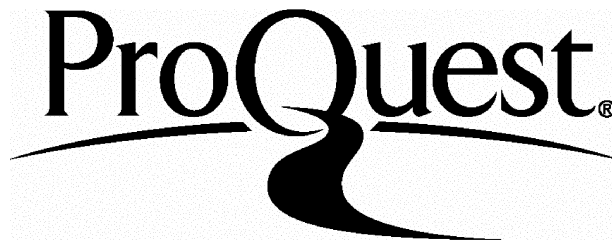
ProQuest Number: 10017341

All rights reserved

INFORMATION TO ALL USERS

The quality of this reproduction is dependent upon the quality of the copy submitted.

In the unlikely event that the author did not send a complete manuscript and there are missing pages, these will be noted. Also, if material had to be removed, a note will indicate the deletion.



ProQuest 10017341

Published by ProQuest LLC(2016). Copyright of the Dissertation is held by the Author.

All rights reserved.

This work is protected against unauthorized copying under Title 17, United States Code.
Microform Edition © ProQuest LLC.

ProQuest LLC
789 East Eisenhower Parkway
P.O. Box 1346
Ann Arbor, MI 48106-1346

Abstract

The aim of this work is to study the human facial profiles by using new techniques applied to the analysis of planar curves.

This involves establishing a method of segmentation, description and classification of profiles, not being restricted to whether the analysis is done on a single profile or a set of them. The particular problems of quantifying changes in facial morphology are investigated.

Mathematical techniques, based on scale space filtering and curvature approaches, are used to describe the changes on the profiles. Special emphasis is given to the analysis of the shape of segments rather than to the movement of points, landmarks or vectors, although these are also explored.

Qualitative descriptions are derived providing a unique representation of the facial profiles, allowing the changes in shape as a result of the treatment, to be visually observed and assessed. Based on these descriptions, the profile is automatically and objectively divided into a number of regions considered suitable for analysis, which are seen to correspond to parts of the face of interest to the clinician (e.g. nose, chin, upper lip, etc.). Quantitative descriptions are also derived for the various segments, through curvature and bending energy plots, and other complementary measures such as length, compactness, roundness and skew. These allow the segments to be classified in terms of their concavity.

The data used are two-dimensional cross sections (profiles) that are a representation of a three-dimensional (3D) model of the human head. Possible sources of data are : traces from lateral radiographs, profiles obtained from 3D data sets generated from Computerized Tomography scans and or from Optical Surface scans. Computer programs were developed for the analysis of the data on a PC-based Transputer system.

Possible areas of applications would be : psychology, pattern recognition, orthodontic and surgical treatments, forensic science and computer vision.

LIST OF CONTENTS

Title Page	1
Abstract.....	2
List of Contents	3
List of Illustrations	7
List of Tables.....	10
Acknowledgements.....	11
Quotation	12
Preface	13
1. Introduction.....	14
1.1. The Human Face	14
1.2. Measuring the Face	14
1.3. Clinical Approach and Motivation.....	15
1.4. Analyzing Facial Data	16
1.5. Aim of Work.....	17
2. Shape Analysis : A General View.....	18
2.1. Statistical Theory of Shape.....	18
2.1.1. D'Arcy Thompson's Contribution.....	18
2.1.2. Bookstein's Contribution	20
2.1.3. Other Contributions	22
2.1.4. Summary	24
2.2. Shape Coding Techniques	25
2.2.1. Simple Scalar Quantities.....	27
2.2.2. Chain Code.....	27
2.2.3. Series Expansions.....	27
2.2.4. Shape Perception	28
2.2.5. MultiScale Techniques	31
2.2.6. Skeleton or Axis of Symmetry.....	34
2.2.7. Summary	37
3. The Study of the Human Face	38
3.1. Initial Perception	38
3.2. Analysis of the Face in Two-Dimensions	42
3.3. Analysis of the Face in Three-Dimensions	45
3.4. Analysis of the Facial Profiles	47
3.4.1. Recognition	47

Contents

3.4.1.1. Francis Galton's Contribution.....	47
3.4.1.2. Leon Harmon's Contribution.....	51
3.4.1.3. Other Contributions.....	54
3.4.2. Fourier Analysis.....	55
3.5. Clinical Analysis of the Face	56
3.5.1. Cephalometric Methods	57
3.5.2. Characterizing Shape	58
3.5.3. Landmarks	60
3.6. Summary	61
4. Method of Analysis	64
4.1. Basic Requirements	64
4.1.1. Landmark versus Curvature Methods	65
4.2. Considering Different Techniques.....	66
4.3. Scale Space Filtering Techniques.....	67
4.3.1. Scale Space Image	69
4.3.2. The Use of Gaussian Convolution	71
4.3.3. Qualitative Descriptions	71
4.3.3.1. The Zero Crossing Contours.....	72
4.3.3.2. Feature Identity and Localization	73
4.3.3.3. The Interval Tree.....	74
4.4. The Analysis of Planar Curves.....	76
4.4.1. The Curvature Scale Space.....	77
4.5. Implementation.....	80
4.5.1. Transputers and OCCAM2.....	80
4.6. Data Acquisition	81
4.6.1. The UCL-MGI Optical Surface Scanner.....	82
4.7. Data Visualization	84
4.8. Summary	86
5. Analyzing Facial Profiles	88
5.1. Outline of Analysis	89
5.2. Discrete Representations of Continuous Curves	90
5.3. Extraction of Facial Profiles	90
5.4. Parametric Curve Representation	92
5.5. Sampling Considerations	95
5.6. Computing the Convolution.....	97
5.7. Qualitative Descriptions.....	103
5.7.1. Curvature Scale Space.....	103
5.7.2. Interval Tree	110
5.8. Profile Segmentation	112
5.8.1. Exploring Curvature Extrema.....	114
5.9. Quantitative Descriptions.....	117
5.9.1. Correcting Spatial Distortions	117
5.9.2. Selecting Natural Scales.....	120
5.9.3. Curvature Value.....	123
5.9.4. Bending Energy	125
5.9.5. Other Quantitative Measures	127
5.10. Evaluation of the Method.....	130

5.10.1. Sensitivity to Noise.....	130
5.10.2. Stability and Repeatability	138
5.10.2.1. Experiment I.....	138
5.10.2.2. Experiment II.....	141
5.10.2.3. Experiment III	144
5.10.3. Sensitivity to Local and Global Shape Changes	147
5.10.3.1. Locally Altering Curve Segments	147
5.10.3.2. Globally Altering Curve Segments.....	156
5.11. Summary.....	159
6. Applications.....	162
6.1. Cleft Palate Case	164
6.1.1. Describing Curve Segments.....	170
6.1.1.1. Using the Qualitative Descriptions	170
6.1.1.2. Using the Quantitative Descriptions	170
6.1.1.3. Using the Bending Energy Concept	173
6.2. Skeletal II Case	177
6.2.1. Describing Curve Segments.....	184
6.2.1.1. Using the Qualitative Descriptions	184
6.2.1.2. Using the Quantitative Descriptions	184
6.2.1.3. Using the Bending Energy Concept	187
6.3. Skeletal III Case.....	189
6.3.1. Describing Curve Segments.....	195
6.3.1.1. Using the Qualitative Descriptions	195
6.3.1.2. Using the Quantitative Descriptions	195
6.3.1.3. Using the Bending Energy Concept	197
6.4. Growth Study.....	200
6.5. Facial Recognition	202
6.5.1. Setting up the Data	203
6.5.2. Matching Scheme	203
6.5.3. Facial Parameters	204
6.6. Summary.....	208
7. Discussion and Conclusions	209
7.1. Conclusions.....	211
7.2. Further Work	212
Bibliographical References	213

1. The Analysis of Facial Profiles using Scale Space Techniques , J.C. Campos, A.D. Linney and J.P. Moss, *IEE Electronics Division, Colloquium on Machine Storage and Recognition of Faces*, Digest no. 1992/017, 24th January, pp.10/1-10/3, 1992.
2. The Analysis of Profiles using Curvature Analysis , J.P. Moss, J.C. Campos and A.D. Linney, *European Journal of Orthodontics*, vol.14, no.6, December, pp.457-461, 1992.
3. The Analysis of Facial Profiles using Scale Space Techniques , J.C. Campos, A.D. Linney and J.P. Moss, *Pattern Recognition*, vol.26, no.6, June, pp.818-824, 1993.

LIST OF ILLUSTRATIONS

Figure 2-1- D'Arcy Thompson's Cartesian transformation grid.....	19
Figure 2-2 - Bookstein's biorthogonal analysis.	20
Figure 2-3 - Homogeneous transformation as a symmetric tensor.	21
Figure 2-4 - The RFTRA method on craniometric analysis.	23
Figure 2-5 - Significant features of a curvature plot obtained when traversing along a curve.	29
Figure 2-6 - Attneave's cat.....	29
Figure 2-7 - Segmenting plane curves using curvature negative minima.	30
Figure 2-8 - The primitive codon types.	31
Figure 2-9 - Scale space technique.	32
Figure 2-10 - Set of primitives based on curvature changes.....	33
Figure 2-11 - Examples of medial axis transform.....	35
Figure 2-12 - Smooth Local Symmetry	35
Figure 3-1 - Leonardo da Vinci's proportions of the human face.	39
Figure 3-2 - Caricatured expression	40
Figure 3-3 - Leonardo da Vinci's comparative nose studies.	40
Figure 3-4 - L. Pacioli's and A. Dürer's measurements of the human face.	41
Figure 3-5 - A. Bertillon's measurements of the face.	43
Figure 3-6 - Eight fundamental surface types.	46
Figure 3-7 - Facial identification: Galton's method for profile measurement.....	48
Figure 3-8 - Galton's profile skeleton.	49
Figure 3-9 - Example of Galton's method.	51
Figure 3-10 - Harmon's face identification method.	52
Figure 3-11 - Typical cephalometric tracing.....	59
Figure 4-1 - Multiscale representation.....	69
Figure 4-2 - Sequence of gaussian smoothings.	70
Figure 4-3 - Scale space image depicted as a surface.....	70
Figure 4-4 - The Scale Space Image description.....	72
Figure 4-5 - The interval tree description.	75
Figure 4-6 - The circle of curvature.	76
Figure 4-7 - Diagram of the UCL-MGI optical surface scanning system.	82
Figure 4-8 - The scanner's coordinate system.	83
Figure 4-9 - A typical display of the optical surface scan data.....	85
Figure 5-1- Block diagram of analysis of human facial profiles.	89
Figure 5-2 - Coordinate system of the graphics display.	90
Figure 5-3 - Extraction of facial profiles.	91
Figure 5-4 - The parametric representation following the path length parameter (t).	93
Figure 5-5 - The vertical profile outline and its parametric representations.	94
Figure 5-6 - The result of resampling a discrete contour segment.....	96
Figure 5-7 - Resampling the profiles with different spacing intervals.....	97
Figure 5-8 - Example of the convolution of two functions.	98
Figure 5-9 - Buffer padding methods.	100
Figure 5-10 - Comparison of curve extension methods.....	101
Figure 5-11 - The truncation effect on the gaussian kernel (and derivatives).	102
Figure 5-12 - Sequence of smoothed vertical profiles.....	104
Figure 5-13 - Sequence of smoothed horizontal profiles.....	105
Figure 5-14 - The curvature scale space description of a vertical profile.	106

Contents

Figure 5-15 - The curvature scale space description of a horizontal profile.....	107
Figure 5-16 - Relationship between zero crossing contours and features of a vertical profile.....	108
Figure 5-17 - Relationship between zero crossing contours and features of a horizontal profile.	109
Figure 5-18 - The interval tree description of a vertical profile.....	110
Figure 5-19 - The interval tree description of a horizontal profile.....	111
Figure 5-20 - The profile segmentation.....	113
Figure 5-21 - The extrema scale space description of a vertical profile.	115
Figure 5-22 - The profile segmentation at extrema of curvature.....	115
Figure 5-23 - Comparison of a zero curvature and extrema scale space descriptions.....	116
Figure 5-24 - Correcting the shrinking effect caused by gaussian smoothing.	119
Figure 5-25 - Comparing the Interval Tree and Minima of Significance.	121
Figure 5-26 - Selecting scales from the Interval Tree description.....	122
Figure 5-27 - The curvature plot of a vertical profile.	124
Figure 5-28 - The bending energy plot.	126
Figure 5-29 - The bending energy plot.	127
Figure 5-30 - Additional metric information.....	128
Figure 5-31 - Effects of added noise on the <i>horizontal profile</i> outline.....	132
Figure 5-32 - Curvature scale space with added <i>normally distributed noise</i>	133
Figure 5-33 - Curvature scale space with added <i>quantization noise</i>	134
Figure 5-34 - Effects of added noise on the <i>vertical profile</i> outline.....	135
Figure 5-35 - Curvature scale space with added <i>normally distributed noise</i>	136
Figure 5-36 - Curvature scale space with added <i>quantization noise</i>	137
Figure 5-37 - Set of 12 automatically identified landmarks.....	139
Figure 5-38 - Landmark variation (experiment I).....	140
Figure 5-39 - Set of 12 automatically identified landmarks.....	142
Figure 5-40 - Landmark variation (experiment II).	143
Figure 5-41 - Curvature scale space descriptions (experiment III).	145
Figure 5-42 - Segmented profiles (experiment III).....	146
Figure 5-43 - The <i>unmodified mid-line vertical profile</i> outline and its CSS description.	149
Figure 5-44 - The <i>modified profile</i> outlines and their CSS descriptions - (<i>section 1</i>).150	
Figure 5-45 - The <i>modified profile</i> outlines and their CSS descriptions - (<i>section 2</i>).151	
Figure 5-46 - The <i>modified profile</i> outlines and their CSS descriptions - (<i>section 3</i>).152	
Figure 5-47 - The <i>modified profile</i> outlines and their CSS descriptions - (<i>section 3</i>).153	
Figure 5-48 - The <i>modified profile</i> outlines and their CSS descriptions - (<i>section 3</i>).154	
Figure 5-49 - The <i>modified profile</i> outlines and their CSS descriptions - (<i>section 4</i>).155	
Figure 5-50 - The <i>original and modified profile</i> outlines and their CSS descriptions - (<i>global alteration</i>).	158
Figure 5-51 - Alternative display of the <i>original and modified profile</i> outlines - (<i>global alteration</i>).	159
Figure 6-1 - Facial profile's landmarks and segments.	163
Figure 6-2 - Facial profiles of the cleft palate patient.....	165
Figure 6-3 - Qualitative descriptions (cleft palate patient - <i>before surgery</i>).....	166
Figure 6-4 - Qualitative descriptions (cleft palate patient- <i>after surgery</i>).	167
Figure 6-5 - Profiles and the zero crossing contours (cleft palate case).	168
Figure 6-6 - Curvature plot (cleft palate case).....	171
Figure 6-7 - Segment's quantitative measures (cleft palate case).	172

Figure 6-8 - Bending energy plot - Effects of surgical treatment (cleft palate case).	174
Figure 6-9 - Bending energy plot - closeness to the average (cleft palate case).....	175
Figure 6-10 - Bending energy plot - Shape signatures for the cleft palate case.	176
Figure 6-11 - Bending energy plot - Shape signatures for the cleft palate case.	176
Figure 6-12 - Classification of skeletal relationship.....	177
Figure 6-13 - Classification of incisor relationship.....	177
Figure 6-14 - Facial profiles of the skeletal II patient.	178
Figure 6-15 - Qualitative descriptions (skeletal II case - <i>before surgery</i>).	180
Figure 6-16 - Qualitative descriptions (skeletal II case - <i>after surgery</i>).....	181
Figure 6-17 - Profiles and the zero crossing contours (skeletal II case).	182
Figure 6-18 - Curvature plot (skeletal II case).	185
Figure 6-19 - Segment's quantitative measures.	186
Figure 6-20 - Bending energy plot - Effects of surgical treatment (skeletal II case).	187
Figure 6-21 - Bending energy plot - Shape signatures for the skeletal II case.	188
Figure 6-22 - Bending energy plot - closeness to the average (skeletal II case).....	188
Figure 6-23 - Facial profiles of the skeletal III case.....	189
Figure 6-24 - Qualitative descriptions (skeletal III case - <i>before surgery</i>).....	191
Figure 6-25 - Qualitative descriptions (skeletal III case - <i>after surgery</i>).	192
Figure 6-26 - Profiles and the zero crossing contours (skeletal III case).	193
Figure 6-27 - Curvature plot (skeletal III case).....	196
Figure 6-28 - Segment's quantitative measures.	197
Figure 6-29 - Bending energy plot - Effects of surgical treatment (skeletal III case).	198
Figure 6-30 - Bending energy plot - Shape signatures for the skeletal III case.	199
Figure 6-31 - Bending energy plot - Shape signatures for the skeletal III case.....	199
Figure 6-32 - Bending energy plot - closeness to the average (skeletal III case).	200
Figure 6-33 - Profile segmentation (growth study).....	201
Figure 6-34 - Curvature diagrams (growth study).	202

LIST OF TABLES

Table 2-1 - Summary of shape coding techniques	26
Table 3-1 - Shapes of profile segments.	50
Table 5-1 - Classification of digital curvature estimation methods.	123
Table 5-2- Table with the segment's quantitative descriptive measures.	129
Table 5-3- Landmark variation (experiment I).	139
Table 5-4- Variation of the landmark's coordinate values (experiment I).	140
Table 5-5- Landmark variation (experiment II).	142
Table 5-6- Variation of the landmark's coordinate values (experiment II).	143
Table 6-1- Table with the segment's shape and quantitative descriptive measures (before surgery).	169
Table 6-2- Table with the segment's shape and quantitative descriptive measures (after surgery).	169
Table 6-3- Table with the segment's shape and quantitative descriptive measures (before surgery).	183
Table 6-4- Table with the segment's shape and quantitative descriptive measures (after surgery).	183
Table 6-5- Table with the segment's shape and quantitative descriptive measures (before surgery).	194
Table 6-6- Table with the segment's shape and quantitative descriptive measures (after surgery).	194
Table 6-7 - Scores used as a measure of similarity of profiles (<i>first experiment</i>).	205
Table 6-8 - Scores used as a measure of significance of facial parameters (<i>first experiment</i>).	206
Table 6-9 - Scores used as a measure of similarity of profiles (<i>second experiment</i>).	207
Table 6-10 - Scores used as a measure of significance of facial parameters (<i>second experiment</i>).	207

Acknowledgements

This work could not have been completed without the dedication, contribution, support and encouragement of many friends and colleagues. Therefore, I would like to acknowledge here my debt and gratitude to them.

My special thanks to two people, Dr. A.D. Linney and Prof. J.P. Moss, who introduced me to this new world and fascinating area of research, in which one takes the challenge to study and measure the human face, in its infinite diversity, its myriad of subtle variations of form and texture, all elements that compose the unique “face” of an individual.

Dr. A.D. Linney , not only for supervising this work, but above all for his open and constant support, encouragement, friendship, patience and humor. His valuable suggestions many times set my research in the right track, and greatly contributed to its final presentation and content.

Prof. J.P. Moss (UCL and the Royal London Hospital), for his enthusiasm and dedication. He also has supported me along the way, and taught me the importance of research directed to clinical applications.

Thanks to all members of the Medical Graphics and Imaging group at the Department of Medical Physics, University College London for their help. In particular, to Dr. Robin Richards which patiently guided me through the ways of the OCCAM programming; to Dr. Anne Coombes, for her encouragement and inspiring work on analyzing the surface of the face, to P.Goodwin for her support and friendship, and to A.C. Tan for his precious tips on many aspects of the hardware and software I used. Also to Dr. R. Fright, for his valuable work on 3D registration of faces, which opened new possibilities on analyzing faces, expanding my own work.

I am grateful as well to my family, for the constant support and encouragement. My mother Antonieta, my sister Ana, and brothers Orlando and Carlos Alberto. Special thanks to Luicyr, Dirce, Bety, Mamy and Nancy.

I dedicate this work in memory of my dear and much loved father.

Finally, my deepest gratitude to my wife Soraia Crystal. Her love, support, creativity and honesty have been the driving forces throughout my life, and specially during the time this work was being written.

Quotation

“ A universe comes into being when a space is severed or taken apart. The skin of a living organism cuts off an outside from an inside. So does the circumference of a circle in a plane. By tracing the way we present such a severance, we can begin to reconstruct, with an accuracy and coverage that appear almost uncanny, the basic forms underlying linguistic, mathematical, physical, and biological science, and can begin to see how the familiar laws of our own experience follow inexorably from the original act of severance. ”

G. Spencer-Brown

Loss of Form,
N.Y., E.P. Dutton, pp.xxix, 1979.

“ none of our explanations can be true... in some sense there is no ultimate truth accessible to us for the simple reason we have to make a cut in the Universe in order to do the experiment at all. We have to decide what is relevant and what is irrelevant. ”

J. Bronowski

The Origin of Knowledge and Imagination,
New Heaven, CD : Yale University Press, pp.69, 1978.

Preface

The study of the human face has always attracted the attention of writers, sculptors, painters, and scientific researchers.

The face plays a vital part in many aspects of our life. It often influences the way we perceive and evaluate others; it conveys information about our sex, age, identity and emotions; it affects social interactions. The face constitutes one of the main elements on our ability to recognize other people. Culturally, facial appearance has a far too great importance and people with facial deformities, due to accidents or birth, have problems to cope with their facial disfigurement.

Hence, the extensive research on the human face, through areas such as perception, recognition and morphometrics, pursued across the disciplines of sociology, psychology, arts, forensic and dental sciences, plastic and reconstructive surgery, amongst others. Consequently, the contributions come from varying perspectives and with somewhat different concerns. They all share, however, the appreciation for the tremendous importance of this topic.

Despite the growing number of experiments and published works, the human face constitutes a subject of research in which many fundamental questions can still be addressed through its wide range of applications.

I too, fascinated by this subject, started and developed my research work, which this Ph.D. thesis now describes. The aim of this work is to study human facial profiles, through automatic methods of segmentation, description and classification. The concept of curvature variation along the contour is applied, which stresses the significance of changes in shape occurring between landmarks rather than in their relative movements. The particular problem of quantifying changes in facial morphology are investigated, with special emphasis given to clinical applications of reconstructive plastic surgery and orthodontic treatments.

Chapter One

1. Introduction

1.1. The Human Face

The human face has, since ancient times, attracted and fascinated mankind. It has been described by poets and writers; depicted by painters; interpreted and analyzed by social scientists; examined and studied by medical scientists.

The face plays a vital part on many aspects of our life and culture. The age and sex of an individual may be directly determined through the face. In many cases, the identification of people has the face as one of its major elements, like a '*fingerprint*' clue. Changes in facial expression carry a lot of information about a range of emotional feelings. Human social interactions are established and greatly influenced by facial appearance, to such a degree that people with facial deformities, due to accidents or birth, have many problems in coping with their facial disfigurement.

It is not surprising the extensive research activities on the face, pursued across the disciplines of sociology, psychology, arts, forensic and dental sciences, plastic and reconstructive surgery, amongst others.

1.2. Measuring the Face

Although observation is a valid scientific method of study, also applied in the case of human faces, measurement is by far the most popular. It seems to be common amongst many disciplines to explore forms and means of dividing and measuring the face in order to develop their ideas, concepts and methodologies. Investigators make use of calipers, photographs, X-rays, video cameras, computers, mathematical models, etc.

Sociological and psychological approaches have devised some experiments to study face perception and the role of facial appearance in social interactions (V. Bruce et al 1990, T.R. Alley 1988).

The study of the human face is particularly important for clinical and biomedical applications. Several of their treatment planning methods are directly based on defining landmarks, segments and geometric constructs to analyze the face. Therefore, any improvements on the techniques for measuring and analyzing the face are bound to have a great impact on these applications and on the results that they may achieve.

Some very important contributions come from the recent and ever increasing use of methods of analysis introduced by the mathematical and computer sciences. Powerful computer graphics workstations have been developed leading to the involvement and rapid growth of areas like artificial intelligence, pattern recognition, computer vision, graphics and image processing.

In addition to that, techniques of recording and visualizing the facial surface in three dimensions have been developed, offering a new and accurate means of measurement and analysis.

1.3. Clinical Approach and Motivation

An important motivation for this work was a practical problem faced during the project '*System for the Simulation and Planning of Facial Reconstructive Surgery Using Computer Graphics*' (DHSS report 1989) in its final stage, during which an evaluation was carried out. The aim was to assess, from a qualitative and quantitative point of view, the predicted surgery performed using a computer graphics system. One of the criteria of this evaluation was based on the extraction of a set of facial profiles and on their comparison using statistical methods. Therefore a suitable metric to describe the changes which have occurred need to be derived.

The clinical analysis of facial form is one of the main applications of the methodology developed on this work.

Introduction

Cephalometric methods provide the basis for most treatment planning techniques on aesthetic, reconstructive and orthognathicsurgery. The most widely used involves the study of posteroanterior and lateral roentgenographic views of the head, where a number of homologous landmarks are identified. Another type is based on the study of proportions of the face and measurements of facial features extracted from standardized photographs.

Over the past twenty years, the advances in surgical techniques and anesthesia, combined with the advances in computer science have increased the scope for facial reconstructive surgery and orthodontic treatment. It has also added a considerable degree of complexity to the treatment planning. Methods that provide a prediction in terms of facial appearance and soft tissue movement have become increasingly more important (DHSS report 1989).

Following this line of work, several cephalometric procedures have been defined for the mid-sagittal facial profile and have proved quite useful. However, they are restricted to a particular profile and the qualitative judgments are always made based primarily on clinical experience.

All of these considerations clearly point to the need to develop more objective approaches to the clinical analysis when based on facial profiles.

1.4. Analyzing Facial Data

Presenting and analyzing facial data is still an area of open debate in many applications, specially the clinical one. As mentioned before, several methods make use of points, lines and angles in an attempt to quantify changes on the facial profiles. The main criticism here is that they mainly look at the relative movement of points, not describing the changes that took place between these points. As it has been pointed out in a previous study (DHSS report 1989) : *“There is too much of the face for it to be described by so few landmarks”*.

The perception and description of the facial form is more realistic and accurate when considering the analysis of entire segments and or surfaces. This

approach of analysis can be, in a broader sense, related to the mathematical description of *shape* - a concept widely accepted and still difficult to define. Although this problem can be expressed in general terms and a general methodology can be developed, the identification of which information is relevant to a particular problem and in what way it should be presented are very important issues in the choice of a method of shape description.

Mathematical techniques to describe the facial shape and the changes occurring in the face may be applied to the analysis of (a) *surfaces*, by using three dimensional (3D) data, or (b) *profiles*, by using two dimensional (2D) data. However, a relationship between the two may be established in cases where sets of two dimensional data are a representation of a three dimensional object. In either case a qualitative and or quantitative description may be achieved.

Although such techniques have been explored in the past, they are both open research fields and I will be concentrating my work on the latter, that is, in the context where shape is defined within a two dimensional field, the shape of plane objects as defined by their contours or “silhouettes”.

1.5. Aim of Work

The aim of this Ph.D. work is to study human facial profiles. This involves establishing a method of automatic segmentation, description and classification of profiles, not being restricted to whether we are analyzing a single one or a set. The particular problem of quantifying changes in facial morphology are investigated.

Through segmentation a profile may be objectively divided into a number of regions considered suitable for analysis, which are seen to correspond to parts of the face of interest to the clinician (e.g. nose, chin, upper lip, etc.).

Although the identification and location of landmarks is a very important issue in profile analysis, the emphasis given on this study is not so much in relative movements of landmarks. Rather, it concentrates on the changes in shape of the segments between the landmarks, by using the concept of curvature variation along the profile.

Chapter Two

2. Shape Analysis : A General View

In the next two chapters the relevant literature regarding shape analysis is reviewed. The number of applications in which shape analysis is, in some way or another, used is considerable.

In order to introduce a few concepts and ideas, this chapter gives initially a more general view on the topic of shape analysis, involving different problems and techniques. After that, in the following chapter, special attention is given to applications that focus on the analysis of the human face, particularly when using facial profiles.

The literature on shape analysis seems to cover two different but complementary areas of study : the statistical theory of shape and the techniques used to code shape.

2.1. Statistical Theory of Shape

The first area of study deals with the pursuit of a statistical theory for shape description and it dates back to the beginning of this century. Disciplines such as astronomy, archeology, chemistry and biology were, amongst many others, raising a number of interesting problems which motivated new ideas and the development of new mathematical methods. The standard of rigor of the work produced was generally high which restricted the audience mainly to mathematicians.

2.1.1. D'Arcy Thompson's Contribution

D'Arcy W. Thompson (1917,1942) introduced his work in zoology. He was the first to use geometric transformations in the study of morphogenesis. He demonstrated that an outline of a part of an organism on a coordinate grid (Cartesian grid) could be

deformed or transformed by mathematical methods into the outlines of different but related species (see figure 2-1).

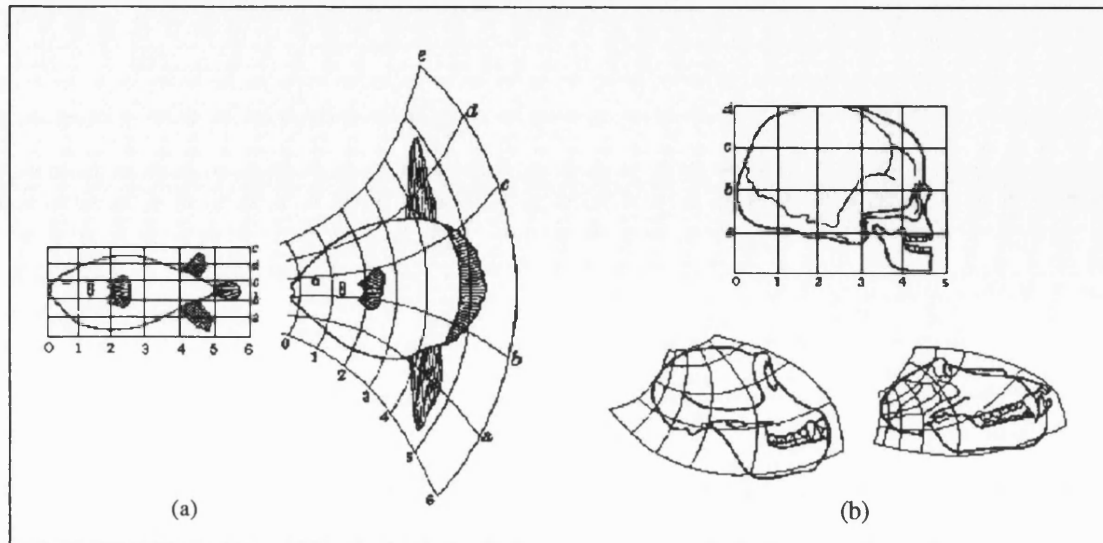


Figure 2-1- D'Arcy Thompson's Cartesian transformation grid.

- (a) from *Diodon* to *Othragoriscus*
 - (b) from human skull to chimpanzee (left) and to baboon (right).
- (Adapted from Thompson 1917)

R.H. Benson and colleagues (1982) point out that the typical transformation of the Thompson's grid, i.e. generally complete, uniform and possibly symmetrical, has great difficulty in expressing real biological changes. Their main argument is that although it may be true that whole structures often vary together as a result of a high degree of morphological integration, the majority of transitions between closely related morphological shapes will not involve global deformation.

However, spite of some limitations, Thompson's method presents a *graphic* representation of the transformation of biological forms, making it possible to appreciate the overall as well as local shape changes.

A similar role in botany was played by the work of F.D. Bower (1930).

2.1.2. Bookstein's Contribution

F.L. Bookstein (1978a,1984,1986,1989,1990,1991) has also made some interesting contributions to this field. Inspired by Thompson's work he explored the idea that shape change is measured by distortion and not by the subtraction of two measurements. His work in *morphometrics*, the quantitative description of biological form using geometry and statistics, makes use of a set of labeled points, or landmarks, that correspond biologically from form to form. By using them he constructs a *biorthogonal grid*, formed by parallel curves intersecting at right angles and bounded by the landmark polygon. The intersections of the curves provide a picture of the distortion, expressed in its natural coordinate system, where the changes are embodied in the stretching or shrinking of lengths on the grid relative to their homologues (see figure 2-2).

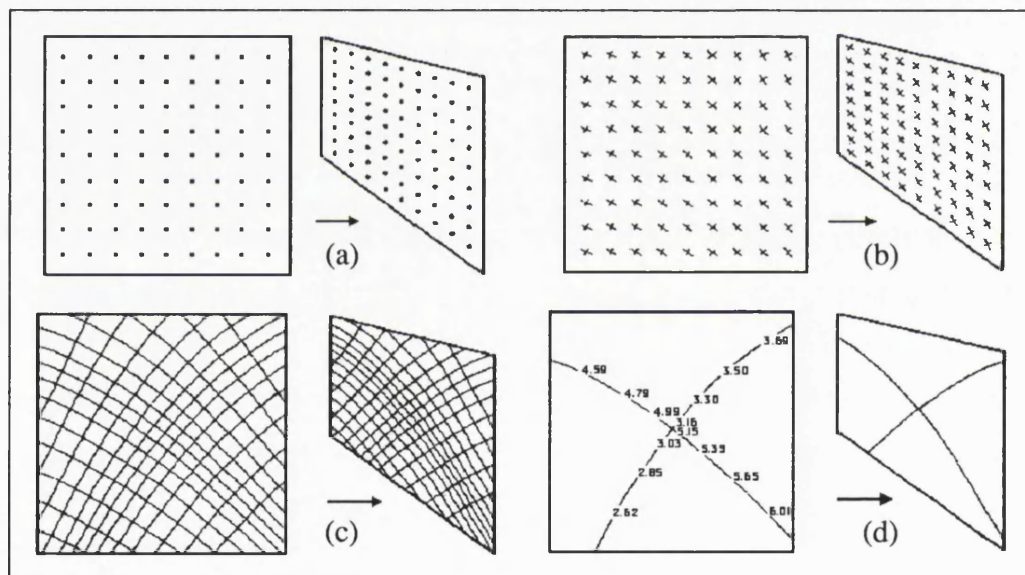


Figure 2-2 - Bookstein's biorthogonal analysis.

The shape changes which transforms a square into a general quadrilateral.

- a) set of homologous points on a square grid.
- b) a sample of homologous directions at 90 degrees in both images of (a). At every point of the image pair there exists just one such cross, an algebraic function of the form of the distortion locally.
- c) a biorthogonal coordinate system, whose curves are aligned everywhere with the tensor field of crosses sampled in (b). This system explicitly depicts the shape change in its natural coordinates of the distortion itself.
- d) two coordinate curves and ratios of corresponding lengths sampled along them. These summarize the shape change. (Adapted from Bookstein 1978a)

With the biorthogonal grid technique Bookstein showed that a given configuration of landmark points may be measured either by distances or ratios of distances, or by the rearrangement of the configuration as a whole (i.e. as a deformation between two forms).

As an extension of his previous analysis, Bookstein suggested the use of a model based on a triad of landmarks to describe changes in shape. The *symmetric tensor*, as it is called, is a mathematical representation of the linear deformation from one configuration of a triangle of landmarks into another (see figure 2-3). Briefly, an internal ellipse is computed for each triangle. The major and minor axes (named principal dilatations) are calculated for each ellipse and these axes are then used to form ratios. Differences in ratios are viewed as changes in shape.

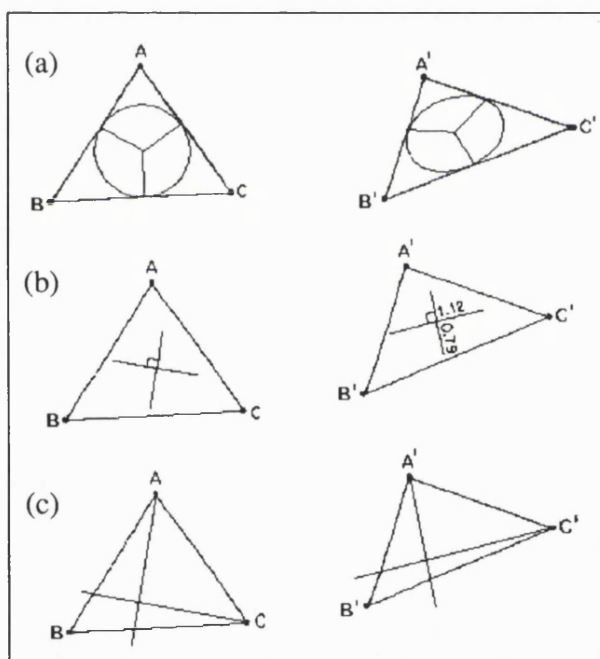


Figure 2-3 - Homogeneous transformation as a symmetric tensor.

- a) dilatations represented by the radii of the ellipse into which a circle is deformed.
 - b) the principal directions are axes of the ellipse, and the principal dilatations are proportional to their length.
 - c) distances measured parallel to these directions are perpendicular both before and after the deformation. Such distances may be indicated by using transects joining one vertex of the triangle to a point of the opposite side.
- (Adapted from Bookstein 1978a)

He demonstrated that the tensors also make possible the statistical analysis of populations of shapes, and the use of conventional multivariate statistical methods.

This method of tensor analysis is applied on his study on the geometry of craniofacial growth invariants (Bookstein 1983), where two examples were used: (1) to extract the statistically most stable definition of "growth axis" (displacement of

menton from cranial base) in a group of children aged 6 to 14 years; (2) to describe the shape change of the rat calvarium between the ages of 7 and 150 days.

In a more recent work, Bookstein (1989) proposes the use of the analogical model of bending or “warping” thin-plate metal sheet splines to describe shape changes or deformations.

2.1.3. Other Contributions

K.V. Mardia (1989) and coworkers (1989b,1991,1993) also review some statistical methodology which can be used in shape analysis. These are applied to an object outline (e.g. digitized bones) or a set of landmarks. They also investigate Bayesian methods of identifying the shape of objects in images (e.g. a rectangular object on a gray level image) and likelihood models for reconstructing shapes in images, amongst others. Here, the shape of the object is represented by a template (e.g. outline, landmark positions) plus a probability value for its variations. Particular attention is given to the concept of shape in the context where an outline of an object or a set of landmarks are based on location, scale and rotation invariant coordinates. These coordinates are called *shape coordinates*.

Following Bookstein’s work on “warping” thin-plate metal sheet splines to describe shape changes or deformations, Mardia and T.J. Hainsworth (1993) worked directly with landmark coordinates as measured in the images (a typical gray-level representation of an object). A thin-plate spline deformation takes landmarks in the image to the corresponding positions in the template, where the smooth deformation is chosen to minimize the “bending energies”. They also showed that the thin-plate splines may be used for merging images.

The use of homologous landmark data sets and the view that the form of an object consists of both size and shape may also be seen in some anthropological studies made by S.R. Lele et al (1991). Their method is based on the Euclidean Distance Matrix (EDM) representation of the form of an object. This matrix of dimension $k \times k$ (where k is the number of defined landmarks) is symmetric and consists of distances between all possible pairs of landmarks. Then a statistical model

is applied to assess the difference between two forms originally represented by their EDM.

J.T. Richtsmeier (1989) used Finite Element Scaling analysis in primatology studies in order to indicate those landmarks that differ most between specimens. A comparative study using the two previous methods may be seen in J.T. Richtsmeier (et al 1991).

A.F. Siegel and R.H. Benson (1982) presented the method of *Resistant-Fit Theta-Rho Analysis* (RFTRA), developed to identify and measure homologous regions of change in shape. It combines a fitting method with vector analysis. Their fitting method (called repeated median algorithm) uses medians of ranked changes in proportion instead of least squares to compute the scale, rotation and translation transformation factors. A graphic representation of the two superimposed morphologies is then produced with vectors indicating the general displacement of a set of homologous points towards uniform deformation. This is illustrated in figure 2-4, which shows the result of the method when applied to explore the craniometric changes between primate and hominid skulls. The authors claim that the differences shown by the RFTRA method are more readily identified in accordance with the structural differences perceived on biological grounds.

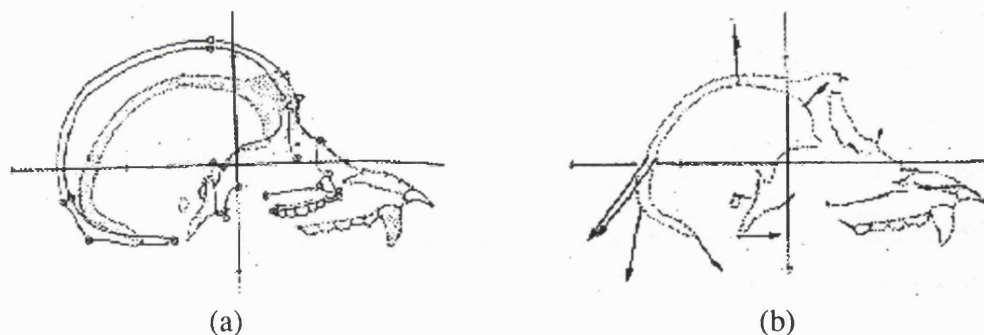


Figure 2-4 - The RFTRA method on craniometric analysis.

Comparison between chimpanzee troglodytes and Homo Sapiens : (a) result of RFTRA analysis; (b) Vectorial changes represented by the landmarks on (a) (Adapted from Siegel 1982)

The work of D.G. Kendall (1977,1984,1986,1989) is, along with others, considered of great importance on this field of statistical analysis of shape. Attracted

by the statistical topic on the fringes of archeology, he poses a quite interesting observation, which shows not only the importance of the statistical tests but also the importance of how and when to use them : “...when one looks at Stonehenge one accepts the underlying circular structure without asking for statistical authentication...” , and he proceeds: “But there are other archeological situations in which a linear structure is accepted by some and dismissed by others. Who is right ?”.

He lays down a theoretical background to formulate and solve statistical problems, mainly dealing with shape characteristics of empirical sets of points. He introduces the concept of *size* and *shape spaces* associated with a set of k landmarks in m dimensions. Apart from archeology, other applications for his methods are to astronomy, geography and physical chemistry.

Furthermore, it is possible to distinguish, amongst others, the work of C.G. Small (1988), R.A. Reyment (1988), N. MacLeod et al (1988) and C.E. Oxnard (1973,1978) .

2.1.4. Summary

We have seen how the pioneering work of D.W. Thompson, at the beginning of this century, using geometric transformations to describe overall and local shape changes amongst related species led F.L. Bookstein to lay the foundations and expand his own methods.

With a strong emphasis on biological applications, Bookstein’s work on multivariate morphometrics explores the use of new and existing tools for representing the biological structure within the context of geometrical and multivariate statistical analyses, as well as for dealing with the special biological relations among different cases of landmark configurations, where the notion of homology is fundamental.

On the other hand, coming from different and differently motivated approaches, mathematicians like D.G. Kendall and K.V. Mardia, amongst others, are

developing theoretical work that tries to unify some recent statistical methodologies which can be used in the field of shape theory.

In the end, although the amount of work produced is considerable (papers, essays, books, etc.) it does not seem to have defined a well and generally accepted theoretical formulation for shape analysis. There are some points of interactions, differences of emphasis, different approaches and motivations which indicates that this field of study has not yet been rigorously developed.

2.2. Shape Coding Techniques

In the second area of study reported in the literature, we find a more general approach based on shape coding techniques and their applications. These methods have been widely explored in the pattern recognition, artificial intelligence, orthodontics, computer graphics and image processing literature. There is an enormous quantity of papers published on this area with a great diversity of approaches. Some very good reviews are given by D. Ballard (1982), A. Rosenfeld (1976), T. Pavilidis (1977,1978,1980) and S. Marshall (1989), which are briefly described next.

Shape, in this context, is defined within a two dimensional field, i.e. shape of plane objects as defined by their contours or “silhouettes”. The coding then takes place where the shape of a line or curved segment is described on some mathematical basis. It is possible to introduce some structure into the analysis of shapes by classifying the methodologies used. Some of the criteria are now described.

One criterion is based on the use of *Scalar Transform* and *Space Domain* techniques. Scalar Transform techniques transform one shape into an array of numbers, which are usually most appropriate as input for classical statistical analysis. Space Domain techniques transform a shape into another shape or picture, and this is useful as input to syntactic and structural analysis.

When the boundary of the object is considered, another distinction may be made. The *External* analysis considers only the boundary of a shape while the *Internal* analysis considers the area within the boundary of the shape.

Shape Analysis: Coding Techniques

A final distinction depends on whether the description contains only information to distinguish similar shapes that may be encountered or it contains sufficient information to be able to reconstruct a faithful representation of the original shape. These approaches are described as *Information Nonpreserving* and *Information Preserving*, respectively. The first is directly associated with *Recognition* tasks where the processes involved should be invariant to changes in scale, position and orientation (e.g. bending energy and simple scalar quantities such as areas, perimeter length, etc.). The second is directly associated with *Data Compression* tasks, although the bounds of Information Preserving techniques are not too clear because some techniques only allow imperfect reconstruction (e.g. Fourier transforms when combined with filtering).

A summary of shape coding techniques (as suggested by S. Marshall) is given on table 2-1, following the above criteria for methodology classification.

Techniques	Scalar Transform (ST) Space Domain (SD)	Internal (I) External (E)	Data Preserving (P) Data Non-preserving (N)
Simple Scalar Quantities	ST	I	N
Moments of Area	ST	I	P
2D Fourier Transform	ST	I	P
Chord Distribution	ST	I	N
Linesums/projections	ST	I	P
Transform Techniques	ST	E	P
Stochastic Methods	ST	E	P
Bending Energy	ST	E	N
Medial Axis Transform	SD	I	P/N
Convex Subsets	SD	I	P
Freeman Chain Code	SD	E	P
Polygon Approximation	--	E	--
Chain Coding	SD	E	P
Scale Space Techniques	SD	E	P
Normal Contour Distribution	SD	E	N
Hough Transform	SD	E	P

Table 2-1 - Summary of shape coding techniques .

2.2.1. Simple Scalar Quantities

Simple scalar quantities and metric properties such as area and length of perimeter are considered so fundamental that they have been employed in one form or another by a large number of research workers. However, measures such as $(\text{perimeter})^2 / (\text{area})$, as used by Green (1970) to describe closed contours, are not robust classifiers because significantly different contours may be represented by similar numerical values (Young et al 1974).

2.2.2. Chain Code

This method of shape coding, also known as Freeman coding, is a well established technique (H. Freeman 1961,1970). Each point on a curve may be coded according to a choice of only eight possible directions which the curve could take. If the Cartesian axis of the curve is used as a reference, the coding will be absolute. On the other hand, if the reference is the direction of a previous segment, the coding will be relative. As S. Marshall pointed out in his review, the Freeman code essentially represents a coarse quantization of curvature.

Although a curve may be fully described by a code of this type, it is highly sensitive to noise, as the errors tend to accumulate throughout the chain. Also, arbitrary changes in scale and rotation are difficult to incorporate.

2.2.3. Series Expansions

Methods that form a series expansion to represent the contour (e.g. Fourier transform and Moments) and then use only the first few terms of the series have been followed by a relatively few research works, possibly because the expansion coefficients obtained do not always have a clear geometrical interpretation (Zahn et al 1972, Alt 1962) .

However, P.E. Lestrel (1978) showed that Fourier analysis is a tool well-suited for quantitative studies of complex biological shapes when considering size and shape. One particular aspect of the Fourier analysis is that the Fourier series can be

utilized as a curve fitting function since it will converge to an arbitrary form as more terms are added to the series. This was explored by P.E. Lestrel (et al 1986) in a study of the cranial base shape variation with age. It was shown to be an alternative way of overcoming some of the difficulties inherent in the use of conventional measurements.

Another aspect of Fourier analysis is that in the Fourier transform domain the harmonics are related to degrees of slowly or rapidly changing shape over the analyzed contour. Typically, the shape is then characterized by the magnitude in each of the different harmonics needed to describe a specific contour. D.J. Halazonetis (et al 1991) used this approach to study the shape of the mandible in the period around the pubertal growth spurt. The Fourier coefficients were analyzed statistically in relation to age, sex, cranial pattern and mandibular growth rotation.

Some applications of Fourier methods to the analysis of facial profiles are also discussed in the next chapter.

2.2.4. Shape Perception

Another largely employed method makes use of some important aspects of shape perception, as suggested by psychologists such as F. Attneave (1954,1956) and D. Hoffman (et al. 1982,1984).

They demonstrated that the curvature values (seen as the amount of bend) along line drawings and silhouettes hold great power when describing the shape of contours for object recognition. Amongst these values, there are three singularities of curvature, as illustrated in figure 2-5 : the extreme of positive curvature maxima (labeled M+), the extreme of negative curvature minima (labeled M-) and the zeros of curvature (not labeled but easily identified as the point where the curve crosses the horizontal axis).

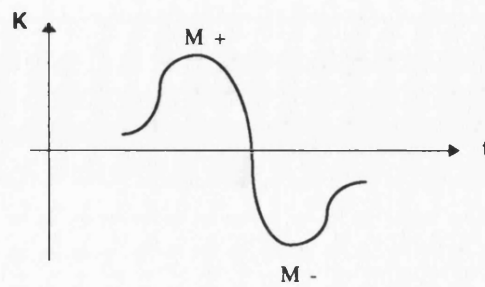


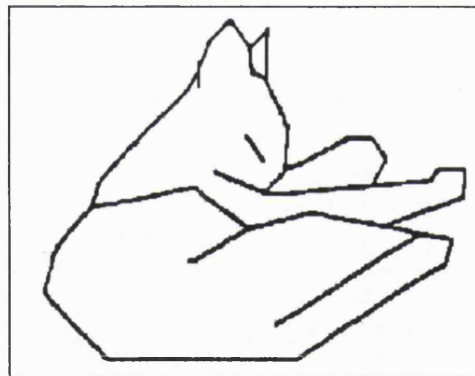
Figure 2-5 - Significant features of a curvature plot obtained when traversing along a curve.

The curvature (K) is represented by the vertical axis, and the position along the contour (t) by the horizontal axis.

F. Attneave demonstrated that points of high curvature (positive maxima and negative minima) are chosen when visually making a summary of a shape and segmenting a contour. Using the photograph of a cat, Attneave created a drawing using line segments connected at estimated points of high curvature as shown in figure 2-6.

Figure 2-6 - Attneave's cat.

Line drawing presentation using points of high curvature estimated on a photograph of a cat. (Adapted from Attneave 1954)



Such a presentation was reliably recognized as a cat. He suggested that such points were high in information content. It is not too surprising that such points and measures of curvature in general, play an important role in most methods of shape analysis (e.g. Ledley 1964).

Hoffman and co-workers provide some psychological evidence that contours are segmented at extrema of negative minima. In other words, to segment an image curve into parts, the concave cusps are used. Thus, in figure 2-7, the plane curves in (a) and (b) are divided into parts by noting the extrema of negative curvature. However, as W. Richards (et al 1986) points out, to find these extrema, one must first

specify which side of the curve should be considered as the object. In figure 2-7(a), when the curve is traversed counterclockwise, the object is to the left of the curve, assuming the appearance of a face. Now, in figure 2-7(b) the opposite traverse direction is adopted and the extrema of positive and negative are exchanged, transforming the parts of the face into the parts of an apple.

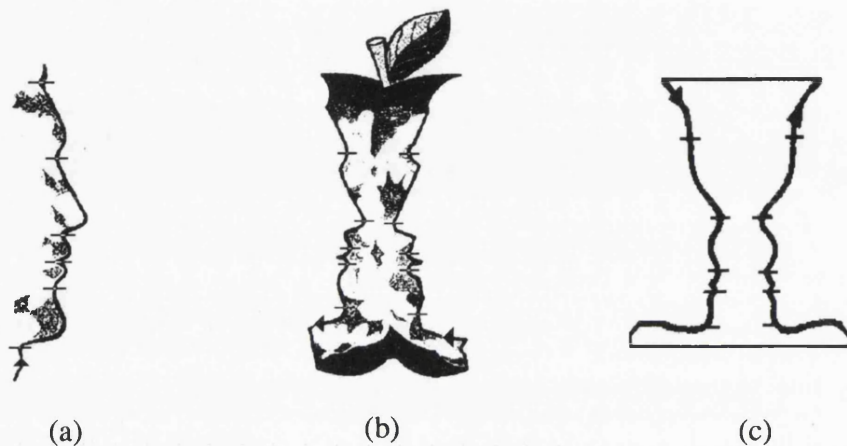


Figure 2-7 - Segmenting plane curves using curvature negative minima.

The extrema of negative curvature are indicated by slashes. Black arrows indicate the direction of traversal of curve. The object is considered to be to the left of the direction of the traversal . (a) image seen as a face ; (b) image seen as an apple ; (c) image seen as a vase.

A similar illusion was also noted by W. Turton (1819) in which the parts of the face, composed by a pair of facial profiles, are transformed into the parts of a vase (see figure 2-7(c)) .

To describe the segments bounded by minima of negative curvature, Hoffman and colleagues introduce the concept of “codons”, which are curve segments lying between minima of curvature.

Codons have zero, one or two inflection points (or points of zero curvature) yielding a total of five codon types. These are illustrated in figure 2-8, where zeros of curvature are indicated by dots and minima by slashes. The symbols **O+**, **O-**, **1+**, **1-**, **2** are the labels for the individual codons.

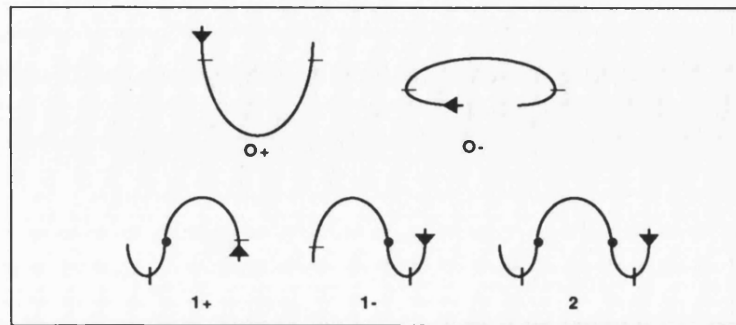


Figure 2-8 - The primitive codon types.

Zeros of curvature are indicated by dots and minima by slashes. The labels O+, O-, 1+, 1- and 2 are the labels for the individual codons. (Adapted from Hoffman 1982)

The codon representation will appear as a sequence of digits such as 21-1+21-. There are 5^5 , or 3,125 unconstrained sequences of five codons, but of these only 25 outlines are possible if they are constrained to be closed and smooth (W. Richards et al 1985).

2.2.5. MultiScale Techniques

Many shape coding techniques operate on a single scale or resolution, where the effects of noise and quantization require some degree of smoothing. Consequently, the final result of any processing operation is strongly influenced by the selected scale. In order to overcome this problem, a description that is continuous across a range of scales (or multiscales) was developed.

A number of multiscale descriptions have been suggested (A. Rosenfeld et al 1971, D. Marr et al 1979, 1979b) as for example, chain pyramids (P. Meer et al 1988) and strip trees (D. Ballard 1981). However, the complexity of some descriptions appeared to increase the volume of data instead of presenting a real solution to the problem. The scales should somehow be related to one another to organize and simplify the description. Marr (1982) suggested that the scales are “physically significant” when the inflection points coincide over several scales.

Following these ideas and the work of Stansfield (1980), A. Witkin (1983) introduced a further approach to multiscale descriptions called *Scale Space Filtering*.

The technique yields a hierarchical representation based on curvature variation as the signal or outline is modified over a range of continuous scale values. The “scale parameter” is introduced by smoothing the signal (or outline) with a Gaussian mask of variable size. This is illustrated in figure 2-9.

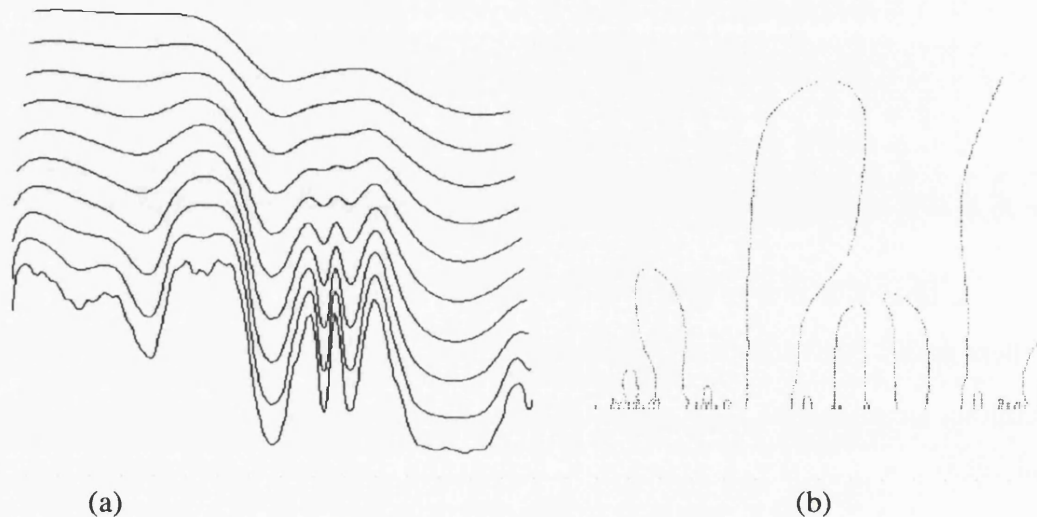


Figure 2-9 - Scale space technique.

- (a) Scale space filtering technique: a sequence of gaussian smoothings of a waveform (first one at the bottom). The scale parameter is increasing from bottom to top.
- (b) Hierarchical representation: zero crossing contours, which indicate the location of the inflection points (points where curvature=0) along the waveform, for a range of scales. The y-axis represents the scale values, where the coarsest scale is on top. The x-axis represents the path length along the waveform, increasing from left to right.

A.L. Yuille (et al 1983, 1983b) have provided some theoretical background for the scale space representation. F. Mokhtarian (et al 1986,1988,1992) extended Witkin's approach by representing the curves by their zero crossings of curvature. However, because such an approach is directly related to the methodology used in my work, it will be explored in more detail in the chapter “Method of Analysis”.

Witkin's work also inspired M. Brady and H. Asada to construct a scale space representation, which they named "Curvature Primal Sketch" (Brady 1984, Asada 1986). This is another multiscale approach for representing significant changes in curvature along the bounding contour of planar shapes. They proposed the use of a set of primitives based on curvature discontinuity, such as : the corner, smooth join, crank, end and bump, as illustrated in the figure 2-10 . These primitives are first defined as ideal parameterized functions modeled in what they called "orientation space" (i.e. relating the orientation of the tangent to the contour to distance along the

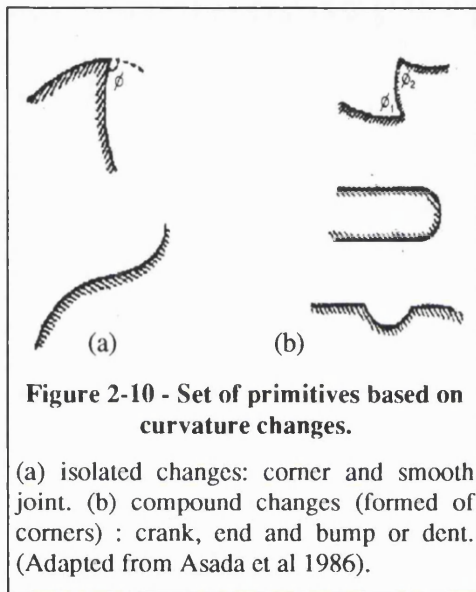


Figure 2-10 - Set of primitives based on curvature changes.

(a) isolated changes: corner and smooth joint. (b) compound changes (formed of corners) : crank, end and bump or dent. (Adapted from Asada et al 1986).

contour) and then analyzed at several scales through a convolution process with the first and second derivatives of a Gaussian. The "signature" for each primitive is given by the behavior of the minima and maxima of the derivatives with respect to the range of scales. The contour of the object to be classified is also filtered with a set of Gaussians of increasing scale to derive the scale space representation of the contour. Finally, instances of the signature of the primitives are identified at the larger scales

of the object and tracked through the finer scales, giving the location, along the contour, of the knot points that correspond to the primitive instances.

The concept of curvature primitives and multiscale representation was also used by P.L. Rosin (1993). He applied curvature primitives called "codons" , i.e. curve segments lying between minima of curvature (see section 2.2.4), with the extension of representing the curves at all their "natural scales" (defined as the scales that best describes the shape of interest - Rosin 1992). Similarly to the scale space techniques, a qualitative description is achieved (called the codon-tree) by linking codons at different scales. The use of such descriptions to model matching was demonstrated.

In seeking a scale space approach to describe contours, F. Leymarie and D. Levine (1988) proposed a new representation based on *mathematical morphology* operations (Matheron 1967, Serra 1982). They named it “Morphological Curvature Scale-Space”. Briefly, they first obtain a discrete curvature function of contours of objects in an image, based on a modified chain-code representation (this function is further smoothed with a Gaussian template). Secondly, features are extracted from the curvature function, such as peaks and segments of constant curvature, by employing the four basic morphological operations: *erosion*, *dilation*, *opening* and *closing* . These are fundamentally neighbour operations, executed locally, at each point of the function, by following a “structural element” of a specific size and shape (e.g. circle, square and line). In this case, a flat structural element (line) of varying width was considered. Finally, the multiscale representation is generated by uniformly increasing the size of this structural element.

When applied to the representation of images, the idea of scale space, suggested by Witkin (1983), has also been developed by Koenderink (1984, et al 1986), Babaud (et al 1986) and Lindeberg (1990). A good reference work may be found in Lindeberg (1994) in which the author explores the scale space theory and its applications to computer vision.

2.2.6. Skeleton or Axis of Symmetry

Some coding techniques explore the local symmetry of planar shapes in terms of the “axis” they define. The entire boundary of the shape is transformed into an axial representation (Rosenfeld 1986), also known as “skeletons”. Rosenfeld identified these classes of planar shapes as “ribbonlike”, which are generated by specifying a geometric figure, such as a disk or line segment, that moves along an arch or axis (the size of such figures may change as it moves).

Following this approach, H. Blum (1973 , Blum and Nigel 1978) introduced the *Medial Axis Transform* (MAT) or *Symmetric Axis Transform* (SAT). The rectangle on figure 2-11 is used to illustrate the technique. Let us consider a set of circles that touch at least two points on the boundary of a given shape (see figure

2-11(a)). The MAT is defined by the locus of circle centres and is shown on figure 2-11(b).

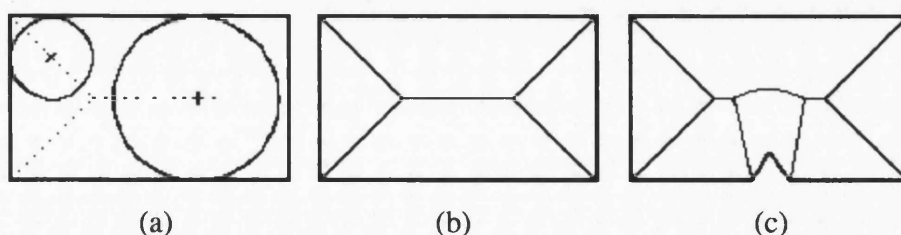


Figure 2-11 - Examples of medial axis transform.

One of the main disadvantages of this method is that small perturbations in the boundary can result in large changes in the structure of the MAT, as illustrated by figure 2-11(c). This directly suggests that smoothing may reduce such effects. Multiscale techniques are once more used to develop a description tree containing a hierarchy of medial axis components defined at a range of scales. This variant on the medial axis transform, called *Multiscale Medial Axis Transform*, was introduced by S.M. Pizer (et al 1987).

Another shape representation related to the MAT is the technique of *Smoothed Local Symmetries* (SLS), introduced by M. Brady (1982,1983,1984). The SLS represent the object using the bounding contour and the region that the boundary encloses. It was developed from the ideas underlying the medial axis transform and generalized cones (see Brady 1983), making explicit the local symmetry axes present in the shape.

Figure 2-12(a) shows the geometry of a local symmetry. The SLS axis is defined as the locus of line segment midpoints P , where α is the angle between the outward normals and the line AB .

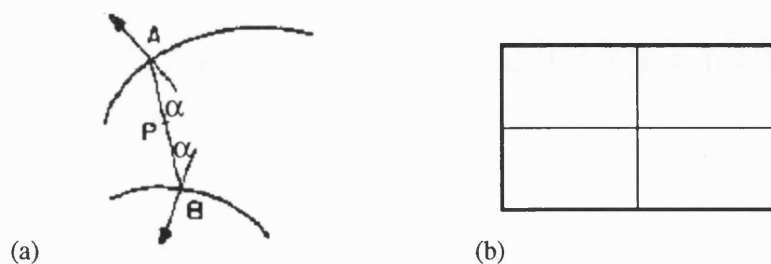


Figure 2-12 - Smooth Local Symmetry .

(a) Geometry of smooth local symmetry ; (b) The SLS axes of a rectangle.
(Adapted from Brady et al 1984).

Figures 2-11(b) and 2-12(b) illustrate the difference between the symmetry axes of a rectangle when defined by the Medial Axis Transform and the Smooth Local Symmetry techniques, respectively.

M. Leyton (1987,1988) added another important psychological role to the curvature extrema points and symmetry axes: using them to infer “process-history”. He called this new analysis *Process-Infering Symmetry Analysis* (PISA). It is the notion of shape being the outcome of processes that formed it. He argued that such a process history of a shape can be recovered from its curvature extrema, and also proposed a process grammar (codon-based) which describes the effect of processes inferred from changing one shape into the other. He proved the duality between curvature extrema and symmetry structure, allowing him to use symmetry axes to infer process history.

The application of the concepts of axial representation, curvature features and multiscale decomposition of shapes may be seen in two distinct works, addressing different problems.

One is applied to the study of biological shapes as investigated by F. Leymarie (et al 1992). They claim that the skeleton is a powerful representation for characterizing the shape deformations and evolution of shape subparts of nonrigid natural forms. The process by which the skeleton is obtained (named skeletonization) enables the integration of both region and boundary features. In particular, they use the “grassfire transform” as a skeletonization process, combined with an active contour model (called the snake) to simulate the fire propagation. Their results show that the derived shape description method is well suited to tracking amorphous forms such as cells.

The other application relates to machine perception, and has been investigated by H. Rom (et al 1991). They focus on the question of the shape description being the basis for recognition tasks. They suggest a hierarchical approach for achieving a natural (intuitive) description of planar shapes and the decomposition of the shape into its parts. Starting from a quadratic B-spline approximation of a closed 2D curve,

all the possible axes on the whole shape are computed through the Smooth Local Symmetries technique. This is then followed by a selection process where at each step, local and well defined parts are described and removed, yielding a hierarchical interpretation of the shape. Parts are sections of the contour bounded by consecutive negative curvature curve sections. Global relationships between different parts of the shape is handled using parallel symmetries (F. Ulupinar et al 1990). Their method was tested on several shapes including a man, snake, bean and airplane shapes.

2.2.7. Summary

As a whole, the number of existing techniques may be seen as a direct result of the variety of areas of application. Each individual method has its own advantages to a particular application which again, emphasizes the importance of identifying the information relevant to the problem under consideration and the way in which it should be presented.

Nonetheless, the general methodologies mentioned above draw a clear picture of the importance of the contributions made by some of the theories of vision to this area of shape coding techniques. With the use of concepts such as curvature maxima in shape perception, Attneave's work is immediately followed by a number of researchers exploring and expanding his initial ideas. Multiscale techniques are useful in providing a qualitative and hierarchical description of the contour, by using the parameter "scale" as a function of the amount of blurring or smoothing necessary to remove details of the contour. They all seem to suggest that the notion of curvature is a very powerful representation for contours.

Although with a large number of practical applications, great emphasis has been placed on the development of theoretical work involving the techniques of multiscale, axes of symmetry and extrema of curvature.

Chapter Three

3. The Study of the Human Face

The study of the human face has always attracted the attention of writers, sculptors, painters and scientific researchers. The measurement, analysis and observation of the face has a long and interesting history which goes back beyond the time of the ancient Greeks.

Even though the reasons were quite diverse, the necessity of having a *description of the face* seems to be the obvious motivation amongst all the investigators. It was a common practice, with these descriptions, to explore forms and means of dividing the face in order to develop their ideas, concepts and methodologies.

3.1. Initial Perception

A mathematical system of proportions for the human figure, including the head and face, has a long standing interest throughout history.

Considering the question of harmony, balance and above all of proportion, the philosopher Plato defined beauty as resulting from the “*golden section*”, that is, a special way of subdividing an object so that the ratio of the whole to the larger part is equal to the ratio of the larger part to the smaller. As the researcher J. Liggett (1974) explains: “ *this formula implied that all beautiful things have some kind of division about one third of the way along their length. Therefore, for the greeks, in the ‘perfect’ face the brow would be one third of the way down from the hairline, and the mouth one third of the way up from the point of the chin. The width of the face would be two-thirds of its height* ” .

A different proportion, however, was adopted by mediaeval artists who believed that the perfect face was divided into sevenths, and that the width of the face should be twice of the length of the nose.

In the Renaissance, Leonardo da Vinci showed similar interest in facial proportions when working on an extremely detailed system of correspondences between all the parts of the entire body. Exploring the representation of the face, Leonardo da Vinci, in his "Treatise on Painting" (Richter 1970, § 315), stated : *"From the eyebrow to the junction of the lip with the chin, and the angle of the jaw and the upper angle where the ear joins the temple will be a perfect square. And each side by itself is half the head."* (see figures 3-1(a) to (c)).

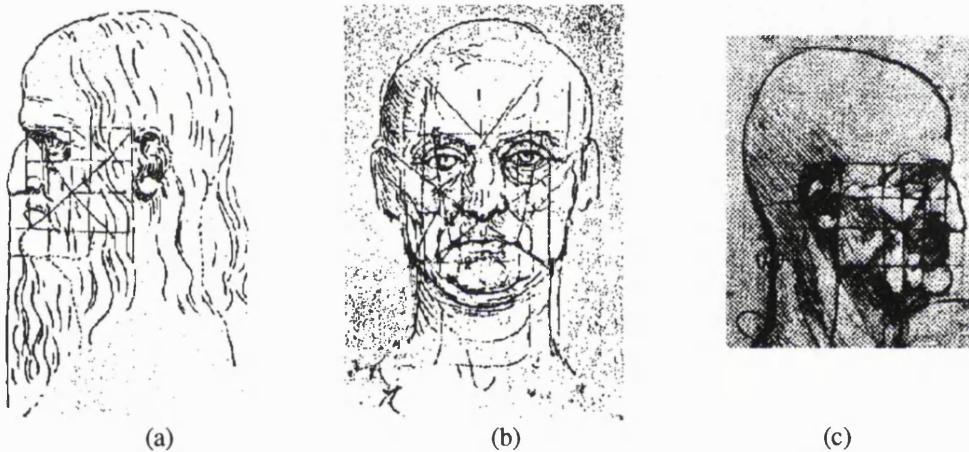
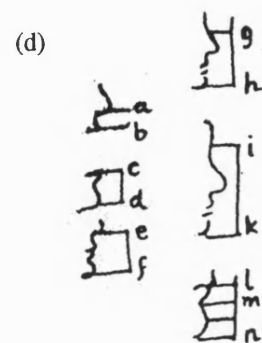


Figure 3-1 - Leonardo da Vinci's proportions of the human face.

- (a) Profile of Leonardo taken from a Venice drawing ;
- (b) Self-portrait by da Vinci (Turin Royal Collection) ;
- (c) Drawing by Leonardo (Venice Academy) ;
- (d) Proportions of the face in profile, some of which are described on the text.



Again, on the proportionality of the parts of the face on profile he writes (Richter 1970, § 315) : *" The space from the chin to the base of the nose e f is the third part of the face... The space from the mouth to the bottom of the chin c d is the fourth part of the face..."* (see figure 3-1(d)).



**Figure 3-2 -
Caricatured expression**

figure 3-2).

Leonardo also suggested that “relevant traits” may be established by dividing the face into four main parts : forehead, nose, mouth and chin. With those parts focused in the mind, one should be able to analyze the face (including cultural elements such as vices and virtues) and retain it with a simple glance. On studying the various shapes that these parts can assume he could produce, from the normal face, variations such as fool’s and monstrous faces (see

K.H. Veltman (1986) correlates this idea with Leonardo’s method, applied in his architectural plans, of playing with variables, i.e. adding, multiplying and subtracting basic shapes to and from one another. This is evident in his approach to the problem of noses, also outlined on the Treatise on Painting. He begins by classifying the nose with three variables: straight, concave and convex, and then combines these in various ways, including the transition from the nose to the brow, as illustrated in figure 3-3.

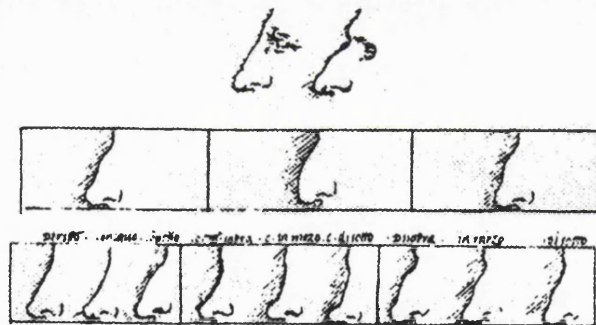


Figure 3-3 - Leonardo da Vinci’s comparative nose studies.

Exploring even further his ideas, Leonardo could create entirely new figures by transforming one face into another. On one of his drawings it is possible to follow the transformation of a horse’s face into a man’s face, and a lion’s face into a man’s face.

Apparently Da Vinci was not alone in this topic of ratios and proportions. The Italian scholar Fra Luca Pacioli wrote the “Trattato de Divina Proportione”, in 1509, in which he too, investigates the head and face (see figure 3-4(a)).

The German Albrecht Dürer, on his work “Four Books of Human Proportions”, published after his death in 1528, presents a system of measurements and proportions for the different parts of the human body, including instructions in the drawing of the head. On figure 3-4(b) the head is seen from in front, in profile, and from above. Figure 3-4(c) shows one of his studies on constructed heads by introducing oblique lines into his constructional grid (Conway, 1958).

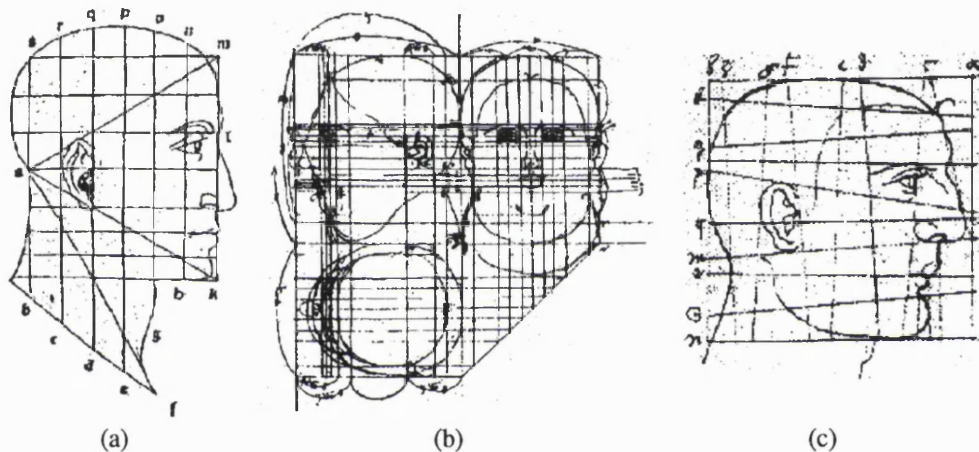


Figure 3-4 - L. Pacioli's and A. Dürer's measurements of the human face.

(a) Presumed portrait of Leonardo da Vinci used by Luca Pacioli in his *Trattato de Divina Proportione* (Venice, 1509) ; (b) Dürer's drawings of a woman's head (Brit.Mus. MSS. vol.II, 2I) ; (c) Example of Dürer's study on constructed heads.

In many aspects, some ideas outlined by Leonardo were evolved in greater detail by Dürer, including studies on the nose and the transformation of faces. In fact, Dürer's work inspired D'Arcy Thompson's pioneer development of a theory of such transformations, working on the life sciences, which were later extended to the statistical and biological branches of the mathematical sciences (see chapter 2).

As a whole, this initial perception of the human face and the search for a mathematical description reflect the knowledge and technology available at that time. With their scientific art, they were trying to solve practical problems. Their canons

were not only intended as a means of artistic workmanship, but primarily to achieve harmony.

3.2. Analysis of the Face in Two-Dimensions

Two-dimensional data has been extensively used for the study and measurement of faces. A technique widely employed in this approach is the use of photographs. A number of methods have been proposed for identifying, describing and measuring facial features out of photographs taken from the anterior and lateral views of the face. Such an approach to the study of faces has been consistently investigated in applications which include the recognition of faces, largely for security and forensic purposes.

One early use of this technique was introduced by Alphonse Bertillon (Rhodes, 1956). In France, about the year of 1840, photographs were added to the physiological description of criminals and used by the police. Beginning by cutting up photographs of the face and juxtaposing the isolated features of different individuals by mounting them side by side on pieces of cardboard, Bertillon developed a new method of classification and identification which combined photography with a number of anthropometric measurements of the individual (later, fingerprints were added as clues of identity). In his method (Bertillon 1885, 1890) he describes the meticulous cataloging of several anthropometric measurements, including standing and sitting heights, length of the right ear and of the left foot, amongst others.

On the face, Bertillon used the photographs in full face and profile (right hand side) to record the structure and patterns of the existing features. This is illustrated in figure 3-5, which also show some of his ideas on classifying the shape of the nose.

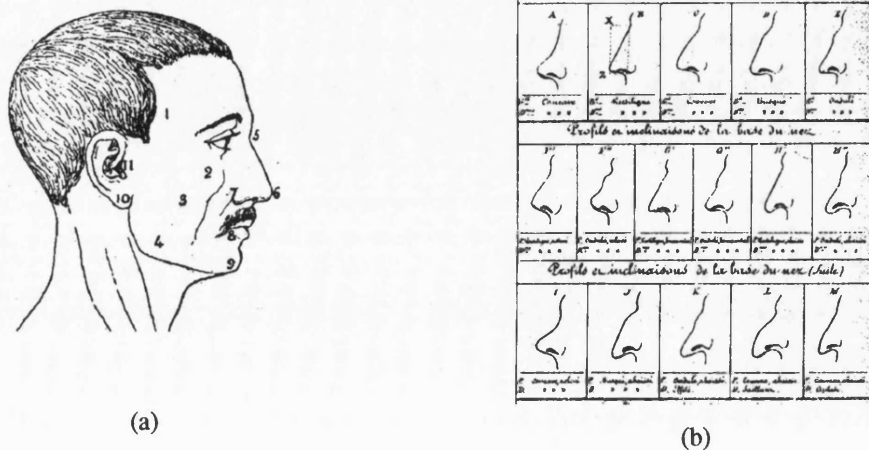


Figure 3-5 - A. Bertillon's measurements of the face.

- (a) Face in profile. The numbers indicate the main features used on his system.
- (b) Bertillon's classification of the nose .

(Adapted from Bertillon 1885)

A less scientific approach to facial description, but nonetheless interesting, may be found in A.L. Allen's book entitled "Personal Descriptions" (Allen, 1950). As a police superintendent, his main interest was in personal identification. Acknowledging that the existing literature was too technical for the average person to understand, his aim was "to present the facts in a simple manner, so that one would know what to look for and how to describe what has been seen". Although his descriptions are basically verbal with no attempts to systematic measurements, he proposes a classification system based on the various shapes of the forehead, nose, ears, mouth and chin.

More recently, a number of computer-based systems have been developed for the study, automatic extraction of features and identification of faces (see A. Samal et al 1992 and A. Coombes 1993 for a survey). W. Bledsoe (1964) used photographs of faces to manually mark the coordinates of various points of features like the eyes, the nose, etc. The distances between these points were then used when trying to identify an individual from a database with two thousand faces. On automating this system, C. Bisson (1965) digitized the photographs and used the "average intensity difference" along the horizontal and vertical axes to extract edges of the facial features, which

were then used on the measurements. Frame-grabbing is another method commonly used to generate digital images of faces.

T. Kanade (1977) proposed a face-identification system based on a fully automated method of feature extraction. He applied picture processing techniques, combined on a scheme with feedback (i.e. the various stages of processing may be repeated if not satisfactory), allowing a more flexible and adaptive process. Photographs of faces in full view were scanned and then, with a Laplacian operator, converted into a binary image representing contour sections where brightness changes significantly according to a threshold level. Starting from the top of the head and moving down towards the chin, approximately thirty points are located, indicating the eyes, nose, lips, mouth and the contour of the face. With this information, the original images were re-analyzed in order to obtain a more detailed description of the located features. His identification routine consisted of a simple distance metric as a measure of the similarity between pictures represented by a feature vector of sixteen parameters. The reported success rate was fifteen out of twenty faces.

Sakai and colleagues (1972) used a similar approach of identifying features in a prearranged order. Other researchers have applied different techniques.

X. Jia (et al 1992) reported on the use of an extended feature set for automatic face recognition. Their data consisted of image intensity values of a frontal view of the face, obtained from a TV camera with controlled illumination. Features like eyes, nose tip and mouth are identified and located using the change of gradients of horizontal and vertical intensity projections which are further processed by filter and edge detection operators. A set of ten geometric features is defined including: length of the face, chin, forehead and nose; width of mouth and neck, amongst others. Following this approach, image intensity graphs have been used by Nixon (1985), and isodensity maps by Nakamura (et al 1991).

Kaya and Kobayashi (1972) proposed the use of principal component analysis to face recognition, and Kelly (1970) used template matching. Yuille (et al 1989), Shackleton (et al 1991) and Bennett (et al 1991) used deformable templates. These

are geometric models which operate globally over the template region, by defining an energy function that incorporate a *priori* knowledge about the shape (e.g. peak, valleys, edges, etc.) and intensities of the features. The best fit of the template to the image occurs when the energy function is minimized.

3.3. Analysis of the Face in Three-Dimensions

By arguing that facial features are three-dimensional in nature, some researchers have proposed methods based on the properties of the surface of the face. There are many types of three-dimensional (3D) surface description. While in a digitized (or greyscale) image the information is extracted by grouping pixels together according to the rate of change of their intensity over a region, in 3D images the pixels are grouped according to the rate of change of depth, corresponding to pixels lying on the same surface such as a plane, cylinder or sphere.

In fact, on dealing with surfaces, different mathematical descriptions are introduced, based on differential geometry. They basically consider that the geometry of the surface, in itself, defines the shape of an object, which can be visualized when the surface is illuminated (see P. Besl 1988 and A. Coombes 1993 for a review).

Descriptions of shape in 3D have been largely investigated by computer vision scientists which have established some criteria for a standard representation (see Marr et al 1978 and Brady 1983). These lead to two distinct approaches, based on image measurements of the **depth** and of the **surface normal**. In the first one, the depth information is obtained from range images containing explicit three-dimensional information, i.e. the geometry of the object is represented in terms of their (x,y,z) coordinates. Depth data have been made possible in recent years by technological advances in camera optics, CCD cameras, laser rangefinders and computers used on the production of reliable and accurate acquisition systems (Faugeras et al 1983, Arridge et al 1985, Boulanger et al 1985, Doemens et al 1986, Porril et al 1987). An actual three-dimensional system utilized in this thesis is described later. The second approach uses the image intensity values to derive the surface normals of an object. In this description many methods have been used to extract the shape of the object,

including shape from shading (Horn 1975), shape from texture (Witkin 1981), shape from contours (Brady et al 1984b), shape from stereo (Woodham 1981, Blake 1986), and shape from topographic primal sketch (Haralick et al 1983), amongst others.

The use of surface curvatures (the Gaussian and mean curvatures) to segment a surface into surface type primitives has been demonstrated, using different computational methods, by Yokoya (1987) and by Besl (1988), when recognizing objects in a scene. This work inspired Coombes and colleagues (1990) to show how the facial surface could be described in the same way. With a refined method, Coombes (et al 1990a, 1991) mathematically described the facial shape and changes occurring in the face in terms of eight “fundamental surface types” (see figure 3-6). Two faces were compared, from range data, representing before and after stages of surgery treatment. Their results show a strong relationship between the surface type description and the clinical observations.

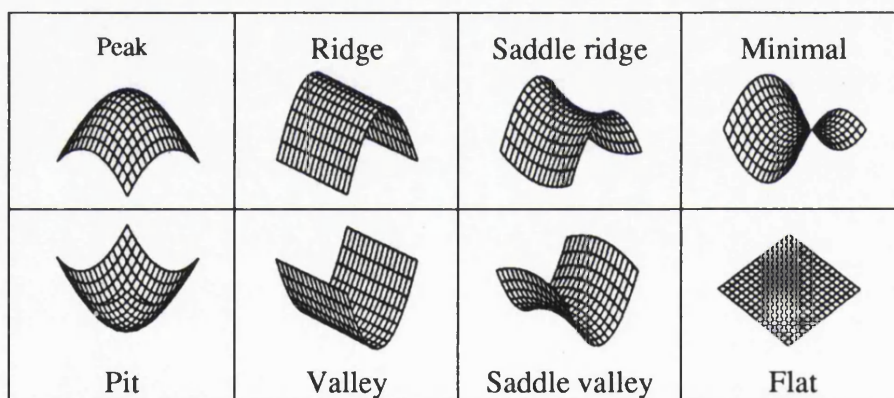


Figure 3-6 - Eight fundamental surface types.

(Adapted from Coombes 1993).

A. Coombes (1993) later defined the Surface Type Image (STI) representations as being produced based on the eight fundamental surface types, defined from the sign of the Gaussian and mean curvatures. Varying the thresholds on the curvature allowed a series of hierarchical STI's to be produced revealing information about the level of curvature of the face.

Other researchers have also applied similar methodologies to describe the facial surface for various tasks (Lee 1990, Gordon 1991, Masui 1990, Bruce 1993).

3.4. Analysis of the Facial Profiles

Many techniques and methods of analysis which involve shape description have been proposed when considering yet another two-dimensional approach to the study of faces, and that is the use of facial profiles. They are reviewed on this section.

3.4.1. Recognition

Systems for automatic recognition of faces and its particular problem of identification is an application that has been widely explored by research workers. The face is most commonly represented by a *feature vector* derived from face profiles (silhouettes). The feature values are obtained using a set of characteristic points on the profile, such as for example the tip of the nose and notch between the nose and upper lip. The features are usually described in terms of distances and angles between the characteristic points.

3.4.1.1. Francis Galton's Contribution

An early use of this approach to face identification and description was developed by Sir Francis Galton (1888, 1888a). Galton had been, for a number of years, working with photographic research and portraiture (Pearson 1924). From his previous investigations in composite photograph, he sought to measure the degree of resemblance or of difference in portraits. Intrigued by our restricted ability of describing form of irregular outlines of different kinds and to describe hereditary resemblances and types of features, he carried out some experiments.

When measuring a profile given by its silhouette (such as the shadow cast projected on a wall) or from photographs of a lateral view of the face, Galton suggested the use of a “unit of measurement” which is given by the distance between two parallel lines, as illustrated in figure 3-7. The first line is obtained from points **B** and **C**, namely, the line which touches the concavity between the brow and nose, and the convexity of the chin. The second line is parallel to **BC**, passing through the point **N**, just touching the nose.

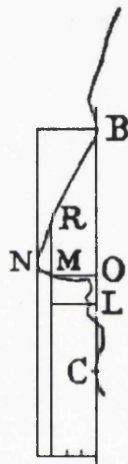


Figure 3-7 - Facial identification: Galton's method for profile measurement.

First, one line is defined through the points **B** and **C**. After that, a second line, parallel to the first and passing through the point **N**, is constructed. The unit of measurement is given by the distance between the two parallel lines. (Adapted from Galton 1888).

From this unit, two more points are identified on the profile : points **O** and **L** . To achieve this, the unit is divided into four equal parts and a line is drawn on the division closest to **N** and parallel to **BC**, defining the points of reference **R** and **M**. By dropping a perpendicular from **M** upon **BC** the point **O** is determined. The perpendicular to **BC** passing through the mouth (i.e. the concavity between the upper and lower lips) will determine the point **L**.

The measurements extracted from the defined points would be the distances **OB**, **OC** and **OL**. In addition to these, Galton suggested the measurement of the “radius of the circle of curvature” of the following facial features: the depression between the brow and the nose, and of that between the nose and the lip. He also suggested the measurement of the general slope of the base of the nose.

Galton realized that the difficulty lies in selecting the best and most meaningful measure that can represent the general form of the profile. Although he had tried many different sets, all with more or less efficiency, he could not decide which one to adopt.

Following his previous work, Galton (1910) later developed a method of numerically describing facial profiles. On this method, five cardinal points were used to draw a rough representation of the profile, as illustrated in figure 3-8. They correspond to the following features of the face : (1) the point in the deepest part of the fronto-nasal notch, labeled **B**; (2) the tip of the nose, labeled **N**; (3) the notch between the nose and the upper lip, labeled **U**; (4) the point half way between the furthest positions at which the lips would touch one another if they were lightly closed, labeled **L**; and (5) the tip of the chin, labeled **C** (F. Galton, 1910). Assuming a pair of orthogonal axes centered on C, with the vertical axis passing through B, the five points B, N, U, L and C may be precisely located. These profile measures were normalized by establishing the length of the line segment given by the points B and C to be always fifty millimeters.

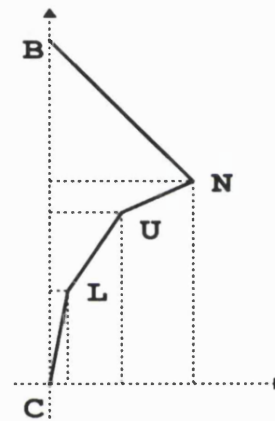


Figure 3-8 - Galton's profile skeleton.

To describe the shape of the profile adjacent to the cardinal points, and those of intermediate links (with the exception of the last point, the chin), Galton used a series of curved segments, each one represented by an index in tabular form.

Study of the Human Face

Expressed as single numerals, between one to nine varieties of shapes were given for each cardinal point, as illustrated in table 3-1 (adapted from Galton 1910).

		1	2	3	4	5	6	7	8	9	0
fronto-nasal notch	<i>b</i>										
ridge of the nose	<i>g</i>										
tip of the nose & outline underneath	<i>n</i>										
naso-labial notch & start of upper lip	<i>u</i>										
the parting of the lips	<i>lp</i>										
sizes of upper & lower lips	<i>ll</i>										
size and position of notch between lower lip and chin	<i>k</i>										

Table 3-1 - Shapes of profile segments.

Table with the shapes of the profile segments adjacent to the cardinal points given on figure 3-8.

Furthermore, Galton thought of using a telegraphic system to encode and transmit his numeralised profiles. He showed that four telegraphic “words” are sufficient to convey that information.

Therefore, the formulae describing the profiles consisted of twenty “figures” or numerals, arranged in four groups of integer digits, with five digits in each group. Referring to the labels in table 3-1, the first three groups refer to points N, U and L respectively. The first group gives the values of N_x , *n* and N_y . The second group gives the values of U_x , *u* and U_y . The third group gives the values of L_x , *lp* and L_y . The last group, preceded by a dot, refers to the peculiarities of *b*, *g*, *ll* and *k* respectively.

In figure 3-9, a facial portrait is used to illustrate Galton’s method on profile recognition. Figure 3-9(a) shows the original portrait, figure 3-9(b) shows its

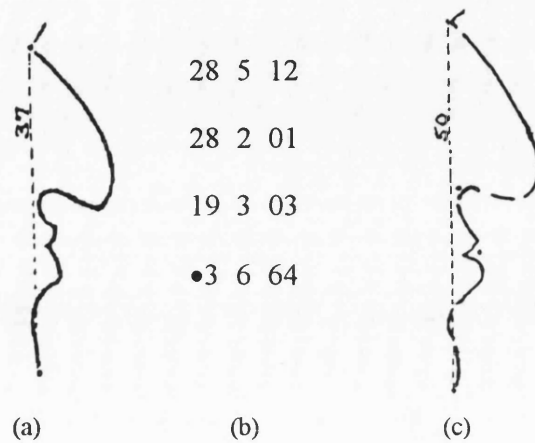


Figure 3-9 - Example of Galton's method.

(a) original portrait.

(b) portrait's formulae : $N_x=28$; $N_y=12$; $U_x=28$; $U_y=01$; $L_x=19$ and $L_y=03$.

The small letters are: $n=5$; $u=2$; $lp=3$; $b=3$; $ll=6$ and $k=64$

(c) reconstruction from the formulae.

(Adapted from Galton 1910)

It can be seen that the five cardinal points are the same ones used in his previous work (as described above) namely: the concavity of the notch between the brow and the nose (labeled B), the convexity of the chin (labeled C), the tip of the nose (labeled N), the notch between the nose and the upper lip (labeled O), and the parting of the lips (labeled L) .

3.4.1.2. Leon Harmon's Contribution

Leon D. Harmon (1976, L.D. Harmon and W.F.Hunt 1977) also adopted a similar approach to the identification of faces, but using photographs (taken at a standard distance) where the profiles were extracted and reduced to outline curves by an artist. These tracings were then digitized and processed by a minicomputer, where each profile trace was represented by approximately 300 sample points.

They used nine fiducial points which basically correspond to the cardinal points in Galton's work, plus two points for the upper and lower lips, one for the throat and one for the forehead. These nine fiducial marks were automatically determined, as for example, for the bridge of the nose, a line is drawn from the nose tip to the forehead and the point between these fiducials which is most distant from the nose-forehead line is recorded; the throat is the tangency point of the line intersecting the chin fiducial and tangent to the inside of the profile below the chin; for the lips and mouth fiducials, the radius of curvature is computed (starting downwards from the nose bottom) until a pattern of three minima has been found with the curvature alternately to the inside, outside, inside; the forehead is obtained by swinging the chin point around the nose tip point to intersect the trace at the forehead.

The distances between points, angles between them, areas of some triangles formed by these points, and the protusion of the nose, amongst others, are used as “geometric features”, which provided the basic components for generating a multidimensional vector, expected to be unique for each face.

Figure 3-10 illustrate the fiducial points and list the eleven components of the feature-vector (adapted from Harmon et al 1978).

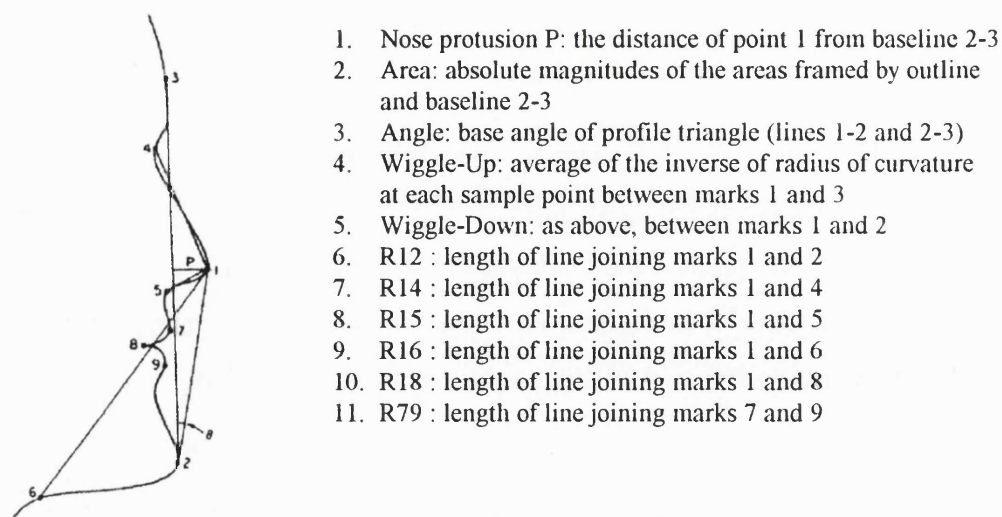


Figure 3-10 - Harmon's face identification method.

On the left: the nine fiducial marks and some feature-vector components relating to line segment length, areas, angles, etc. On the right: a list of feature-vector components is shown.

On a population of 256 male faces, the pairwise dissimilarity was measured by a normalized Euclidean distance between the two sets of features X and Y :

$$D^2(X,Y) = \sum_{i=1}^N \frac{(x_i - y_i)^2}{\sigma_i^2}$$

where σ_i^2 is the population variance for the component i . After checking the “unknown” profile against the population, an ascending ranking order is established with the most similar profile at the top of the list.

Their results on identifying the most and the least similar pairs of profiles emphasize that what the computer “decides” as similar (or different) does not necessarily agree with what the human decides. Their justification is that we largely base our judgments on feature shapes (e.g. nose and chin contours) while such shapes are not used in their present machine analysis. When testing the independence of the feature vector components, the highest correlation coefficients, indicating a dependent relationship, were for the protrusion, area and angle, closely followed by R12 and R18. Clearly, some feature-vector components could be eliminated without diminishing individual identification, which they proposed to systematically test on a future experiment. Normalized histograms showing the distribution of the features over the entire population were also presented.

In a subsequent experiment, Harmon and colleagues (1978) used a new population of 121 subjects (94 males and 27 females), with each person having three poses taken approximately one week apart. The artist’s tracings were still maintained in this study. They refined the algorithms used in their preliminary work to eliminate sources of errors, especially notable for fiducial mark detection and high sensitivity of the area and wiggle measurements due to sample coarseness and to matrix orientation. The relative utility of the various feature-vectors used for identification was considered and their eleven-dimensional feature space was reduced to ten by deleting Protrusion, mainly because this feature is highly correlated with Area and Angle. Improved statistical decision procedures were also adopted. It consisted of a combination of a classification method by distance comparison and a set partitioning technique. The latter would partition the candidate population to a relatively small

subset file by rejecting all vectors which “couldn’t possibly fit”, reducing the number of Euclidean distance calculations. The noise effects such as soft tissue and lower mandibular variations, data quantizing and errors produced by the artist’s tracings for data entry were claimed to be minor and well handled by the procedures involved.

Another extension and refinement of their previous technique was presented by Harmon and colleagues (1981). A new population was added to the experiments, consisting of 112 subjects, with four poses each. This time, the profiles were automatically obtained from faces directly scanned using a camera and a high contrasted background. Two extra fiducial marks were adopted : the minimum point between lower lip and chin, and the forehead maximum. New angles and distance measurements were introduced to the multidimensional vector, bringing to a total of seventeen features. Their results show that when a fourth pose was introduced as an “unknown” for file identification, the recognition accuracy was 96%. Experiments of asserted identity and rejection of strangers (i.e. population membership) were also reported to be highly satisfactory.

3.4.1.3. Other Contributions

G.J. Kaufman (et al 1976) also used a feature based approach, where the components were coefficients computed from the polar form of the autocorrelation function. They used full profile silhouettes from a binary, black and white television camera image, which were further processed to remove noise, smooth and extract edges. Ten subjects were used (making up ten pattern classes), with each one having twelve full facial profiles taken over a period of several weeks. From this population of 120 facial silhouettes a twelve-dimensional circular autocorrelation feature vector was computed and a distance-weighted k-nearest neighbor decision (as described by J.Carl et al 1972) used on a set of experiments. Their results show that using an adaptive training procedure the accuracy of the system for recognition was 90 percent (in a ten class problem). The technique of moment invariance was also used to form the feature vector and the results compared with the circular autocorrelation features. It was found that the recognition accuracy this time was worse by approximately 20

percent difference, indicating that, for this problem, circular autocorrelation seems superior.

C. Wu and J. Huang (1990) used cubic B-spline functions to extract six interesting points from the face profile, later used to derive a set of twenty four features used for recognition. They used back-lighting photography to obtain the outline curves automatically. Eighteen subjects were used, described as “from a group of oriental faces, from small to large and from young to old”. Three profile images were collected for each subject. The six interesting points are determined using a similar approach to that of Harmon and colleagues. The mean, variance and standard deviation values are used to calculate the minimal distance, used to rank the candidates when matching the profiles for recognition. Based on their experimental results, the authors claim their system to be reliable.

3.4.2. Fourier Analysis

Another approach applied by some investigators, when studying facial profiles, is the use of Fourier analysis. For this particular application, Fourier analysis allows a transformation from the spatial domain (as the measures are distances) into the frequency domain (where frequency is equal to $1/\text{distance}$). The fundamental frequency is given by the first harmonic. The next higher frequency is the second harmonic, which is equal to one-half the wavelength of the fundamental frequency. The third harmonic is equal to one-third of the fundamental frequency, and so on. In this way, the separate harmonics or components can be analyzed and their contributions to the total form identified. When utilized as a curve fitting function, the Fourier series will converge onto the form under examination as more components are added in the series.

However, the main drawback of this approach is the difficulty of relating the values of the coefficients to the shape of a particular region along the contour. Changing the value of a coefficient changes the whole contour shape in a way which is not easy to predict and identify. Nonetheless, such approach has been reported in the literature.

K. Lu (1965) used Fourier series to obtain a harmonic analysis of the human face, represented by the frontal and lateral views, with the aim of identifying patterns of growth and symmetry. In the frontal view study, the data consisted of twenty four frontal cephalograms (X-ray photographs) from boys of four to six years of age (normal growing children). By choosing the midpoint between the two fronto-zygomatic sutures as the origin, and using polar coordinates, forty points were defined along the frontal outline. The Fourier coefficients were calculated and their effect on the shape of the face examined. The results show that a combination of lengthening, narrowing and shortening global effects over the upper, mid and lower parts of the face may be associated to specific coefficients of the series. In the profile study, the data consisted of one hundred lateral cephalograms from a five years record (three to seven years of age) of a group of twenty children (ten boys and ten girls). The profiles were defined by thirty six points between the nasion and menton landmarks. The computed Fourier coefficients represented the average of ten individuals in each sex-age group. From the results, K. Lu correlates specific coefficients to the vertical growth of the face, as well as their change of magnitude with age (i.e. *“the coefficient B_2 increases with age for the girls and is greater than that for the boys”*). He also claims that the change due to growth between any two ages may be obtained by the difference of the two respective sets of coefficients.

V. Delfino (et al 1985) reported on the use of Fourier sine-cosine series coefficients to describe fronto-facial profiles of fossil Hominid skulls. The series order was ninety four harmonics for a normalized set of 190 points. They explored the harmonic's amplitude and phase, as well as their individual effect on the series. The results seem to indicate a major diversity in fronto-facial profile growth between the analyzed skulls, which they justify by being *“mainly expressed by the different congruence of the first and second harmonics”*.

3.5. Clinical Analysis of the Face

Orthodontists and maxillo-facial surgeons, amongst other clinicians, have long been interested in the study of facial morphology, including growth and the aesthetics of the face (e.g. Enlow 1990). Many clinicians have emphasized the use of neoclassical

rules of proportionality (some of which were described earlier on this chapter) in assessing the soft-tissue face and in planning surgical treatment (Reidel 1950, Subtelny 1959, Ricketts 1957). However, many of these canons have been challenged. With further anthropometric studies, new data is available, which is analyzed in terms of the means and standard deviations of measurements and indices, allowing differences and similarities between groups to be statistically compared (Farkas 1981, Farkas et al 1985, Farkas 1987).

Over the past few years, the advances in surgical techniques and anesthesia, combined with the advances in computer technology, have increased the scope for facial reconstructive and orthodontic treatments. The importance of methods that provide a prediction in terms of facial appearance and soft-tissue movement have been intensified.

3.5.1. Cephalometric Methods

Cephalometric methods are widely used in the study of craniofacial morphology and the clinical analysis of facial form. It is a traditional method used by orthodontists.

Initially, studies using craniometric as well as other anthropometric methods were limited to the use of dried skulls, bones and cadavers. Anatomical landmark points, lines and reference planes were most commonly used as a basis for study and comparison, with calipers used for the measurements. Despite the invaluable foundation provided by those studies, a significant advance came with the discovery of X-rays, by the German physicist W.C. Röntgen in 1895, and its consequences on the clinical sciences (Glasser 1934).

Although radiography was an accepted clinical procedure and cephalometric measurements were being applied to external structures of the living head, these two different techniques were not merged until the independent studies of B.H. Broadbent (1931) and H. Hofrath (1931) were published, introducing *cephalometric radiography* (or *cephalometrics* as it is more frequently known). With this new tool, the frontal and lateral views of the bone and soft tissue of a living head could be consistently recorded. Thus, eliminating the uncertainty of measuring through soft tissue, the

craniometric landmarks of the face and cranial base may be registered, and used for treatment planning (Zide et al 1981, 1982) and for monitoring changes due to growth (G.F. Walker et al 1971), orthodontic or surgical treatments (K.L. Denis et al 1987).

The cephalometric technique produces fundamentally two dimensional information of the head. Three dimensional information may also be obtained, with the use of geometry, if two cephalograms (lateral and frontal) are taken orthogonally and concurrently (Savara 1965, Cutting et al 1986). However, the difficulties, reliability and errors involved in this method has limited its use (Miller et al 1965). For this reason, a large amount of research and clinical work has been reported on two dimensional studies of the midline profile.

3.5.2. Characterizing Shape

In conventional cephalometrics, the face is measured after locating, on the projected images derived from lateral X-ray radiographs, a number of landmarks. Form (or shape) is then characterized in terms of distances between pairs of landmarks, distances between landmarks and lines through landmarks, and angles between pairs of lines.

As a whole, these landmarks are mainly based on the skeletal and then extrapolated to the soft tissue profile. Usually, the measurements are obtained from tracings on matted acetate paper using ruler and protractor.

A typical cephalometric tracing is shown in figure 3-11, illustrating some landmarks and planes .

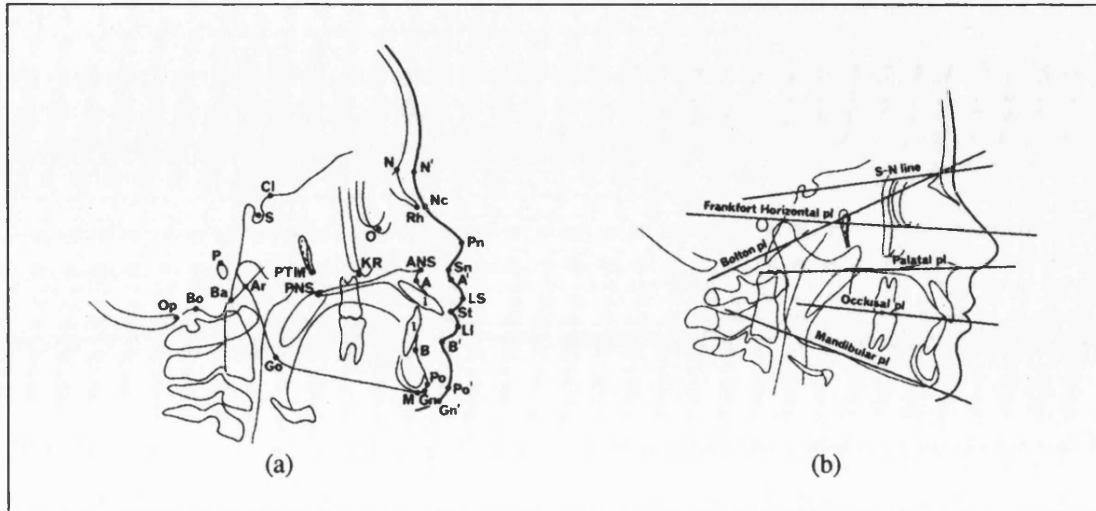


Figure 3-11 - Typical cephalometric tracing.

- (a) Skeletal and soft tissue landmarks.
- (b) Lines and planes derived from above landmarks.

(Based on Chaconas 1980).

Often, the measurements obtained from a cephalometric analysis play an important part in orthodontic diagnosis and treatment planning, where the assessment of skeletal, dental and soft tissue relationships are performed. They aim to *describe* the patient's condition and to *predict* the outcome of the treatment basically by categorizing cases according to type, defining the amount by which an observed case departs from some accepted norm, and indicating the extent of change during treatment.

Consequently, it is clear why concern is expressed by the clinicians for establishing a reference basis and standards for the description of morphology and longitudinal comparisons. Some examples are the Bolton Triangle (Broadbent 1937), Sella-Nasion and the anterior cranial base (Brodie 1941, Björk 1947), Ricketts (1981) and Downs (1948) indices, the Frankfort horizontal plane, the facial line (formed by points N-Po), and the facial angle (i.e. the angle formed by the facial line with the Frankfort horizontal - Ricketts 1961), amongst others.

While looking for the "normality" (or a standardized representation) with relation to landmarks, lines and angles, other important aspects also used for

characterizing shape, such as functionality and aesthetics, had to be considered when applying cephalometric methods.

With the widespread use of cephalometrics, a large number of landmarks and points of orientation have been suggested for comparison. Computer programs have been written that allow orthognatic surgical planning to be interactively performed on the computer screen (Bhatia 1984, Hussain 1988). However, even with the use of computer technology, investigations which aimed to take the different methods and test them against each other did not succeeded in arriving at an objective consensus (Ricketts 1981). Clinicians and researchers seem to maintain their own personal preferences.

General objections have been raised. Park and Burstone (1986) tested the efficacy of using a cephalometric dentoskeletal standard as a clinical tool to produce predictable facial aesthetics in a study on adolescent patients. Their results suggested that any given dentoskeletal standard has questionable validity in producing desirable aesthetics or reproducible profiles following treatment. Moyers (et al 1979) analyzed some of the problems and difficulties of conventional cephalometric methods, arguing that they fail to represent the dynamics of craniofacial growth and its physiologic changes. They proposed a different approach based on some new morphometric techniques (see Bookstein 1986).

3.5.3. Landmarks

Landmarks are at the core of the cephalometric analysis. Much of the work reported has consisted of an operator identifying and locating landmarks and then proceeding with the standard cephalometrical measurements.

One of the main objections to the use of landmarks has been that they cannot be located accurately and repeatedly. Both hard and soft tissue tracings present the observer with anatomical structures that are not so well defined, increasing the uncertainty on the part of the observer. This has been investigated by Carlson (1967), Gravely (et al 1974), Wisth (et al 1975) , Savara (et al 1966) and Cohen (1984).

Baumrind (et al 1971) demonstrates that the errors in landmark identification are too great to be ignored, even when replicating assessments of the same radiograph; and that the magnitude of errors varies considerably from landmark to landmark. There is a systematic error in determining the landmark locations, and the magnitude and distribution of the error is dependent on the feature. When considering the identification of facial features, Broadway's investigation (et al 1962) showed that the error between observers in deciding the location of a feature is greater than the error of an observer in locating the same feature on different occasions. Training and experience directly affects the level of errors involved.

The subjectivity of the human operator was also pointed out as the cause of errors in locating landmarks by Richardson (1966) and Cohen (et al 1984). They demonstrated that the reproducibility in locating landmarks has little or no gain with the use of high resolution digitizing tablets (typically 0.017 mm resolution) .

In addition, landmarks and their movement offer no information on the shape of the segments joining them (Bookstein 1978a).

3.6. Summary

In this chapter we have seen how the geometric properties of the human head and face have captured the imagination of scientists and artists for centuries. The need for a description of the face has lead to a number of systems of proportions, or canons, being developed, depending upon the motivation, knowledge and techniques used at the time.

The concept of beauty of male and female faces was originally suggested by the Greeks, when considering the relationship between various parts of the face.

Renaissance artists used similar ideas when developing their studies in painting. Some remarkable examples of Leonardo da Vinci's work on the proportions of the face were shown, including a system of classification of the nose according to its variation in shape. Other ideas found in Leonardo's work such as the

transformation of one face into another were explored even further by Albretch Dürer, who also worked on a facial canon.

The use of photography in methods of describing the face were also outlined showing that the chief application is identification, or recognition. Early ideas and techniques were dramatically improved with the use of computer systems. With the data on a digital format, fully automated methods of feature extraction form the basis of face identification systems. A number of computer based techniques, from image processing and pattern recognition, are used on such systems and were briefly presented, including techniques for the manipulation of surfaces, used in three-dimensional descriptions of the face.

When dealing with methods of analysis based on facial profiles, detailed descriptions were given of existing systems and techniques. Generally, these systems are based on the use of feature vectors, obtained using a set of characteristic points (or landmarks) on the profile (e.g. the tip of the nose), and then a description in terms of distances and angles between the landmarks.

Finally, the clinical view of describing the face was discussed. Anthropometric studies of the head and face are combined with cephalometric analysis and widely used in treatment planning and orthodontic diagnosis. These clinical analyses have at their core the use of landmarks. A large amount of clinical work has been reported on two dimensional studies of the midline profile only.

From the material presented and discussed in this chapter it is possible to identify the importance attached to the use of landmarks and its role in the overall analysis. Some objections that have been raised were presented. For landmark based methods, their limitation lies in the accuracy and repeatability with which the landmarks can be identified. Another important point to be made, with respect to reliability in measurement, is that such methods involve the individual's ability to locate a specified landmark, making the analysis highly subjective. Landmarks also fail to adequately describe the segments *in between* the points they define.

A solution to this problem is presented in this thesis, in the form of a method which uses multiscale techniques to automatically identify landmarks and describe the shape of segments between landmarks. This is described in detail in the next chapter.

Chapter Four

4. Method of Analysis

In this chapter, the methodology adopted in this work is described.

As we have seen in the previous chapter, although the world is three dimensional, there are important applications involving shape analysis defined within a two dimensional field. The image processing literature shows that representing two dimensional shape is one of the most challenging and least well understood areas (Brady 1983, Foley 1990). Although advances have been made, the problem is still receiving growing attention. Computerized recognition and vision systems still lay well behind human descriptive abilities which are often taken for granted.

Below, some basic requirements and criteria are discussed when considering the use of techniques for the mathematical description of the human face when represented by profiles. From these, a number of approaches are considered and evaluated, leading to the technique of scale space filtering and its particular application to planar curves. Based on the latter, the method developed in this thesis was derived. Some aspects of the implementation of this method are also discussed.

Finally, the method of acquiring and displaying 3D data of the face, which has been selected to generate the data sets used in this work, is described.

4.1. Basic Requirements

The face is a smooth continuous surface, full of subtle variations and nuances which are reflected in the profiles they generate. The importance of being able to identify and describe local features is immediately noticed, for example, when two profiles are compared for either clinical or recognition purposes. Small scale differences, changes on the nose or lips, for example, are usually more important than variations across the entire profile. Therefore, flexibility on describing both local and global features is

advantageous (e.g. through hierarchical approaches). The idea of a description that uniquely specifies the profile (as a “fingerprint” representation) is very attractive for both recognition and clinical applications.

The description should be simple, visual and correspond to the way we perceive the face (i.e. the nose is convex, the mouth concave, etc.). Qualitative and quantitative assessments should also be possible.

The method should be robust against noise and invariant under rotation, uniform scaling, and translation of the profile, otherwise, applications where reliable recognition or matching is needed will not be possible.

4.1.1. Landmark versus Curvature Methods

The use of landmarks in methods designed to describe two dimensional curves and to study facial profiles have been the subject of a number of criticisms, some of which were presented in the previous chapter. Mainly, their limitation lies in the accuracy and repeatability to which the landmarks can be identified; they rely on an individual’s ability to locate them (making the analysis highly subjective); landmarks and their movement offer no information on the shape of the segments joining them.

The identification and location of points or landmarks, however, is a very important issue specially in the analysis of facial profiles. They play an important role in segmenting the profile as a pre-cursor for analysis and that is the main point explored here. From research carried out by several workers (Broadway 1962, Cohen 1984, Richardson 1966, Moyers 1979) it may be assumed that a significant source of error is human subjectivity. Therefore, by automating the process of landmark location, the human subjectivity would be eliminated and hence play a definite part in producing more repeatable and reliable results.

Furthermore, in this work, the emphasis given is not so much in relative movements of landmarks as in the *changes in shape of the segments between the landmarks*. Shape representation and analysis is of fundamental importance and of the many approaches that have been proposed (see chapter 2), one of the most powerful

concepts that has emerged is the notion of curvature of planar curves (Levine 1985). Curvature represents a measure of the rate of change in orientation at each point along the curved path. Thus, a curve may be defined by the curvature values at all its points, for example in terms of regions of positive or negative curvature values. Singular curvature points themselves may be used to subdivide the curve into parts and, if necessary, characterize them in terms of features such as maxima, minima or inflection points.

There is a considerable research background that supports the use of curvature as a representation of curves or contours, from areas such as psychological, mathematical and computational sciences (Attneave 1954, Blakemore 1974, Hoffman 1984, many of which have been discussed on section 2.2).

Thus, in conclusion the following criteria have also been considered when assessing the methodology for analyzing facial profiles :

- a) the well recognized importance of curvature variation along the contour;
- b) the view of curvature as a result of processes acting on the shape;
- c) the use of metric information extracted from curvature analysis;
- d) use of curve segments bounded by perceptually relevant points.
(e.g. inflection points, maxima and minima of curvature).

4.2. Considering Different Techniques

Several techniques of shape representation may be judged by these criteria, and many of them have already been discussed in the previous chapters (see sections 2.2 and 3.2). For instance, chain coding (Freeman 1970) and polygonal approximations (Pavlidis 1977b, 1980) do not normally meet the criteria of invariance (rotation, scaling and translation) and are highly sensitive to noise. Single scalar quantities (Green 1970, Young 1974, Danielsson 1978) involve a substantial reduction in data, and do not uniquely specify a single curve. Fourier descriptors (Persoon 1977) and moment invariants (Teh 1980) compute only global features of the contours, meaning

that the shape distortions indicated by their coefficients (or low-order moments) cannot be locally identified.

The “codon” representation proposed by Hoffman (1982) satisfies the curvature criteria on segmenting the contour at minima of curvature. However, it works on a fixed scale sequence not reflecting the considerations of finer and coarse detail information, necessary for hierarchical descriptions. Although Rosin (1993) later overcame this difficulty, codon representations still fail to satisfy the requirement that small changes to part of the curve should create a small local change in the representation. Furthermore, the elements of the description, i.e. the codons, impose a rigid segmentation of the contour. These observations also apply to the “curvature primal sketch” technique introduced by Asada (1986), which uses only a limited number of well defined shapes that are approximated by analytical functions.

Although the last two approaches make use of scale space filtering techniques, as proposed by Witkin (1983), it is the approach developed by Mokhtarian (1986) that seems to satisfy most of the criteria listed above, and for this reason, was adopted in the methodology of this thesis.

There follows a more detailed description of the technique of scale space filtering, followed by Mokhtarian’s suggested approach.

4.3. Scale Space Filtering Techniques

In computer vision (and indeed in other fields related to automatic signal processing) considerable attention and effort has been dedicated when dealing with the basic problem of scale. The problem of scale relates to the fact that objects in the world (or details in images) only exist as “meaningful entities” over limited ranges of scale. An interesting example which demonstrates the importance of the concept of scale has been given by Lindeberg (1994) concerning the experimental sciences: “*The physical description depends strongly on the scale at which the world is modeled. In biology, the study of animals can only be performed over a certain range of coarse scales...an*

Method of Analysis

organism looks completely different seen through a microscope when individual cells become visible... ” .

These are well known qualitative aspects of scale which have, only during the past few decades, been formalized into a mathematical theory. The notion of scale in measured data may be translated in terms of the spatial extent of some neighborhood around the point of measurement, meaning that a local measurement depends on a *parameter of scale*. A number of researchers (Rosenfeld 1976, Ballard 1982, Witkin 1983) have argued that it is imperative to specify the scale of measurement in order to achieve any description, and that different scales yield different descriptions. Therefore, the question of which scale (or scales) is correct and how to organize them had to be addressed (see section 2.2.5 for further discussion).

A solution to this problem was suggested by Witkin (1983) using a methodology which represents the measured data at multiple scales. At that time, Witkin used in his examples a waveform, that is, a continuous one-dimensional *signal* varying along a time scale. Thus, for consistency reasons, the same notation will be considered in this section.

The way in which this multiscale representation of a signal is achieved is by generating an ordered set of derived signals where fine scale information is successively removed, with the idea of representing the original signal at different levels of scale (see figure 4-1). Such a set is also known as a “*one-parameter family*” of derived signals. This operation of systematically eliminating finer scale details is what Witkin called *Scale Space Filtering*.

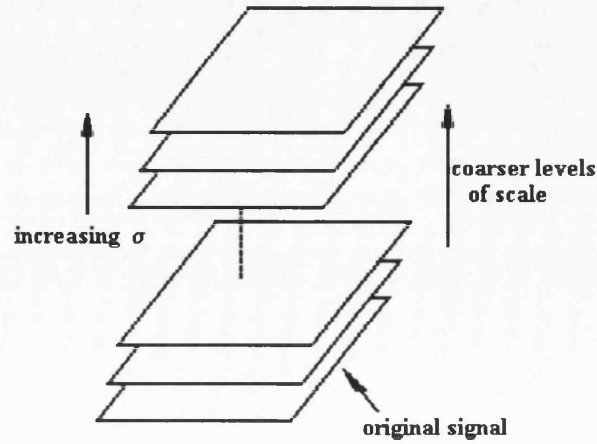


Figure 4-1 - Multiscale representation.

This figure shows an ordered set of derived signals (family), representing the original signal at different levels of scale (or detail). The scale parameter σ describes the current level of scale. (Adapted from Lindeberg 1993).

4.3.1. Scale Space Image

Formally, with a continuous signal $f(x)$ Witkin showed that it is possible to introduce a parameter of scale by smoothing the signal with a mask of variable size. This can be computed by a *convolution* process, where the mask used is a one-dimensional *gaussian function* of standard deviation σ as the *scale parameter*.

The convolution of the signal $f(x)$ with the gaussian function $G(x, \sigma)$ is given by :

$$F(x, \sigma) = f(x) * G(x, \sigma) = \int_{u=-\infty}^{u=+\infty} f(u) \cdot \frac{1}{\sigma\sqrt{2\pi}} \cdot e^{-\frac{(x-u)^2}{2\sigma^2}} du \quad (4-1)$$

$$G(x, \sigma) = \frac{1}{\sigma\sqrt{2\pi}} e^{-\frac{x^2}{2\sigma^2}} \quad (4-2)$$

where “ $*$ ” denotes convolution with respect to x .

Figure 4-2 illustrates a one parameter family of derived signals, the *scale space*, where each plotting describes the original signal at a different level of scale (or detail). The original signal, at the top, has been successively smoothed by convolution gaussian kernels of increasing values of σ .

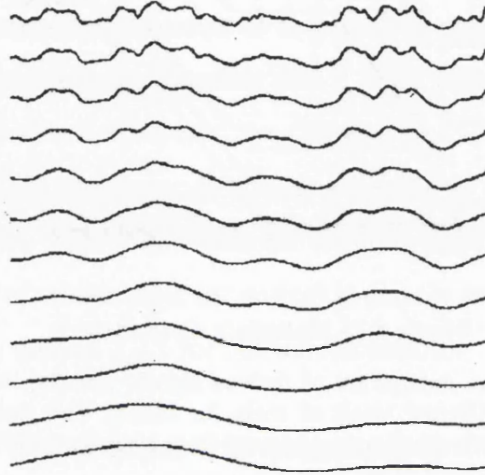


Figure 4-2 - Sequence of gaussian smoothings.

A sequence of gaussian smoothings of a signal, with σ increasing from top to bottom. Each plotting is a constant σ value. (Adapted from Witkin 1983).

Witkin called the function F , defined in the equation (4-1), the *scale space image* of f . Another way of visualizing the scale space image, as suggested by Witkin, is in terms of a surface, as illustrated in figure 4-3.

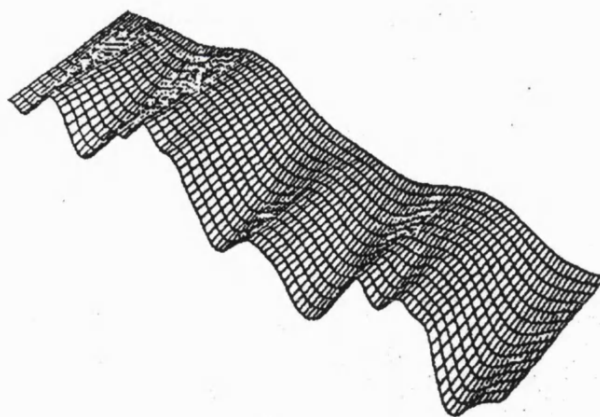


Figure 4-3 - Scale space image depicted as a surface.

The sequence of gaussian smoothings of figure 4-2, portrayed as a surface in perspective. (Adapted from Witkin 1986).

4.3.2. The Use of Gaussian Convolution

Witkin was mainly interested in observing the behavior of extrema and inflection points obtained when the signal was smoothed at nearby scales. However, he realized two fundamental points of the smoothing process when going from a finer to a coarser scale: (i) that fine scale features should disappear monotonically with increasing scale, and (ii) that artifacts should not be introduced by this process.

The gaussian is not the only convolution kernel used to compute a description that depends on scale. For example, Difference of Gaussians and Gabor functions have been used (see also Yuille et al 1983). However, a number of properties make the gaussian very attractive :

- a) the gaussian is symmetric and strictly decreasing about the mean, i.e. decreases smoothly with distance;
- b) the convolution behaves well near the limits of the scale parameter σ .
It approaches the original signal for small σ , and approaches the signal's mean for large σ ;
- c) the gaussian is readily differentiated and integrated;
- d) as σ decreases, additional zero crossings may appear, but existing ones cannot disappear. (Yuille et al 1983)

Babaud (et al 1986) have shown that the gaussian is the only convolution kernel guaranteed to satisfy all these criteria.

4.3.3. Qualitative Descriptions

Following the smoothing transformation, Witkin observed that the number of zero crossings in the second derivative decreased monotonically with scale, constituting a basic characteristic of the scale space image representation.

Method of Analysis

From the scale space description, two qualitative descriptions may be derived : the *zero crossing contours* and the *interval tree*.

4.3.3.1. The Zero Crossing Contours

At any fixed value of σ , the extrema of slope (or inflection points) are given by the zero crossings in the second derivative, computed using the relation :

$$\frac{\partial^2 F}{\partial x^2} = f^* \frac{\partial^2 G}{\partial x^2} \quad (4-3)$$

and satisfying the constraints :

$$\frac{\partial^2 F}{\partial x^2} = 0 \quad , \quad \frac{\partial^2 F}{\partial x^3} \neq 0 \quad (4-4)$$

These fixed scale zeroes, when computed through the range of scales, lie on *zero crossing contours*. As Witkin points out, a “*contour*” actually represents a *single arm* of an *arch* , and may be viewed as a zero crossing that moves continuously on the x-axis as σ is varied.

Thus, the zero crossing contour description is derived by finding all the inflection points at all values of σ . It represents a qualitative description of the structure of the signal over all scales, in terms of inflection points (see figure 4-4).

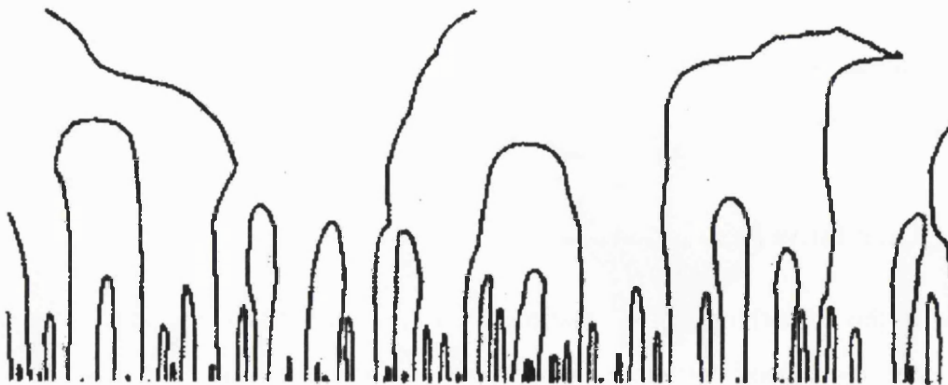


Figure 4-4 - The Scale Space Image description

Contours of zero crossings of the second derivative in the scale space image. They form paths across scales that may form arches. The vertical axis represents the scale with the coarsest value at the top. The horizontal axis represents the location of the inflection points along the signal. (Adapted from Witkin 1983).

Regarding the behavior of zero crossings, Yuille (et al 1983, 1983b) demonstrated that :

- a) two contours can merge into one closed contour as the scale parameter increases. This will form an *arch* , closed above but open below;
- b) a closed contour can split into two branches;
- c) considering an increasing σ value, no new zero crossings are created.

4.3.3.2. Feature Identity and Localization

Having established the scale space description, Witkin observed that there was a physical meaning attached to it, embedded in the zero crossing contours. He related a “*physical event*” (or “*something*” that created an inflection point) to each zero crossing contour, and assumed that when changing σ a small amount and smoothing the signal, the same events may be seen (broadly) at a different scale (instead of a new set of events).

As mentioned earlier, the contours in the scale space description mark the appearance and motion of inflection points as the signal is smoothed. The effects of smoothing, such as the removal of fine scale features, and the broadening and flattening of the features that persist, are also present on the zero crossing contours. The latter effect causes a spatial distortion which is undesirable when the location of points is necessary.

However, this may be overcome by tracking points at a coarse scale down to their fine scale location. Thus, in this “coarse-to-fine” tracking description, the coarse scale is used to **identify** inflection points, and the fine scale to **localize** them. According to Witkin, the *identification* is based on the fact that inflection points observed at different scales, but lying on a common zero crossing contour, arise from a single underlying physical event on the signal. The *localization* is based on the fact that the true location of an event giving rise to a zero crossing contour is the contour's x-axis location when the scale is at its minimum.

Method of Analysis

Therefore, coarse-to-fine tracking reduces each zero crossing contour to a pair of coordinates (x, σ) , specifying the fine scale location on the x-axis and the coarsest scale at which the contour disappears.

Yuille (et al 1983b) have shown that the zero crossing contour description may be seen as a *fingerprint*, i.e. a unique and complete representation of the signal.

4.3.3.3. The Interval Tree

Another important idea found in Witkin's work is concerned with the organization or grouping of the inflection points and the physical events they reflect, as seen in the zero crossing description.

Although symmetries and repetitions can be used as bases for grouping, Witkin suggested that *scale* be used to organize the zero crossing contours.

This is based on the fact that the zero crossing contours whose scales exceed a given value of σ , partition the x-axis into intervals. As σ is decreased, new zero crossing contours appear dividing the enclosing interval into sub-intervals, and so on until the finest used scale is reached.

In the scale space representation, each of the **intervals** above defines a **rectangle**, which according to Witkin's definition : “ *is bounded above by the scale at which the interval emerges out of an enclosing one, bounded below by the scale at which it splits into sub-intervals, and bounded on either side by the x-locations of the events that define it (i.e. the zero crossing contours)* ”.

This simplification allows the scale space image to be reduced to a simple hierarchical representation called the *interval tree*, illustrated in figure 4-5.

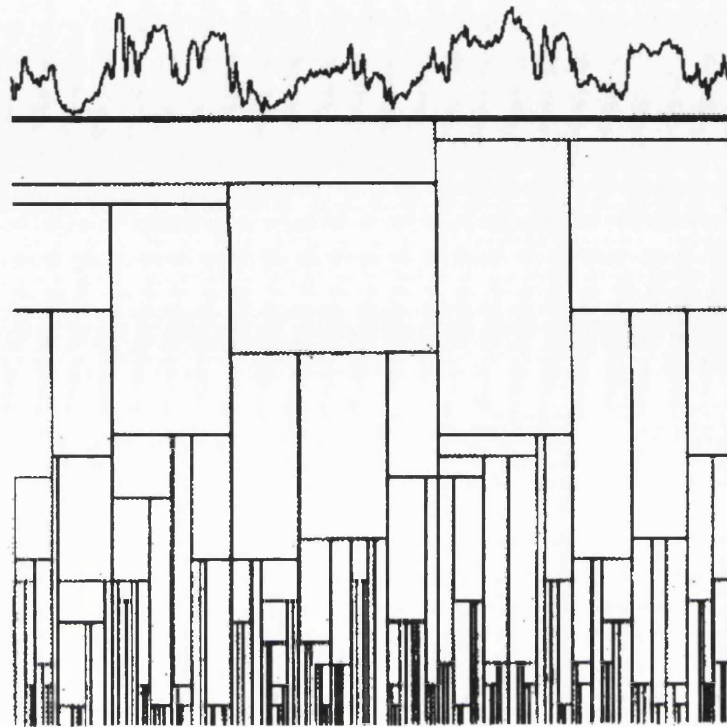


Figure 4-5 - The interval tree description.

The signal is shown at the top, which indicates the root of the tree. Each rectangle is a node indicating an interval on the signal (x-axis) and the scale range over which the interval exists (y-axis). (Adapted from Witkin 1983).

Each rectangle is a node on the tree, indicating the location and extent of a region on the signal, and the scale limits over which this region exists. The tree nodes may be classified as : (i) *parent node* : denoting the larger interval from which a node emerged; (ii) *offspring node* : denoting the smaller interval into which a node subdivides.

Furthermore, the extent of a node in the scale domain (i.e. the y-axis) is seen as its persistence or *stability*. Witkin empirically observed a strong correspondence between the stability of an interval on the tree and its perceptual salience on the signal (i.e. features that tend to leap out at the eye).

4.4. The Analysis of Planar Curves

Applying the scale space filtering techniques to the analysis of planar curves, Mokhtarian (et al 1986,1988,1992) showed that a scale space image can also be obtained.

Initially, they expressed the planar curve C in terms of two *parametric functions* $x(t)$ and $y(t)$, where t is a linear function of the path length ranging over the closed interval $[0,1]$:

$$C\{(x(t), y(t)) \mid t \in [0,1]\} \quad (4-5)$$

Then, they applied the concept of curvature of a planar curve. By definition, the curvature of a planar curve at a point P on the curve is the instantaneous rate of change of the slope angle ϕ of the tangent at point P with respect to the arc length S , and is equal to the inverse of the radius ρ of the *circle of curvature* at point P (also called osculating circle - Anton 1988). This is illustrated in figure 4-6:

$$k = \frac{d\phi}{ds} = \frac{1}{\rho} \quad (4-6)$$

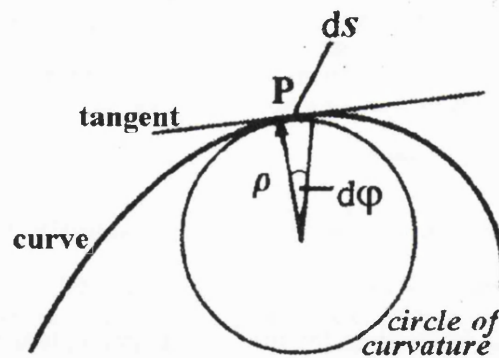


Figure 4-6 - The circle of curvature.

The curvature of the curve at the point P is equal to the inverse of the radius ρ of the circle at that point. The circle of curvature is also called 'osculating circle' because it has a higher degree of contact with the curve at point P than any other circle.

4.4.1. The Curvature Scale Space

The scale space image is derived by finding and combining inflection points on the curve at varying levels of detail. In this case the inflection points are defined when the curvature value is equal to zero (also known as zero crossings), and the levels of detail are obtained by convolving the parametric functions with a gaussian function of varying width (i.e. the scale parameter). This description is called *Curvature Scale Space*.

The curvature can be defined when expressed in terms of the derivatives of the functions $x(t)$ and $y(t)$, from the known expression (a detailed proof may be seen in Mokhtarian 1988) :

$$k = \frac{\frac{\partial^2 y}{\partial x^2}}{\left[1 + \left(\frac{\partial y}{\partial x}\right)^2\right]^{\frac{3}{2}}} \quad (4-7)$$

By denoting

$$\dot{x} = \frac{\partial x}{\partial t} ; \quad \dot{y} = \frac{\partial y}{\partial t} ; \quad \ddot{x} = \frac{\partial^2 x}{\partial t^2} ; \quad \ddot{y} = \frac{\partial^2 y}{\partial t^2} \quad (4-8)$$

the derivatives may be expressed as :

$$\frac{\partial y}{\partial x} = \frac{\dot{y}}{\dot{x}} ; \quad \frac{\partial^2 y}{\partial x^2} = \frac{\dot{x}\ddot{y} - \dot{y}\ddot{x}}{\dot{x}^3} \quad (4-9)$$

and the curvature of the curve may be expressed as :

$$k = \frac{\dot{x}\ddot{y} - \dot{y}\ddot{x}}{\left(\dot{x}^2 + \dot{y}^2\right)^{\frac{3}{2}}} \quad (4-10)$$

Method of Analysis

To compute the curvature of the curve represented at different scales, i.e. from a fine to a coarse level of detail, the parametric functions $x(t)$ and $y(t)$ are convolved with a one-dimensional Gaussian kernel $G(x,\sigma)$ of width σ , according to equations (4-1) and (4-2).

Thus, $X(t,\sigma)$, the gaussian smoothed function of $x(t)$ is then given by :

$$X(t,\sigma) = x(t)*G(t,\sigma) = \int_{u=-\infty}^{u=+\infty} x(u) \cdot \frac{1}{\sigma\sqrt{2\pi}} e^{-\frac{(t-u)^2}{2\sigma^2}} du \quad (4-11)$$

and likewise for $Y(t,\sigma)$.

Since any derivative of $X(t,\sigma)$ is equal to the convolution of $x(t)$ with a gaussian derivative of the same order, i.e.

$$\dot{X}(t,\sigma) = \frac{\partial X(t,\sigma)}{\partial t} = \frac{\partial [x(t)*G(t,\sigma)]}{\partial t} = x(t)*\left(\frac{\partial G(t,\sigma)}{\partial t}\right) \quad (4-12)$$

$$\ddot{X}(t,\sigma) = \frac{\partial^2 X(t,\sigma)}{\partial t^2} = x(t)*\left(\frac{\partial^2 G(t,\sigma)}{\partial t^2}\right) \quad (4-13)$$

the curvature at varying levels of detail is readily available by applying :

$$\ddot{X}(t,\sigma), \dot{Y}(t,\sigma), \ddot{X}(t,\sigma) \text{ and } \ddot{Y}(t,\sigma)$$

to equation (4-10), leading to :

$$k(t,\sigma) = \frac{\dot{X}(t,\sigma)\ddot{Y}(t,\sigma) - \dot{Y}(t,\sigma)\ddot{X}(t,\sigma)}{\left(\left(\dot{X}(t,\sigma)\right)^2 + \left(\dot{Y}(t,\sigma)\right)^2\right)^{\frac{3}{2}}} \quad (4-14)$$

Therefore, the implicit function defined by

$$k(t,\sigma) = 0 \quad (4-15)$$

is the *curvature scale space image* of the planar curve C .

Mokhtarian (et al 1988) have shown that some generalizations, observed in the one-dimensional case for the scale space image (see section 4.3.3), also hold in the two-dimensional case for the curvature scale space image.

Furthermore, Mokhtarian (et al 1988b and 1992) investigated the use of the curvature scale space description as a general purpose shape representation method for closed contours, and have shown that it satisfies a number of basic criteria, some of which are :

- a) Invariance : two curves with the same shape should yield the same representation. When the curve is translated, no changes are caused in the curvature scale space. The same uniform scaling applied to the curve is reflected in the curvature scale space. Rotation of the curve may be identified as a horizontal shift in the curvature scale space, which can be determined by matching the respective curvature scale space descriptions.
- b) Uniqueness : curves with different shape yield different curvature scale space descriptions, and that the planar curve may be reconstructed from its curvature scale space description.
- c) Stability : small changes in the shape of the curve are also reflected as a small change in its curvature scale space description and vice versa. Regarding this criterion, the authors have also shown that the curvature scale space description is stable when uniform and nonuniform noise is present on the curve.

Further illustrations on the curvature scale space are given in the next chapter, when the analysis of a facial profile is described.

4.5. Implementation

The techniques described above, compose the methodology developed in this work and have been translated into computer programs. The choice of hardware and software adopted for their implementation is now discussed.

The computational requirements when dealing with the processing of the face in three-dimensions are quite large. Great speed and graphics capabilities are very important elements of any basic computer system dedicated to that task. Although the work developed here fundamentally involves the processing of information in two-dimensions, those considerations are relevant in view of the methods of data acquisition and profile extraction adopted (these are later described). Moreover, at the division of Medical Graphics and Imaging a computer graphics workstation has been developed, consisting of a PC hosted Transputer network (Moss et al 1987,1989 ; Tan et al 1988,1991; Linney et al 1989,1991 ; Linney 1992). This makes use of parallel processing technology providing fast graphics display at a relative low cost. Amongst its features, the workstation allows the simulation of facial surgery.

Thus, the choice of hardware and programming language were essentially limited to those requirements and the available resources. It was natural then to use a compatible programming language so that the programs could eventually be included in that system. So, in this thesis, all the algorithms and routines were written in OCCAM2 and implemented on a PC Transputer based system.

4.5.1. Transputers and OCCAM2

Transputers are programmable VLSI (very large scale integration) devices, containing communication links for point-to-point inter-transputer connections. The system used here was a specialized unit called Xtram (Tektite 1989), consisting of basically a T800 Transputer module, an Intel 82786 graphics co-processor (with a drawing processor and a display processor) and 8 MBytes of memory. This compact unit was assembled on a PC half-card format board, and hosted by a PC compatible computer system .

OCCAM2 is a programming language designed to enable the Transputer to operate very efficiently. It is a high level language based on concurrency and communication of sequential processes. With OCCAM2, an application is designed and described in terms of an interconnected collection of independent processes, which communicate via point-to-point channels, and may be executed in parallel. The OCCAM2 programs are written and compiled using a Transputer integrated programming environment system (Transputer Development System), containing a text editor, file manager, compiler and a debugging system.

The Transputer, OCCAM2 and the Transputer Development System were designed by INMOS.

4.6. Data Acquisition

The main source of data utilized in this work will now be described. It provided the means of producing accurate measurements of the surface of the face, which were then used to generate a number of arbitrary cross section representations (i.e. facial profiles).

The possibility of using data sets that accurately represent the objects being measured, greatly improve their mathematical description. A number of data acquisition systems for the human body and face, based on three- and two-dimensional methods, have been developed and are commercially available (for a review see Karara 1989, Marshall 1992 and Marz 1993).

My natural choice was to use the system developed at University College London, an **optical surface scanner**, because of its excellent characteristics, easy access, and extensive clinical applications. Furthermore, it offered a data format compatibility that would enable the immediate access to a large database of faces, composed of normal and clinical subjects.

4.6.1. The UCL-MGI Optical Surface Scanner

The optical surface scanning system developed by the division of Medical Graphics and Imaging (MGI) of the Department of Medical Physics and Bioengineering, University College London (UCL) was the main source of data used in this work. The facial profiles were extracted from the surface data generated by this system.

The UCL-MGI system has been fully described by Arridge (et al 1985) and Moss (et al 1989), therefore, only a brief description is given here.

Figure 4-7 illustrates the current scanner set-up and its optical geometry. The basic configuration of the system consists of the following components: an optical bench (with camera, laser and mirrors), a rotating platform, and a PC compatible computer hosting a TV frame grabber and a transputer graphics interface .

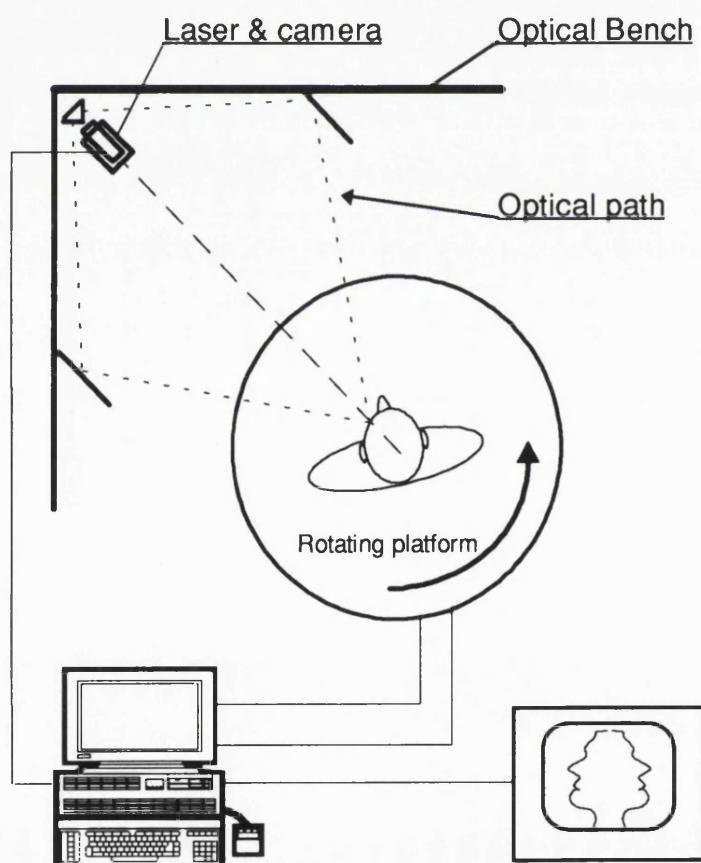


Figure 4-7 - Diagram of the UCL-MGI optical surface scanning system.

(Adapted from Linney et al 1993)

The system is based on the principle of triangulation. A vertical line is projected onto the patient's face by a cylindrical lens placed in front of a laser beam. As the line hits the face, it is distorted according to the shape of that particular surface. An arrangement of three special mirrors (one prismatic and two planar) enable a CCD (Charged Coupled Device) camera to view the vertical line from two oblique angles. The video signals from the camera are then pre-processed, digitized and recorded. This process is repeated as the platform, on which the subject's chair is mounted, is rotated under computer control, causing the laser line to illuminate the face at different positions.

Hence, the data produced are measurements of the radial distances r to the surface of the head from a vertical axis y through the center of the head for different angles θ in the horizontal plane (see figure 4-8).

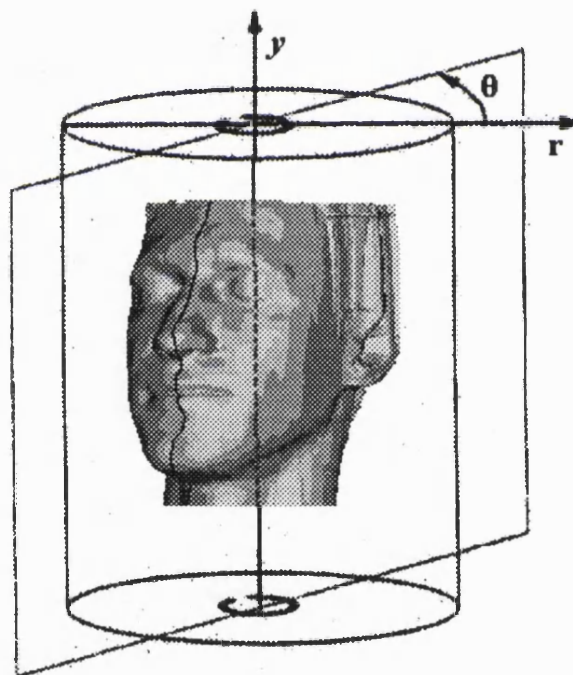


Figure 4-8 - The scanner's coordinate system.

The advantage of such specific optical arrangement is that simulates having two cameras viewing the laser line from either side, avoiding the occlusion of parts of the face, specially the alar base of the nose. However, some loss of data is expected

Method of Analysis

due to the high angle of incidence of areas under the chin and at the top of the head. Facial hair may produce undesirable artifacts as it may not reflect the laser light very well. These can be minimized by dusting the hair with white talc powder.

The speed of the platform being rotated and the scanning interval are adjustable by the operator. Typically, the laser line is recorded at every one degree of rotation. This faithfully records all facial features with a great level of detail. For a full face (approx. 225 degrees of rotation) 225 profiles are recorded. Alternatively, when greater level of detail is needed over a specific region of the face, as for example the ears or the region of the eyes, nose and mouth, the laser line may be recorded at every 0.5° of rotation. The number of points in each profile vary according to the amount of information collected by the camera (after considering the possible losses explained above).

Typically, when collected around the middle part of the face, the profiles contain up to 300 points. The entire scanning takes, on average, fifteen seconds.

The acquired data are stored in computer memory, and later transferred, in a compressed format, into computer files of an average size of 110 Kbytes. From this data, approximately 20,000 three dimensional coordinates (i.e. x, y and z values) on the facial surface may be derived.

The calibration and accuracy of the system has been investigated by Moss (et al 1989). Single profiles can be recorded with a radial spatial resolution better than 0.5 mm, and vertical resolution better than 1.0 mm .

4.7. Data Visualization

The visualization of both two- and three-dimensional information are handled by the Transputer graphics interface. The former is described in more detail in the next chapter.

In the case of the optical surface scan data sets, the technique used applies two well known methods of the computer literature: the Delaunay triangulation (Fuchs et

al 1977, Boissonnat 1985) and the Gouraud surface rendering (Gouraud 1971). The method of Delaunay triangulation is used to generate a patchwork of triangles, named facets, from the stored data.

A three dimensional model of the face can be obtained by shading these facets according to their illumination by a notional light source which may be positioned at any angle (Gouraud method). This rendered image is produced in a few seconds and then displayed on a monitor (see figure 4-9).

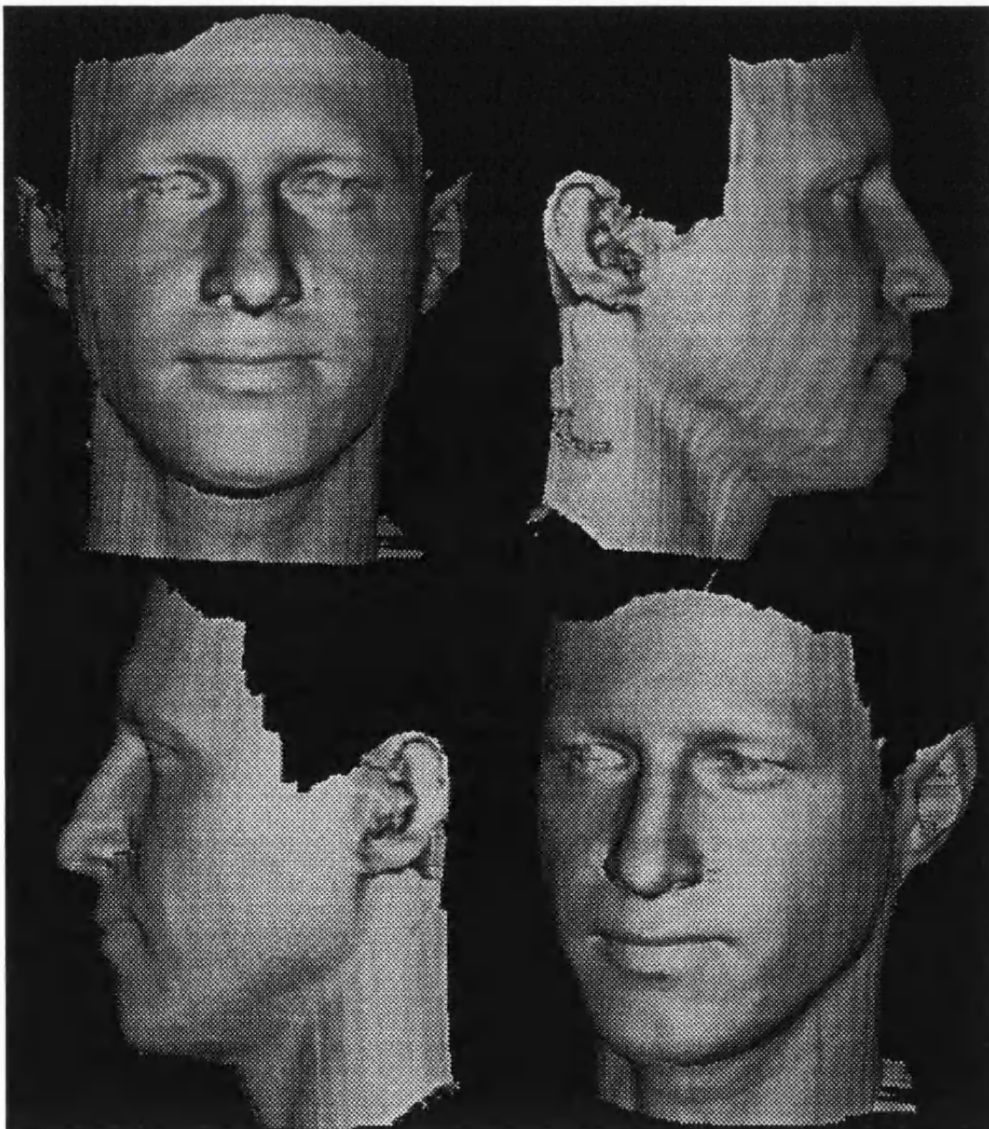


Figure 4-9 - A typical display of the optical surface scan data.

Illustration of rendered surface images displayed in different views: frontal (top left), left (top right), right (bottom left) and general (bottom right).

4.8. Summary

The basic requirements for the description of the shape of the facial profiles were discussed in this chapter. The use of landmark and curvature based approaches were considered and evaluated, pointing out some important aspects of the methodology here proposed: (i) the role played by the identification and location of landmarks in segmenting the profile as a pre-cursor for analysis; (ii) an automatic process of locating landmarks reducing the overall error by eliminating the subjectivity error; (iii) the emphasis given to the changes in shape of the segments between the landmarks rather than their relative movements. Consequently, some criteria have been based on the notion of curvature of planar curves, shown to be one of the most powerful concepts for shape representation.

It has been shown that the technique of scale space filtering and its particular application to planar curves meets a set of requirements for facial profile analysis. The advantage of using scale space filtering is that the inflection points (and/or extrema points) corresponding to a single physical event or profile feature, such as the nose for example, observed through a continuum of scales produces a unified description, rather than an unrelated set of points. When this description is organized by scale, a representation that is appropriate for the segmentation of the profile may be derived. By using inflection points, it is possible to naturally partition the profile into a number of convex and concave curve segments. Because this technique has been adopted as the method developed in this thesis, their complete description was also given.

These techniques have been implemented on a Transputer-based PC system, which has benefits in terms of hardware and software.

Finally, the method of data acquisition utilized as the main source of data in this work was described. It is an optical surface scanner, based on the principle that the distortion of a single line of light which is projected onto the surface of the object, and viewed by a camera placed at an oblique angle, may be used to compute the surface geometry. The “scanning” then takes place by “sweeping” the line over the desired area of the object. This method provides the means of producing accurate

measurements of the surface of the face, which are then used to generate a number of arbitrary cross section representations (i.e. facial profiles).

In the next chapter, the shape description technique based on planar curves is applied to the analysis of facial profiles.

Chapter Five

5. Analyzing Facial Profiles

In this chapter we will explore the analysis of facial profiles based on the methodology discussed in the previous chapter.

The analysis of profiles involves basically the use of methods of description, segmentation and classification of profiles. Each one of these stages, within the analysis process, are presented and discussed.

The main source of data used in this work was the three-dimensional data sets generated by the optical surface scanner. A method of extracting two-dimensional cross sections from these data sets has been developed and is described.

Some basic considerations are also presented concerning the parametric curve representations, sampling and the computation aspects of the convolution process. These constitute important elements for achieving the qualitative and quantitative forms of describing the facial profiles.

Following that, the qualitative descriptions are presented and illustrated for vertical and horizontal profiles. By using such descriptions, it is shown that the profile may be repeatedly and reliably divided into a number of segments. The concept of curvature is then applied to produce different and meaningful ways of quantitatively describing the various profile segments.

Finally, a number of experiments were designed to evaluate the method and are reported here.

5.1. Outline of Analysis

Figure 5-1 is a block diagram illustrating the flow of the analysis.

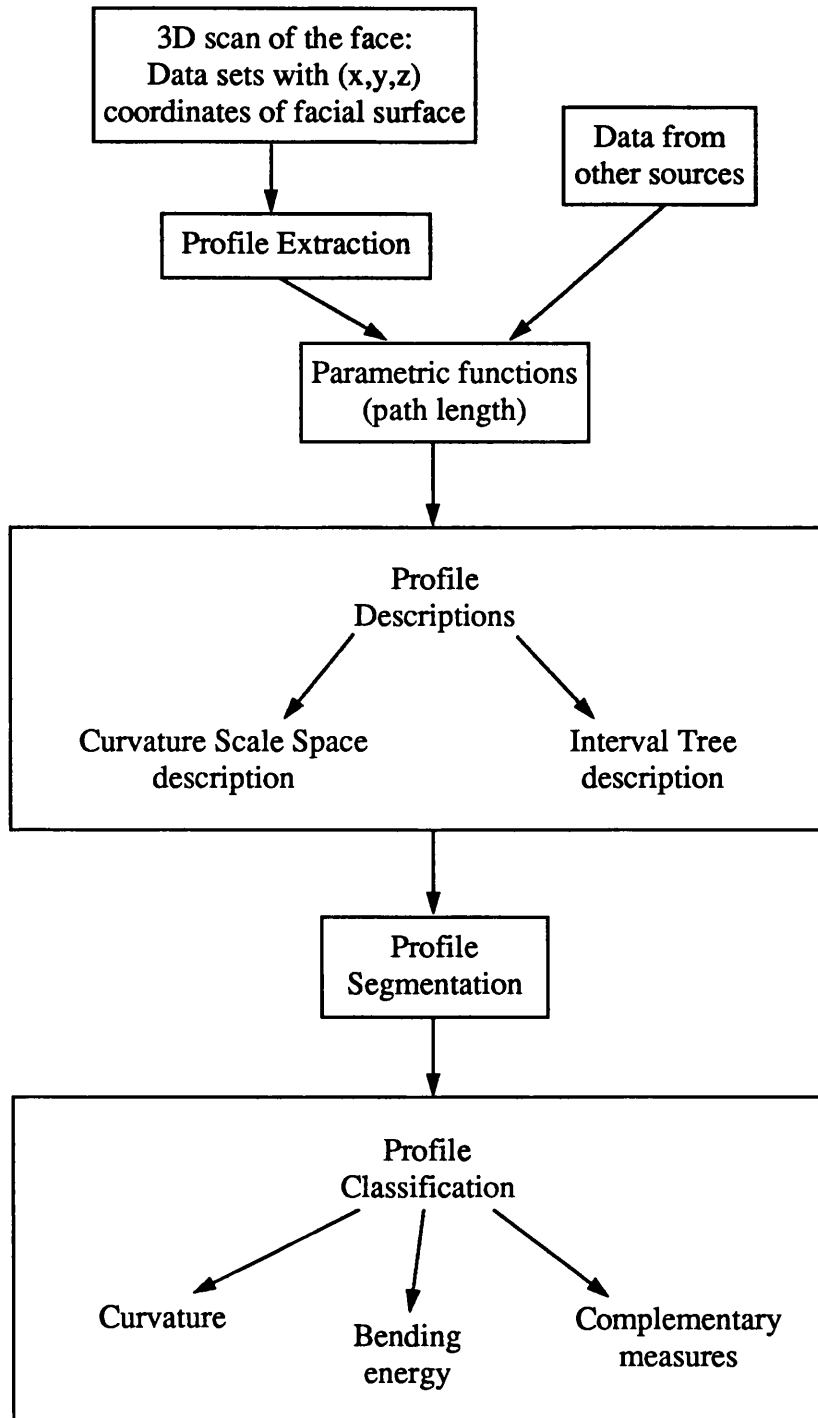


Figure 5-1- Block diagram of analysis of human facial profiles.

5.2. Discrete Representations of Continuous Curves

When the face is converted to a digital format, only a set of discrete points in space are defined, based on a frame of reference or grid. From this *sampling* and *digitization* process, the images generated are in fact only a discrete approximation to the underlying continuous surface, that is the real perceived face.

The digital contours or facial outlines derived from this data set are actually a subset of coordinates in a two dimensional grid. The process in which the facial profiles are extracted is described below.

5.3. Extraction of Facial Profiles

Once the face has been scanned, a computer file of surface profiles is created. From this file, the (x,y,z) coordinate points of the surface of the face are computed. Triangular facets may be defined between triplets of points to represent the facial surface, and displayed using a rendering technique (see section 4.7). The coordinate system adopted for the graphics display routines is illustrated in figure 5-2, where the **x**-axis represents the width, the **y**-axis represents the height and **z**-axis represents the depth.

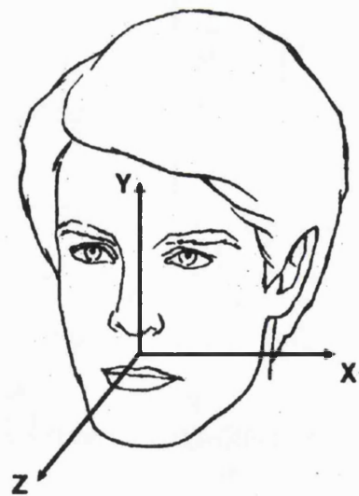


Figure 5-2 - Coordinate system of the graphics display.

Any cross section (profile) may then be extracted as follows : a shaded surface is generated representing a particular orientation of the head, for example the anterior view. A mouse driven cursor is provided to the user, selecting points on the facial surface. The cursor, however, moves in the screen plane instead of moving over the facial surface. At any cursor position, two perpendicular profiles are generated, which are simultaneously displayed on the screen. Considering the coordinate system above, it is easy to see that *vertical profiles* are values of z and y for a constant value of x , and that *horizontal profiles* are values of z and x for a constant value of y . In both cases, the typical distance between profile points is one millimeter (the sampling is further discussed below).

Figure 5-3 illustrates this process. With the face displayed in anterior view, the cursor (seen as a cross shaped mark) is positioned around the tip of the nose, generating both the vertical profile, plotted on the right hand side, and the horizontal profile, plotted at the top, partially overlapping with the image of the face. If desired, computer files are created, one for each profile, storing their coordinate values in text format.



Figure 5-3 - Extraction of facial profiles.

The black dots, representing the cross shaped cursor, moves over the shaded surface of the face generating both horizontal (top) and vertical (right) profiles.

Likewise, an *oblique profile* may be achieved by obliquely aligning the face on the screen.

Therefore, a direct relationship between the defined profiles (represented in two-dimensions) and the surface of the face (represented in three-dimensions) may be established.

5.4. Parametric Curve Representation

As a planar curve representation, facial profiles are seen to be composed of a sequence of convex and concave curve segments. Within the context of the methodology established in this work, the idea is to mathematically describe these curves and their properties such as curvature. In order to achieve this, some fundamental concepts of differential geometry are used (some of which have already been discussed in the previous sections).

The parametric representation is a way of mathematically describing a curve. It is usually applied in combination with other mathematical tools in order to study and describe the geometric properties of the curve. There are several distinct parametric representations for a planar curve (for an overview see Farin 1993). However, it has been suggested (Mokhtarian 1992) that a *natural* parametrization of the curve may be achieved when the parameter used is the *arc length*.

More specifically, through parametrization a path can be determined by taking discrete steps (or samples) along the length of the curve. Considering the nature of the convolution process and the properties of the gaussian function (discussed later in this chapter), it is necessary to adopt uniform samples at regular, small intervals.

The parametrization is computed as follows: let us consider that the curve S , representing a facial profile, is defined by a set of points with coordinate values $X[i]$ and $Y[i]$, for $i=1,2,\dots,n$. From these values, the length along the curve, denoted by $L[i]$, is defined by the sum of the Euclidean distances calculated between every two

consecutive points, i.e.

$$L[i] = \sum_{i=1}^{n-1} \left((X[i+1] - X[i])^2 + (Y[i+1] - Y[i])^2 \right)^{\frac{1}{2}} \quad (5-1)$$

for $i=1,2,\dots,(n-1)$, so that $L[0] = 0$ and the total length is given by $L[n-1]$.

A parametric representation of the curve S may be achieved when following the “path” along the length of the curve (see figure 5-4).

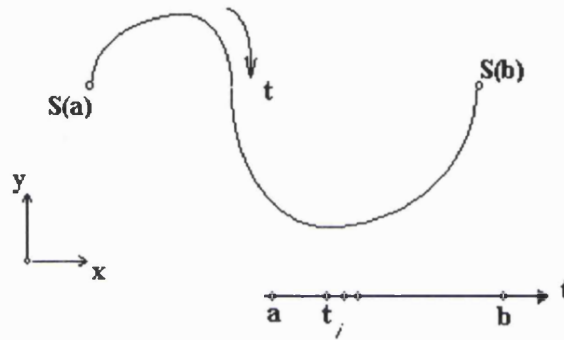


Figure 5-4 - The parametric representation following the path length parameter (t).

The curve S may be described as a parametric representation using the path length (t) along the curve. (Adapted from Farin 1993).

The “arc length” parametrization of the curve (as it is called) is expressed by $X[t_j]$ and $Y[t_j]$, for $j=1,2,\dots,np$. The values of $X[t_j]$ are computed by the equation :

$$\frac{X[t_j] - X[i]}{X[i+1] - X[i]} = \frac{\Delta t - L[i]}{L[i+1] - L[i]} \quad (5-2)$$

and likewise for $Y[t_j]$. The variable Δt is an equidistant partition of the t -axis determined by :

$$\Delta t = \frac{L[n-1]}{n} \quad (5-3)$$

Analyzing Facial Profiles

The array $T[t_j] = L[1] + j\Delta t$, where $t_j = j\Delta t$, containing the path length values is also computed and used for further processing.

Following Mokhtarian's approach, the path length is normalized by the total length of the curve, so that it will range over the interval 0 and 1 (denoted by $[0,1]$). Figure 5-5 illustrates a vertical profile outline and its parametric curve representations.

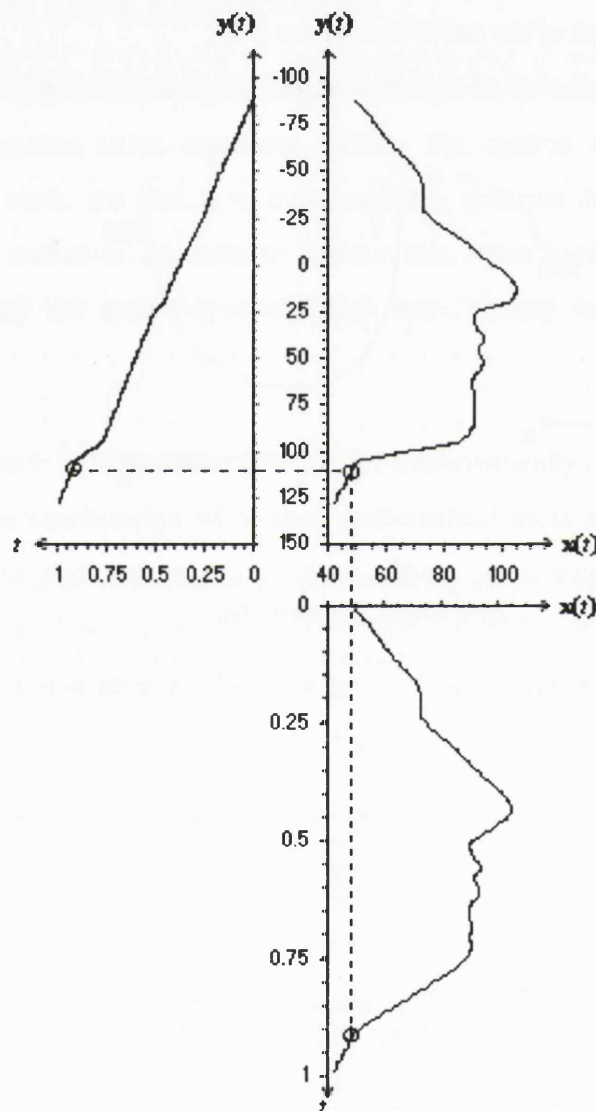


Figure 5-5 - The vertical profile outline and its parametric representations.

The vertical profile is given by the (x, y) coordinate values, which are then parametrized following the path length parameter t over the interval $[0,1]$. The dotted lines show the correspondence between the points on the (x, y) plot and the (x, t) and (t, y) plots.

5.5. Sampling Considerations

When computing this parametric representation of the curve it is important to take into account the effects of sampling nonuniformity and resampling. Due to the characteristics of the standard two dimensional square grid used (see description of the optical surface scanner - section 4.6.1), the spacing between two neighboring points is not necessarily constant. Generally, the distance between the successive points on a squared grid with a spacing h may assume one of two values, h or $h(2)^{1/2}$. In practice, the result of the digitized version of any curve may be thought as a string of points that are linked along one of four orientations: horizontal, vertical, and the 45° and 135° diagonals. Thus, the actual sampling distance varies along the digitized curve or contour.

Shahraray (1985) and Duncan (1991), when studying the nonuniformity of the sampling interval, observed that for many purposes this difference in actual sampling distance should be removed by *resampling* the discrete contour.

Hence, in order to minimize sampling nonuniformity, the arrays $X[t_j]$ and $Y[t_j]$ are *resampled* along the path length with equal spacing h' as:

$$h' = \frac{\sum_{j=1}^{NP} \left\{ \left(X[t_j + 1] - X[t_j] \right)^2 + \left(Y[t_j + 1] - Y[t_j] \right)^2 \right\}^{1/2}}{NP} \quad (5-4)$$

where $X[t_j]$ and $Y[t_j]$ are the parametric representations of the curve (as determined by the equation 5-2) and NP is the resampling parameter. The new resampled array $X'[k]$ is given by the following relation:

$$\frac{X'[k] - X[t_j]}{X[t_j + 1] - X[t_j]} = \frac{h' - T[t_j]}{T[t_j + 1] - T[t_j]} \quad (5-5)$$

and likewise for $Y'[k]$, for $k=1,2,...,NP$.

The resampling is graphically illustrated in figure 5-6, showing the results on a contour segment.

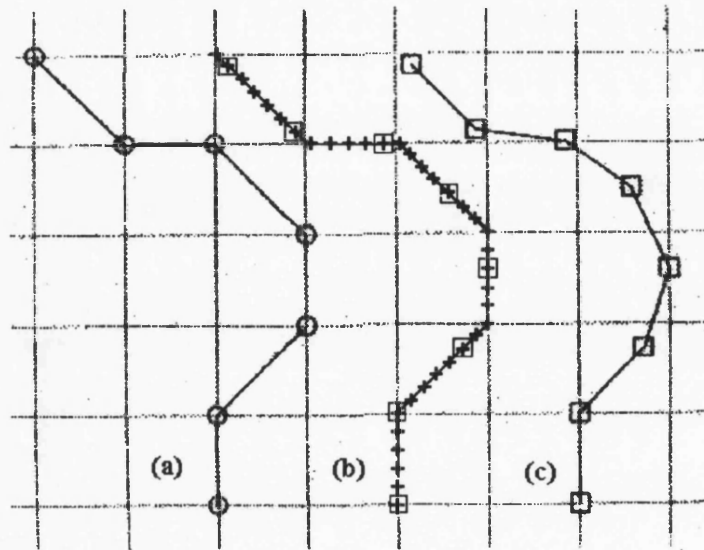


Figure 5-6 - The result of resampling a discrete contour segment.

(a) original digitized curve and points (circles) ; (b) result of parametrization where intermediate interpolated values are obtained (crosses) ; (c) the final resampled discrete curve and points (squares). (Adapted from Shahraray 1985).

From equation (5-4) we observe that the smaller the resampling parameter NP is, the bigger the spacing between profile points will be, resulting in a poorer representation of the existing facial features. An ideal selection of the resampling interval is provided by the Nyquist theorem, which says that the original curve can be perfectly recovered (i.e. digitized) if the sample rate is set to a value greater than twice the highest spatial frequency of interest along the curve (i.e. the most abruptly curving feature). In practical terms this means that if a particular feature of the profile is to be digitized, it must be sampled in such a way that at least two of the sample elements will fall upon the feature itself.

For our purposes, the resampling parameter is set to a fixed value, so that the resulting resampled profiles may be compared with each other. When measuring the face, especially for clinical applications, it is important that facial features are represented with as much detail as possible. In our case, the extracted profiles may

contain up to 300 points. Having experimented with different values, it has been decided to adopt $NP = 250$ when resampling the profiles for further analysis.

The effect of the resampling parameter NP is illustrated in figure 5-7, for a vertical profile outline.

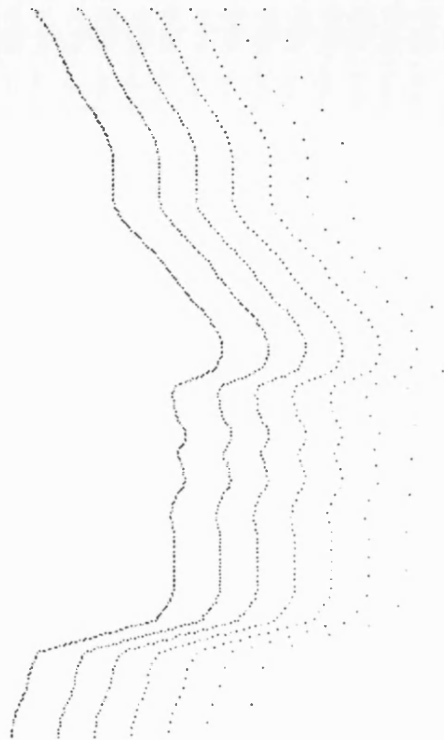


Figure 5-7 - Resampling the profiles with different spacing intervals.

This figure illustrates the effect of the resampling parameter NP . The original profile is on the left with $NP = 314$, followed by six resampled versions with $NP = 250, 200, 150, 100, 50$ and 25 , respectively.

5.6. Computing the Convolution

Before presenting how the quantitative descriptions are derived, it is important to discuss first the algorithm implemented to compute the convolution between two functions.

An initial distinction to be made is between two basic types of signals : the *continuous signals*, where the signal is defined for a continuum of values of the independent variable, and the *discrete signals*, where the signal is defined only for a

discrete set of values of the independent variable. In this context, *signals* are used to describe a wide variety of physical phenomena and are mathematically represented as a function of one or more independent variables, for example, voltage as a function of time.

The convolution process, as defined by the expression (4-1), assumes that one is dealing with continuous signals. For situations where the signal is discrete, however, the implementation to be performed computationally follows the numerical method given by the equation below (W. Press et al 1978) :

$$H_j = (R * V)_j = \sum_{i=-M/2+1}^{i=M/2} V_{j-i} \cdot R_i \quad (5-6)$$

In equation (5-6) the convolution integral of equation (4-1) is computed as a sum, which produces reasonable approximations to the continuous numerical values (Lindeberg 1994). The function denoted by V represents the discretized signal. The other function R , the convolution mask, typically a peaked function of finite length M , that falls to zero in both directions from its maximum. Moreover, the convolution of two functions, denoted by $(R * V)$, is mathematically equal to their convolution in the opposite order, i.e. $(V * R)$.

W. Press gives a clear graphical interpretation of the convolution process: “ *the effect of the convolution is to smear the signal V according to the recipe provided by the response function R* ”. This is illustrated in figure 5-8.

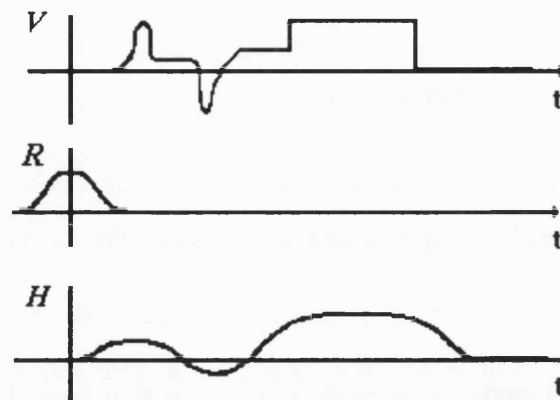


Figure 5-8 - Example of the convolution of two functions.

A discrete signal $V(t)$ is convolved with a response function $R(t)$, yielding the output $H(t)$.
(Adapted from Press 1978).

Equation (5-6) may be re-written using one of the parametric representations, for example $X'[k]$, and the discrete gaussian kernel $G(i,\sigma)$, resulting :

$$XG_k = (X' * G)_k = \sum_{i=-M/2+1}^{i=M/2} X'_{k-i} \cdot G(i,\sigma) \quad (5-7)$$

and likewise for YG_k .

Because we are dealing with open curves, a way must be found to compute the convolution values for points where part of the mask extends beyond the end of the curve. This is achieved by setting up a “buffer zone” at the beginning and end of both parametric representations.

Following this approach, a number of possible solutions have been reported (Mokhtarian 1986, Rosin 1992). In this work, two methods were tested using profile outlines. The aim was to evaluate the effect of this “buffer padding” procedure on the final result of the convolution process.

Using the first method, the curve is treated as *constant* beyond the boundary points, i.e. from the parametric representation $X'[k]$ for $k = 1, 2, \dots, NP$, the padded values are :

$$\begin{aligned} PX_u &= X'[1] & \text{for} & \quad -M/2 \leq u < 1 \quad \text{and} \\ PX_u &= X'[NP] & \text{for} & \quad NP < u \leq (NP+M/2) . \end{aligned}$$

Using the second method, the curve is extended at each end by *duplicating and reflecting* the curve points. This is done by reflecting about the straight line drawn from the end point to the previous $M/2$ th point and then reflecting again about the normal to that line at the curve end point. So, for $X'[k]$ above, the padded values are :

$$\begin{aligned} PX_u &= ((-1.0 * (X'[(M/2+1)+u] - X'[1])) + X'[1]) & \text{for} & \quad -M/2 \leq u < 0 , \quad \text{and} \\ PX_u &= ((-1.0 * (X'[u-1] - X'[NP-1])) + X'[NP-1]) & \text{for} & \quad NP < u \leq (NP+M/2) . \end{aligned}$$

The two methods are illustrated below (figure 5-9). Because they are applied in exactly the same manner for both ends of the curve, only one end of the curve is used in this illustration as shown on 5-9(a). Figure 5-9(b) represents the first method and 5-9(c) the second method.

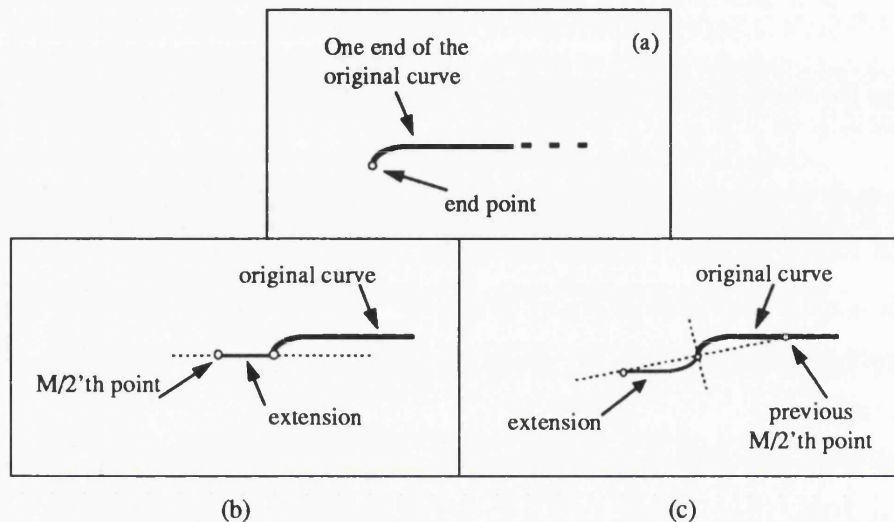


Figure 5-9 - Buffer padding methods.

On these diagrams only one end of the curve is shown, as illustrated on (a). They illustrate the methods of extending the curve (at each end) with $M/2$ points by : (b) repeating boundary points and (c) duplication and reflection.

A comparison of the effects of the two methods is shown in figure 5-10. On (a) and (b), the original curve is represented by the thicker outline, which after being extended by either method and smoothed, is represented by the normal thin outline. Figure 5-10(a) shows the result when using the first method, and 5-10(b) when using the second method. Notice how the curve's end point on 5-10(a) has moved to the right, whereas on 5-10(b) it maintained the same position. On figure 5-10(c) the entire curve has been used. The curve was extended, on both ends, using each method and then smoothed over a range of values, every one producing a different outline. To highlight the differences of each method, the curves were displayed close to each other, in pairs. For each smoothed outline, the result of the first method is displayed on the left, and result of the second method is displayed on the right. The differences may be seen on both extremities of each curve.

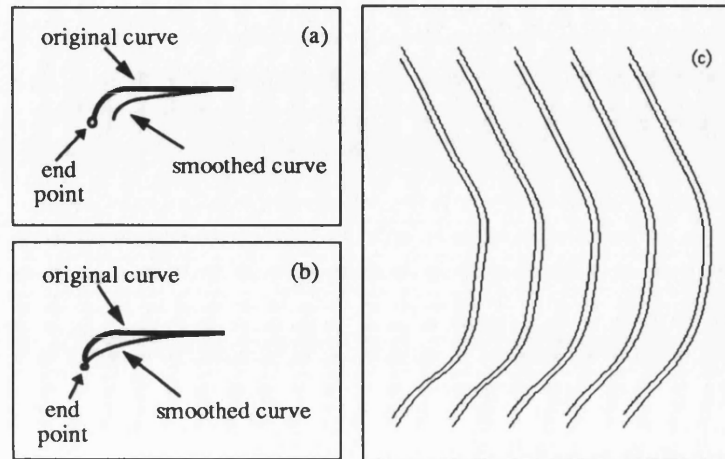


Figure 5-10 - Comparison of curve extension methods

Partial view of the original curve (thick outline) and the result of smoothing (thin outline) when the end points are extended by (a) first method and (b) second method. On (c) the entire outline is used to show the effect of the two methods. The difference is observed on both ends of the curve for a range of smoothed outlines.

If any of the above methods is consistently applied, the results for similar curves will be similar. However, the second method preserves the location of the curve end points which is advantageous when handling the smoothing effects caused by the convolution process (i.e. broadening and flattening). Furthermore, the method is robust and easy to implement. For these reasons, this method was adopted in this work to handle the curve end points.

To determine the value of M (equation 5-7), it is necessary to look at the behavior of the convolution kernel, that is the gaussian function. The gaussian kernel is defined over an infinite range but can be safely truncated at a fixed distance from its center.

In the literature, very few authors state the values used in their methods. Lowe (1988), for example, suggested this distance to be 3σ , a multiple of the scale value σ , and this has been followed by other workers (Rosin 1993, Worring 1993). However, when experimenting with low values of σ (e.g. 1 or 2), the results showed that the distance of 3σ does not produce a satisfactory approximation of the kernel, specially those of the derivatives. Consequently, the result of the convolution process and the computation of the zero crossings are affected.

For truncations greater in width than 3σ , a satisfactory approximation of the kernel (and of the derivatives) is produced, regardless the values of σ used (i.e. low or high).

This is illustrated in figure 5-11(I), for $\sigma = 1$. Distances of 3σ , 5σ , 8σ and 10σ were used and are indicated by the characters (a), (b), (c) and (d), respectively. The gaussian and its first and second derivatives are labeled G, DG and D2G. A close observation of (a) shows how the truncation by 3σ affects the approximation of the derivatives DG and D2G. Figure 5-11(II) illustrates a good approximation of the gaussian and that of its derivatives. When comparing the curves on figures 5-11(II) and (I), a better approximation for all three functions is observed on either approximations represented by (b), (c) or (d).

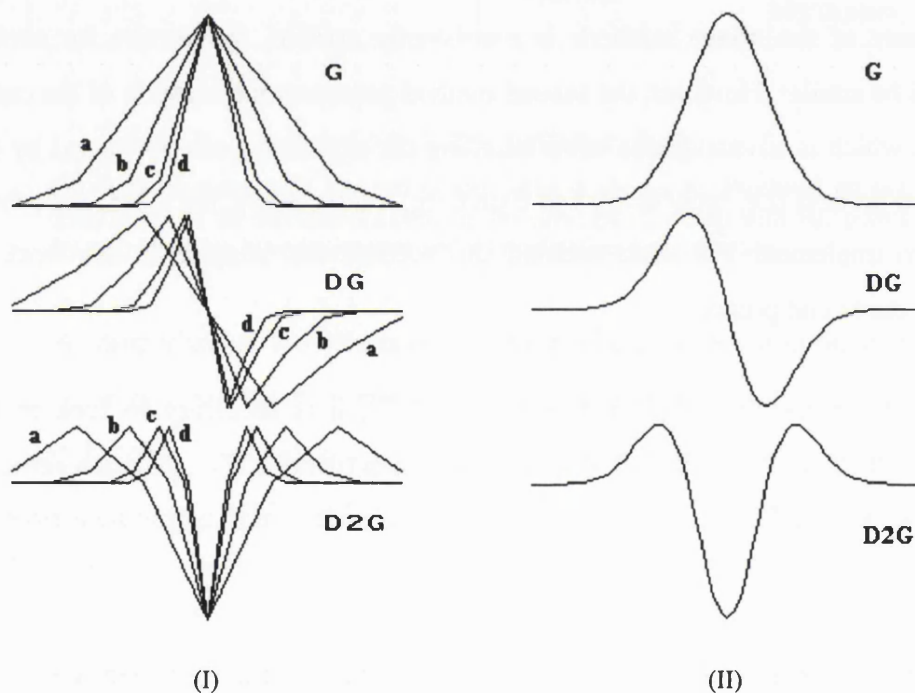


Figure 5-11 - The truncation effect on the gaussian kernel (and derivatives).

The discrete approximations of the gaussian and of its first and second derivatives are indicated by G, DG and D2G. On (I), they were truncated, from their center, with the fixed distances of 3σ , 5σ , 8σ and 10σ (for $\sigma = 1$) yielding the approximations indicated by (a), (b), (c), and (d), respectively. A good approximation of all functions is illustrated on (II) .

Because low values of σ are always included in the computation of the qualitative descriptions to be derived, the value of 5σ is adopted here, yielding a

satisfactory discrete approximation. The discrete gaussian kernel is given by the equation (5-8) with $m = 5$:

$$G(i, \sigma) = \left(\frac{1}{\sigma \sqrt{2\pi}} e^{-i^2 / 2\sigma^2} \right)_{i=-M/2, M/2}, \frac{M}{2} = m\sigma \quad (5-8)$$

The importance of the shape of the derivatives of the kernel has also been observed by Worring (1993).

5.7. Qualitative Descriptions

The next step in the analysis is to derive the qualitative descriptions, through scale space filtering techniques, as discussed in the previous chapter. They are the *curvature scale space* and the *interval tree*.

By itself, each one fully describes the planar curve that represents a given facial profile, and may be explored as such. In addition, they provide a reproducible and objective basis for a natural segmentation of the profile.

In the illustrations presented below, two profiles are used as examples, extracted midway across the face in the vertical and horizontal directions.

5.7.1. Curvature Scale Space

The curvature scale space description is derived by finding and combining inflection points on the curve at varying levels of detail. The inflection points (or zero crossings) are computed from the curvature values, given by equation (4-14), and the levels of detail are obtained by convolving the curve with the gaussian function, using an increasing scale parameter (for further discussion see section 4.3.3.1).

Analyzing Facial Profiles: Qualitative Descriptions

The figures 5-12 and 5-13 shows a sequence of profiles produced by gaussian convolution, illustrating the smoothing effect, that is the broadening and flattening of the facial features. The scale parameter increases between each profile by a factor of two, ranging from a fine scale (equal to one) to a coarse scale (equal to nineteen). The fine scale is on the left hand for figure 5-12, and at the bottom for figure 5-13.

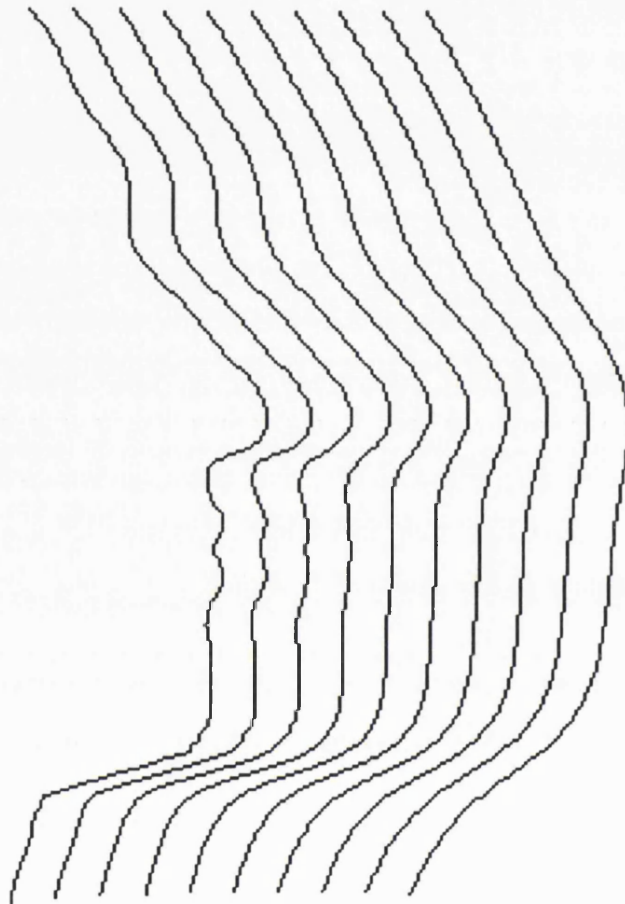


Figure 5-12 - Sequence of smoothed vertical profiles.

The degree of smoothing is determined by the width of the gaussian mask (scale parameter). The scale parameter is increasing from left to right, ranging from a fine (equal to one) to a coarse scale value (equal to nineteen).

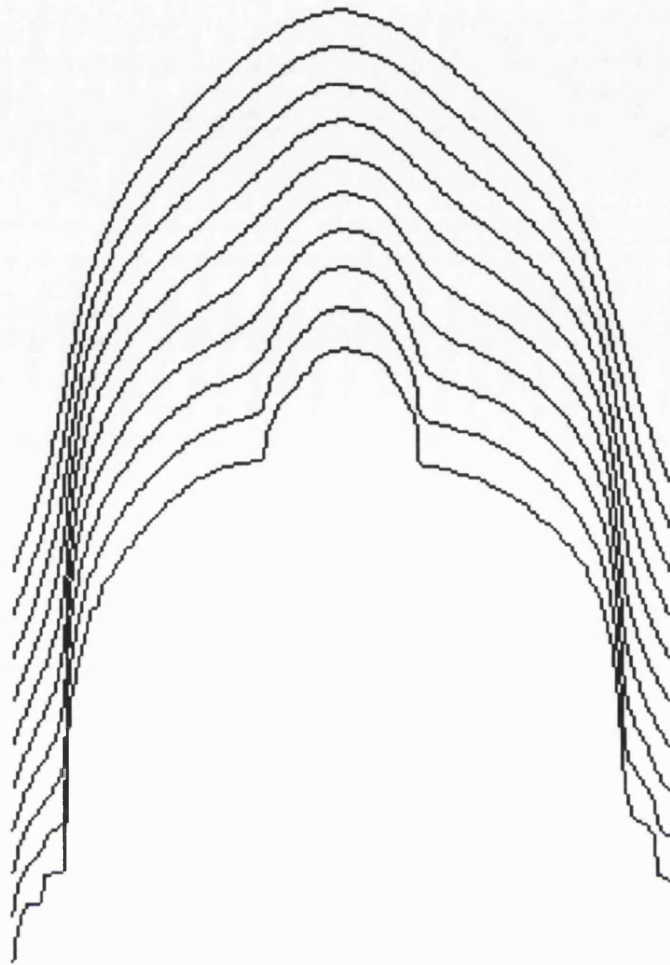


Figure 5-13 - Sequence of smoothed horizontal profiles.

The degree of smoothing is determined by the width of the gaussian mask (scale parameter). The scale parameter is increasing from bottom to top, ranging from a fine (equal to one) to a coarse scale value (equal to nineteen).

The minimum scale value applied is the smallest integer value of σ allowed in the gaussian kernel (equation 5-8). By this criterion, the smoothed outline will represent the original profile with as much fine details as possible so that the inflection points can be accurately located. Therefore, the value 1.0 has been chosen as the finest scale to be used when deriving the qualitative descriptions.

There is not a fixed rule to determine the maximum scale value, or the limit to the amount of smoothing that is performed. One method is to specify in advance the number of inflection points and gradually increase the scale until that number is

Analyzing Facial Profiles: Qualitative Descriptions

reached. Another method is to stop the process when the number of inflection points does not change in a pre-determined duration of scale values ($\Delta\sigma$) above some threshold level (e.g. the number specified on the first method). Finally, in the method adopted here, the scale value is gradually increased until no inflection points can be detected on the smoothed profile.

Figures 5-14 and 5-15 shows the curvature scale space descriptions automatically generated from the vertical and horizontal profiles. The x-axis is the length along the profile and the y-axis represents the scale values, where the coarsest scale has the highest value. A scale increment of 1.0 has been used to generate the descriptions shown on both figures. The *zero crossing contours* plotted represent the inflection points along the profile and their movement over a range of scales. As a visual aid, the profile is plotted versus the path length, so that the zero crossing contours may be visually related to the facial features they describe.

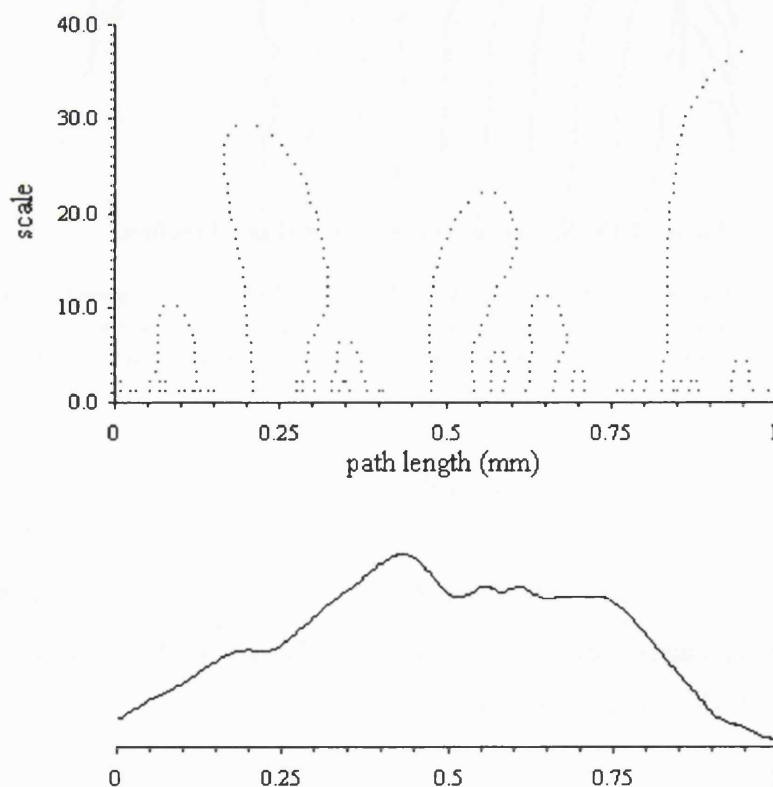


Figure 5-14 - The curvature scale space description of a vertical profile.

The behavior of zero crossings over a range of scales. The x-axis represents the path length parameter (in millimeters) and the y-axis represent the scale parameter increasing from bottom to top. The curvature scale space description is shown at the top and the profile at the bottom.

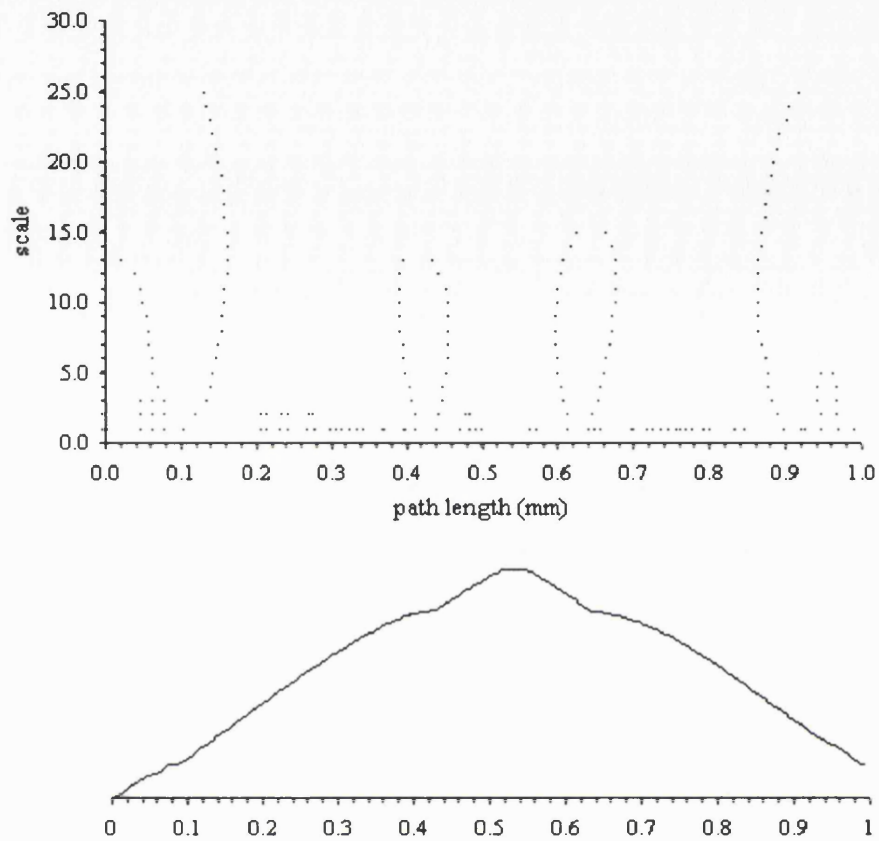


Figure 5-15 - The curvature scale space description of a horizontal profile.

The behavior of zero crossings over a range of scales. The x-axis represents the path length parameter (in millimeters) and the y-axis represent the scale parameter increasing from bottom to top. The curvature scale space description is shown at the top and the profile at the bottom.

Analyzing Facial Profiles: Qualitative Descriptions

Alternatively, another display may be produced to help understand the zero crossing contours and visually relate them to the underlying features of the profile. This is done by plotting the inflection points over the smoothed profiles, for the complete range of scales used on the curvature scale space description (see figures 5-16 and 5-17). This representation is particularly helpful when clinical applications are considered.

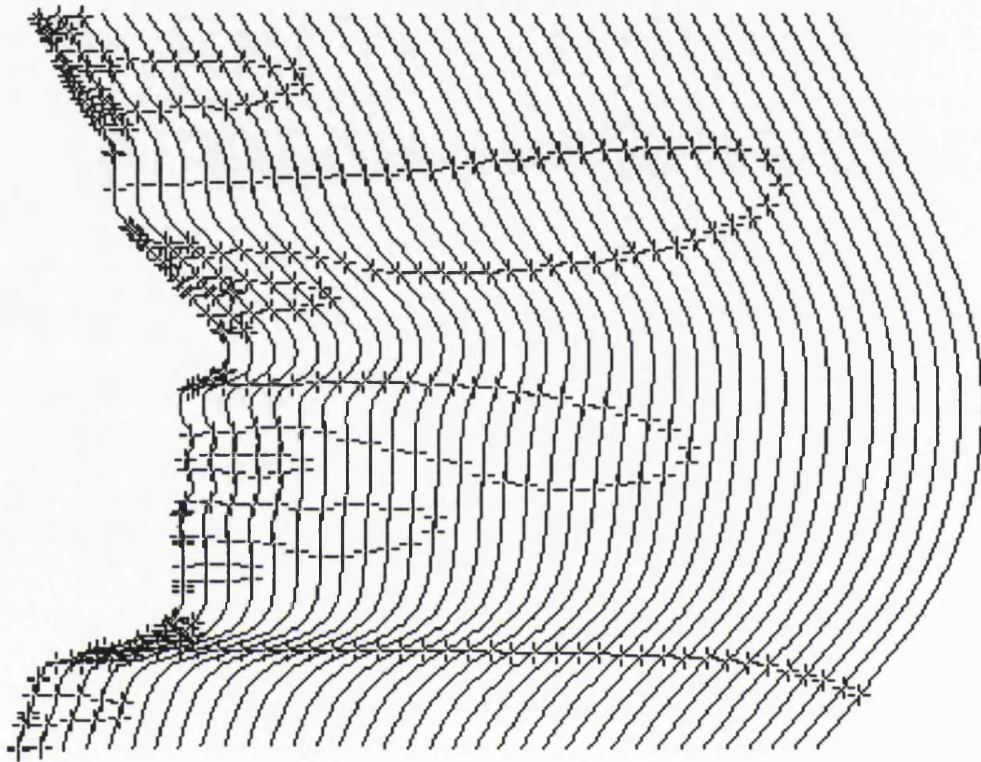


Figure 5-16 - Relationship between zero crossing contours and features of a vertical profile.

The inflection points are plotted over the smoothed profiles for the complete range of scales used on the description. The scale parameter is increasing from left to right.

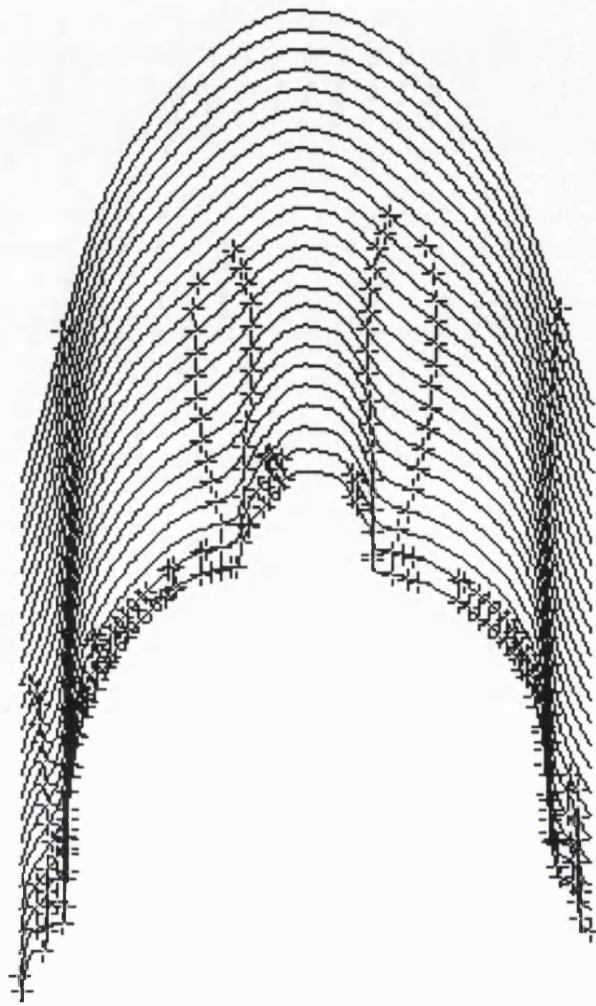


Figure 5-17 - Relationship between zero crossing contours and features of a horizontal profile.

The inflection points are plotted over the smoothed profiles for the complete range of scales used on the description. The scale parameter is increasing from bottom to top.

Notice for example, on figure 5-16, the contours generated by the segments representing the mouth and subnasale regions. They clearly show the advantage of using scale space filtering, because of the way it unifies the inflection points that correspond to those profile features, observed through a continuum of scales.

In the next section, the *scale* is used as a basis for the organization or grouping of the inflection points and the curve features they reflect (as presented by the curvature scale space description), in order to obtain a representation that is appropriate for the segmentation of the profile.

5.7.2. Interval Tree

The zero crossing contours on the curvature scale space description cannot be directly used to segment the profile, mainly because they reflect the spatial distortions introduced by the gaussian convolution process. However, when grouped together by scale, these distortions are eliminated, yielding a representation (known as interval tree) which is appropriate for segmenting the profile.

Figures 5-18 and 5-19 shows the interval tree descriptions, automatically generated from the curvature scale space descriptions of the vertical and horizontal profiles (seen on figures 5-14 and 5-15) . The x-axis is the length along the profile and the y-axis represents the scale values, where the coarsest scale has the highest value. Each *rectangle* is a node on the tree, indicating the location and extent of a region or an *interval* on the curve, and the scale limits over which this region exists.

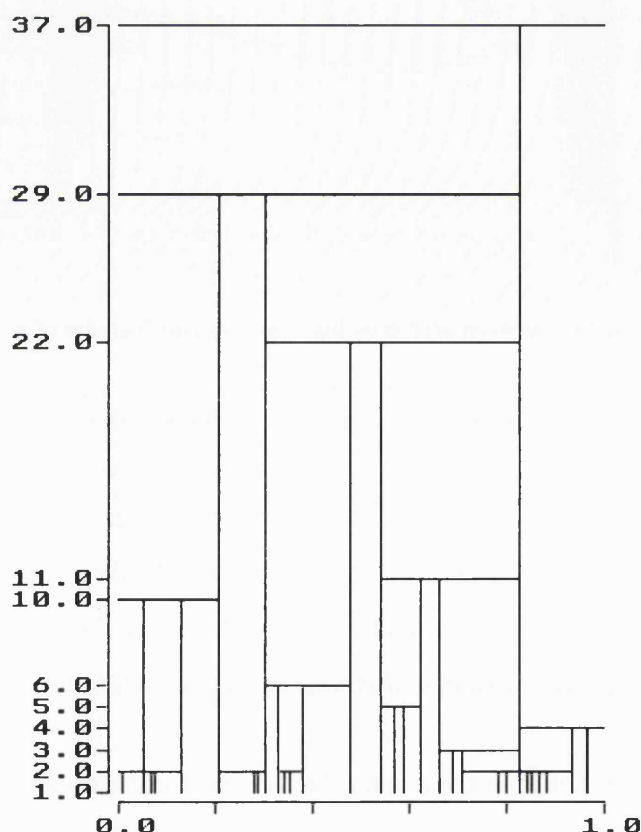


Figure 5-18 - The interval tree description of a vertical profile.

The x-axis represents the path length parameter (in millimeters) and the y-axis represents the scale parameter decreasing from top to bottom. A set of intervals is represented by rectangles, indicating their location and extent (x-axis), as well as the scale duration (y-axis) . The root of the tree is at the top.

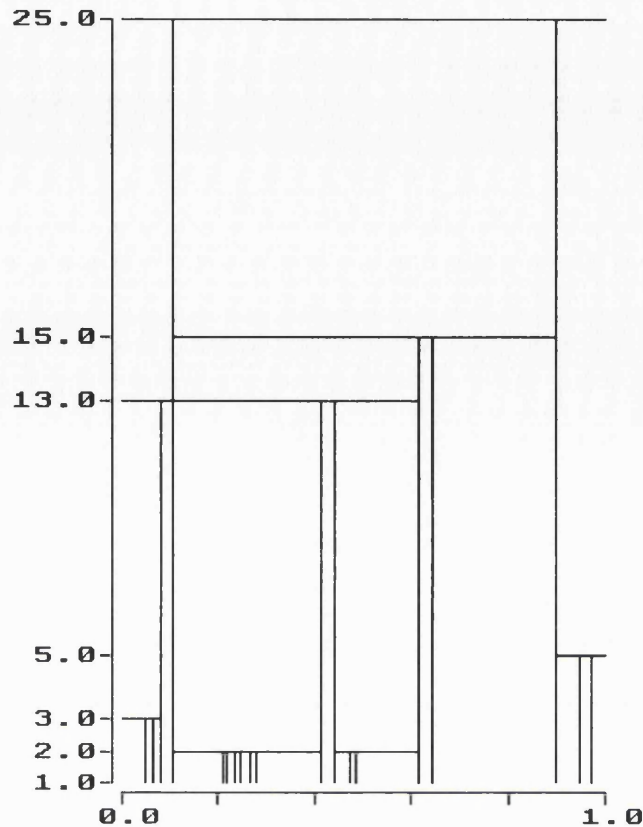


Figure 5-19 - The interval tree description of a horizontal profile.

The x-axis represents the path length parameter (in millimeters) and the y-axis represents the scale parameter decreasing from top to bottom. A set of intervals is represented by rectangles, indicating their location and extent (x-axis), as well as the scale duration (y-axis). The root of the tree is at the top.

The interval tree description is automatically derived by locating the inflection points at a coarse scale and then tracking them back at the adjacent finer scale, until the smallest used scale is reached (starting from the root, located at the top of the tree). In this manner, a number of rectangles are defined which are directly related to the features of the profile outline. These rectangles are bounded on both sides by the x-axis locations of the zero crossing contours (indicating the location of a underlying feature); bounded above by the coarsest scale at which the zero crossing contour ends; bounded below by the scale at which a new zero crossing contour appears, splitting the rectangle into sub-intervals. This is achieved by a specially designed algorithm.

By exploring the intervals so defined, it is possible to obtain a segmentation of the facial profile which best describes all of its existing features. This is discussed in the next section.

5.8. Profile Segmentation

Each rectangular interval of the tree description subdivides the curve into sections or segments. For example, by moving a straight line up or down the scale values, parallel to the x-axis on the interval tree description, a set of rectangles is intersected. At the higher levels of scale, only a few, large rectangles, are intersected, and consequently, the defined curve segments are larger. Similarly, at lower levels of scale, many small rectangles are intersected, producing smaller curve segments. In addition, by merging or splitting the rectangular intervals according to the classification of their nodes (e.g. parent or offspring) a new segmentation may be generated.

Coarse scale values are useful to show which features have persisted during the smoothing process and therefore may be considered as relevant. Moreover, they simplify the segmentation by eliminating small details and digitization artifacts. However, an important distinction must be considered. Although a segmentation is possible at coarser levels of scale, where fine detail and even entire features might have been removed, the primary interest is at the finest scale value, where all the information (i.e. curve details and features) is present. Because in the tree description all scales have been integrated, features identified at a coarse scale can be located at the finest scale.

There are a number of different ways of exploring the tree description in order to segment the curve representing the facial profile (this is further discussed later in this chapter). However, to achieve a meaningful segmentation, the most important features of the general profile, such as the nose and lips (when on the mid-line), need to be clearly represented.

By adopting this approach, tree intervals are selected as to objectively segment the profile into a number of regions suitable for analysis. For example, the segments including the nose or the chin would correspond to parts of the face that are of relevance to a clinical application.

Figure 5-20 illustrates the segmentation process for a vertical profile. Following the horizontal line placed at the scale value of 10.0 (darker horizontal line with one inverted arrow end), eight segments are automatically defined on the profile, as indicated by their bounding points (crosses) plotted along the profile displayed on the right hand side.

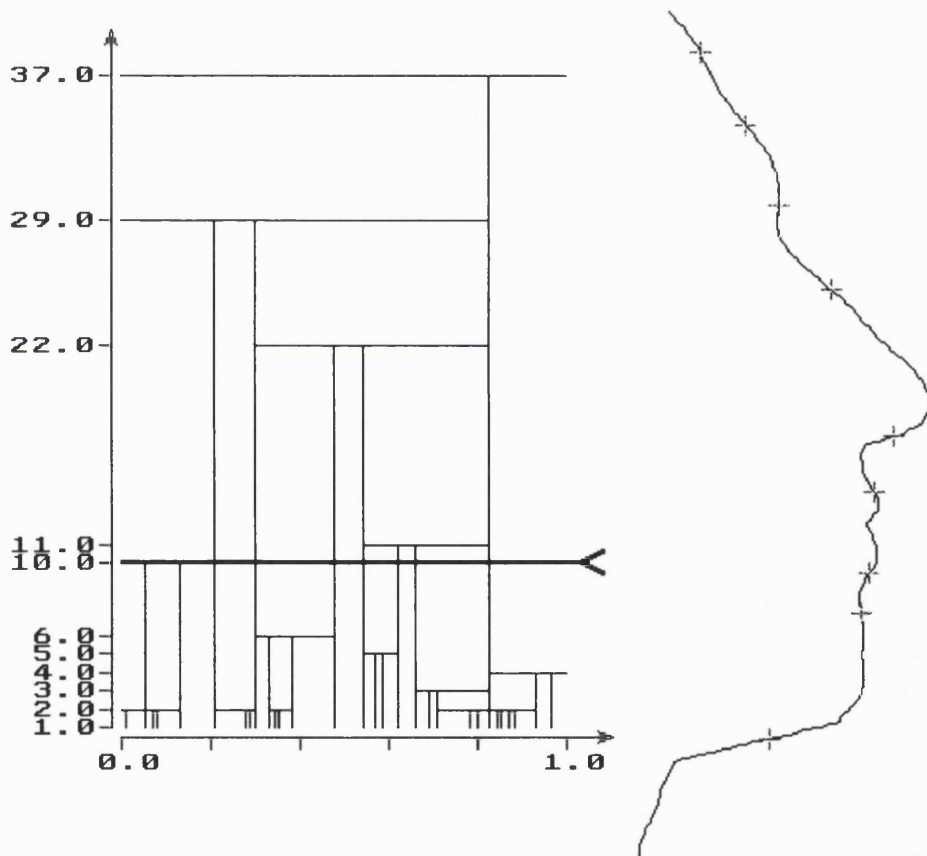


Figure 5-20 - The profile segmentation.

At the scale value 10.0, the outline is automatically segmented by 9 landmarks, as shown on the right side of the figure. On the interval tree description (left), the x-axis represents the path length parameter (in millimeters) and the y-axis represents the scale parameter decreasing from top to bottom.

Note that each segment is defined by two boundary points plus the points that lie between them. In addition, the points that define these boundaries may be treated as landmarks. When a particular segmentation is accepted, a computer file is created to store the coordinated points of the profile plus the bounding points of each segment. This file may be used for further processing.

5.8.1. Exploring Curvature Extrema

As discussed in section 2.2.4, the zero crossings are not the only invariant features of a curve that may be described by the curvature values. The maxima and minima of both positive and negative curvature values, known as *curvature extrema*, have also been applied by a number of research workers. Only a few, however, have considered such curvature features within the context of a multiscale representation (e.g. Richards et al 1986, Teh et al 1989, Pei et al 1992 and Rosin 1993).

When such curvature features are considered within the context of a multiscale representation, a new qualitative description of planar curves may be attained : the *extrema scale space*. The procedure followed to derive this description is similar to the case of curvature scale space, described in section 5.7 .

Firstly the extrema scale space is derived by finding and combining the extrema points on the curve at varying levels of detail (or scale). This is achieved by either (i) comparing every curvature value (equation 4-14) with its preceding and succeeding neighbors, or by (ii) computing the change in curvature, as given by the equation below (5-9) :

$$k'(t, \sigma) = \frac{\left(\dot{X}(t, \sigma) \cdot \ddot{Y}(t, \sigma) - \dot{Y}(t, \sigma) \cdot \ddot{X}(t, \sigma) \right) \left(\dot{X}^2(t, \sigma) + \dot{Y}^2(t, \sigma) \right) - \left(\ddot{X}(t, \sigma) \cdot \ddot{Y}(t, \sigma) \left(\dot{X}^2(t, \sigma) - \dot{Y}^2(t, \sigma) \right) \right) + \left(\dot{X}(t, \sigma) \cdot \dot{Y}(t, \sigma) \left(\ddot{X}^2(t, \sigma) - \ddot{Y}^2(t, \sigma) \right) \right)}{\left(\dot{X}^2(t, \sigma) + \dot{Y}^2(t, \sigma) \right)^3} \quad (5-9)$$

Secondly, the spatial distortions, introduced by the smoothing process, are eliminated by grouping the curvature points according to their scale values. Finally, the curve may be segmented by selecting or combining the defined rectangular intervals. This is illustrated in the figures 5-21 and 5-22.

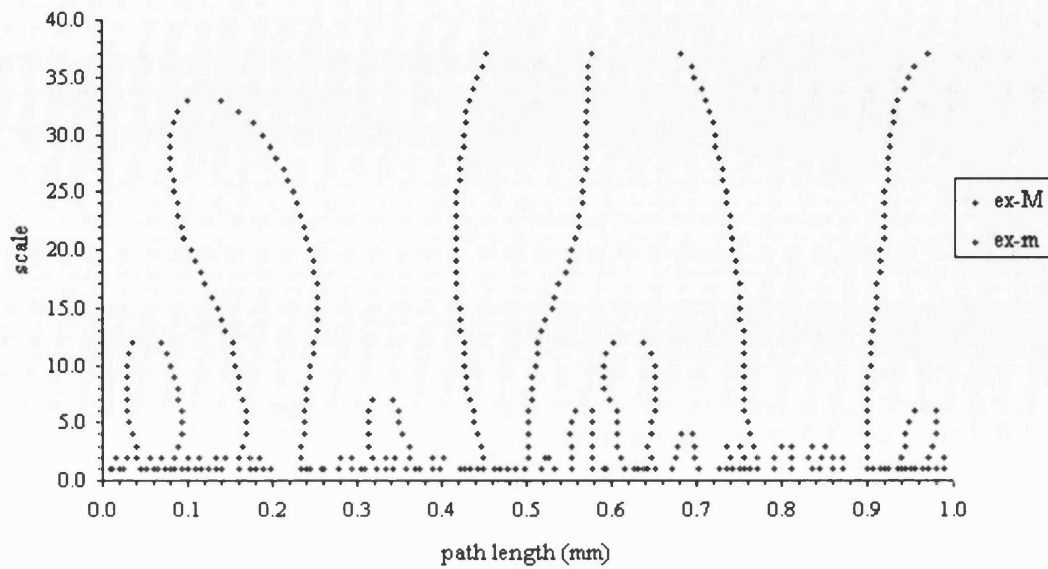


Figure 5-21 - The extrema scale space description of a vertical profile.

The behavior of extrema over a range of scales. The x-axis represents the path length parameter (in millimeters) and the y-axis represent the scale parameter increasing from bottom to top. The maxima is denoted by ex-M, and the minima is denoted by ex-m.



Figure 5-22 - The profile segmentation at extrema of curvature.

At the scale value 10.0, the outline is automatically segmented by 18 landmarks. The maxima of curvature is denoted by **ex-M** (square), and the minima is denoted by **ex-m** (circle).

Figure 5-23 shows the relationship between the zero crossings (or inflection points) and extrema points, when described by their respective scale space contour representations.

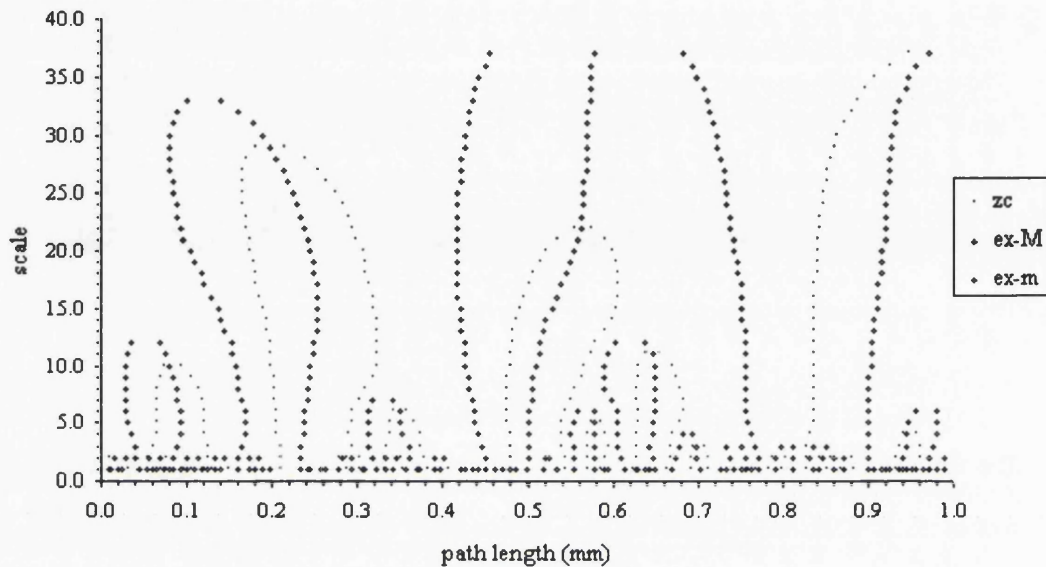


Figure 5-23 - Comparison of a zero curvature and extrema scale space descriptions.

The curvature scale space description (figure 5-14) and the extrema scale space description (figure 5-21), of the same vertical profile, are plotted together along the same axes. The x-axis represents the path length parameter (in millimeters) and the y-axis represent the scale parameter increasing from bottom to top. The zero crossing is denoted by *zc*, the maxima is denoted by *ex-M*, and the minima is denoted by *ex-m*.

Notice how the contours behave : they seem to appear in turns so that between two consecutive zero crossing contours there is one extrema contour. Furthermore, they indicate that the maximum of a zero crossing contour is a significant point of that contour (such point occurs at the contour's highest scale value, or at the top of the arch formed by two zero crossing contours). This point seems to be always associated with a point of extrema of curvature (i.e. either a maxima or minima). As the figure clearly illustrates, the point of extrema usually falls in the gap at the top of the zero crossing contour. When at the top of an arch, the point of extrema is the middle point between two zero crossings.

5.9. Quantitative Descriptions

Proceeding with the analysis, the next step is to introduce forms to quantitatively describe the profile and its segments as well as to measure changes and differences between them when different profiles are compared.

Quantifying facial profile changes due to growth, orthodontic treatment or surgery, is not an easy task. Although some statistical methods for comparing differences in shape and landmark movement are available, they are not so meaningful or easy to use from a clinician's point of view.

In fact, as the literature shows, the discrete measurement of properties of continuous curves is not trivial and have been the object of the research efforts of various workers (Shahraray 1985, Dorst 1987, Duncan 1991, Worring 1993).

Following the methodology of this work, some techniques have been used to establish a difference metric with a view to explore one of the most important properties of planar curves, that is the curvature of the curve. Such an approach emphasizes the shape of the curve segments rather than single points only.

Before presenting them, two questions will be addressed: the shrinking effect caused by the gaussian smoothing, and the selection of the scale at which the curvature should be computed.

5.9.1. Correcting Spatial Distortions

Smoothing a curve with a gaussian filter introduces spatial distortions due to the broadening and flattening of the features. As a result, the curve is systematically shrunk towards the local center of curvature.

Qualitative shape descriptions are not affected by this, as it has been demonstrated in the previous sections. On the other hand, quantitative descriptions require the use of smoothing methods that cause no additional distortion, otherwise

these will be reflected on the measurements taken. If distortions are introduced by the smoothing process, a method of correcting them should be applied.

The correction method adopted in this work, which is described below, is based on a gaussian smoothing operation, and satisfy all the scale space properties that have previously been underlined, specially those related to zero crossings and extrema of curvature.

Lowe (1988) investigated this problem and observed that the averaging nature of the gaussian filter is a source of distortions, causing a *shrinking effect*. Considering a circle of radius r centered at the point $(r,0)$, he determined the shrinkage as a function of the degree of smoothing σ and of the local curvature measure $X''(t)$ (i.e. the second derivative of the convolution). With this shrinkage value he was able to correct the original smoothed curve.

This process is expressed by the equations below, where the shrinkage error for each point of the smoothed curve $X(t)$ is given by :

$$X(t) = r \left(1 - e^{-\sigma^2/2r^2} \right) \quad (5-10)$$

and r is given by :

$$X''(t) = \frac{e^{-\sigma^2/2r^2}}{r} \quad (5-11)$$

Because the values of r are not known in advance, Lowe suggested a method of correction based on lookup table and interpolation. First, a table is built with the shrinkage error values from equation (5-10) as a function of X'' , based on the solution for r from equation (5-11). Then, for each point of the curve the appropriate error value is interpolated from the table and subtracted from the smoothed coordinate value. However, a further interpolation is necessary to compensate the discontinuities of equation (5-10) as X'' approaches zero when changing from positive to negative or vice-versa.

The shrinkage correction is applied to both coordinate functions $x(t)$ and $y(t)$ of the parametric curve. Moreover, as Lowe argued, the correction is a monotonically increasing function of curvature, so that the original zero crossings as well as the maxima and minima of curvature are preserved in the corrected curve.

The result of applying the correction method above to a vertical profile outline is shown in figure 5-24. In figure 5-24(a) the profile is smoothed with a gaussian filter with $\sigma = 10$, and in 5-24(b) the correction is applied after smoothing. To highlight the differences, the smoothed outlines before and after correction are plotted superimposed one upon another, as shown in 5-24(c). The shrinkage is apparent in 5-24(a) where the smoothed outline has been systematically displaced towards the center of each curved region in a much greater degree than the one observed in 5-24(b).

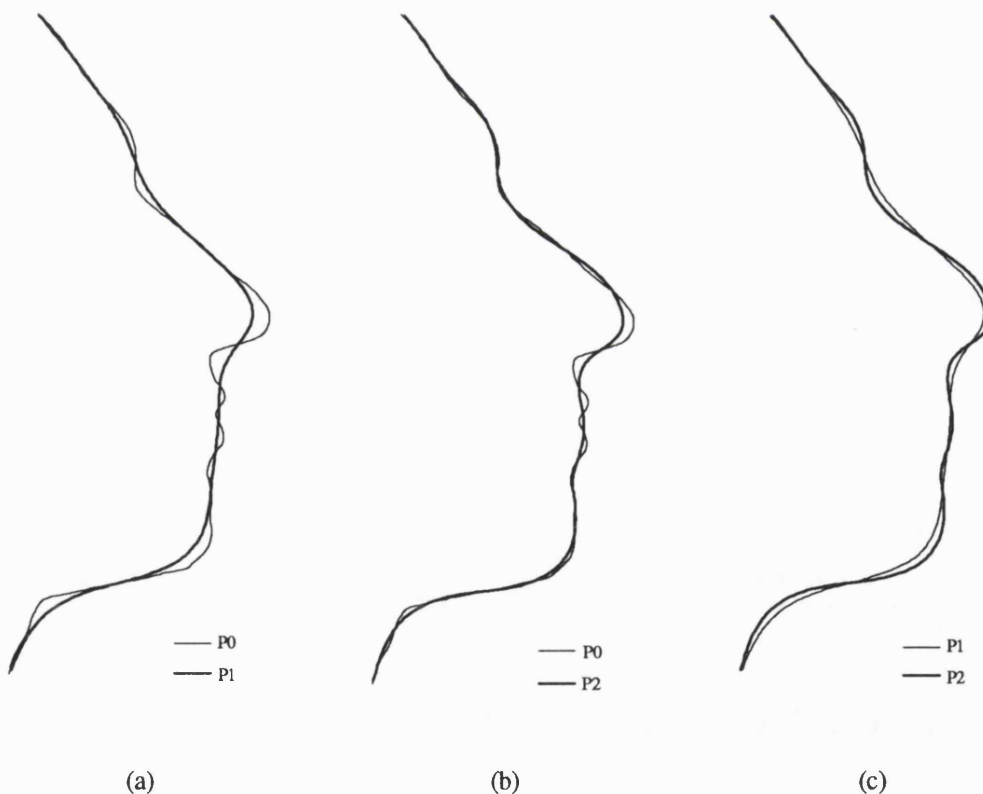


Figure 5-24 - Correcting the shrinking effect caused by gaussian smoothing.

The vertical profile outline (P0) has been smoothed by a gaussian convolution with $\sigma = 10$. The smoothed outline (P1) is displayed in (a). After applying the shrinkage correction the smoothed outline (P2) is displayed in (b). The two smoothed outlines are shown superimposed on (c).

5.9.2. Selecting Natural Scales

The curvature is estimated at every point of the curve. Generally, filtering or smoothing is the method by which excessive noise (e.g. due to quantization) is removed, so that an accurate estimation may be performed.

The immediate question that arises when noise is removed by smoothing is how much smoothing should be performed in order to preserve valid shape information of the existing features ?

As the preceding sections have shown, multiscale methods can adequately represent the curve at various levels of detail by introducing a scale parameter which increases over a range of values. We have also seen, from the interval tree description, that certain features of the curve, when smoothed, are represented (or survive) only at a specific range of scales, suggesting that each feature of interest has a scale that best describes it, while eliminating noise and detail. In other words, it would be possible to represent the curve only at certain scales (called “*natural scales*”), each of which would describe the curve from a different qualitative aspect.

Therefore, the degree of smoothing of the curve to be applied when estimating the curvature values may be determined by the natural scale values, selected directly from the interval tree description.

Although this was the approach adopted in this work, other methods have been proposed and are briefly described. Some initial investigation has been done in this area by Marr (1982) and Witkin (1983), in his work on scale space filtering (described in section 4.3). These ideas were later followed by Richards (et al 1986), Lowe (1988) and also by Bengtsson (et al 1991) and Rosin (1991).

When trying to identify the most significant scales, a common approach found in the literature requires the quantification of “significance” by taking some measurements on the curve at each scale applied when smoothing the curve. Examples of these measurements include maximum curvature, average curvature, number of

curvature extrema and number of zeros of curvature (or zero crossings). Rosin (1991) compared several significance measures on different synthetic curves and concluded that the change in number of zero crossings was the measure that performed better. For each smoothed curve, this measure is given by the sum of all zero crossing points, multiplied by the smoothing scale σ . When computed over a range of scales, this significance measure will present values of maximum and minimum. Rosin demonstrated that when the significance values are minimum (called minima of significance measure) they represent the features of the curve at their natural scales. Rosin describes these values as : “*corresponding to structures in the curve which have been isolated at their natural scales*”.

However, a relationship between the interval tree and the minima of significance measure may be established when considering the number of zero crossings, as illustrated in the graphic below (figure 5-25). A high rate of change in the number of zero crossings may be observed on basically the same scale values for both descriptions. Usually these values indicate the scales of interest at which the curve could be described. A similar relationship has been pointed out by Rosin (1993) when comparing his approach with Witkin’s scale space description.

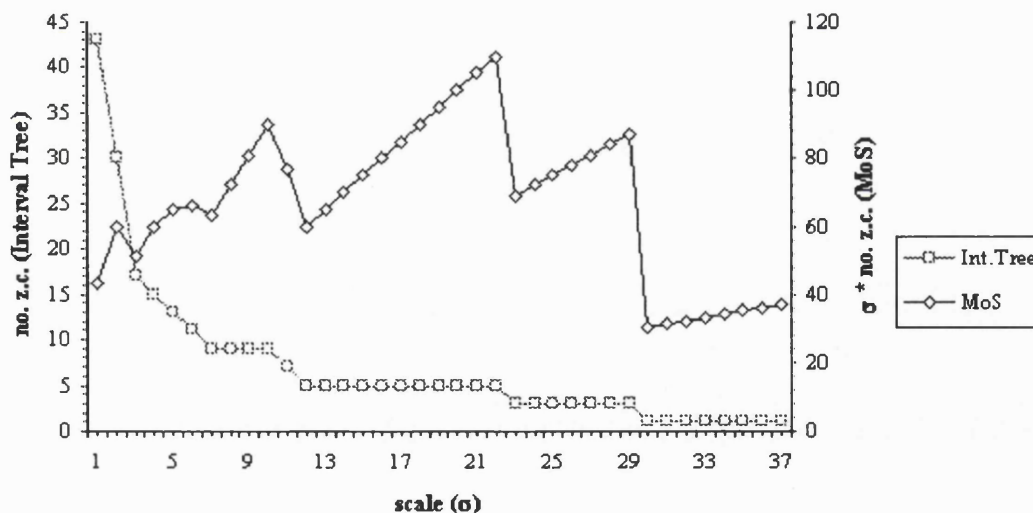


Figure 5-25 - Comparing the Interval Tree and Minima of Significance.

Therefore, there is evidence that supports the use of the interval tree description to select the natural scale (or scales) which will determine the degree of

the curve to be applied when estimating the curvature values.

Figure 5-26 illustrates the vertical facial profile outline smoothed at some of the “natural scales” extracted from the interval tree description of figure 5-18. The scale values are 3, 6, 10, 22 and 37, which correspond to the horizontal boundaries of the rectangular intervals on the tree (i.e. values which mark the appearance and disappearance of the zero crossing contours).

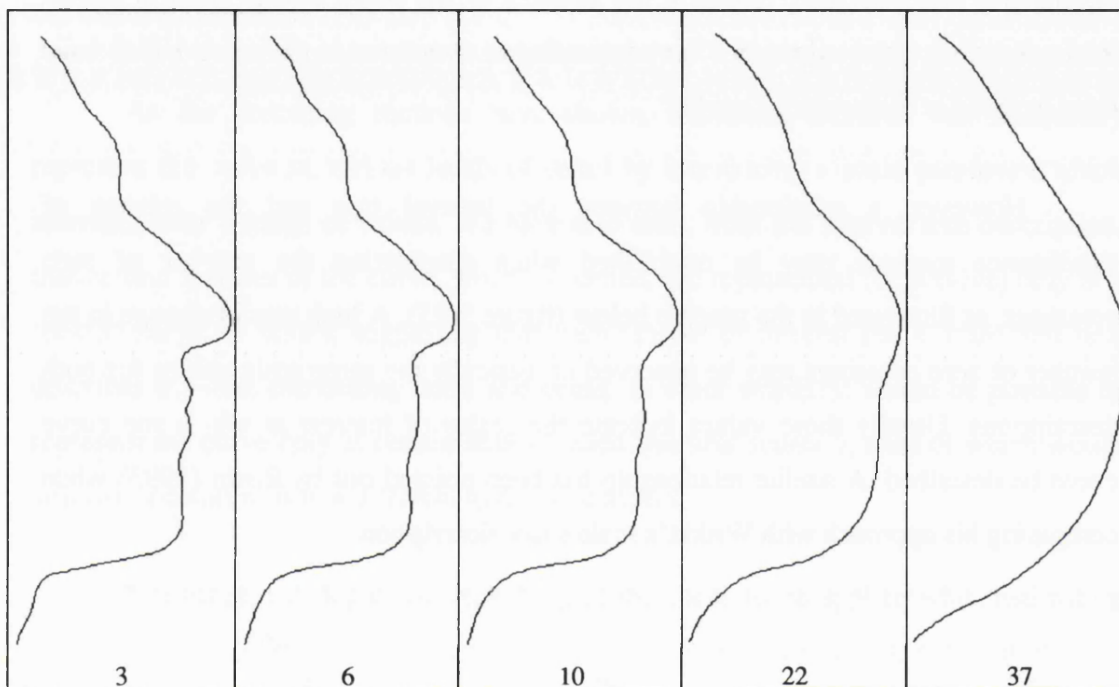


Figure 5-26 - Selecting scales from the Interval Tree description.

The “natural scales” of a given profile are indicated at the bottom, with the respective smoothed profile shown at the top.

Depending on the feature of interest, a specific scale value may be used. In the figure above, some of the facial features such as the brow ridge and lips are present only at the first two scales (3 and 6), whereas the nose and the chin may be seen at the scales 3, 6, 10 and 22. This result shows that the interval tree description does contain the scale values which best describes the features of interest in the profile.

5.9.3. Curvature Value

The curvature value provides useful local shape information by which a segment can be described in terms of its direction of curvature (or concavity).

Three equivalent formulations of curvature may be found in the literature of differential geometry (Lipschutz 1969), which are based on : (i) the orientation of the tangent, (ii) the local touching circle, and (iii) on the second derivative of the curve considered as a path. From them, several methods are derived and have been reported in the literature for computing the curvature of a digital curve (Thomas et al 1989, Asada et al 1986, Mokhtarian et al 1986).

Worring (et al 1993) presented an extensive study on the performance of these methods when estimating the digital curvature. They grouped the existing methods into five classes according to the formulations above. These classes are summarized in the table 5-1 .

Formulation	Method
Orientation of the tangent	I - Chain code II - Resampled chain code III - Line fit
Second derivative of the curve as a path	IV - Path
Touching circle	V - Arc fit

Table 5-1 - Classification of digital curvature estimation methods.

Theoretical and practical considerations were used as a basis for the evaluation of these methods. They quantified the error in terms of two components: first the “curvature bias”, expressing the accuracy as a consequence of the digitization on the grid, and second the “curvature deviation”, expressing the precision of the method.

Analyzing Facial Profiles: Evaluation of the Method

From their experiments, they concluded that : “ *the path based method (IV) is the method to use when the aim is to estimate curvature as well as the smoothed curve* ” .

This method has, in fact, been applied in the methodology established here to compute the qualitative descriptions used for segmenting the facial profiles. As shown in section 4.4 , the equation (4-14) gives the signed curvature of the curve considering the parametric representation of its x and y coordinate points, and a given scale value. For a given curve, the curvature is plotted versus the path length, resulting in a graph called the *curvature plot*, which is illustrated in figure 5-27, for a vertical profile outline.

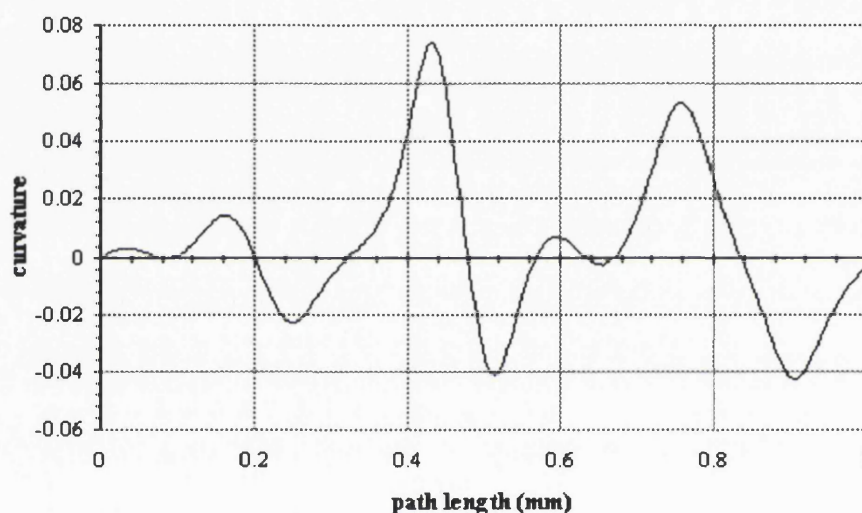


Figure 5-27 - The curvature plot of a vertical profile.

The vertical profile outline has been smoothed with a scale factor of 10.0 .The x-axis represents the path length parameter (in millimeters) and the y-axis represents the curvature values.

In addition to this graphic representation, the curvature values are used to describe the curve segments individually, e.g. through the average value for all segment points or the value at singular points only (i.e. extrema of curvature). When computed, these values are presented in tables, depending upon the application.

5.9.4. Bending Energy

Let us consider that the contour defining the facial profile, in any arbitrary view, is modeled as a thin flexible rod. The properties of such rod when being deformed (e.g. the elastic energy), may be used to define a measure of the shape of the contour.

A similar idea was used in the early days of ship design (e.g. in the 1800s) when a thin, elastic wooden beam called a “spline” was passed between metal weights, to produce a smooth curve. The wooden beam would always assume a position that minimizes its strain energy (Farin 1993).

What it is applied, on our case, is the notion of *bending energy*, that is the energy required to bend a thin rod from one shape into another. The bending energy borrows its concept and mathematical formulations from the elasticity theory (Landau 1986) and has been explored by research workers in describing biological shapes (Young et al 1974, Bowie et al 1977, Smeulders et al 1980, Duncan et al 1991).

From the elasticity theory it is known that the bending energy is proportional to the local curvature squared, as expressed by the equation below :

$$BE = \int_{s_1}^{s_2} K(s)^2 ds \quad (5-12)$$

assuming that the undeformed state is a straight rod. When generalized to account for the bending of a rod having any undeformed state, the integrand of equation (5-12) is written as the squared difference of the local curvature of the rod in its deformed and undeformed states, as expressed by :

$$BE = \int_{s_1}^{s_2} (K_d(s) - K_u(s))^2 ds \quad (5-13)$$

where $K_d(s)$ and $K_u(s)$ are the curvatures for the deformed and undeformed rods, respectively.

The discrete version of equations (5-12) and (5-13) are given below, in order that the shape measurements based on bending energy may be applied to the resampled contour points of our facial profiles :

$$BE = \sum_{i=1}^{i2} (K_d(i) - K_u(i))^2 \quad (5-14)$$

$$BE = \sum_{i=1}^{i2} (K(i))^2 \quad (5-15)$$

Therefore, the concept of bending energy may be explored in two ways. The first one which assumes the initial undeformed state to be a straight line, and consequently, the measurements will reflect the particular shape of either a segment or the entire facial profile, depending upon which one is analyzed. The second one which assumes two generic states of deformation, where the measurements will then reflect the difference or the change in shape of either a particular segment or the entire facial profile.

Similarly to the curvature plots, the bending energy is plotted versus the arc length. The resulting graph is the *bending energy plot*, and is illustrated, for a vertical profile outline, in the next two figures (5-28 and 5-29), as examples of the first and second approaches, respectively.

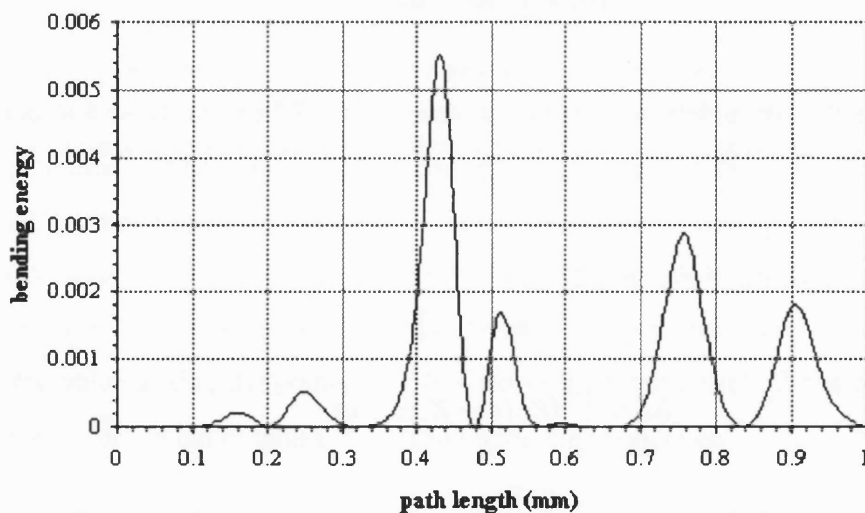


Figure 5-28 - The bending energy plot.

This bending energy plot represents the first approach as described in the text above, i.e. the energy required to bend a straight rod into the shape of the vertical profile outline, has been smoothed with a scale factor of 10. The x-axis represents the path length parameter (in millimeters) and the y-axis represents the bending energy values.

In figure 5-29, the bending energy plot represents the energy required to bend a rod from one initial shape into another (the second approach as described above). In this example, only the profile segments representing the nose and the subnasale segment have been altered. The bending energy was computed for the entire outline. In order to help associating the bending energy values with the profile segments, both outlines are superimposed and displayed on the bending energy plot. The profile markers and the dashed vertical lines indicate the boundaries of all defined segments, derived from figure 5-20.

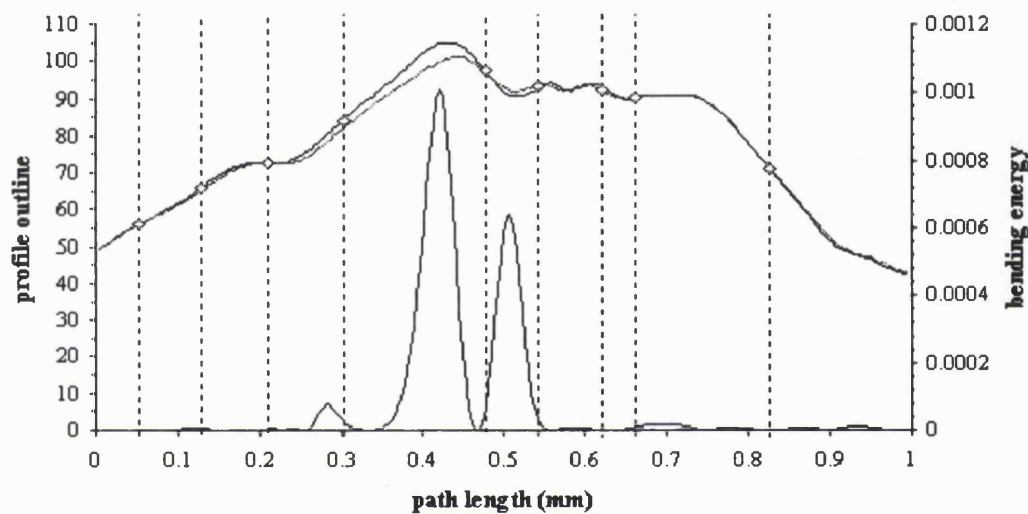


Figure 5-29 - The bending energy plot.

This bending energy plot represents the second approach as described in the text above, i.e. the energy required to bend a rod from a initial shape into its present shape. The vertical profile outlines has been superimposed and displayed in the same plot. The x-axis represents the path length parameter (in millimeters) and the y-axis represents the bending energy values on the right, and the outlines on the left. The markers and dashed lines indicate the boundaries of the defined segments.

In addition to this graphic representation, the bending energy values are used to describe the curve segments individually, e.g. through the average value for all segment points. When computed, these values are presented in tables, depending upon the application.

5.9.5. Other Quantitative Measures

To complement the above measures, some additional descriptive measures have been included in the analysis and are described next. They intended to describe the

Analyzing Facial Profiles: Evaluation of the Method

curve segments only. It is common to find similar metric information being employed in the pattern recognition literature, as discussed in section 2.2 . Some examples are Freeman (et al 1975), C. You (et al 1979), Hoffman (1982) and Rosin (1993).

The first measure is **length**, and is computed by summing the Euclidean distances between all points that compose the segment.

The second measure is **roundness**, and it is determined by integrating the absolute curvature over the entire curve segment.

The third measure is **compactness**, and may be approximated by the ratio of the lengths of two lines: one is the straight line joining the endpoints of the curve and the other is the perpendicular to this line passing through the midpoint of the curve (see figure 5-30(a)).

Finally, **skew** is taken as the last complementary measure. To prevent instability for segments with low curvature, in which small shifts produces substantial change in angle, the skew can be computed as the area of the sector normalized by the length of the curve. This sector is formed by angle of declination of the midpoint of the curve, as illustrated in figure 5-30(b).



Figure 5-30 - Additional metric information.
parameters to calculate (a) compactness , and (b) skew

Analyzing Facial Profiles: Quantitative Descriptions

Once these measures have been computed, they are presented as a table of values, as illustrated below (table 5-2).



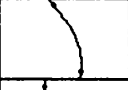






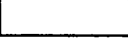
Segment no.	Segment shape	Start	End	no. points	Length (mm)	Average curvature	Average bending energy	Roundness	Compactness	Skew
0		0	12	13	12.37	-1.443	18.76	43.20	27.823	
1		12	31	20	21.21	-0.013	0.26	27.11	0.002	0.002
2		31	51	21	22.38	0.029	0.62	10.03	0.002	0.074
3		51	74	24	25.77	-0.032	0.76	7.73	0.002	-0.043
4		74	118	45	49.11	0.041	1.83	4.52	0.006	0.839
5		118	135	18	18.80	-0.089	1.61	3.02	0.019	-0.013
6		135	155	21	21.84	0.045	0.95	41.10	0.029	0.001
7		155	165	11	11.14	-0.064	0.71	9.32	0.006	-0.005
8		165	205	41	44.24	0.036	1.47	3.50	0.008	-1.172
9		205	248	44	47.78	-0.026	1.12	4.16	0.005	

Table 5-2- Table with the segment's quantitative descriptive measures.

These values refer to the segmented vertical profile outline of figure 5-20.

The shape of each segment, plus its boundary points, is illustrated in the second column of the table. The segments number 0 and 9 are composed by using the first and last landmark points plus the first and last outline points respectively, and are only printed for the sake of completeness.

5.10. Evaluation of the Method

Three aspects have been considered for the evaluation of the method : (i) the sensitivity and stability of the resulting descriptions to noise; (ii) the stability and reproducibility of the segmentation of the profile, and (iii) the sensitivity of the description to local and global changes of the profile outline. These are described below.

5.10.1. Sensitivity to Noise

Real data always contain a certain amount of noise or distortion. For the case of the UCL-MGI optical surface scanner, Moss (et al 1989) reported the estimated error in the data collection to be 1.0 mm along the profile and 0.6 mm between profiles (also see section 4.4). Coombes (1993) reported on the overall assessment of noise in the optical surface scans by generating mathematical spheres with combined amounts of quantization and gaussian distributed noises. When compared with a scanned sphere, the reported results showed that 0.25 mm quantization noise and between 0.1 mm and 0.15 mm of normally distributed noise were present.

In order to evaluate the method, or more specifically, the stability of the curvature scale space description in the presence of noise, two types of noise were added to a given facial profile outline : *quantization noise* and *random noise*.

The quantization noise can normally arise during the digitization process, where the points along the outline are digitized to the nearest pixel by the scanning device. The routine used here to simulate the effect of quantization noise consisted of computing the rounded value for the real numbers representing the surface of the scanned face (i.e. the radial position of the facial surface). Two noisy data sets were generated, from which the horizontal and vertical profiles were then extracted. They correspond to the data being rounded to the nearest 1.0 mm and 3.0 mm. The profiles and the curvature scale space descriptions are shown in figures 5-31, 5-33, 5-34 and 5-36.

Analyzing Facial Profiles: Evaluation of the Method

The normally distributed (gaussian) random noise was also added to the values representing the surface of the scanned face. It was computed by using a standard algorithm (Groeneveld 1979) based on equations 5-16 and 5-17 :

$$x = x + sd * err \quad (5-16)$$

$$err = \sqrt{((-2 * \log(R1)) * (\cos(2\pi * R2)))} \quad (5-17)$$

where **sd** is the standard deviation of noise to be added (in millimeters), and **R1** and **R2** are random numbers between 0 and 1.

The profiles and respective curvature scale space descriptions, generated by adding the amounts of standard deviation of noise of 1.0 mm and 3.0 mm are shown in figures 5-31, 5-32, 5-34 and 5-35 .

The results show that in both cases of the two types of noise, i.e. for a significant amount of noise (1.0 mm) and for an extreme amount of noise (3.0 mm), there is a very close similarity in the basic structures of the derived descriptions. At high scale values the zero crossing contours match well, and at lower values they are influenced by existing shape differences or detail of the profile outlines (see the superimposed descriptions in figures 5-32(d), 5-33(d), 5-35(d) and 5-36(d)).

This suggests that the curvature scale space description is very stable in the presence of noise.

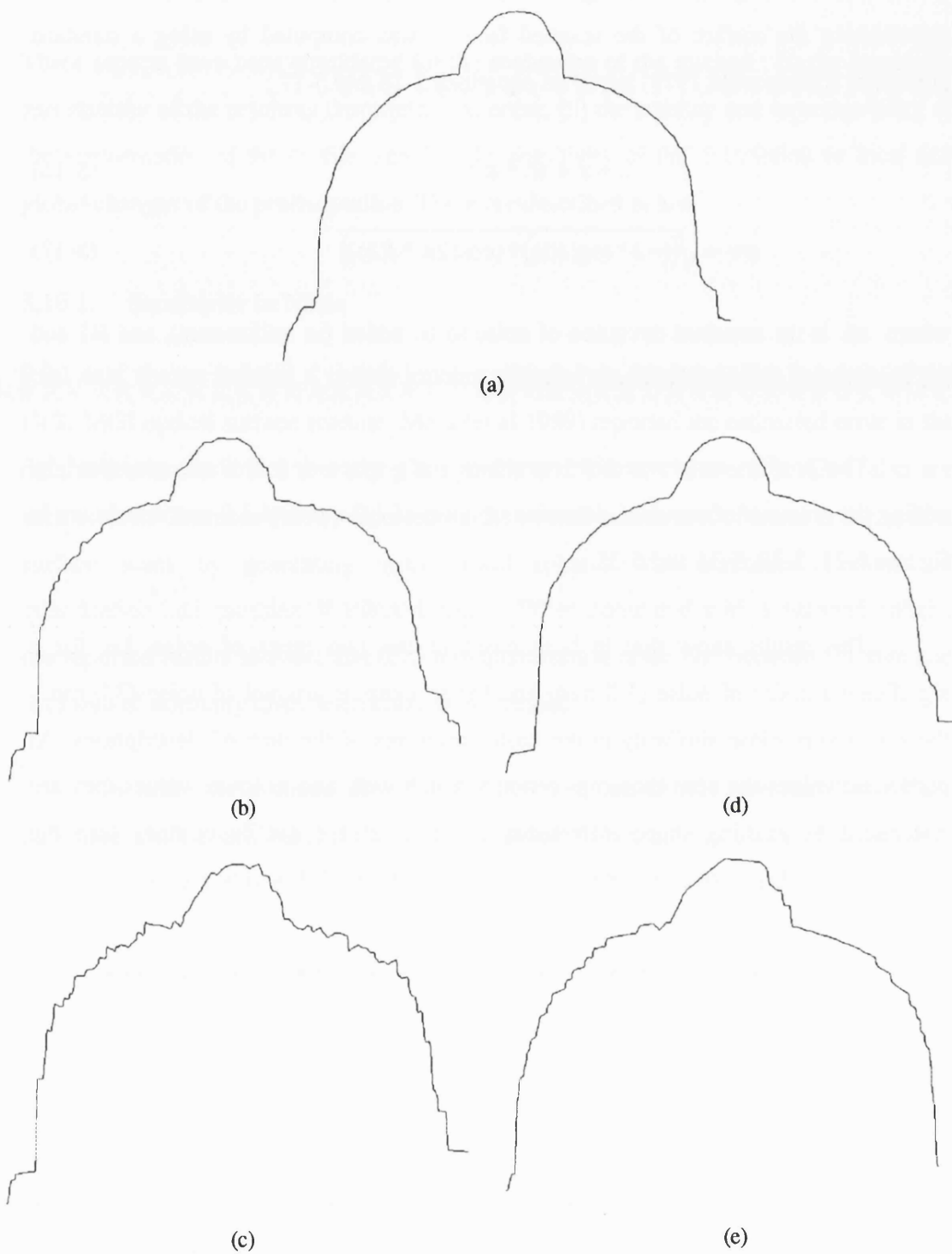


Figure 5-31 - Effects of added noise on the *horizontal profile* outline.

The original profile is shown in (a). The profiles with added 1.0 and 3.0 mm of *normally distributed noise* are shown in (b) and (c), respectively. The profiles with added 1.0 and 3.0 mm of *quantization noise* are shown in (d) and (e), respectively.

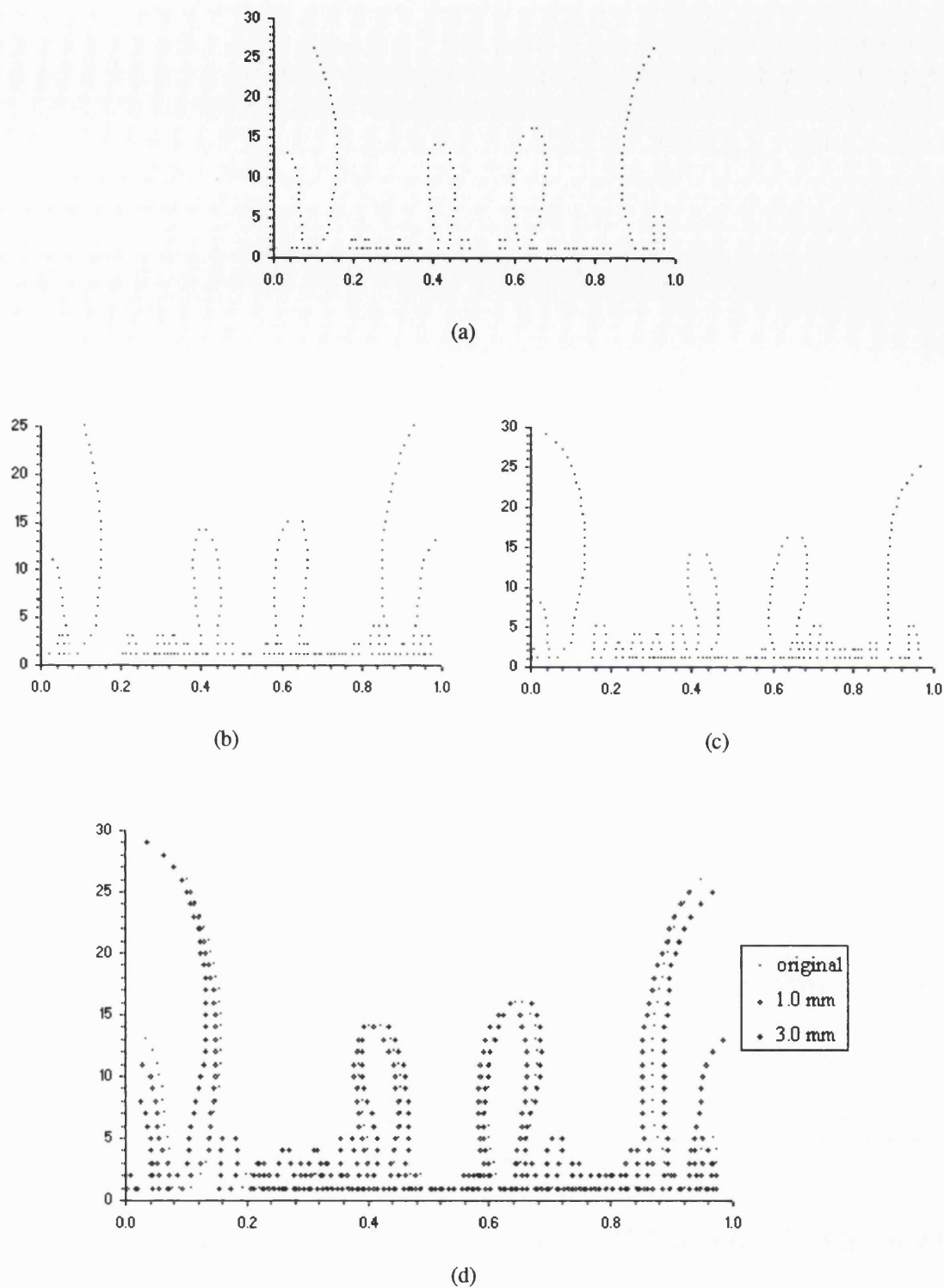


Figure 5-32 - Curvature scale space with added *normally distributed noise*.

This figure illustrates the curvature scale space descriptions of the *horizontal profiles* of figure 5-31. The original profile is shown in (a). The profiles with added 1.0 and 3.0 mm of *normally distributed noise* are shown in (b) and (c), respectively. All three descriptions are superimposed and shown in (d). The x-axis represents the path length parameter (in millimeters) and the y-axis represents the scale parameter.

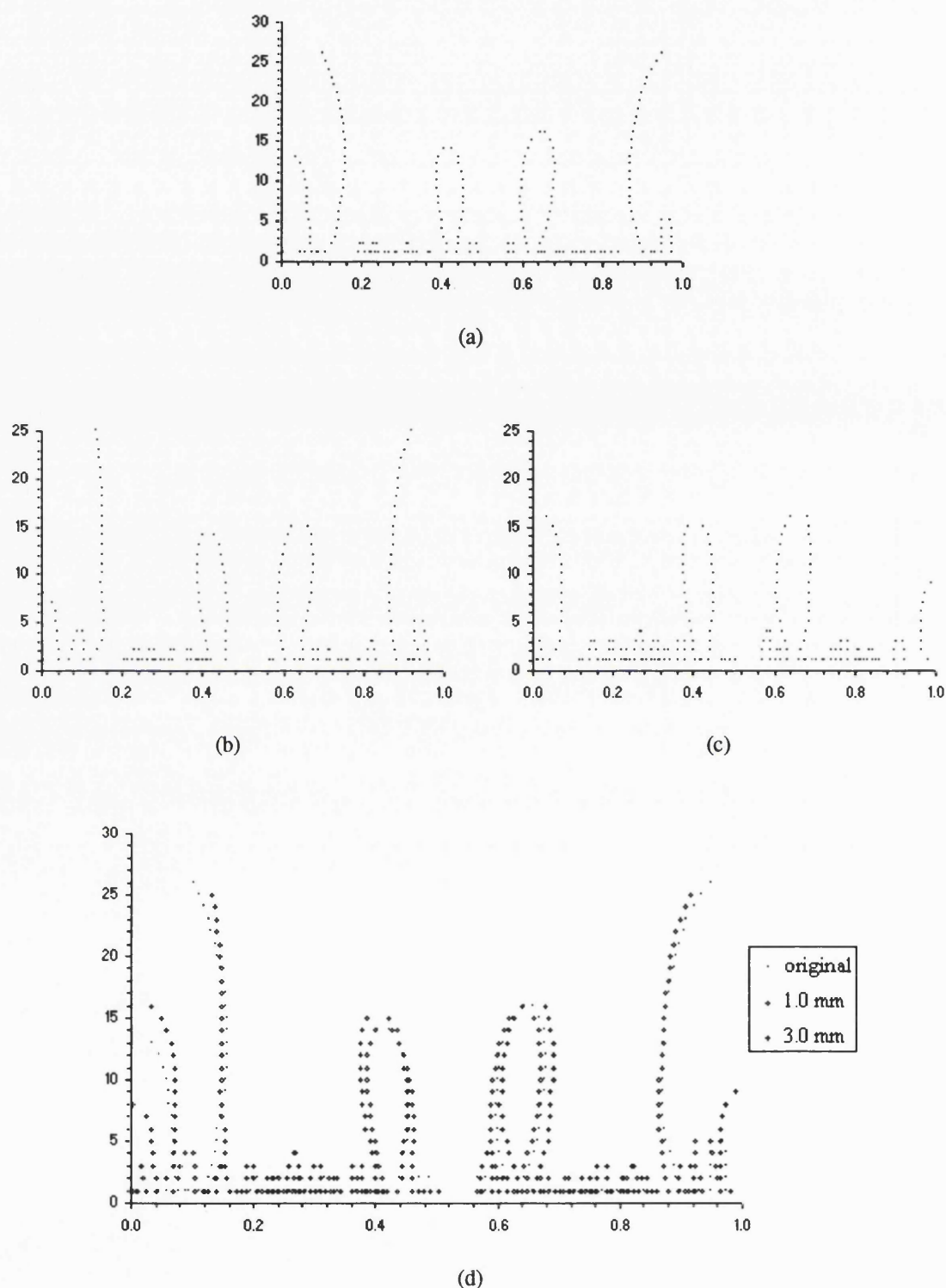


Figure 5-33 - Curvature scale space with added *quantization noise*.

This figure illustrates the curvature scale space descriptions of the *horizontal profiles* of figure 5-31. The original profile is shown in (a). The profiles with added 1.0 and 3.0 mm of *quantization noise* are shown in (b) and (c), respectively. All three descriptions are superimposed and shown in (d). The x-axis represents the path length parameter (in millimeters) and the y-axis represents the scale parameter.

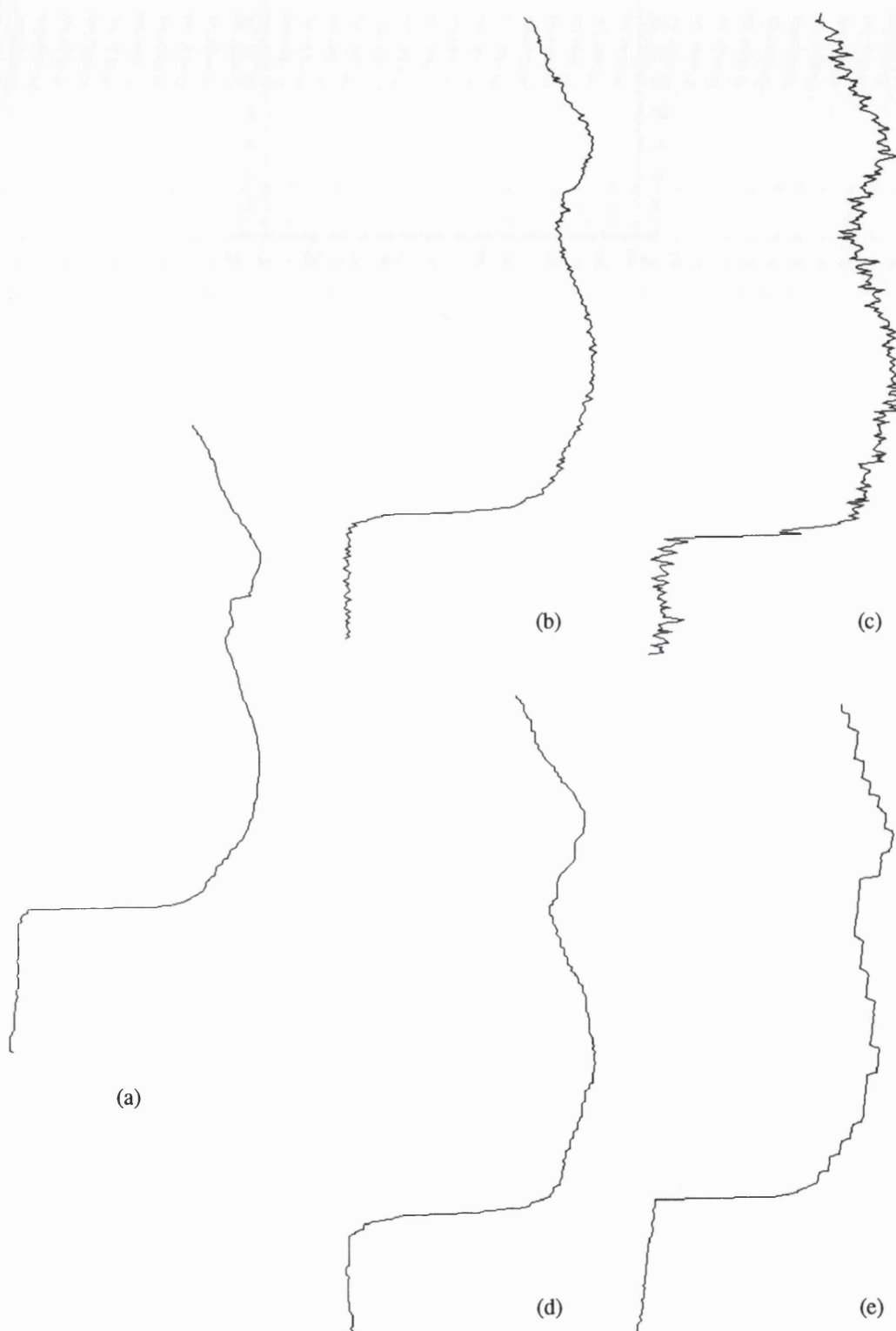


Figure 5-34 - Effects of added noise on the vertical profile outline.

The original profile is shown in (a). The profiles with added 1.0 and 3.0 mm of *normally distributed noise* are shown in (b) and (c), respectively. The profiles with added 1.0 and 3.0 mm of *quantization noise* are shown in (d) and (e), respectively.

Analyzing Facial Profiles: Evaluation of the Method

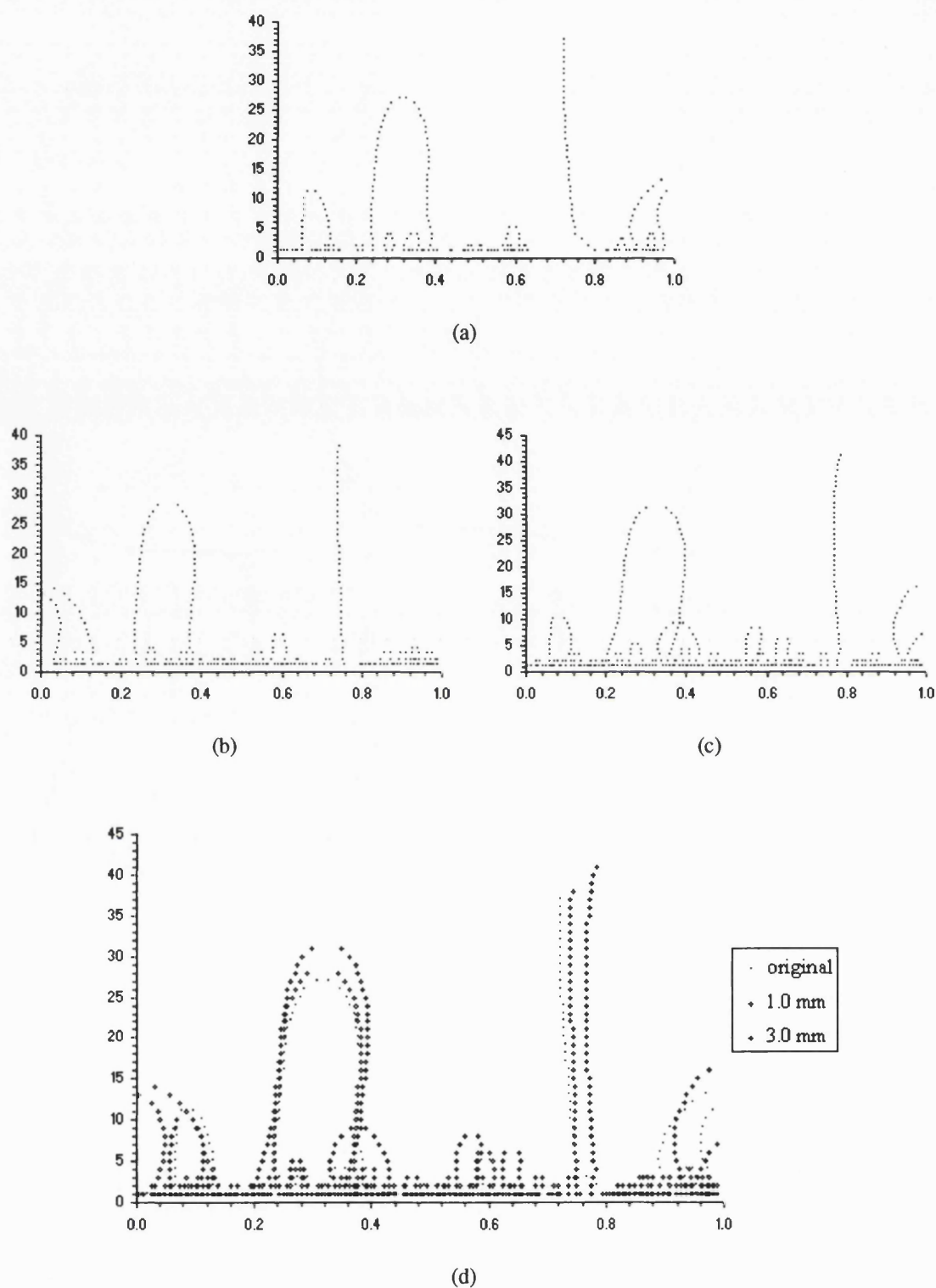


Figure 5-35 - Curvature scale space with added *normally distributed noise*.

This figure illustrates the curvature scale space descriptions of the *vertical profiles* of figure 5-34. The original profile is shown in (a). The profiles with added 1.0 and 3.0 mm of *normally distributed noise* are shown in (b) and (c), respectively. All three descriptions are superimposed and shown in (d). The x-axis represents the path length parameter (in millimeters) and the y-axis represents the scale parameter.

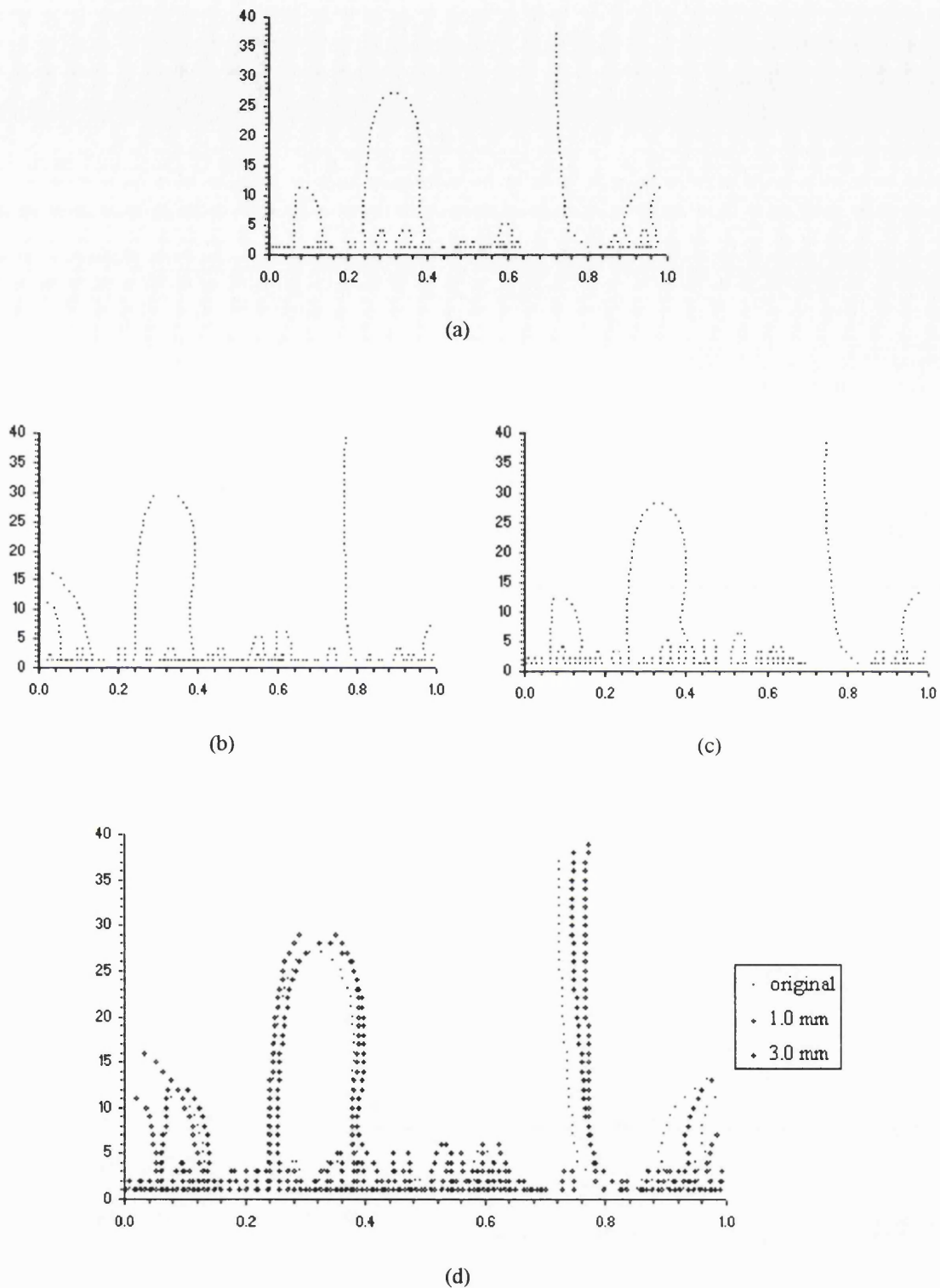


Figure 5-36 - Curvature scale space with added *quantization noise*.

This figure illustrates the curvature scale space descriptions of the *vertical profiles* of figure 5-34. The original profile is shown in (a). The profiles with added 1.0 and 3.0 mm of *quantization noise* are shown in (b) and (c), respectively. All three descriptions are superimposed and shown in (d). The x-axis represents the path length parameter (in millimeters) and the y-axis represents the scale parameter.

5.10.2. Stability and Repeatability

In this section, different aspects or stages of the process of achieving a segmentation of a given profile are considered. Basically, these consist of : (A) extracting a single profile from a database with the (x,y,z) coordinate points of the surface of the face (discussed in section 5.3) ; (B) deriving the qualitative descriptions, i.e. the curvature scale space and the interval tree (discussed in section 5.7) ; and (C) from these descriptions, divide the profile into segments by automatically locating a number of singular curvature points (discussed in section 5.8).

Three experiments were carried out to evaluate the stability and reproducibility of the segmentation process. In the first one, all stages of this process have been included, being executed on one face, at different times and by different operators. In the second experiment only the last stage (C) was included, again done by different operators and at different times. The third and last experiment of this section consider the stages (B) and (C) when dealing with one original profile and with versions of it, obtained after some mathematical transformations.

5.10.2.1. Experiment I

In this experiment, the stability and reproducibility of the segmentation method was tested by repeated recording and measurement. The 3D data set on one face was used, from which the mid-line vertical profile was extracted. The measurements consisted of dividing the profile into eleven segments by automatically defining twelve landmark points. The same segments were aimed at each time. This procedure was repeated on ten separate occasions and by three different individuals, in such a way that two individuals performed the entire procedure three times and one individual performed it four times.

The mean values, standard deviation and standard error for the set of measurements are shown in table 5-3, considering the profile path length and its normalized form. The landmarks are labeled and shown in figure 5-37.

In addition, the mean values, standard deviation and standard error for the ten sets of measurements considering the coordinate values (x-axis and y-axis) are shown

in table 5-4 and graphically illustrated in figure 5-38. The results show very little variation in the location of the landmarks.

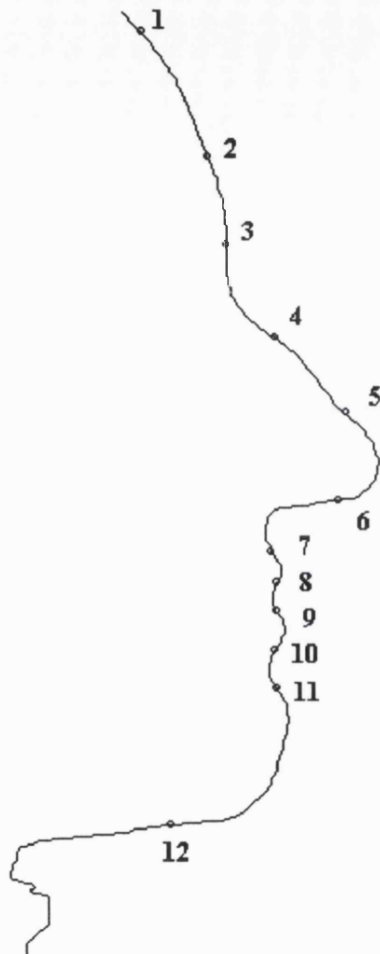


Figure 5-37 - Set of 12 automatically identified landmarks.

The landmarks are labeled and identified along the profile. The *mean values* are displayed in this graph.

landmark	Normalized Path Length (mm)		
	N = 10		
	ave	stdev	stderr
1	0.0225	0.0028	0.0009
2	0.1333	0.0042	0.0013
3	0.2064	0.0039	0.0012
4	0.2868	0.0039	0.0012
5	0.3615	0.0057	0.0018
6	0.4534	0.0072	0.0023
7	0.5281	0.0034	0.0011
8	0.5538	0.0072	0.0023
9	0.5787	0.0058	0.0018
10	0.6101	0.0072	0.0023
11	0.6462	0.0072	0.0023
12	0.7952	0.0166	0.0053

landmark	Path Length (mm)		
	N = 10		
	ave	stdev	stderr
1	4.73928	0.68208	0.21569
2	32.5617	1.48115	0.46838
3	51.2302	0.35093	0.11097
4	72.7064	0.57102	0.18057
5	91.9986	1.27233	0.40235
6	115.307	0.2433	0.07694
7	134.222	1.2718	0.40218
8	140.939	0.53104	0.16793
9	147.367	0.94875	0.30002
10	156.072	0.16033	0.0507
11	164.58	0.63322	0.20024
12	204.017	6.07442	1.9209

Table 5-3- Landmark variation (experiment I).

N is the number of times each set of twelve landmarks was defined. The mean (ave), standard deviation (stdev) and standard error (stderr) are presented.

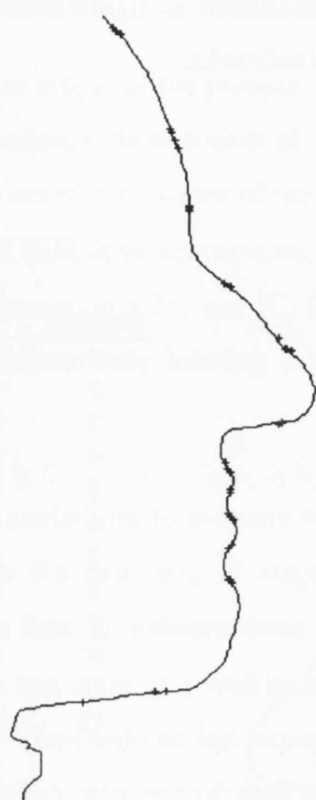


Figure 5-38 - Landmark variation (experiment I).

This figure illustrates the variation of each landmark when automatically identified and located along the profile. All *ten sets of twelve landmarks* are displayed in this graph.

landmark	Coordinate values (mm)					
	N = 10					
	X			Y		
	ave	stdev	stderr	ave	stdev	stderr
1	52.181	0.510	0.161	-110.069	0.590	0.187
2	62.308	0.391	0.124	-84.398	1.343	0.425
3	65.401	0.067	0.021	-66.126	0.424	0.134
4	72.722	0.587	0.186	-46.932	0.425	0.135
5	83.781	0.798	0.252	-31.378	1.037	0.328
6	82.525	0.179	0.057	-13.058	0.144	0.045
7	72.288	0.419	0.133	-2.639	0.990	0.313
8	73.109	0.065	0.021	3.712	0.263	0.083
9	73.001	0.380	0.120	9.854	0.667	0.211
10	72.846	0.198	0.063	18.034	0.302	0.095
11	72.994	0.187	0.059	26.064	0.321	0.102
12	56.598	5.801	1.834	54.215	1.162	0.367

Table 5-4- Variation of the landmark's coordinate values (experiment I).

5.10.2.2. Experiment II

This experiment tested the stability and reproducibility of the method of segmentation by repeated measurement only.

Initially, a mid-line vertical profile was chosen and the curvature scale space and interval tree descriptions were derived. Then, the experiment consisted of dividing the profile into eleven segments by automatically defining twelve landmark points using the interval tree description. This procedure was repeated on ten separate occasions, by three different individuals. The same segments were aimed at each time.

The mean values, standard deviation and standard error for the set of measurements are shown in table 5-5, considering the profile path length and its normalized form. The landmarks are labeled and shown in figure 5-39 .

In addition, the mean values, standard deviation and standard error for the ten sets of measurements considering the coordinate values (x-axis and y-axis) are also shown in table 5-6 and graphically illustrated in figure 5-40.

The results of this experiment shows that once the interval tree description has been derived, the same set of landmarks can be repeatedly and objectively identified, producing an extremely reliable segmentation process.

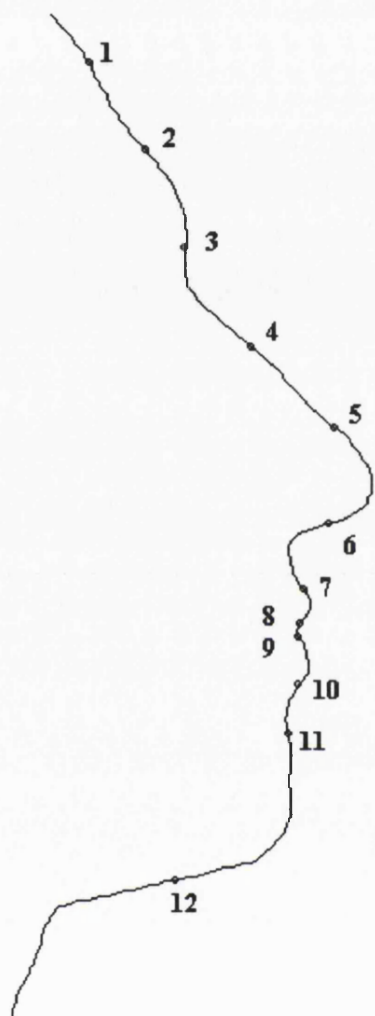


Figure 5-39 - Set of 12 automatically identified landmarks.

The landmarks are labeled and identified along the profile. The *mean values* are displayed in this graph.

landmark	Normalized Path Length (mm)		
	N = 10		
	ave	stdev	stderr
1	0.052	0.00E+00	2.19E-18
2	0.129	0.00E+00	8.78E-18
3	0.209	0.00E+00	8.78E-18
4	0.301	0.00E+00	1.76E-17
5	0.382	7.02E-09	0.00E+00
6	0.478	0.00E+00	0.00E+00
7	0.542	0.00E+00	3.51E-17
8	0.570	1.40E-08	3.51E-17
9	0.586	9.93E-09	3.51E-17
10	0.623	0.00E+00	3.51E-17
11	0.663	0.00E+00	0.00E+00
12	0.827	1.40E-08	3.51E-17

landmark	Path Length (mm)		
	N = 10		
	ave	stdev	stderr
1	12.317	2.25E-07	5.62E-16
2	33.591	0.00E+00	2.25E-15
3	56.044	8.99E-07	0.00E+00
4	81.874	1.27E-06	0.00E+00
5	104.327	0.00E+00	0.00E+00
6	131.240	0.00E+00	8.99E-15
7	150.304	2.54E-06	8.99E-15
8	158.129	1.80E-06	0.00E+00
9	161.446	0.00E+00	0.00E+00
10	172.637	0.00E+00	8.99E-15
11	183.850	5.09E-06	8.99E-15
12	228.540	0.00E+00	8.99E-15

Table 5-5- Landmark variation (experiment II).

N is the number of times each set of twelve landmarks was defined. The mean (ave), standard deviation (stdev) and standard error (stderr) are presented.



Figure 5-40 - Landmark variation (experiment II).

This figure illustrates the variation of each landmark when automatically identified and located along the profile. All *ten sets of twelve landmarks* are displayed in this graph.

landmark	Coordinate values (mm)					
	N = 10					
	X			Y		
	ave	stdev	stderr	ave	stdev	stderr
1	55.989	6.36E-07	2.01E-07	-77.003	1.27E-06	4.02E-07
2	65.925	0.00E+00	0.00E+00	-58.356	1.56E-06	4.92E-07
3	72.768	8.99E-07	2.84E-07	-37.628	6.36E-07	2.01E-07
4	84.153	0.00E+00	0.00E+00	-15.897	2.25E-07	7.11E-08
5	98.504	0.00E+00	0.00E+00	1.242	0.00E+00	0.00E+00
6	97.398	0.00E+00	0.00E+00	22.060	4.50E-07	1.42E-07
7	93.251	0.00E+00	0.00E+00	36.259	0.00E+00	0.00E+00
8	92.584	0.00E+00	0.00E+00	43.419	0.00E+00	0.00E+00
9	92.171	0.00E+00	0.00E+00	46.366	0.00E+00	0.00E+00
10	92.177	2.20E-06	6.96E-07	56.745	0.00E+00	0.00E+00
11	90.418	0.00E+00	0.00E+00	67.441	0.00E+00	0.00E+00
12	70.919	0.00E+00	0.00E+00	99.324	1.27E-06	4.02E-07

Table 5-6- Variation of the landmark's coordinate values (experiment II).

5.10.2.3. Experiment III

In this experiment the stability and reproducibility of the method of segmentation was tested by using four mid-line vertical profiles : one original plus three transformed versions of it, including uniform scaling, translation and rotation.

In every case, the stages (B) and (C) of the segmentation process were performed. Again, the same segments were aimed at each time.

The results are shown below. Figure 5-41 illustrates the curvature scale space description derived for the original profile outline and after each transformation, while figure 5-42 illustrates the segmented profiles.

This experiment shows that the curvature scale space description is stable when the profile outline has been transformed by uniform scaling, translation and rotation. Furthermore, it shows that the segmentation of the profile is very reliable even under these circumstances.

Analyzing Facial Profiles: Evaluation of the Method

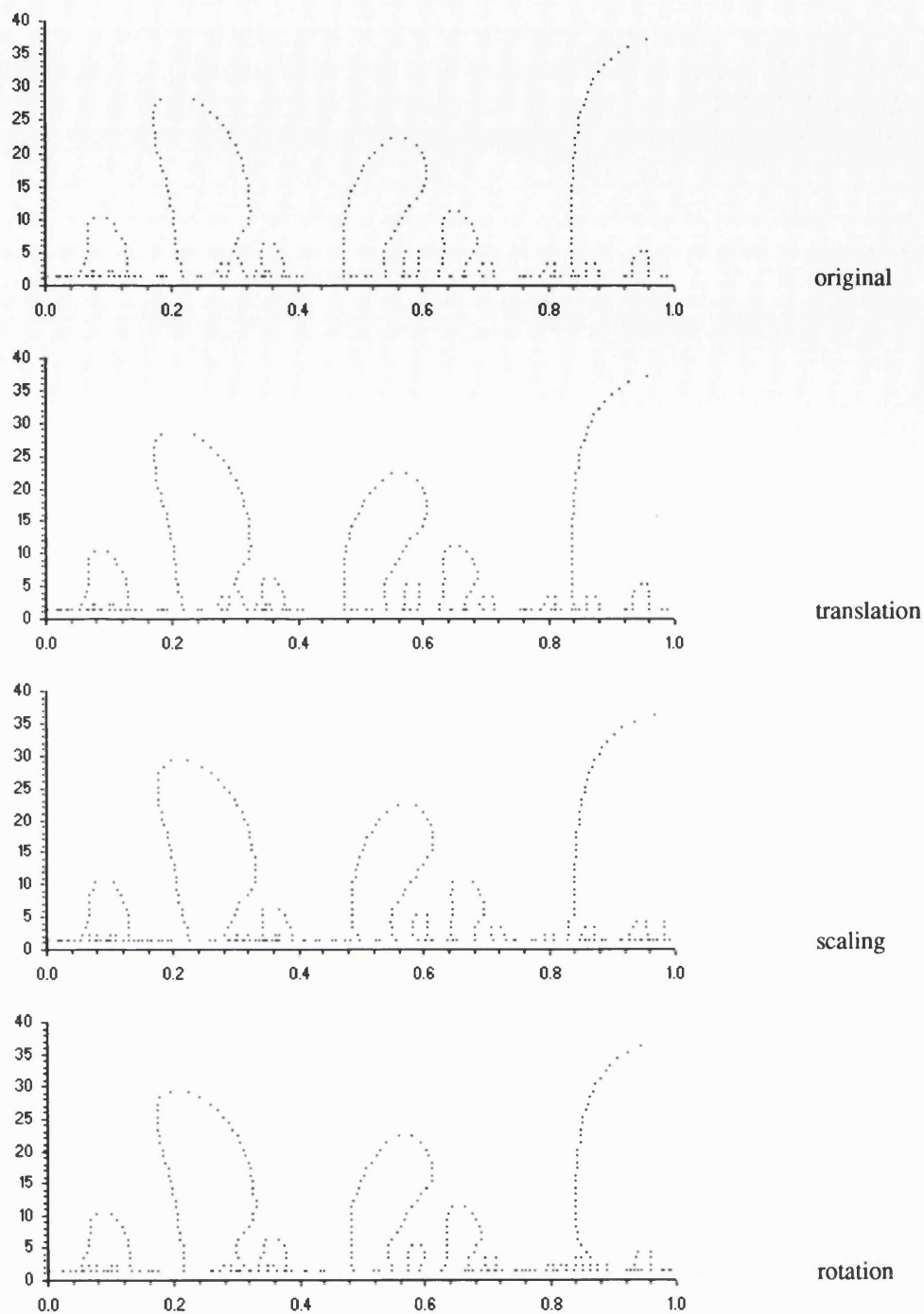


Figure 5-41 - Curvature scale space descriptions (experiment III).

This figure illustrates the curvature scale space description for the original profile and for the profiles generated after each transformation of uniform scaling, translation and rotation. The x-axis represents the path length parameter (in millimeters) and the y-axis represents the scale values. The profiles are illustrated in figure 5-42.

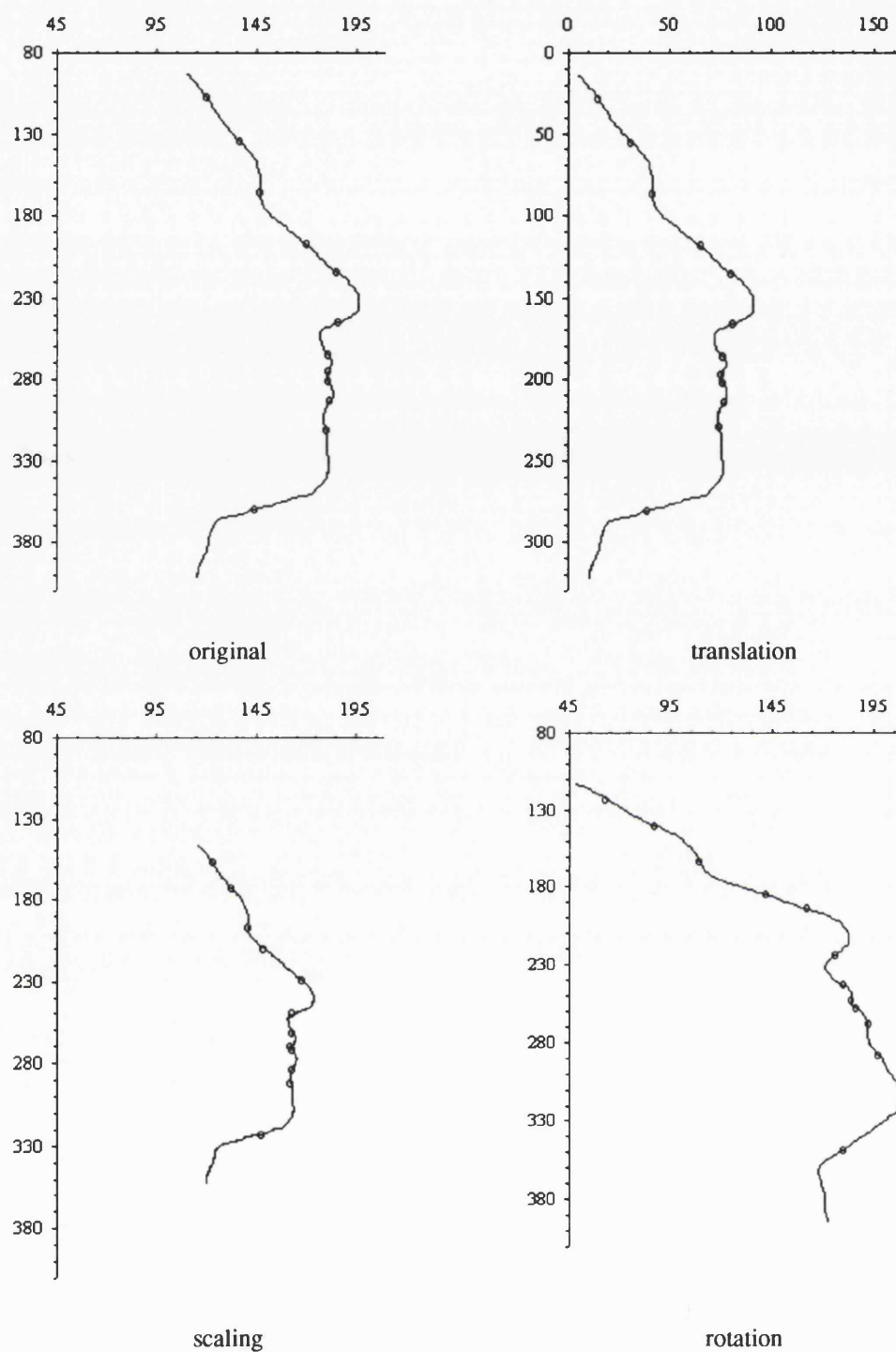


Figure 5-42 - Segmented profiles (experiment III).

This figure illustrates the result of the segmentation process for the original profile and for the profiles generated after each transformation of uniform scaling, translation and rotation. Eleven segments were obtained by automatically identifying and locating twelve landmarks along the profile (indicated by circles). Both axes are in millimeters.

5.10.3. Sensitivity to Local and Global Shape Changes

The curvature scale space description qualitatively reflect the shape of the underlying features of facial profiles. In fact, it provides an invariant and unique description, so that curve segments which have similar shape yield similar descriptions (see discussion on shape representation criteria in section 4.4.1).

The investigation carried out in this section shows how global and localized shape changes are reflected in the configuration (or pattern) of the zero crossing contours of the curvature scale space description (CSS). Although any facial profile would be valid for this test, the mid-line vertical outline carries a special meaning due to the large number of facial features it contains, and also due to its widespread use in clinical applications.

5.10.3.1. Locally Altering Curve Segments

A number of points (including extrema of curvature and inflection points) was selected from the original mid-line vertical profile, and used as control points of a fourth order polynomial function. In this way, a profile could be mathematically generated (i.e. through interpolation), allowing changes to be made locally on different parts of it.

In order to have a better understanding of how and where such changes would happen in the curvature scale space description, the profile was divided into four sections, each one including one or more anatomically meaningful curve segment (e.g. the nose).

The sections were altered in turns, that is when one was being altered the other three remained unchanged. Since the position of the control points would determine the shape of the outline, the alterations were produced by manually moving (i.e. with the user's interaction) these points, individually, so as to affect only their corresponding segments. Even though no special criteria was adopted when altering the shape of the curve segments, the aim was to significantly alter them and at the same

Analyzing Facial Profiles: Evaluation of the Method

time keep a relationship with their neighbors, so that the final outline would resemble possible clinical cases.

The main features of the first section were the brow ridge and the soft tissue nasion. In the second section, the soft tissue nasion, nose and subnasale segment were included. Section three was composed of subnasale segment, lips, mouth and labial-mental fold. Lastly, the forth section contained the labial-mental fold and the chin segments. There is, purposely, an overlapping segment for every section.

In fact, a similar division was adopted by Leonardo Da Vinci when representing “relevant traits” by dividing the face into four main parts, hence creating variations such as fool’s and monstrous faces (see section 3.1).

Figure 5-43 illustrates the unmodified profile and its curvature scale space description. In addition, an alternative display (section 5.7.1) is presented to help understand the patterns of the zero crossing contours and visually relate them to the underlying features of the profile (5-43(c)).

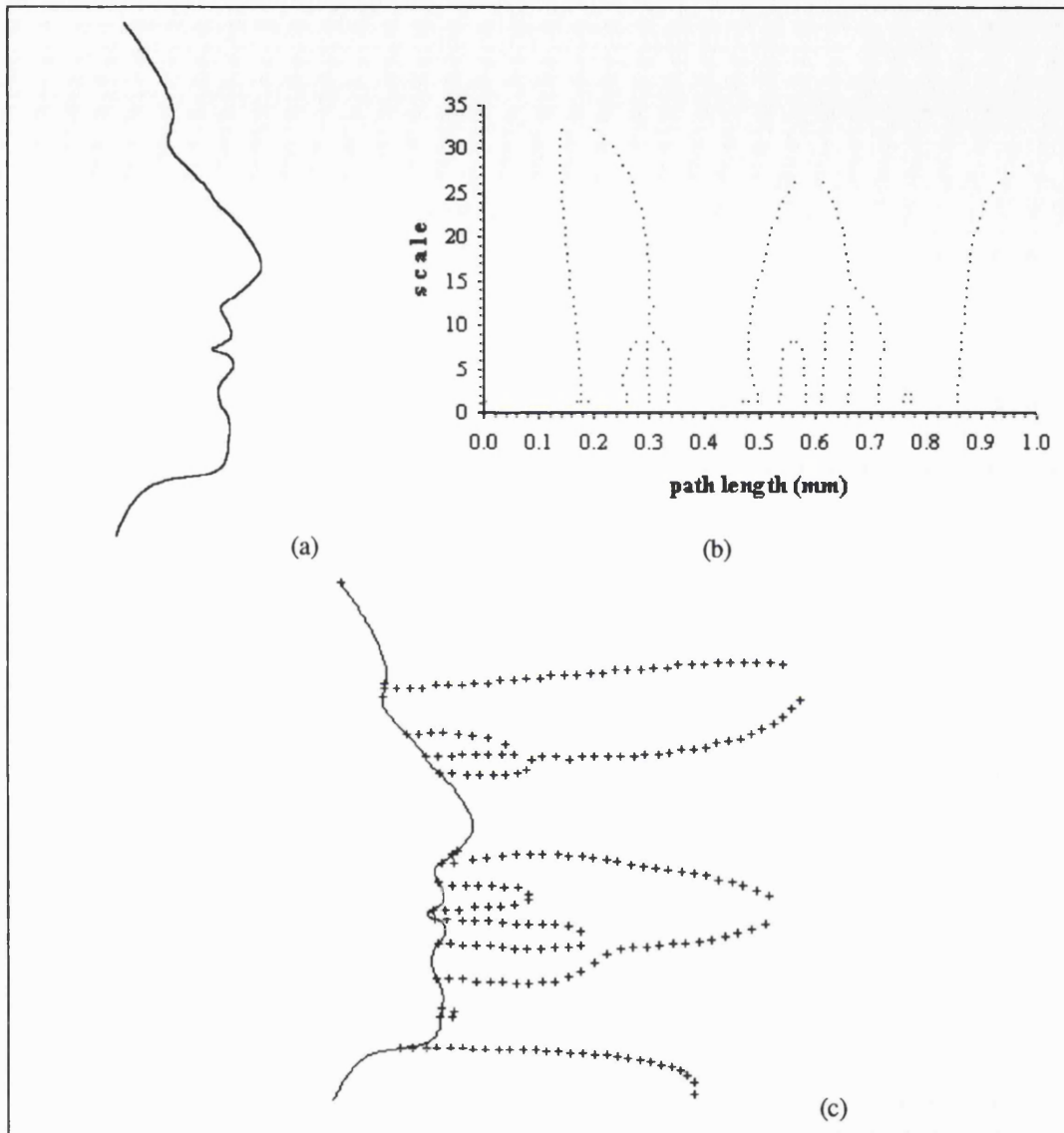


Figure 5-43 - The unmodified mid-line vertical profile outline and its CSS description.

The unmodified profile is shown on (a), and the curvature scale space description (CSS) is shown (b). On (c) the zero crossing contours can be related to the underlying facial features.

Analyzing Facial Profiles: Evaluation of the Method

The profile representing section one (figure 5-44(a)) had the brow ridge segment moved outwards, increasing its convexity, and the soft tissue nasion moved to the left and downwards, also increasing its concavity. The resulting CSS (figure 5-44(b)) shows that only the first few zero crossing contours were affected (located between 0 to 0.4 mm on the x-axis). Their pattern now indicates that a new contour has appeared (around 0.1 mm) and that the third and fourth contours changed, splitting the arches they were forming before.

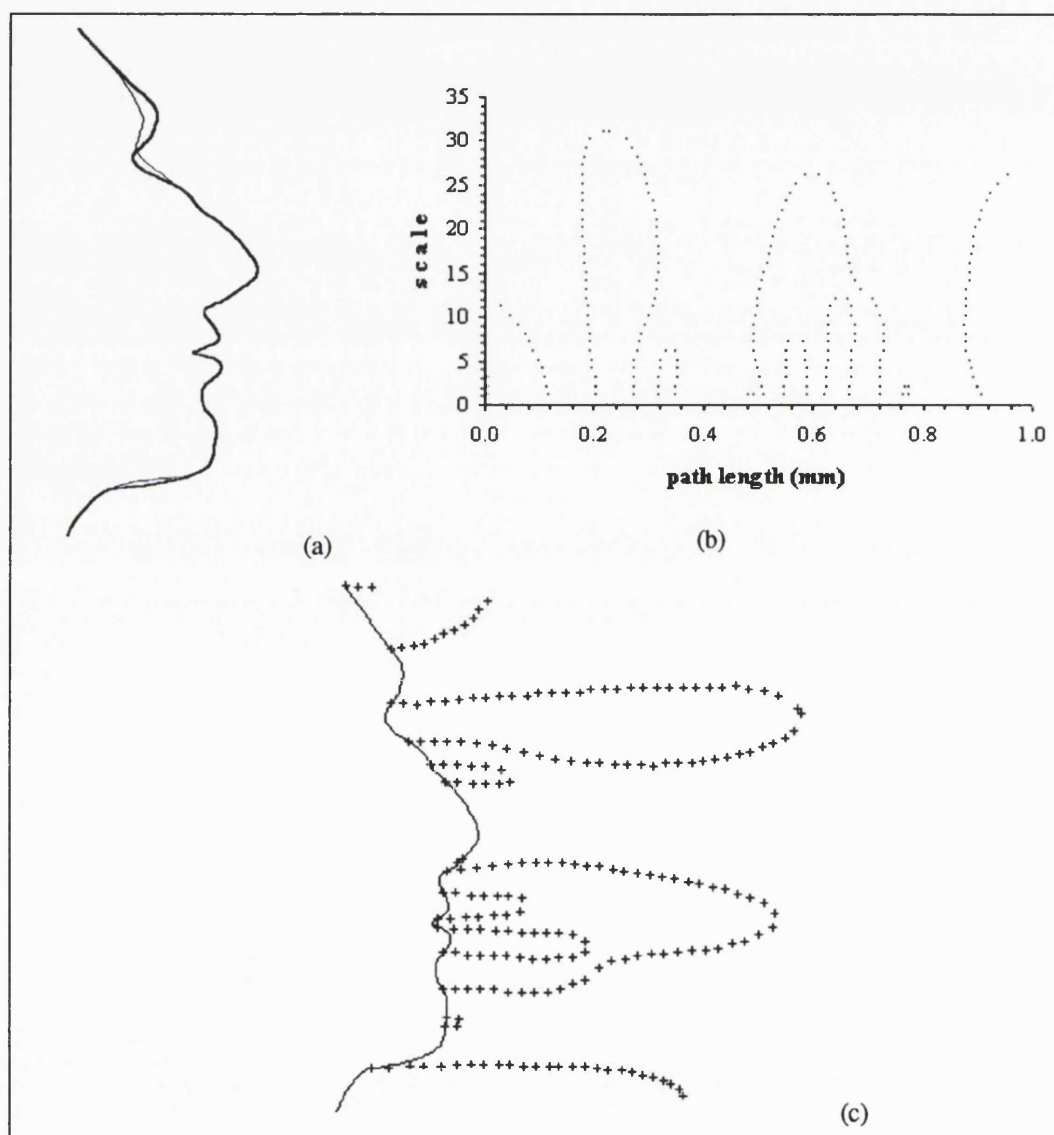


Figure 5-44 - The modified profile outlines and their CSS descriptions - (section I).

Alterations for *section one*. The original profile (light outline) and the modified profile (darker outline) are shown on (a). The curvature scale space description (CSS) is shown on (b). On (c) the zero crossing contours can be related to the underlying facial features.

In the profile of section two (figure 5-45(a)), the soft tissue nasion was made more concave and the nose completely re-shaped, having an accentuated spinal base, pointed tip and a significantly long and slightly concave base, which also affected the subnasale segment. The CSS (figure 5-45(b)) shows some changes on the first two contours, which now don't join at their maximum scale values, indicating the marked alterations of both soft tissue nasion and nose spine. The changes in the fourth zero crossing contour, reflecting the deeper subnasale segment, changed the entire configuration in the middle part of the description.

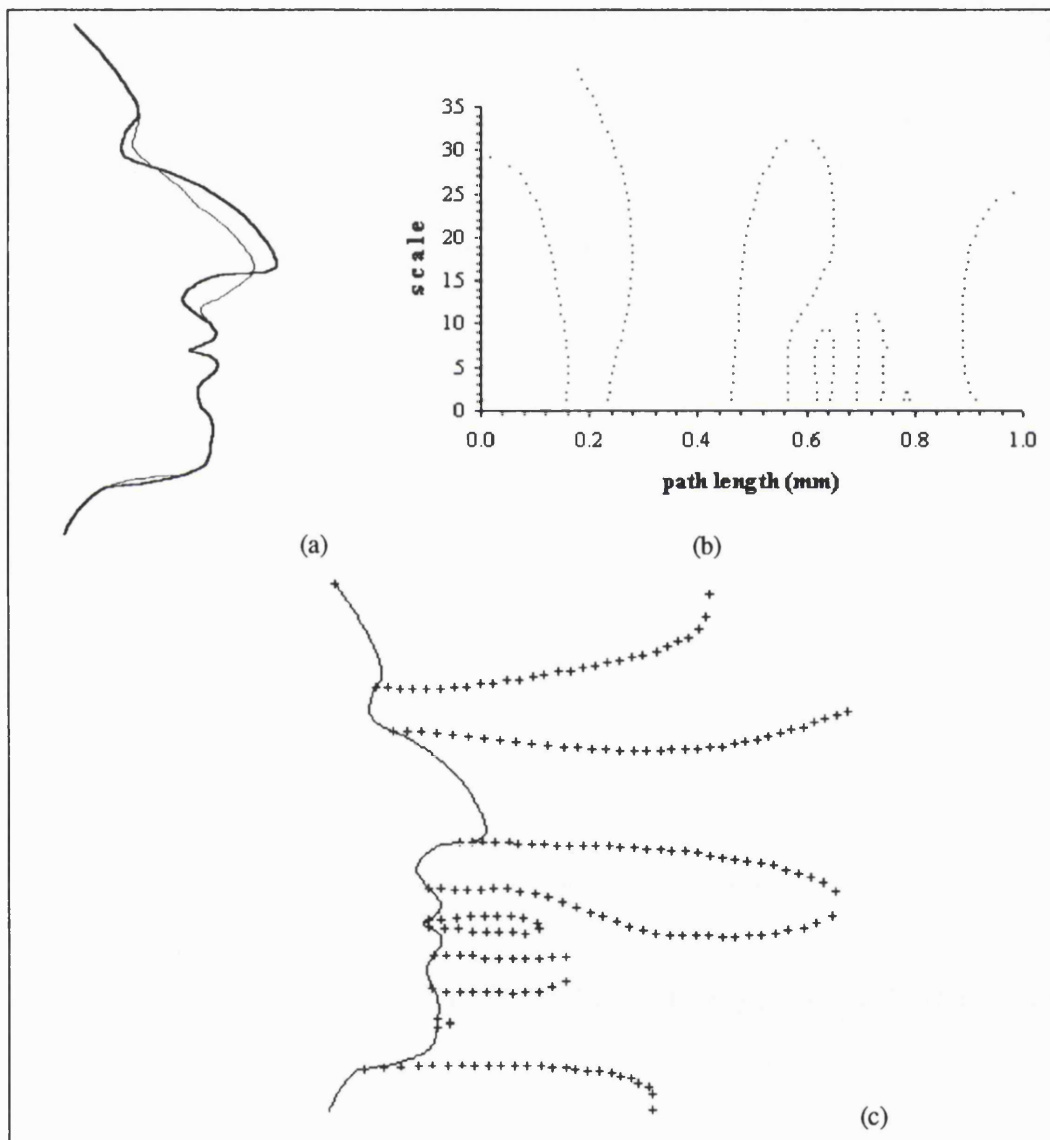


Figure 5-45 - The modified profile outlines and their CSS descriptions - (section 2).

Alterations for *section two*. The original profile (light outline) and the modified profile (darker outline) are shown on (a). The curvature scale space description (CSS) is shown on (b). On (c) the zero crossing contours can be related to the underlying facial features.

Analyzing Facial Profiles: Evaluation of the Method

Three distinct profiles were created for section three, altering the subnasale segment and upper lip in the first outline (figure 5-46(a)), the mouth and lower lip in the second outline (figure 5-47(a)) and the upper and lower lips plus the mouth in the third outline (figure 5-48(a)). Each CSS description showed a particular change in the pattern of zero crossing contours, mainly affecting a specific region (between 0.4 and 0.8 mm) along the path length axis.

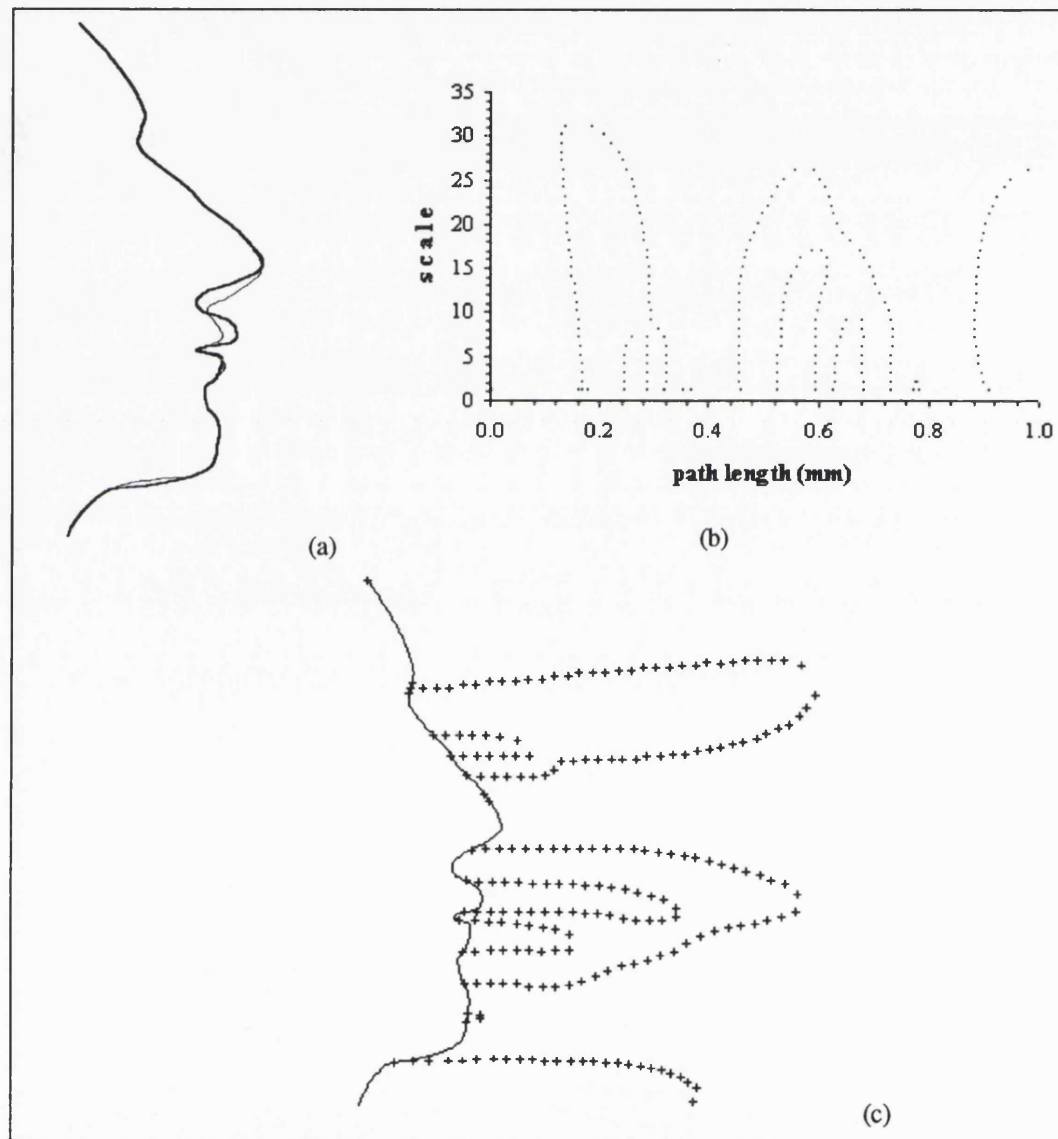


Figure 5-46 - The modified profile outlines and their CSS descriptions - (section 3).

Alterations for *section three, first outline*. The original profile (light outline) and the modified profile (darker outline) are shown on (a). The curvature scale space description (CSS) is shown on (b). On (c) the zero crossing contours can be related to the underlying facial features.

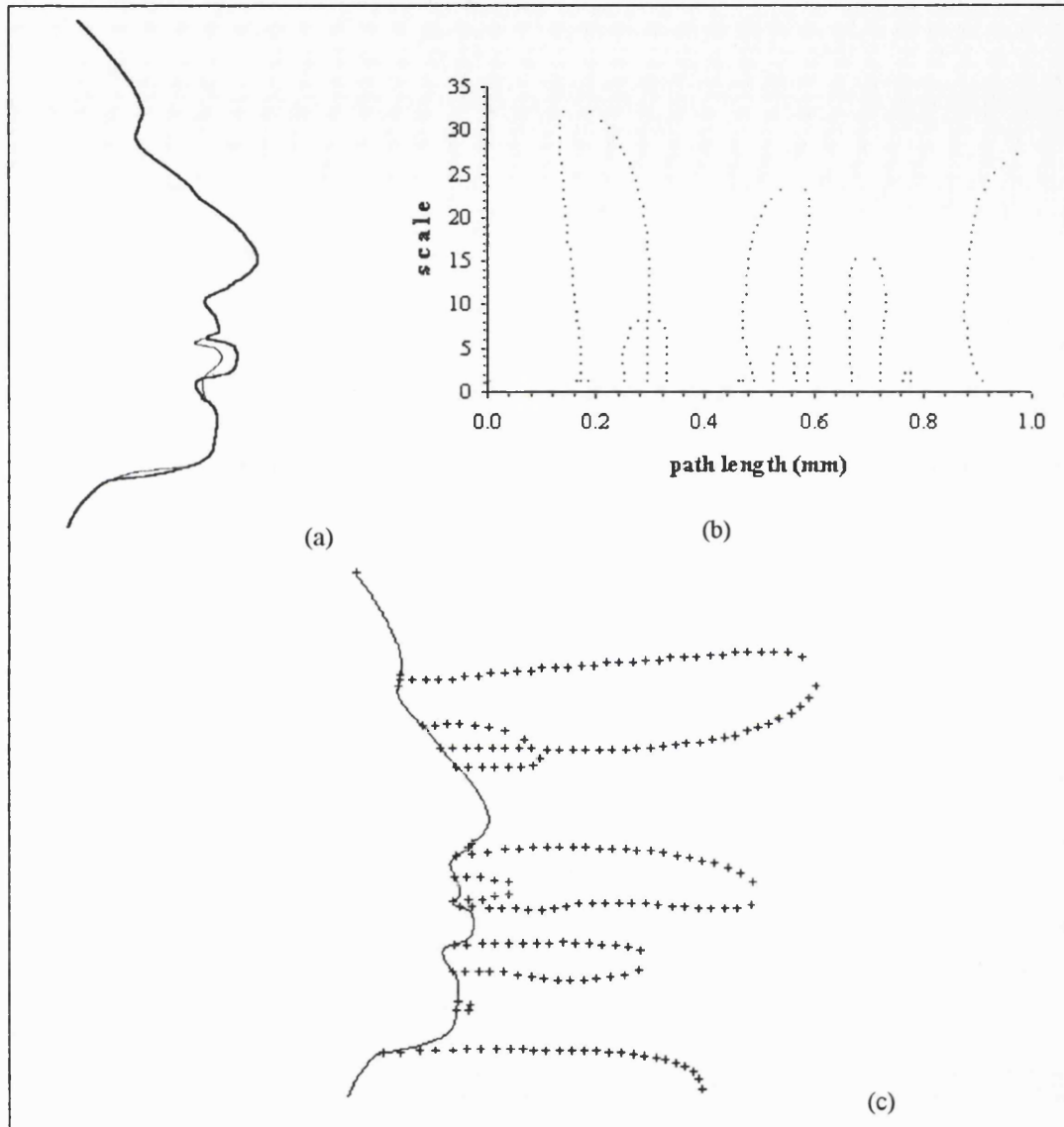


Figure 5-47 - The *modified profile* outlines and their CSS descriptions - (*section 3*).

Alterations for *section three, second outline*. The original profile (light outline) and the modified profile (darker outline) are shown on (a). The curvature scale space description (CSS) is shown on (b). On (c) the zero crossing contours can be related to the underlying facial features.

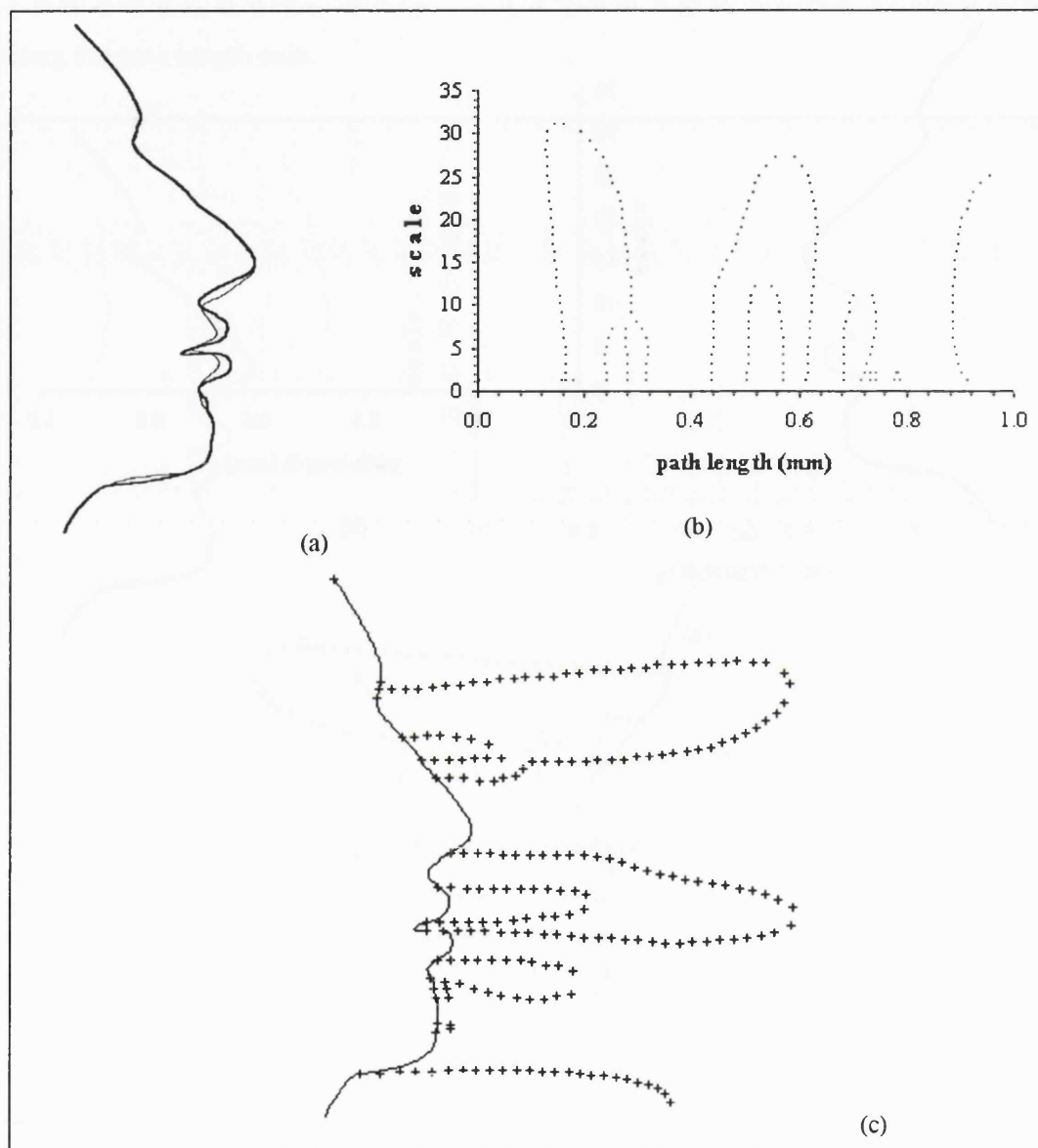


Figure 5-48 - The modified profile outlines and their CSS descriptions - (section 3).

Alterations for *section three, third outline*. The original profile (light outline) and the modified profile (darker outline) are shown on (a). The curvature scale space description (CSS) is shown on (b). On (c) the zero crossing contours can be related to the underlying facial features.

The outline of figure 5-49 refers to section four, displaying a more prominent chin and greater labio-mental fold concavity. Again, the only noticeable changes involve the contours forming the large arch in the central region of the description.

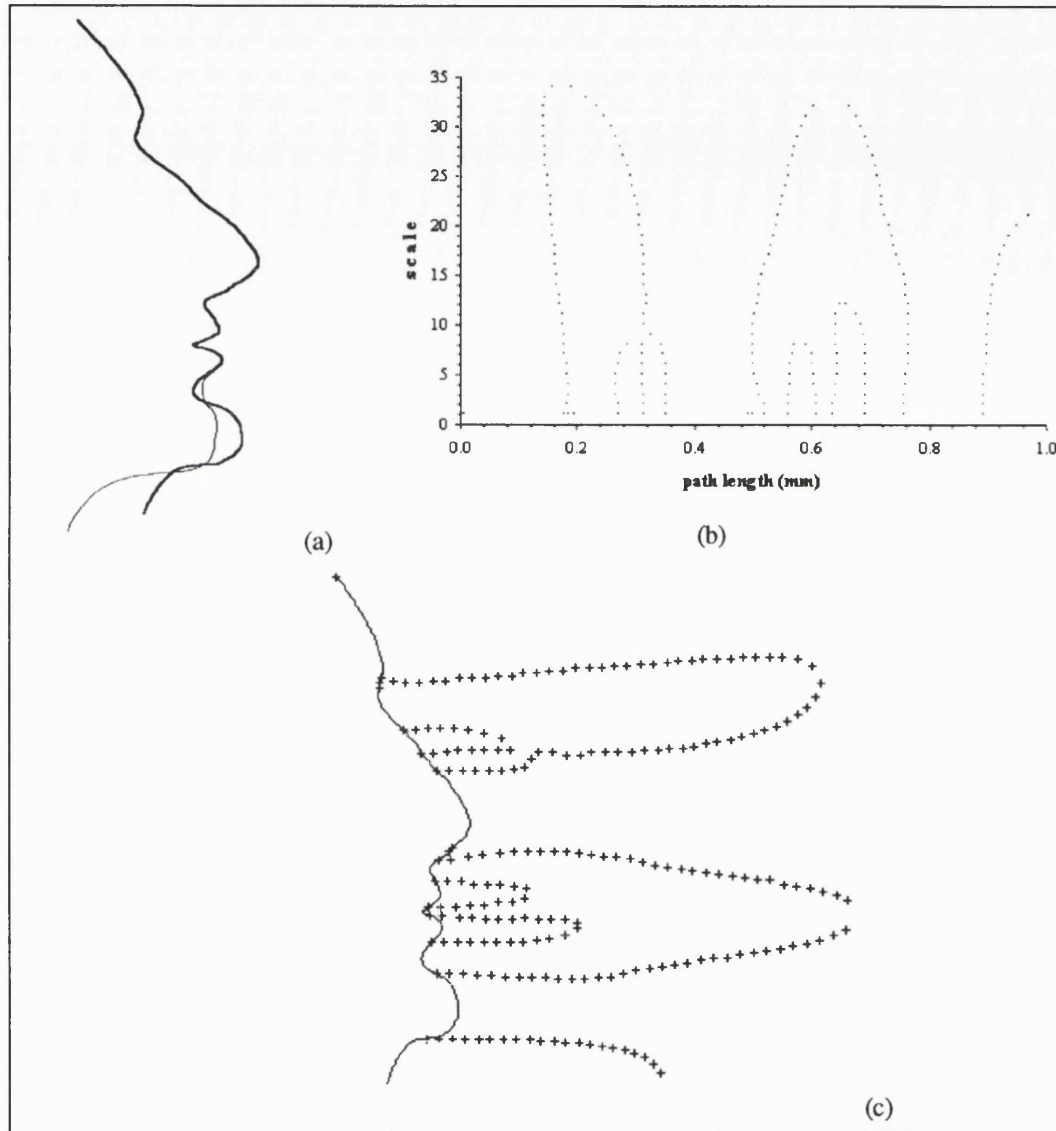


Figure 5-49 - The modified profile outlines and their CSS descriptions - (section 4).

Alterations for *section four*. The original profile (light outline) and the modified profile (darker outline) are shown on (a). The curvature scale space description (CSS) is shown on (b). On (c) the zero crossing contours can be related to the underlying facial features.

These results suggest that the curvature scale space description responds quite well to local shape variation, presenting changes in the pattern of the zero crossing contours which were also localized (along the x-axis).

Another observation to be made from these results is related to the arches seen on the CSS description. As expected, changes on the pattern of the zero crossing contours directly affect the arches they form. In many cases, concave curve segments lead to an arch being formed, as seen in the example of figure 5-45 for the subnasale, mouth and labial-mental fold segments. However, there are other cases in which an arch results from a convex segment, as illustrated by the upper and lower lips in figures 5-44 and 46, for example. This is due to the fact that these concave and convex segments are connected together, and their combined change may alter how the arch is formed. Consequently, an arch formed by two individual zero crossing contours cannot always be directly associated to a specific feature of the profile.

5.10.3.2. Globally Altering Curve Segments

Global alterations imply that all features along the profile outline are affected simultaneously. The use of direct transformations of the profile points by uniform scaling, translation and rotation have been discussed in sections 4.4.4 and 5.10.2.3 .

Another way to achieve global alterations has been reported by Coombes (1993), based on the work of Fright (et al 1993) which used 3D data sets of the human head. Their technique consisted of changing the surface of the entire head in a caricaturing fashion, i.e. by exaggerating the more prominent features when compared with those which are less prominent. The changes were computed radially to a central axis, defined as passing through the top of the head and the tip of the chin. In their work, the surface of an individual's face was altered with respect to an average face. Depending on the extent of the exaggeration, a different caricature could be created.

Adopting the same approach here, I have used a facial data set from the optical surface scanner (see section 4.6.1) which was then altered with respect to a geometric object, in this case an ellipsoid. Therefore, with a zero percentage of the exaggeration applied, the result would be an ellipsoid, and with one hundred percent, the result would be the individual's face. The values of 50% and 200% were used to create two caricatured faces, from which the mid-line vertical profiles were then extracted.

Figure 5-50 illustrates the original and the altered profiles together with their curvature scale space descriptions. The alternative displays of each case is shown in figure 5-51.

The fifty percent caricatured profile (figure 5-50(b)) shows the same basic features as the original profile (figure 5-50(a)), in an apparent reduced way. The CSS shows a remarkable similarity in the pattern of all zero crossing contours, with some reductions in the maximum scale values (i.e. at the top of the contours).

The exaggerated features of the second caricature (figure 5-50(c)) give rise to a different pattern of zero crossing contours, involving basically all areas of the path length axis.

Both results seem to suggest that global shape alterations made in the profile outline are also reflected in the pattern of the zero crossing contours, globally involving the entire x-axis.

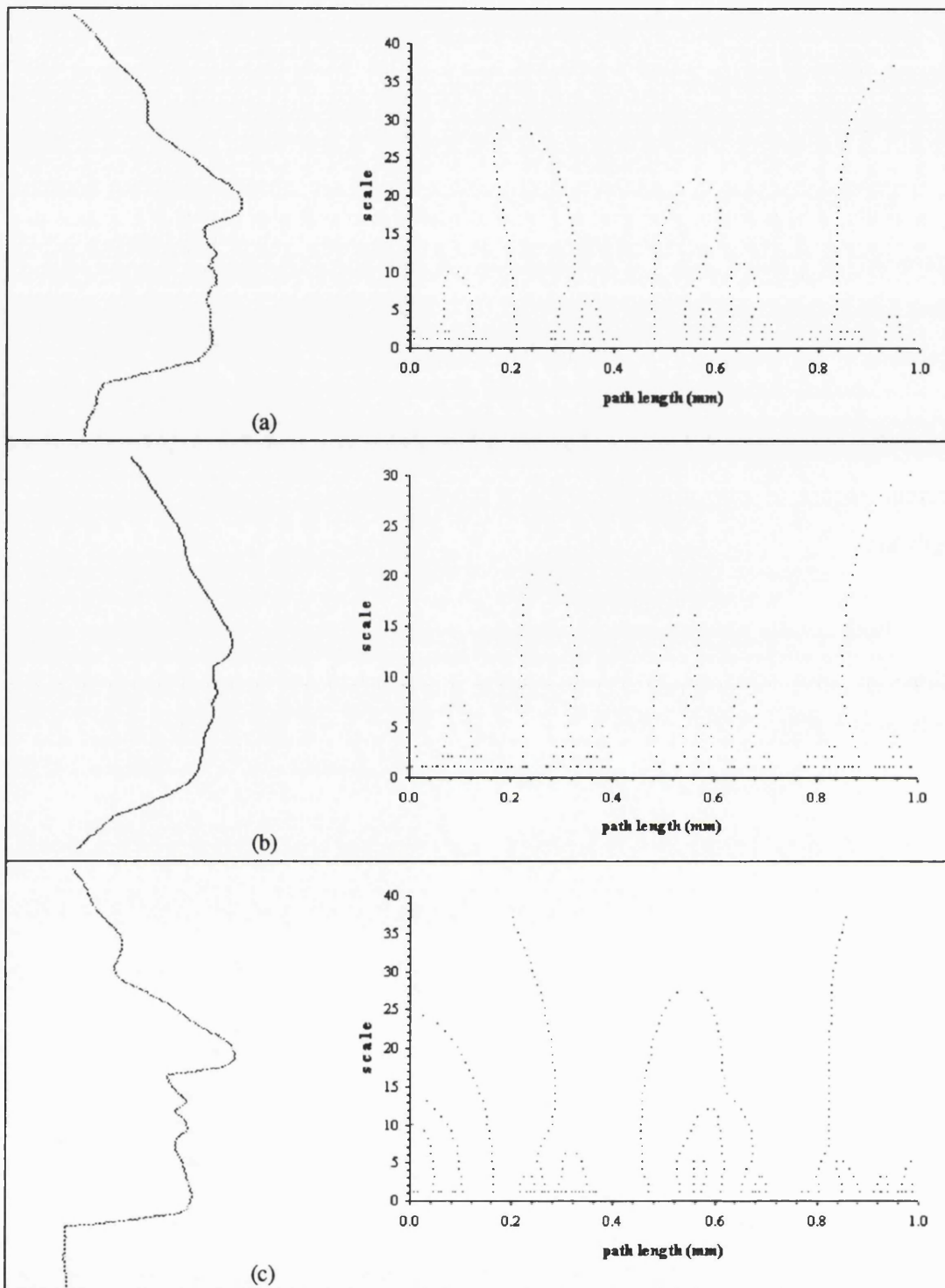
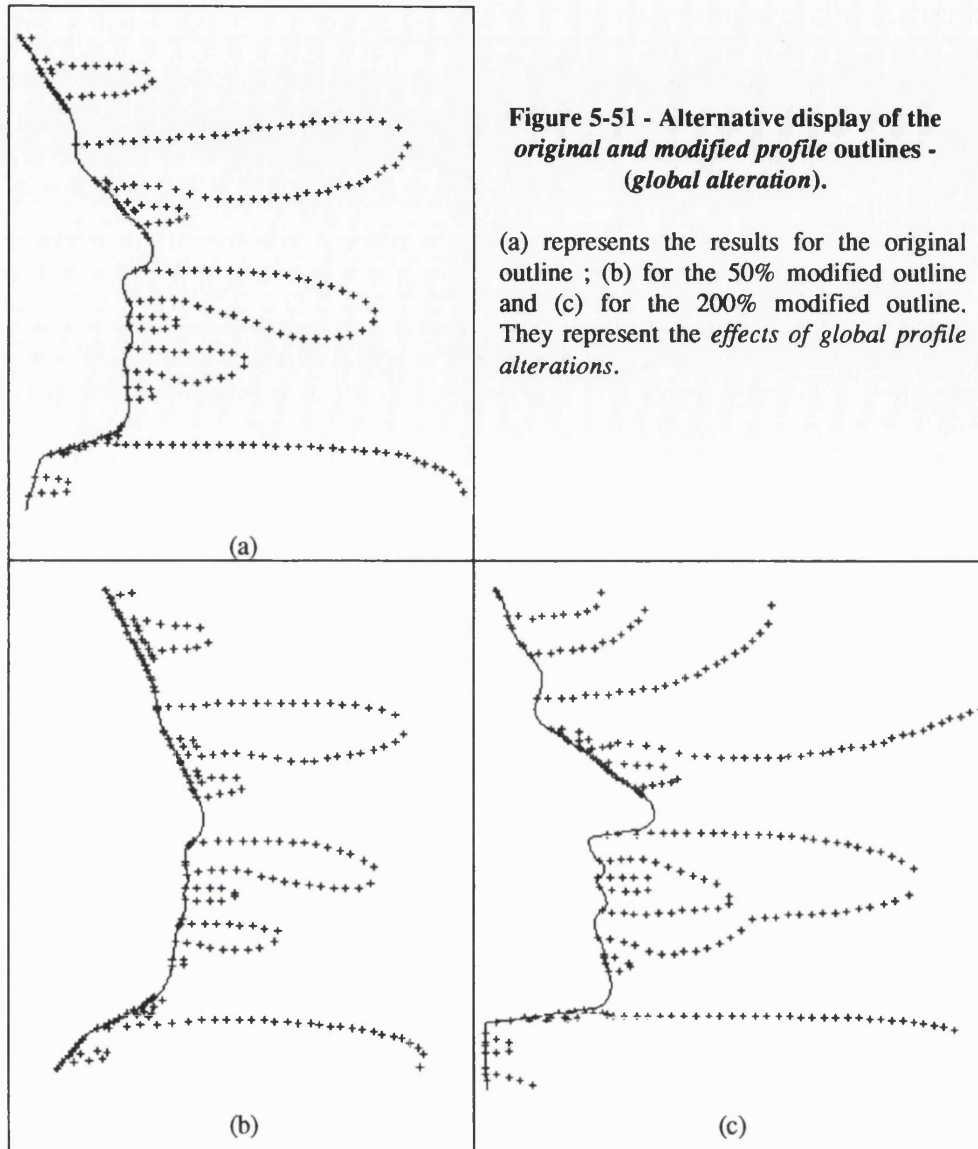


Figure 5-50 - The original and modified profile outlines and their CSS descriptions - (global alteration).

(a) represents the results for the original outline ; (b) for the 50% modified outline and (c) for the 200% modified outline. They represent the *effects of global profile alterations*.



5.11. Summary

A complete description of the method of analysis of facial profiles has been presented in this chapter. Initially, the profiles are extracted from a 3D data set of coordinate points representing the surface of the face. By using the approach of scale space techniques to planar curves, a first qualitative description called curvature scale space is derived, which fully describes the behavior of the inflection points (or zero crossings) along the profile over a continuum of scale values. It has also been shown that a similar description may be derived when considering points of extrema of curvature.

A second description, known as interval tree, is then derived from the first one. In summary, the interval tree is a qualitative description of the profile, organized by scale, in terms of inflection points. Each node on the tree defines a rectangle which is related to a underlying feature on the profile. A rectangle is bounded on both sides by zero crossing contours. The location of zero crossing contours on the x-axis precisely indicate the location of inflection points along the profile.

Furthermore, an inflection point indicates where a curve changes its direction of curvature, i.e. from concave to convex or from convex to concave. Consequently, in this manner, it is possible to naturally represent the profile as a number of convex and concave curve segments. Moreover, since the rectangles have their precise extent, location and scale duration given by the interval tree description, any derived segmentation may be exactly reproduced at any time, by any operator, providing a highly objective segmentation process. This represents a great advantage over the existing segmentation methods which require an operator to locate specific and often poorly defined points on the profile.

The profile segments produced in this manner represent the data to which the qualitative methods are applied. The curvature approach is adopted in this work to quantitatively describe the contours of planar curves, i.e. the defined segments. The notion of bending energy was also used to define a measure of the shape of contour segments. By definition, it is the energy required to bend a thin rod from one shape into another. Additional metric information such as length, compactness, roundness and skew are also used. They complement the shape measures based on curvature, allowing segments of similar shape to be adequately discriminated.

The evaluation of the method was carried out by a series of experiments involving the stability of the curvature scale space description, and the repeatability and reliability of the segmentation of the profile. Further tests also showed the response of the curvature scale space descriptions to local and global shape variation along the profile outline. These experiments suggests that they are a robust shape description for dealing with facial profiles. Moreover, they show the potential of the method to fully describe, qualitative and quantitatively, the shape and shape changes of the profile.

Analyzing Facial Profiles: Evaluation of the Method

Ultimately, it is desirable that the method and its derived descriptions have a clear meaning, especially when clinical applications are considered. This is investigated and discussed in the next chapter.

Chapter Six

"There is nothing permanent in life except change. "

(Hericlitus, 5th century B.C.)

6. Applications

The human face is constantly changing. Although normal growth is one of the main contributing factors, there are other ways in which such changes may be brought about, as for example orthodontic treatment or reconstructive and cosmetic plastic surgery.

The importance of methods that can provide a description of the changes in the face have been discussed in chapter one. In fact, the clinical analysis of facial form has been outlined as one of the main applications of the methodology developed in this work.

In order to evaluate the potential of the methodology here described, as well as to assess its limitations, some typical clinical cases were selected and are analyzed in this chapter. Although a brief clinical description is given for each case, further details may be found on Grabb (et al 1971), White (et al 1976) and Albery (et al 1986), amongst others. Furthermore, facial growth and facial recognition based on profile outlines have also been investigated.

The layout in which the clinical cases are presented is as follows : firstly a brief clinical description is given and the case illustrated with the pre- and post-treatment facial profiles. Secondly, the charts, plots and tables are given, as a result of the analysis. Thirdly, these results are discussed exploring (a) the qualitative descriptions, (b) the quantitative descriptions and (c) the bending energy model. Largely, this discussion is based on nine curve segments generated by the analysis (this automatic segmentation has been discussed in section 5.8). In all cases investigated here, inflection points have been used for that purpose, resulting in the

profile being segmented into a series of convex and concave curves. The diagram below (figure 6-1) illustrates these points and the segments they define, which have been labeled according to a corresponding classical landmark or an anatomical feature. As a reference only, figure 6-1 also illustrates some of the classical anthropometric landmarks visible on the lateral view of the face (Farkas 1981, see also section 3.5.2).

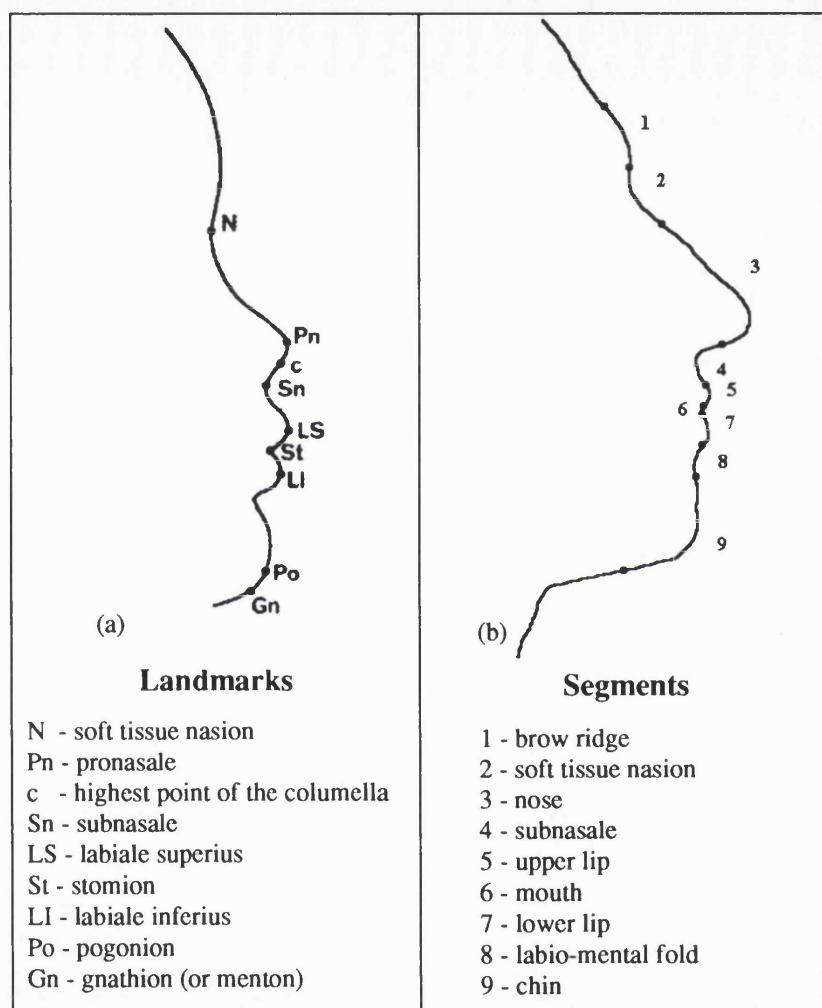


Figure 6-1 - Facial profile's landmarks and segments.

- (a) classical anthropometric landmarks ;
 (b) illustration of the landmarks and segments used in this study.

6.1. Cleft Palate Case

The first clinical application is a cleft palate case. It is a facial deformity which may involve the primary palate (i.e. the anterior hard palate), or the secondary palate (i.e. the soft and hard palate), or both. They may be complete or incomplete, depending on whether the lips are involved or not, and may be unilateral or bilateral.

Figure 6-2(a) illustrates the mid-line facial profile of a patient with a unilateral cleft of the palate. A previous operation left a scar tissue formation in the palate which severely affected the forward growth of the maxilla (upper jaw). This resulted in a very posterior positioning of the bony prominence at the base of the nose and a flattening of the tip and base of the nose. The profile shows the flattening of the tip of the nose and the extremely small and flattened upper lip contour. As a result of this deficiency in the middle third of the face, there is a relative protrusion of the lower lip.

Following surgery, the whole of the upper jaw was separated from the base of the skull and moved anteriorly and downwards and then fixed in this position. It can be seen that the profile has dramatically changed (see figure 6-2(b)).



Figure 6-2 - Facial profiles of the cleft palate patient.

The mid-line vertical facial profiles represent: (a) before and (b) after surgical treatment.

The qualitative descriptions generated by the analysis are presented in the figures 6-3, 6-4 and 6-5 for the pre- and post-treatment profiles, respectively. They were used to mathematically identify and locate ten landmark points, dividing the profiles into nine main curve segments. The segmented profiles are illustrated in figures 6-3(c) and 6-4(c).

The quantitative descriptions generated by the analysis are presented in the tables 6-1 and 6-2.

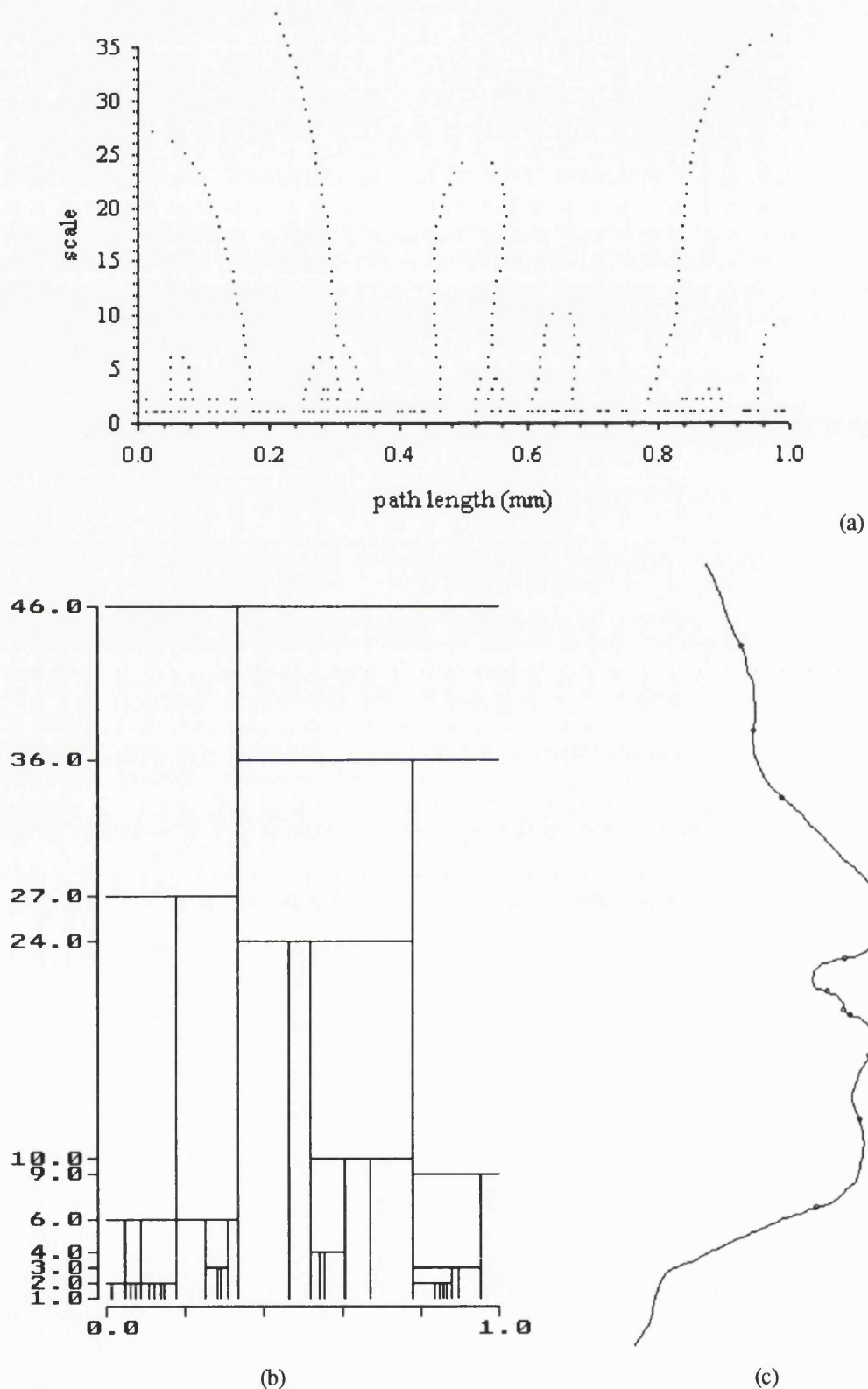


Figure 6-3 - Qualitative descriptions (cleft palate patient - *before surgery*).

The qualitative descriptions are : (a) curvature scale space ; (b) interval tree (the x-axis represents the path length parameter (in millimeters) and the y-axis the scale parameter) . On (c) the landmarks and curve segments are illustrated.

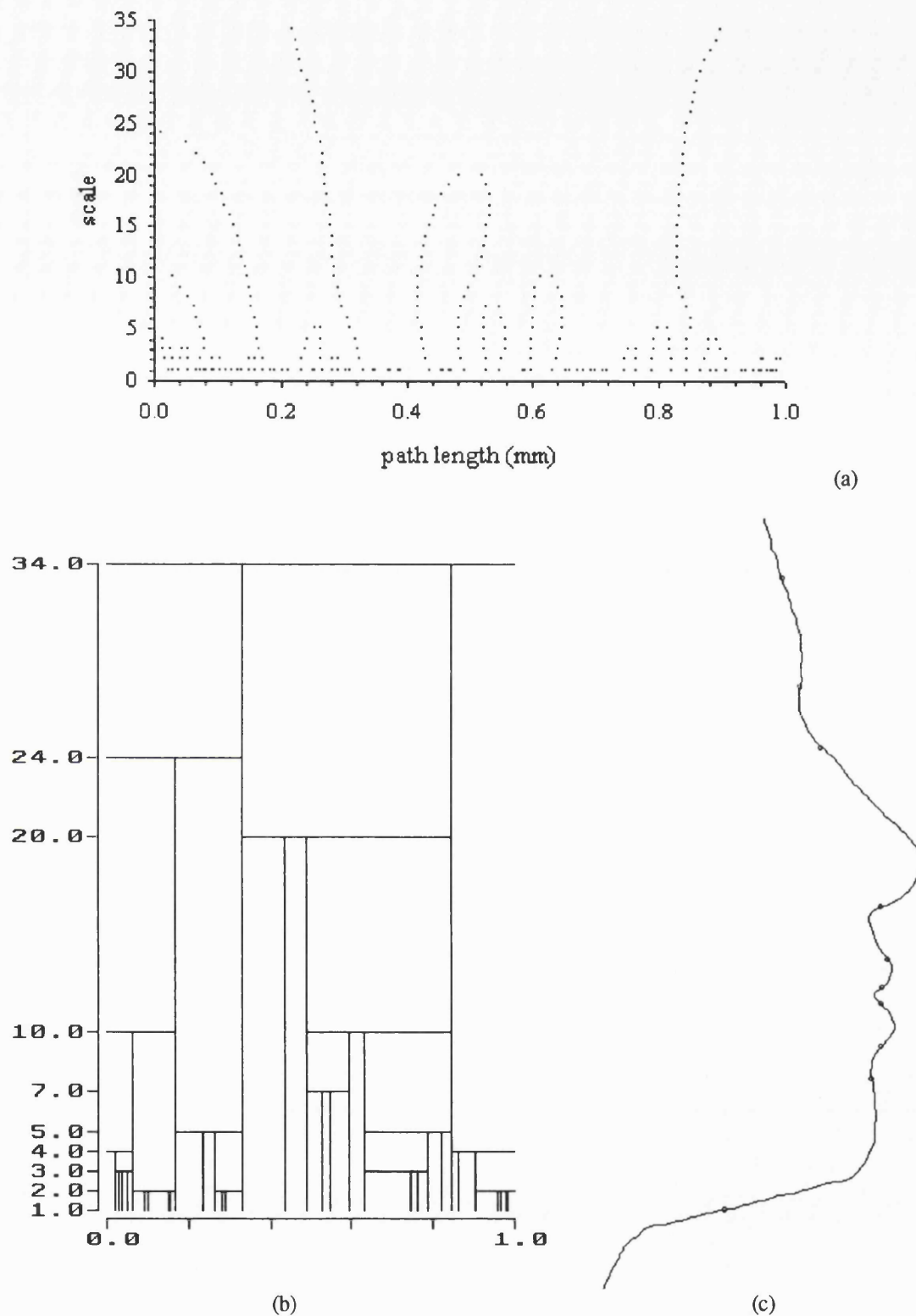


Figure 6-4 - Qualitative descriptions (cleft palate patient-*after surgery*).

The qualitative descriptions are : (a) curvature scale space ; (b) interval tree (the x-axis represents the path length parameter (in millimeters) and the y-axis the scale parameter) . On (c) the landmarks and curve segments are illustrated.

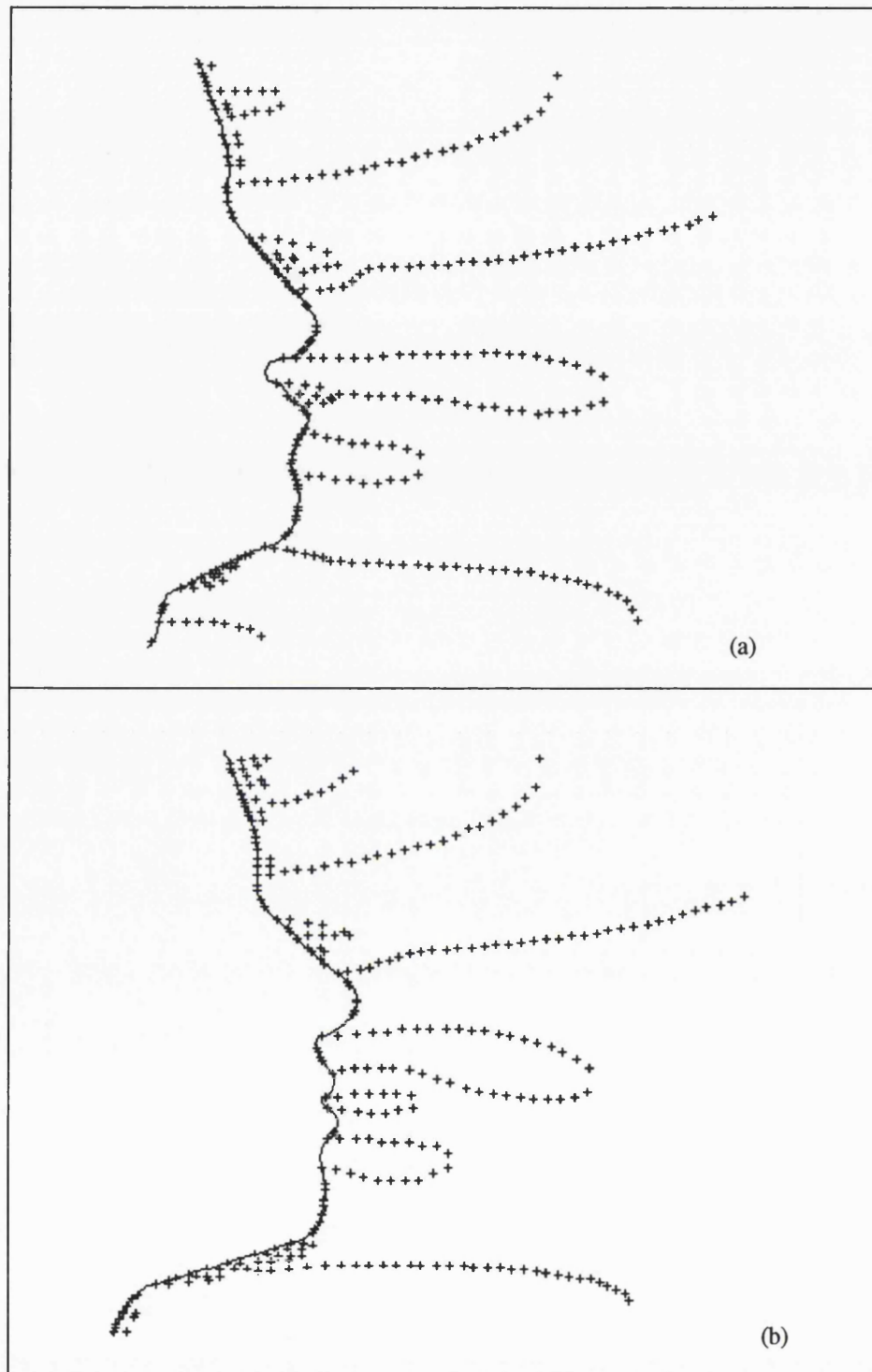


Figure 6-5 - Profiles and the zero crossing contours (cleft palate case).

The *alternative display* where the zero crossing contours can be related to the underlying facial features. (a) before treatment ; (b) after treatment.


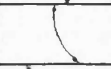

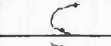
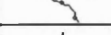




Segment no.	Segment shape	Start	End	no. points	Length (mm)	Average curvature	Average bending energy	Roundness	Compactness	Skew
0		0	22	23	19.56	0.0028	5.81E-05	0.07	2156.44	
1		22	43	22	19.60	0.0169	3.83E-04	0.37	15.59	-0.02
2		43	62	20	17.22	-0.0408	1.80E-03	0.82	9.19	-0.01
3		62	114	53	48.12	0.0394	3.70E-03	2.09	4.12	0.67
4		114	129	16	11.13	-0.1786	4.84E-02	2.86	1.92	0.15
5		129	135	7	5.12	0.0001	3.22E-04	5.9E-04	6.33	-1.56E-04
6		135	137	3	1.75	0.0008	3.49E-06	2.4E-03	9.92	-9.21E-08
7		137	150	14	10.90	0.0972	1.28E-02	1.36	3.47	0.16
8		150	167	18	15.09	-0.0323	2.54E-03	0.58	6.59	-0.01
9		167	193	27	23.67	0.0546	3.31E-03	1.47	4.94	0.20
10		193	248	56	51.10	-0.0098	1.43E-03	0.55	6.74	

Table 6-1- Table with the segment's shape and quantitative descriptive measures (before surgery).

These values refer to the segmented vertical profile outline of figure 6-3(c) (cleft palate case).



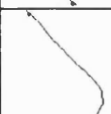





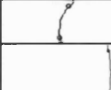
Segment no.	Segment shape	Start	End	no. points	Length (mm)	Average curvature	Average bending energy	Roundness	Compactness	Skew
0		0	16	17	14.08	-0.002	4.29E-06	0.03	239.16	
1		16	42	27	25.85	0.010	2.48E-04	0.28	17.92	0.02
2		42	57	16	14.89	-0.043	2.02E-03	0.69	10.40	0.02
3		57	107	51	48.82	0.031	3.75E-03	1.61	4.12	-0.61
4		107	122	16	12.47	-0.083	1.36E-02	1.32	6.20	0.03
5		122	130	9	6.31	0.058	5.19E-03	0.52	16.26	-0.01
6		130	136	7	4.40	-0.075	6.28E-03	0.52	19.36	3.45E-05
7		136	148	13	9.95	0.052	4.93E-03	0.67	9.70	0.05
8		148	156	9	7.55	-0.040	1.89E-03	0.36	21.86	-1.22E-03
9		156	210	55	53.91	0.024	1.64E-03	1.34	3.88	-1.31
10		210	248	39	36.08	-0.025	1.09E-03	0.98	6.15	

Table 6-2- Table with the segment's shape and quantitative descriptive measures (after surgery).

These values refer to the segmented vertical profile outline of figure 6-4(c) (cleft palate case).

6.1.1. Describing Curve Segments

The qualitative and quantitative descriptions generated by the analysis reveal the changes that occurred in the facial profile.

6.1.1.1. Using the Qualitative Descriptions

The zero crossing contours of the curvature scale space descriptions relating to before and after treatment conditions show a similar pattern (see figures 6-3(a) and 6-4(a)). However, a significant change may be noticed in the central region of the description, including the three distinct arches. Arches usually correspond to concave outline segments, and in this case, they refer to (from left to right, starting at 0.44 mm): the subnasale segment (4), mouth (segment 6) and the labio-mental fold (segment 8). Consequently, the gaps between and adjacent to the defined arches correspond to convex outline segments. These are : the nose (segment 3), the upper and lower lips (segments 5 and 7) and the chin (segment 8).

From the post-operative condition, their pattern indicates a marked change in this area of the face, reflecting an increase in concavity, specially noticeable in the first two arches (i.e. with segments 4, 5 and 6).

6.1.1.2. Using the Quantitative Descriptions

The analysis produced nine curve segments as illustrated in figures 6-3(c) and 6-4(c). These were then represented by a number of quantitative descriptive measures which are given in the tables 6-1 and 6-2. However, a greater insight may be gained when these values are graphically represented.

The first quantitative analysis is done by using the curvature plot (described in section 5.9.3). It provides useful local shape information by describing the entire profile and its segments in terms of its concavity (or direction of curvature). In order to emphasize these local shape changes, the curvature plots of before and after surgical treatment have been displayed along the same axes and are shown in figure

6-6. As a visual aid, the profile outline has also been displayed on the same plot, so that a direct interpretation of the curvatures values can be made.

The result shows the distinct areas affected by the surgical correction, namely the base of the nose, the subnasale, the upper lip and the mouth.

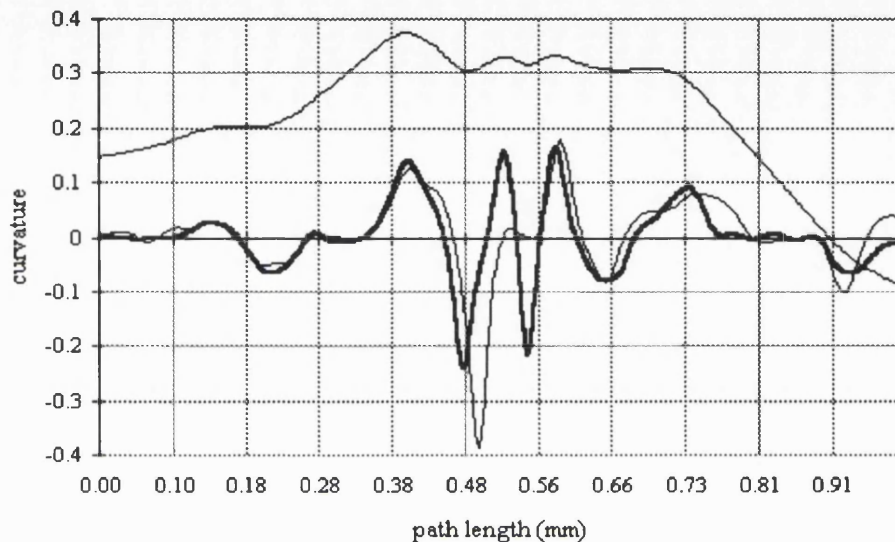


Figure 6-6 - Curvature plot (cleft palate case).

A scale value of 4 has been used in this analysis, indicating the local shape changes *before (thin line)* and *after (thick dark line)* surgical treatment.

The second and perhaps complementary analysis, graphically represents all nine curve segments by their mean curvature values, as illustrated in figure 6-7(b). The length of each segment is also graphically illustrated in figure 6-7(a).

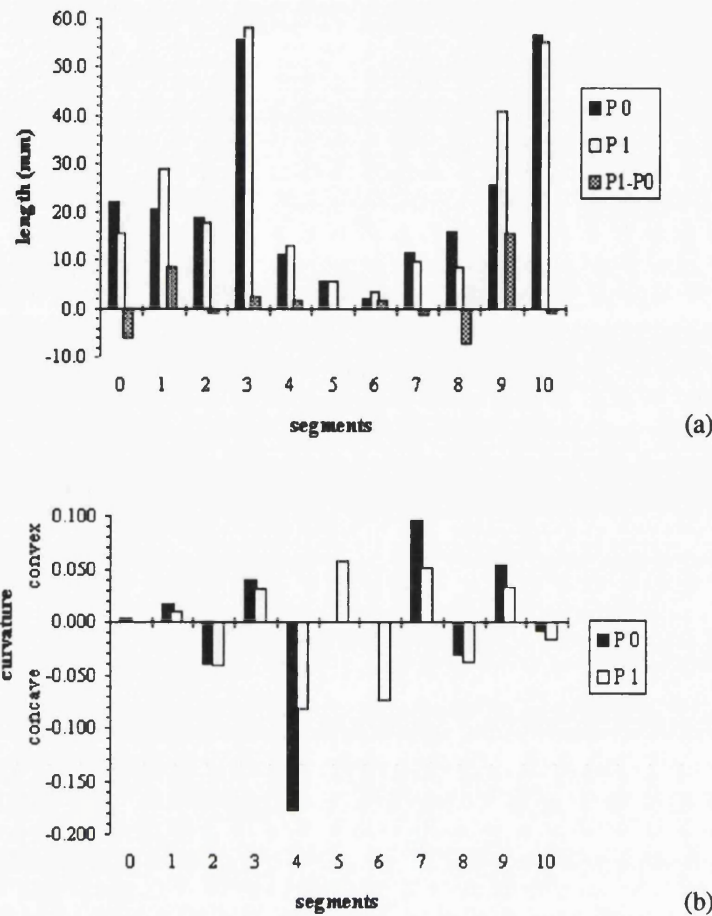


Figure 6-7 - Segment's quantitative measures (cleft palate case).

P0 and P1 represent the *pre- and post-treatment conditions*, respectively. On (a) the length of each segment is graphically illustrated. The dotted columns represents their difference. On (b) the mean curvature values are shown.

For the pre-surgical condition (black columns-figure 6-7(b)) the segments 1 and 2 shows the gentle concavity in the region of the brow ridge and of the bridge of the nose (i.e. the soft tissue nasion). Segment 3 represents the nose, and segment 4 the region of the upper lip at the base of the nose. From the diagram, it can be seen that this is the most concave area. The segment representing the upper lip and the mouth area showed no concavity (the values were too close to zero to be visible on that scale). Analysis of normal profiles has shown that the mouth appears as a segment with large but variable concavity (Moss, Campos and Linney 1992). The lower lip (segment 7) showed a large convexity. The concavity of the labio-mental fold (segment 8) is also identified, and the convexity of the chin was gentle (segment 9).

For the treated face (white columns) the curvature values show that the soft tissue nasion (segment 2) has not changed significantly. The convexity of the nose has slightly decreased (segment 3). Due to the maxillary advancement there is a movement of the soft tissues, which are indicated by : the marked change in the concavity of the subnasale segment (4), in the convexity of the upper lip (segment 5), and by the increased concavity of the mouth (segment 6). There is a decrease in the convexity of the lower lip (segment 7) and an increase in the concavity of the region of the labio-mental fold. The chin has become slightly less prominent.

Further analysis on the changes of the various segments can be made on the basis of their length. Similarly to the curvature chart, the diagram of figure 6-7(a) shows how the segments have changed in length due to treatment. The overall changes are illustrated by the dotted columns, where positive values indicate that the segment has elongated, and negative values indicate that they have decreased.

6.1.1.3. Using the Bending Energy Concept

The concept of bending energy has also been used to investigate the changes in the shape of the various segments due to surgical treatment. More specifically, it has been used to determine: (i) the effects of the surgical treatment by comparing pre- and post-operative profiles; (ii) the “shape signatures” for a particular facial anomaly, by comparing the pre-operative profile with a mean normal facial profile (average), and (iii) how close the post-treatment profile is to the average, by comparing the post-operative profile with the mean normal facial profile.

This is achieved by using the analogical model described in the section 5.9.4 , where one outline represents the undeformed state of a thin flexible rod and the other represents the deformed state.

Figure 6-8 shows the amount of energy required to change the shape of the pre-operative profile into the shape of the post-operative profile. In addition to that, indicates the main areas of the profile affected by these changes. A profile outline is also displayed on the bending energy plot, so that the changes may be visually related to the various segments on the profile.

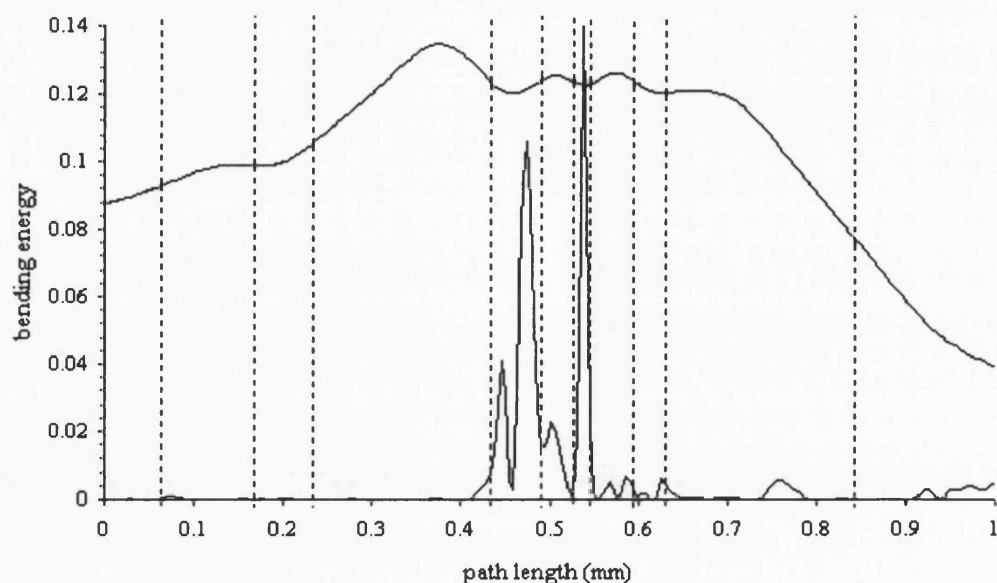


Figure 6-8 - Bending energy plot - Effects of surgical treatment (cleft palate case).

This plot shows the effects of the surgical treatment. A scale value of 3 has been used in this analysis, indicating the local shape changes on the *profile before treatment* when compared with the *profile after surgical treatment* (displayed on the diagram). The dashed vertical lines identify the bounds of the main segments.

Another way of exploring the bending energy approach is to consider the measurements made on a group of normal subjects (faces), where the resulting mean facial profile is then used as the undeformed state of the thin flexible rod. Assuming that the treated profile is used as the deformed state, the bending energy measurements will determine how close it now is to the average profile. Therefore, this quantitative analysis could enable an audit system to be established. In the other hand, when the pre-operative profile is used as the deformed state, the bending energy measurements will represent the deformations away from the mean normal facial profile, for the case of a cleft palate profile. This quantitative analysis represents the shape signatures for this particular facial anomaly.

As the patient analyzed here was seventeen by the end of the treatment, a group of thirty females of seventeen years old was used to derive the mean face (further information in this process may be seen in Coombes 1993 and in Fright and Linney 1993). The result of this analysis is shown below (figures 6-9, 6-10 and 6-11).

Figure 6-9 shows the analysis of the surgically corrected face (profile) when using the scale value of five, thus emphasizing local shape changes when quantifying the results of the treatment as compared to the average.

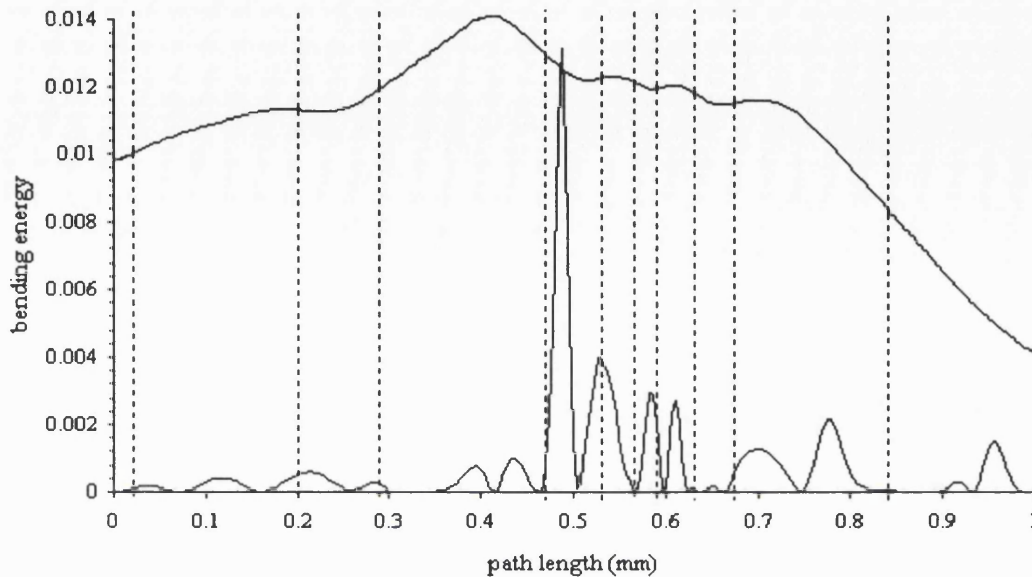


Figure 6-9 - Bending energy plot - closeness to the average (cleft palate case).

A scale value of 5 has been used in this analysis, indicating locally how close the *post-operative profile* is to the *mean normal profile* (illustrated on the diagram). The dashed vertical lines identify the bounds of the main segments.

Figure 6-10 shows the analysis when using the scale value of three, emphasizing local shape changes. In figure 6-11, the coarser scale value of twelve has been used to measure global shape changes. The last two results suggest that the primary shape deformation or the difference between the group of normal and cleft palate patients occurs in the middle third region of the profile outline.

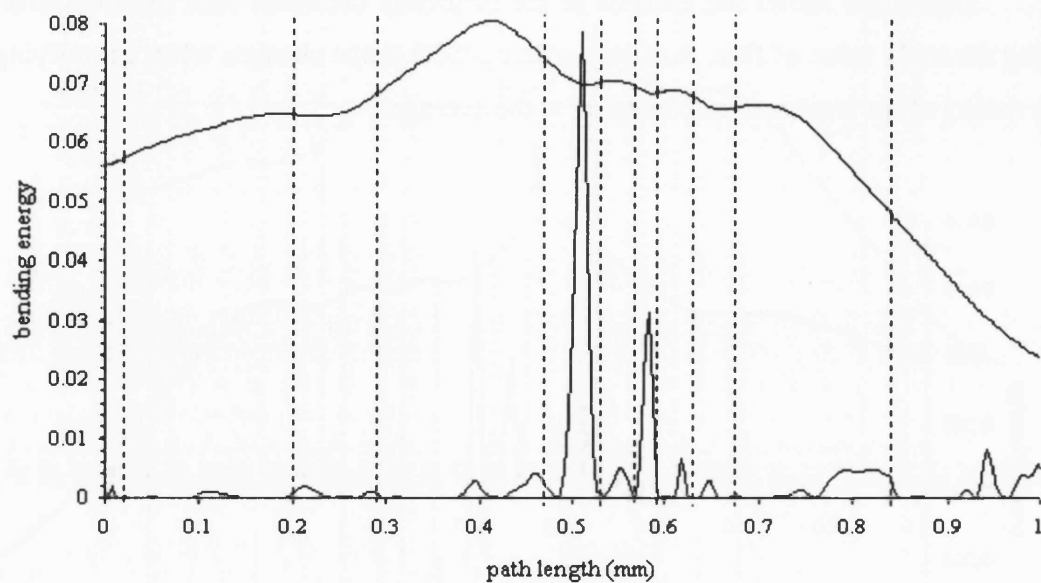


Figure 6-10 - Bending energy plot - Shape signatures for the cleft palate case.

A scale value of 3 has been used in this analysis, indicating the local shape changes (regional deformities) on the *pre-operative profile* when compared with a *mean facial profile* (illustrated on the diagram). The dashed vertical lines identify the bounds of the main segments.

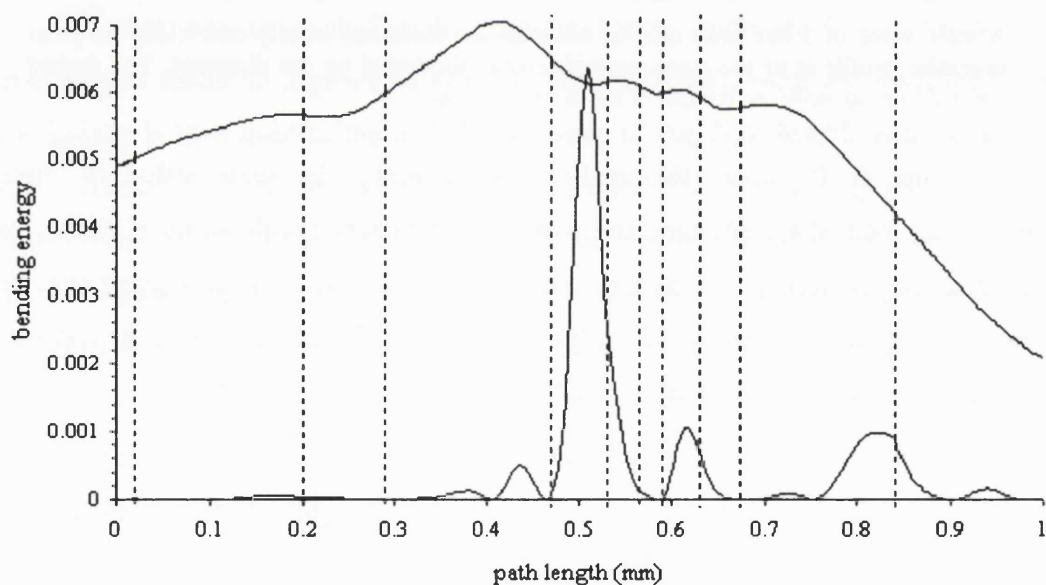


Figure 6-11 - Bending energy plot - Shape signatures for the cleft palate case.

A scale value of 12 has been used in this analysis, indicating the global shape changes on the *pre-treatment profile* when compared with a *mean facial profile* (illustrated on the diagram). The dashed vertical lines identify the bounds of the main segments.

6.2. Skeletal II Case

The bony base relationship (or skeletal base relationship) greatly influences the appearance of the face. The alveolar processes which contain the teeth and form the dental arches are based in this skeletal structure. Following a standard classification of the skeletal relationship, three classes are defined (see figure 6-12) : (i) skeletal I : when the maxillary bony base lies slightly forwards of the mandibular bony base (considered a normal relationship); (ii) skeletal II : when the mandibular bony base is retrognathic relative to the maxillary base; (iii) skeletal III : when the mandibular base is prognathic relative to maxilla, or the maxillary base is retrognathic relative to the mandibular base, or a combination of both. The classification of incisor relationship is also associated with these classes, as illustrated in figure 6-13.

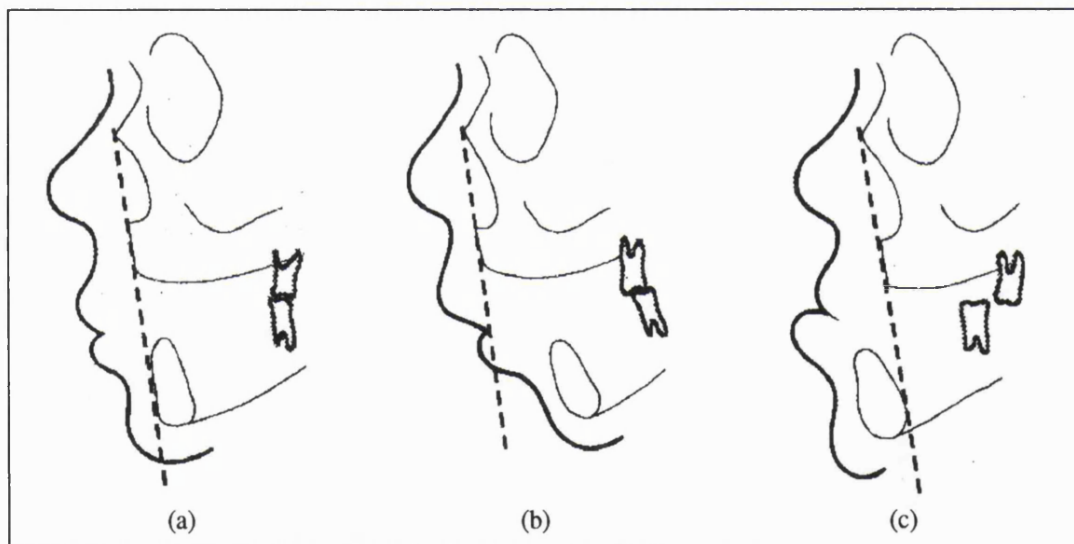


Figure 6-12 - Classification of skeletal relationship.

(a) skeletal I ; (b) skeletal II and (c) skeletal III. (Adapted from Albery et al 1986).

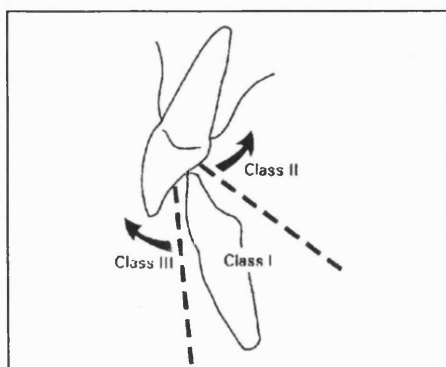


Figure 6-13 - Classification of incisor relationship.

(Adapted from Albery et al 1986).

Applications: Skeletal II

The second clinical application is a skeletal II case, and is illustrated by the mid-line profile of figure 6-14(a). The profile shows the relatively small base of the nose and the large lips. As a result of the retrognathic mandibular base, the chin appears extremely small and too far backwards, producing the effect of a double chin when seen in profile.

Following surgery, the maxillary base was moved retrusively and the mandible was moved forward. The patient also had a genioplasty which moved the chin forward. The resulting profile is illustrated in figure 6-14(b), showing the dramatic changes.



Figure 6-14 - Facial profiles of the skeletal II patient.

The mid-line vertical facial profiles represent: (a) before and (b) after surgical treatment.

The qualitative descriptions generated by the analysis are presented in the figures 6-15, 6-16 and 6-17 for the pre- and post-treatment profiles. Similarly to the previous case, the profiles were divided into nine curve segments, corresponding to the same anatomical facial features. The segmented profiles are illustrated in figures 6-15(c) and 6-16(c).

The quantitative measurements generated by the analysis are presented in the tables 6-3 and 6-4.

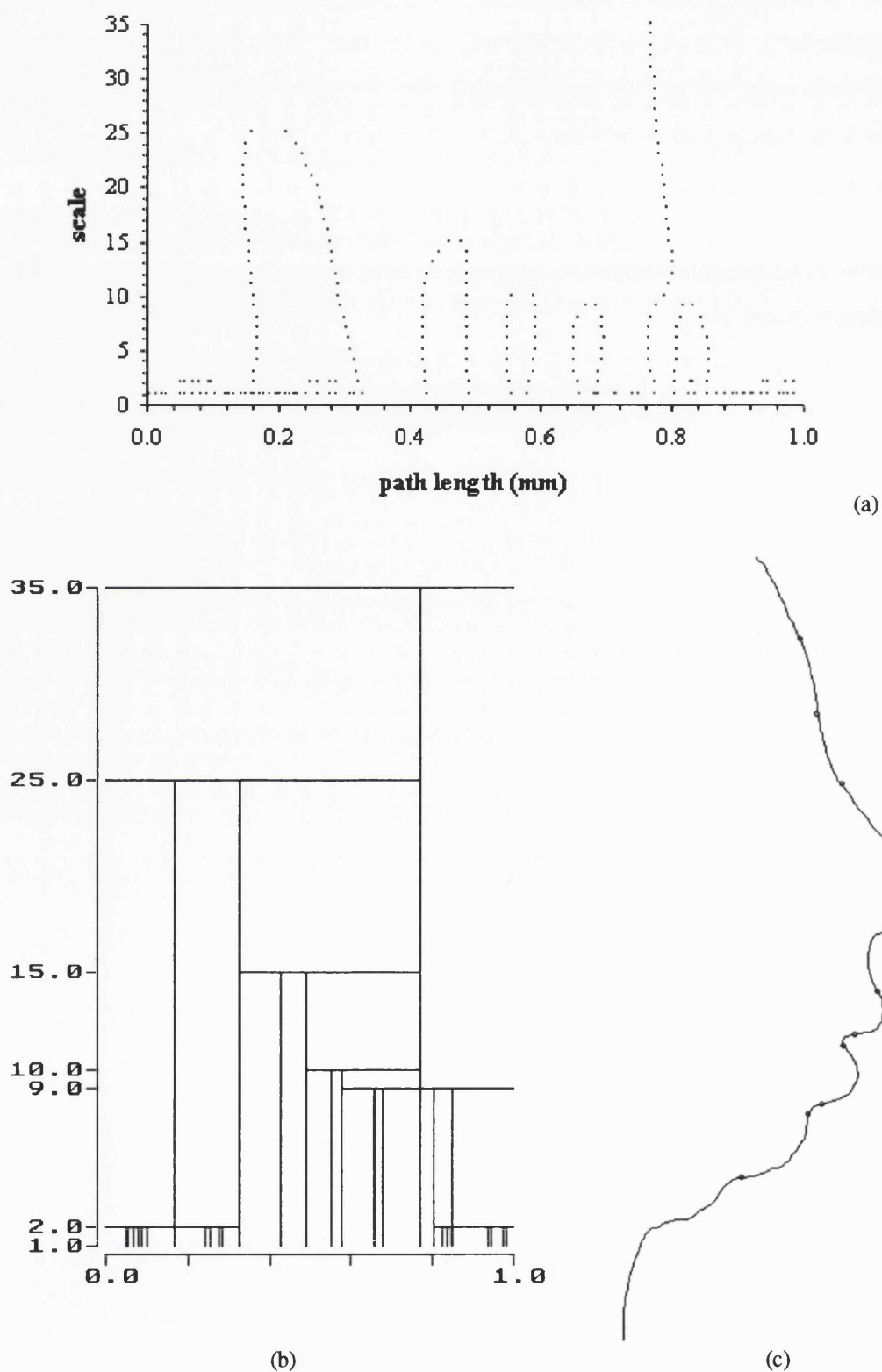
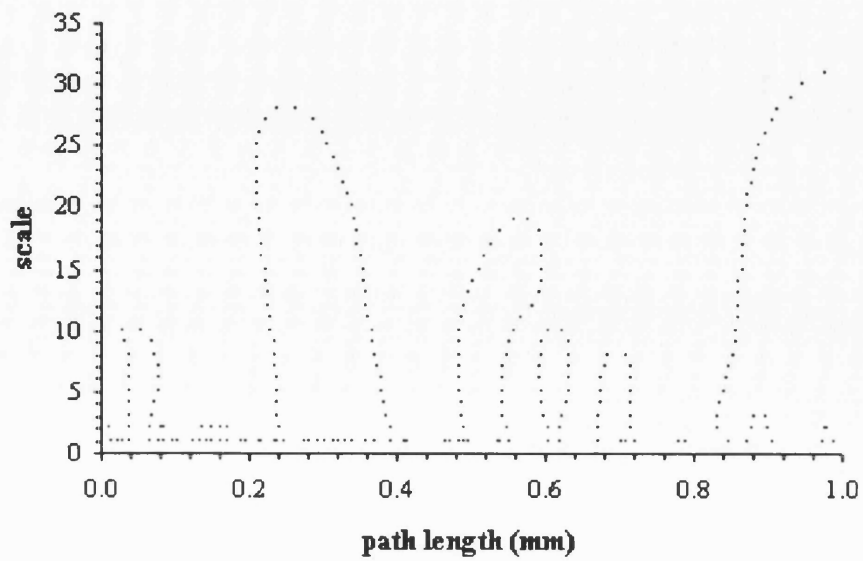
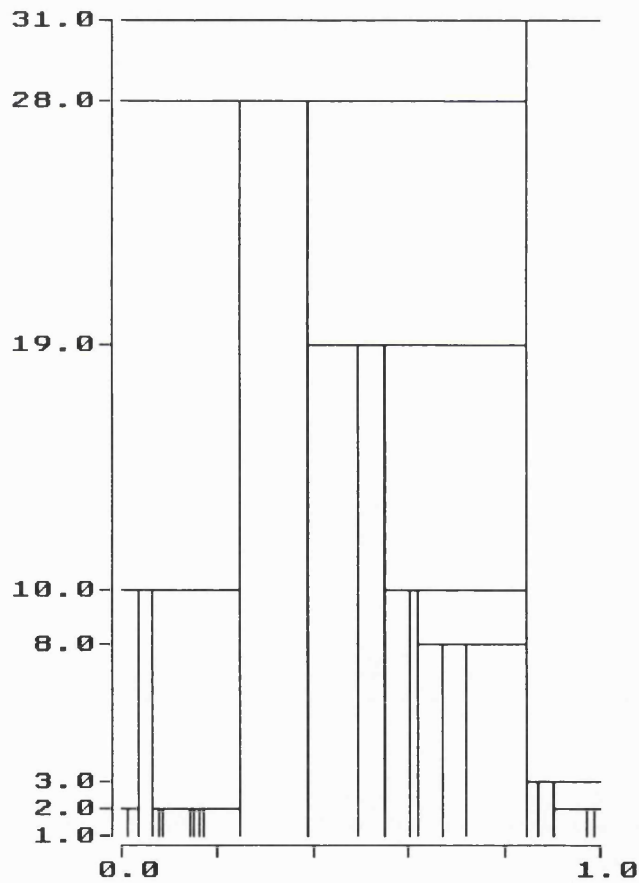


Figure 6-15 - Qualitative descriptions (skeletal II case - before surgery).

The qualitative descriptions are : (a) curvature scale space ; (b) interval tree (the x-axis represents the path length parameter (in millimeters) and the y-axis the scale parameter) . On (c) the landmarks and curve segments are illustrated.



(a)



(b)



(c)

Figure 6-16 - Qualitative descriptions (skeletal II case - *after surgery*).

The qualitative descriptions are : (a) curvature scale space ; (b) interval tree (the x-axis represents the path length parameter (in millimeters) and the y-axis the scale parameter) . On the landmarks and curve segments are illustrated.

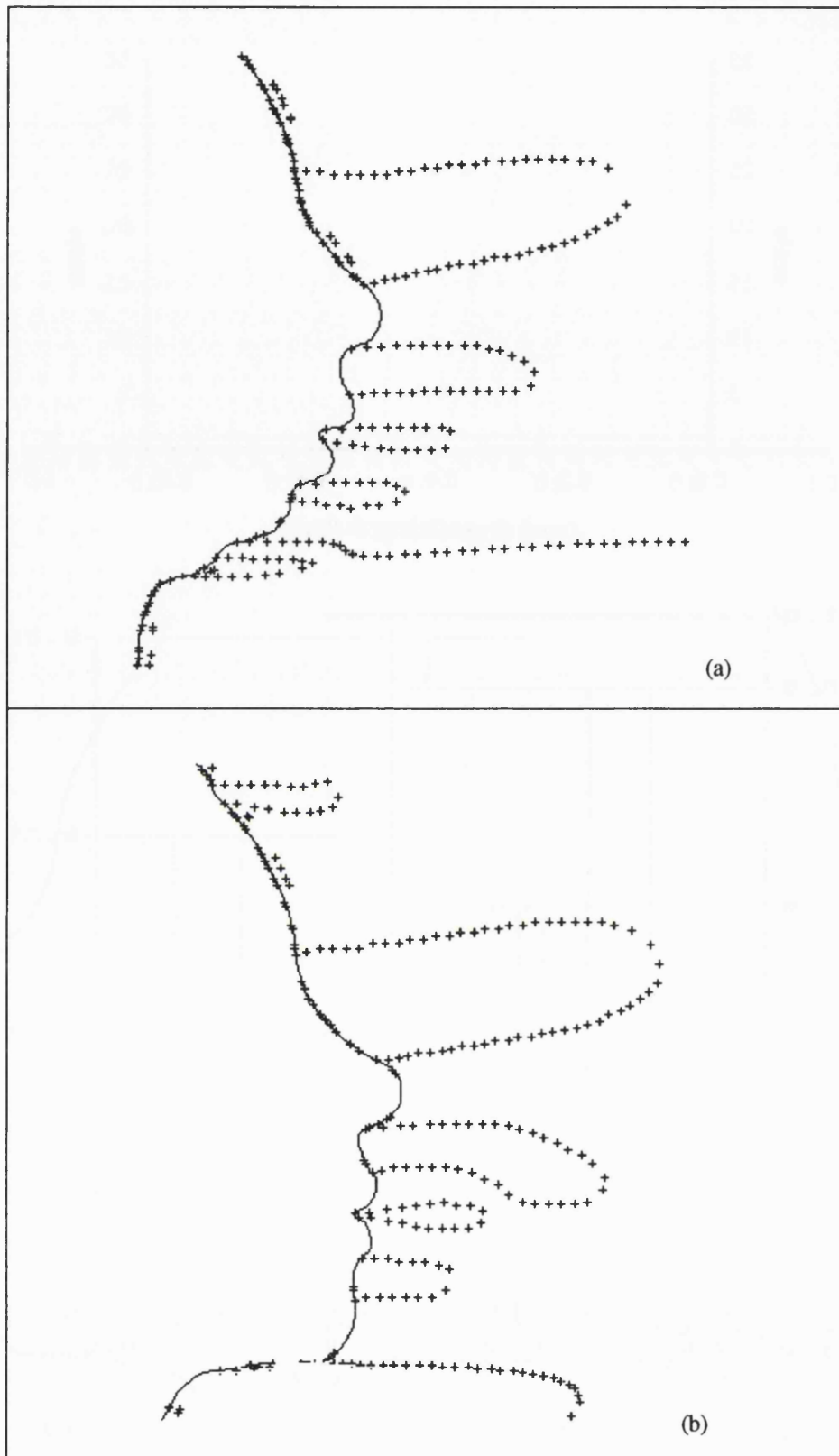


Figure 6-17 - Profiles and the zero crossing contours (skeletal II case).

The *alternative display* where the zero crossing contours can be related to the underlying facial features. (a) before treatment ; (b) after treatment.


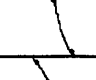


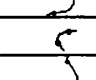
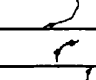
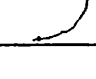
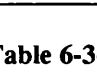
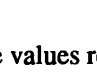
Segment no.	Segment shape	Start	End	no. points	Length (mm)	Average curvature	Average bending energy	Roundness	Compactness	Skew
0		0	24	25	23.99	0.009	8.2E-05	0.22	34.82	
1		24	42	19	19.74	0.006	6.0E-05	0.12	55.24	-0.003
2		42	60	19	19.46	-0.015	2.4E-04	0.28	25.66	-0.003
3		60	105	46	44.76	0.025	1.8E-03	1.17	5.19	-0.472
4		105	122	18	15.62	-0.025	9.4E-04	0.45	15.14	0.014
5		122	137	16	12.22	0.028	1.1E-03	0.46	17.34	0.015
6		137	143	7	4.43	-0.023	5.7E-04	0.16	69.49	1.13E-04
7		143	163	21	16.69	0.020	7.8E-04	0.41	15.42	-0.020
8		163	168	6	4.85	0.001	9.4E-06	0.01	7.68	-0.004
9		168	192	25	24.70	0.014	2.7E-04	0.34	16.78	-0.030
10		192	248	57	57.09	-0.018	5.5E-04	1.00	5.49	

Table 6-3- Table with the segment's shape and quantitative descriptive measures (before surgery).

These values refer to the segmented vertical profile outline of figure 6-15(c) (skeletal II case).





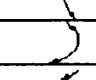
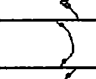
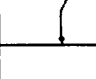
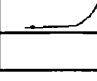

Segment no.	Segment shape	Start	End	no. points	Length (mm)	Average curvature	Average bending energy	Roundness	Compactness	Skew
0		0	43	44	42.99	0.005	0.21	39.48	4.9E-05	
1		43	57	15	15.34	0.010	0.15	46.42	1.1E-04	0.003
2		57	73	17	17.21	-0.016	0.27	27.71	3.3E-04	-0.001
3		73	123	51	48.69	0.023	1.17	4.82	2.9E-03	-0.856
4		123	137	15	12.27	-0.039	0.59	13.86	2.2E-03	-0.005
5		137	149	13	10.02	0.014	0.18	38.79	3.7E-04	0.005
6		149	153	5	2.99	-0.021	0.10	118.17	4.5E-04	1.25E-05
7		153	167	15	11.73	0.008	0.12	47.99	2.7E-04	-0.003
8		167	178	12	11.15	0.002	0.02	186.26	2.1E-05	0.004
9		178	212	35	34.53	0.037	1.28	4.52	1.8E-03	-0.677
10		212	248	37	37.08	-0.025	0.92	6.81	7.9E-04	

Table 6-4- Table with the segment's shape and quantitative descriptive measures (after surgery).

These values refer to the segmented vertical profile outline of figure 6-16(c) (skeletal II case).

6.2.1. Describing Curve Segments

The qualitative and quantitative descriptions generated by the analysis also reveal the changes that occurred in the facial profile for this clinical case.

6.2.1.1. Using the Qualitative Descriptions

The zero crossing contours of the curvature scale space description relating to the before treatment condition (see figure 6-15(a)) show the existence of a significantly concave segment after the chin (indicated by the long and almost vertical contour starting just after the 0.76 mm length marker). This contour configuration is not normally seen in a similar description of a normal profile, but here it clearly portrays the double chin profile. This may be confirmed by the description of the post-operative profile (see figure 6-16(a)), where the contours depict the corrected chin.

Once again, the pattern of the zero crossing contours forming three arches on the central region of both descriptions indicate the marked change in their corresponding area of the face (from the subnasale segment to the labio-mental fold segment). They reflect an increase in concavity, mainly noticeable in the first arch.

6.2.1.2. Using the Quantitative Descriptions

The curvature plot for this clinical case is shown in figure 6-18. The result shows the changes in curvature of the nose, its base and the subnasale segment. It shows the reduction in concavity of both lips and the mouth. Furthermore, it shows a significant amount of change in the labio-mental fold and chin areas.

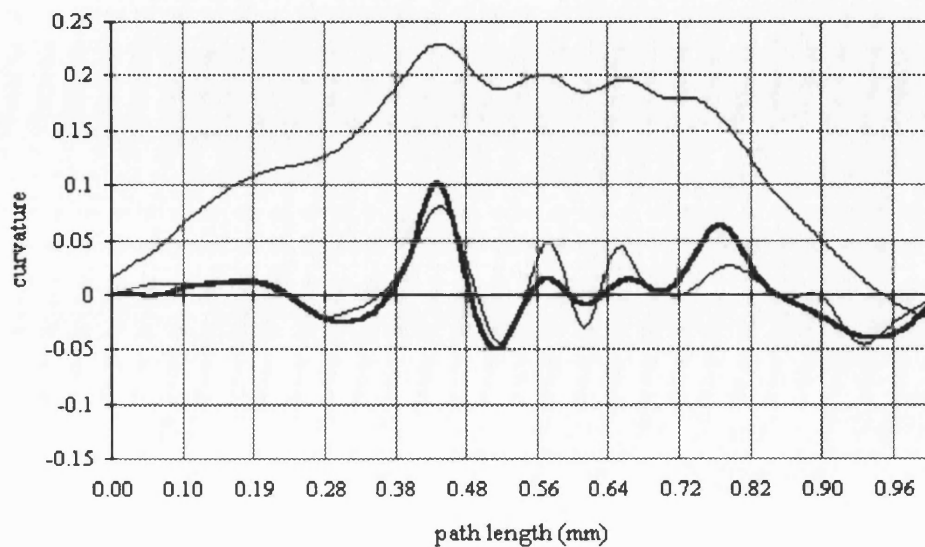


Figure 6-18 - Curvature plot (skeletal II case).

A scale value of 9 has been used in this analysis, indicating the local shape changes *before* (thin line) and *after* (thick dark line) surgical treatment.

The analysis of the segment's mean curvature values (figure 6-19(b)), similarly depicts the same changes. It indicates the increase in the convexity of the brow ridge and a small increase in the concavity of the nasion, too. Segment 3 shows a less convex nose, and segment 4 shows a more concave subnasale area. The same significant changes seen on the lips, according to the curvature plot, are also described by their mean curvature values. For the last two segments, the columns show the precise amount of change corresponding to each one of them, with the greatest change being on the chin.

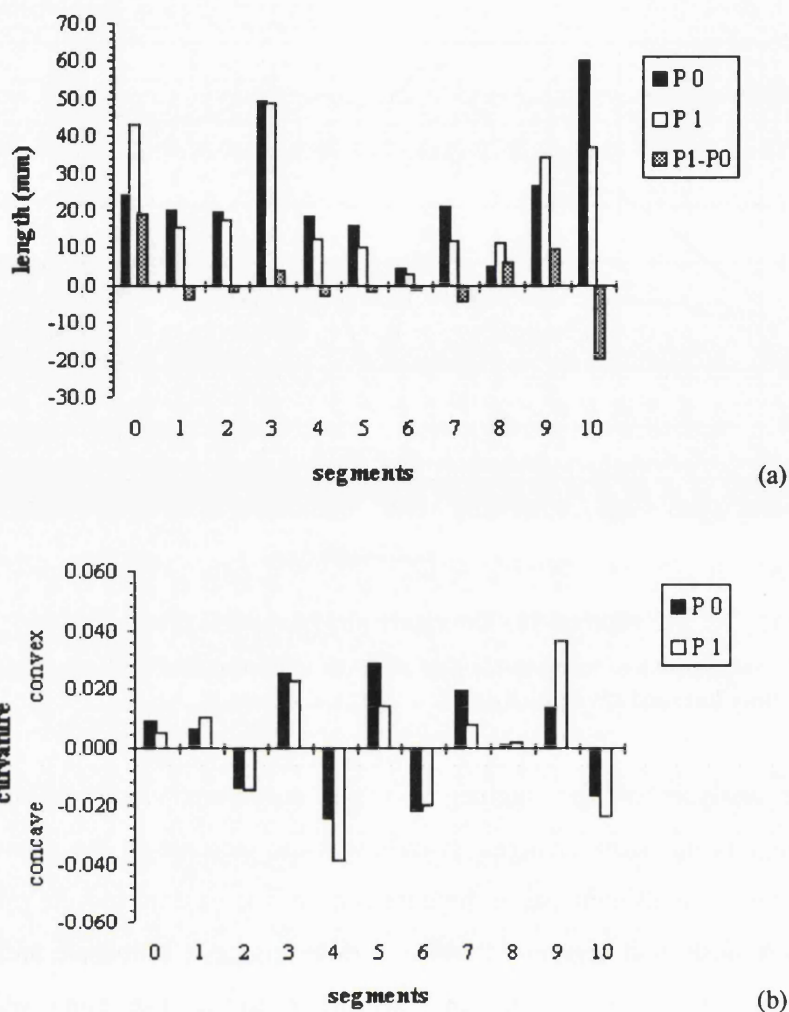


Figure 6-19 - Segment's quantitative measures.

On (a) the length of each segment is graphically illustrated. The dotted columns represents their difference. On (b) the mean curvature values are shown. **P0** and **P1** represent the pre- and post-treatment conditions, respectively.

The length chart (figure 6-19(a)) shows a small increase for the nose, a small and gradual shortening from the subnasale to the mouth segments, followed by a greater reduction in the lower lip (segment 7). The labio-mental fold and the chin are shown to have been elongated.

6.2.1.3. Using the Bending Energy Concept

The bending energy plot of figure 6-20 quantifies the shape changes brought about by the surgical treatment. The scale value of eight used in this plot identify the local shape changes, the significant ones being in the lips and chin area.

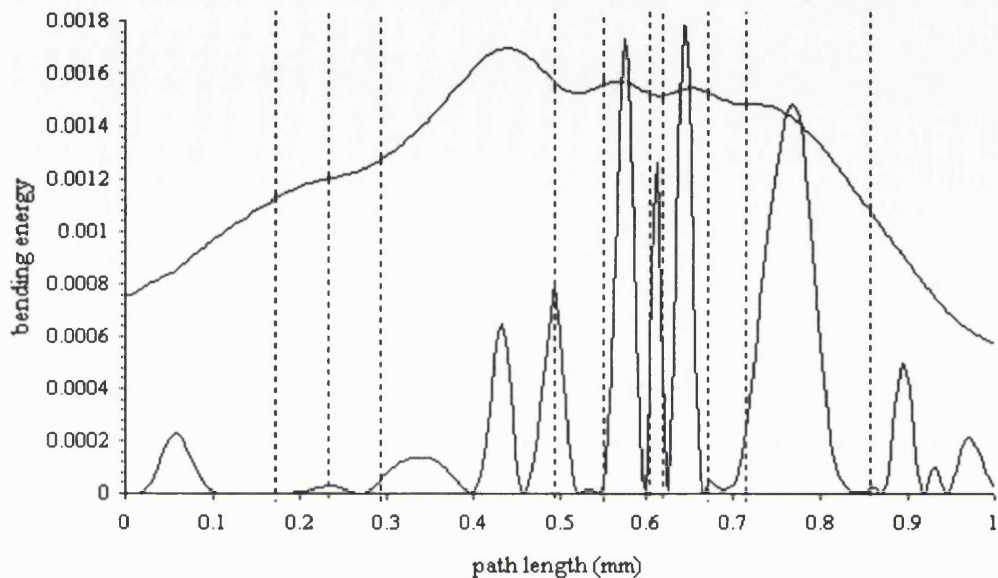


Figure 6-20 - Bending energy plot - Effects of surgical treatment (skeletal II case).

This plot shows the effects of the surgical treatment. A scale value of 8 has been used in this analysis, indicating the local shape changes on the *profile before treatment* when compared with the *profile after surgical treatment* (displayed on the diagram). The dashed vertical lines identify the bounds of the main segments.

The next figure (6-21) shows the bending energy analysis that represents the shape signatures for the skeletal II class of facial anomaly. Because the same conditions of age and sex also applied to this case, the mean facial profile of a seventeen year old female, defined for the previous case, was used here. This plot emphasizes global shape changes by using the coarser scale value of fifteen. The results suggest that the main shape deformation or the difference between the group of normal patients and this skeletal relationship class occurs in the lower half region of the profile outline, with the primary deformation around the chin area.

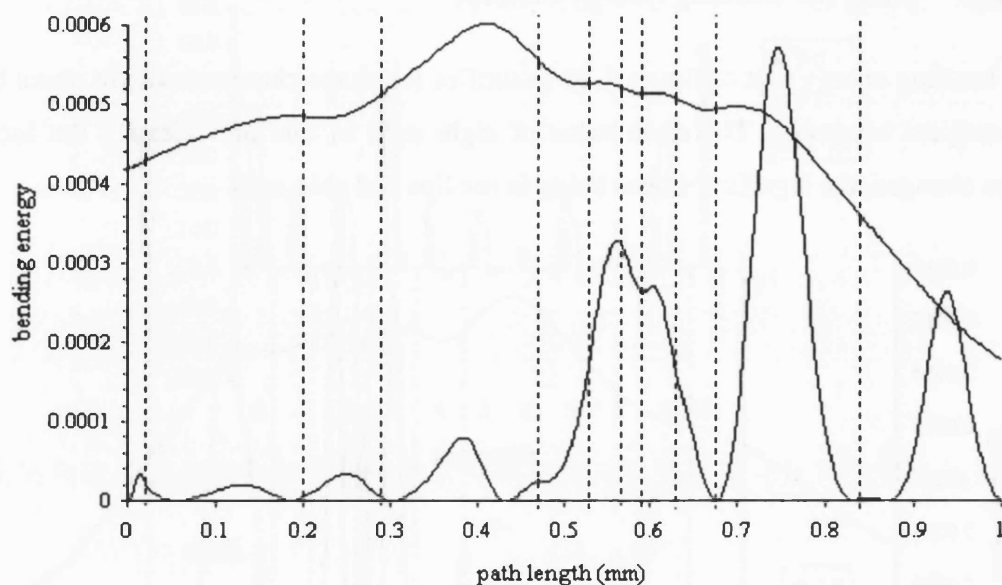


Figure 6-21 - Bending energy plot - Shape signatures for the skeletal II case.

A scale value of 15 has been used in this analysis, indicating the global shape changes on the *pre-treatment profile* when compared with a *mean facial profile* (illustrated on the diagram). The dashed vertical lines identify the bounds of the main segments.

The main shape differences between the treated profile and the average are shown in figure 6-22. This plot emphasizes global shape changes by using the coarser scale value of ten.

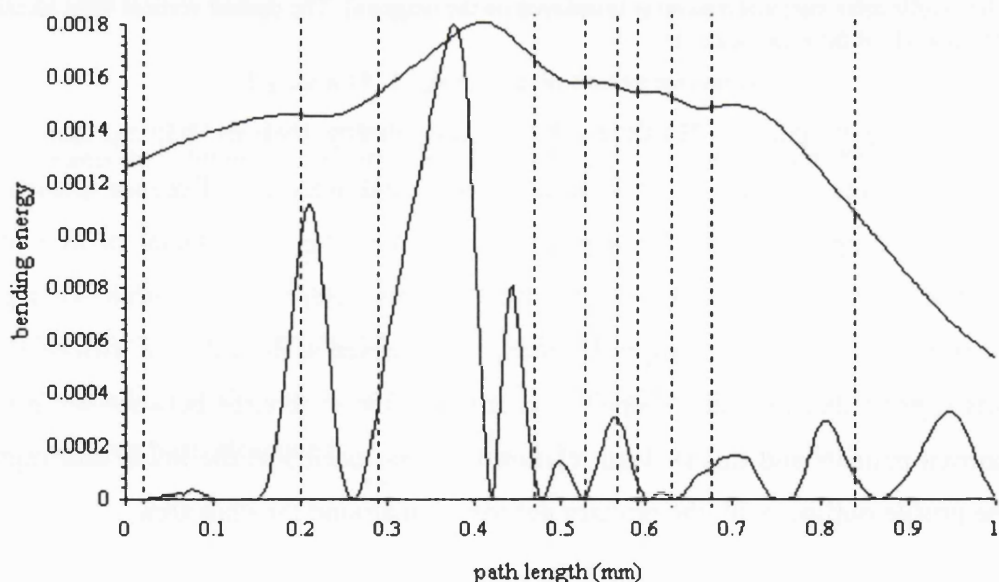


Figure 6-22 - Bending energy plot - closeness to the average (skeletal II case).

A scale value of 10 has been used in this analysis, indicating the global shape changes on the *post-treatment profile* when compared with a *mean facial profile* (illustrated on the diagram). The dashed vertical lines identify the bounds of the main segments.

6.3. Skeletal III Case

The third clinical application is a skeletal III case (clinically defined in section 6.2), and is illustrated by the mid-line profile of figure 6-23(a). The profile shows a retrognathic maxillary base, markedly affecting the positioning of the bony prominence at the base of the nose. The contour of the upper lip appears flat, and the chin prominent and long. A large mandibular facial height, typical of this condition, is also apparent.

The results of the bimaxillary corrective surgery are illustrated in the facial profile of figure 6-23(b). The maxilla was advanced with a Le Fort I maxillary osteotomy, and the prominence of the lower face reduced by a mandibular osteotomy (with a subsigmoid pushback).

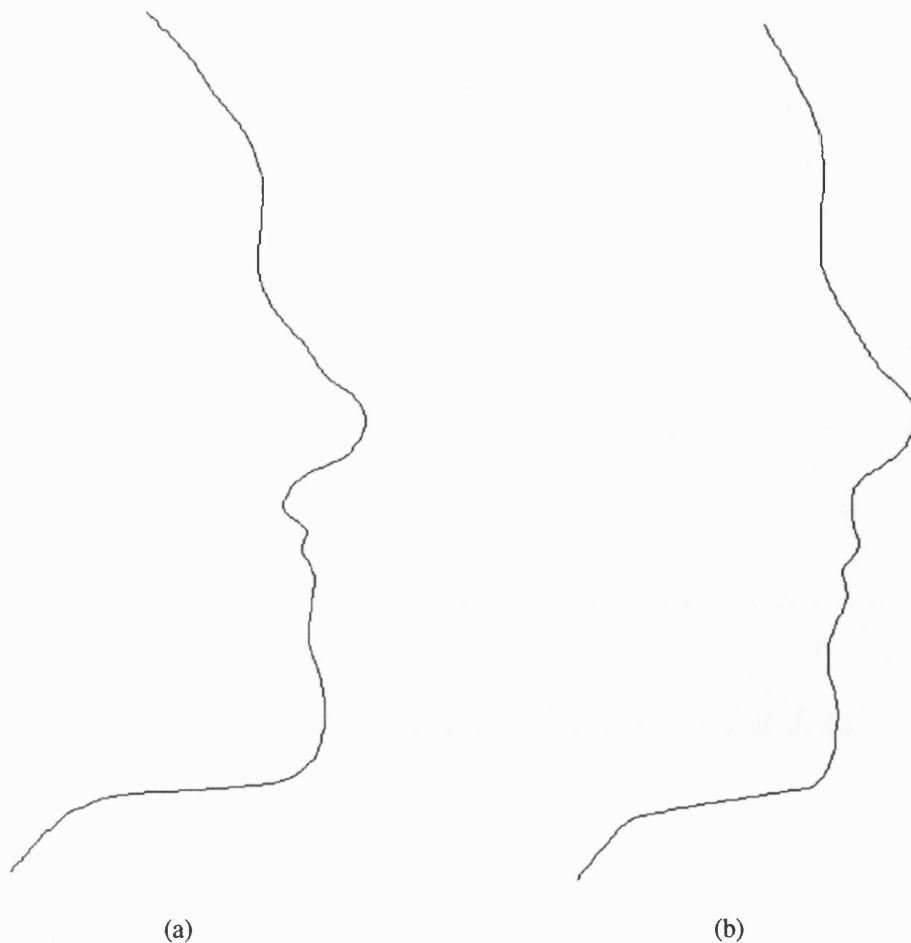
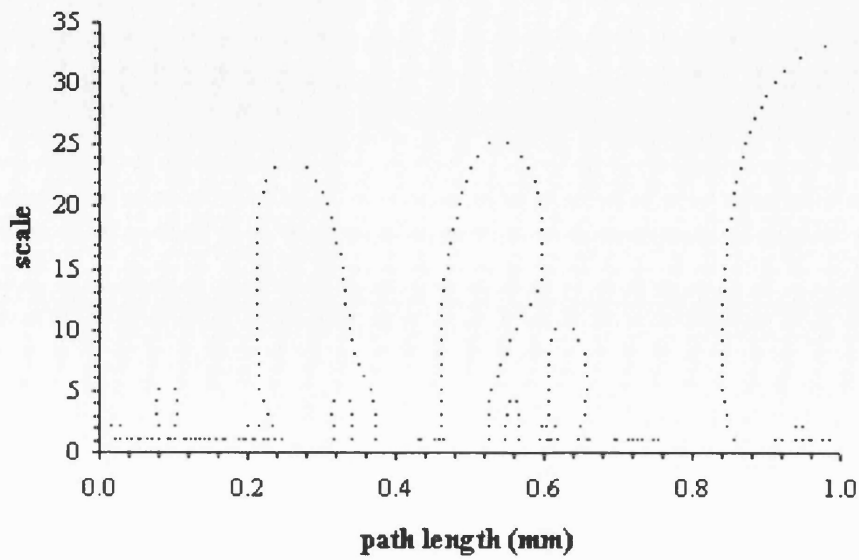


Figure 6-23 - Facial profiles of the skeletal III case.

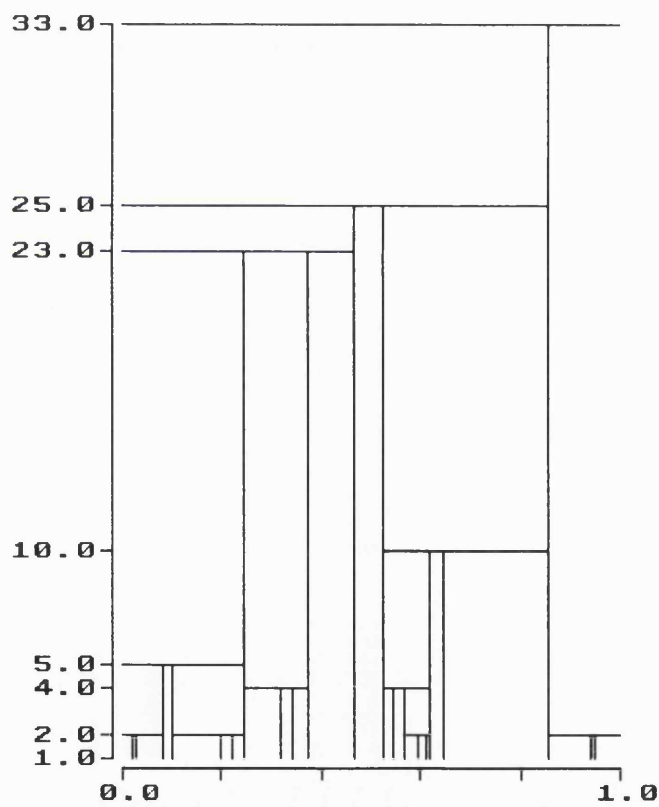
The mid-line vertical facial profiles represent: (a) before and (b) after surgical treatment.

Applications: Skeletal III

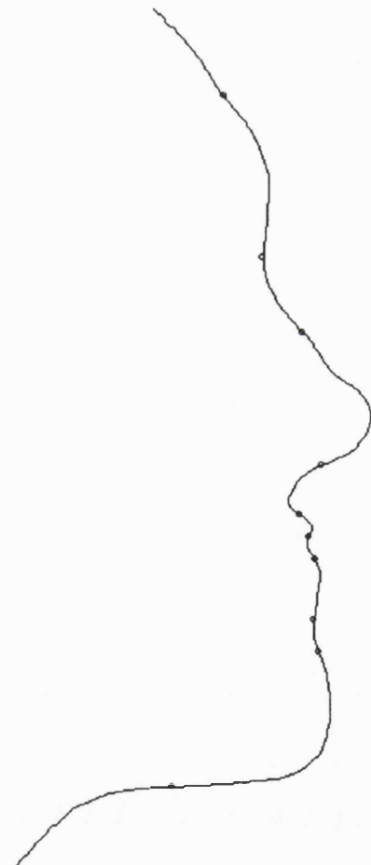
Figures 6-24, 6-25 and 6-26 present the qualitative descriptions generated by the analysis for the pre- and post-treatment profiles. Again, the profiles were divided into nine main curve segments, corresponding to the anatomical facial features outlined above. The segmented profiles are illustrated in figures 6-24(c) and 6-25(c). The quantitative measurements are presented in the tables 6-5 and 6-6.



(a)



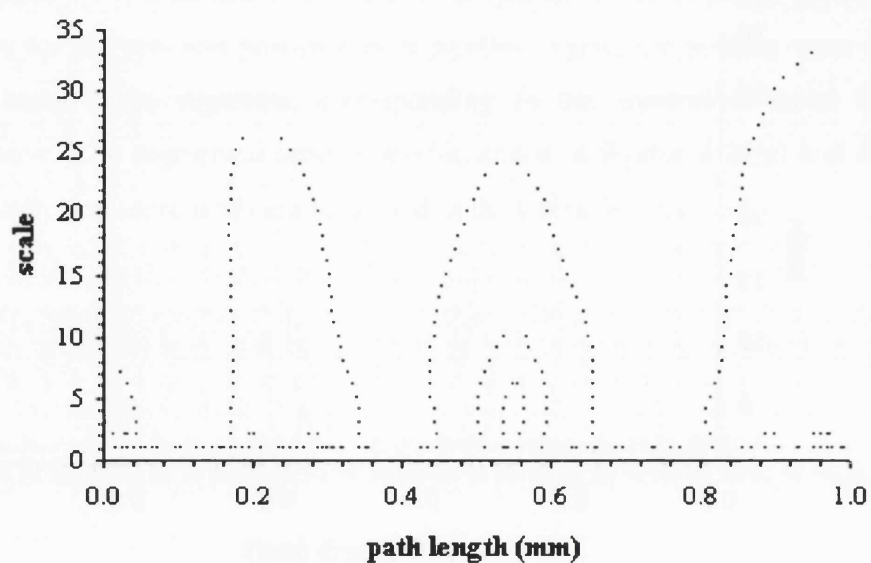
(b)



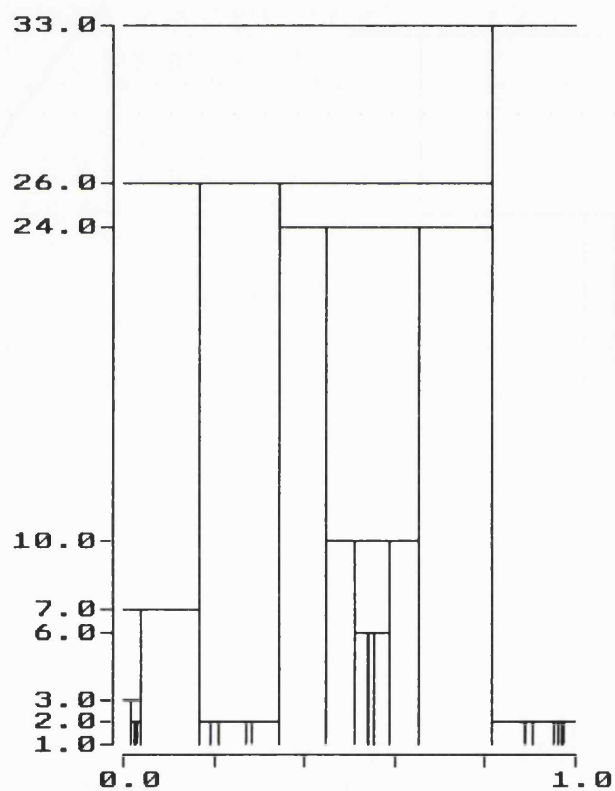
(c)

Figure 6-24 - Qualitative descriptions (skeletal III case - *before surgery*).

The qualitative descriptions are : (a) curvature scale space ; (b) interval tree (the x-axis represents the path length parameter (in millimeters) and the y-axis the scale parameter) . On (c) the landmarks and the segmented profile are indicated.



(a)



(b)



(c)

Figure 6-25 - Qualitative descriptions (skeletal III case - *after surgery*).

The qualitative descriptions are : (a) curvature scale space ; (b) interval tree (the x-axis represents the path length parameter (in millimeters) and the y-axis the scale parameter) . On (c) the landmarks and the segmented profile are indicated.

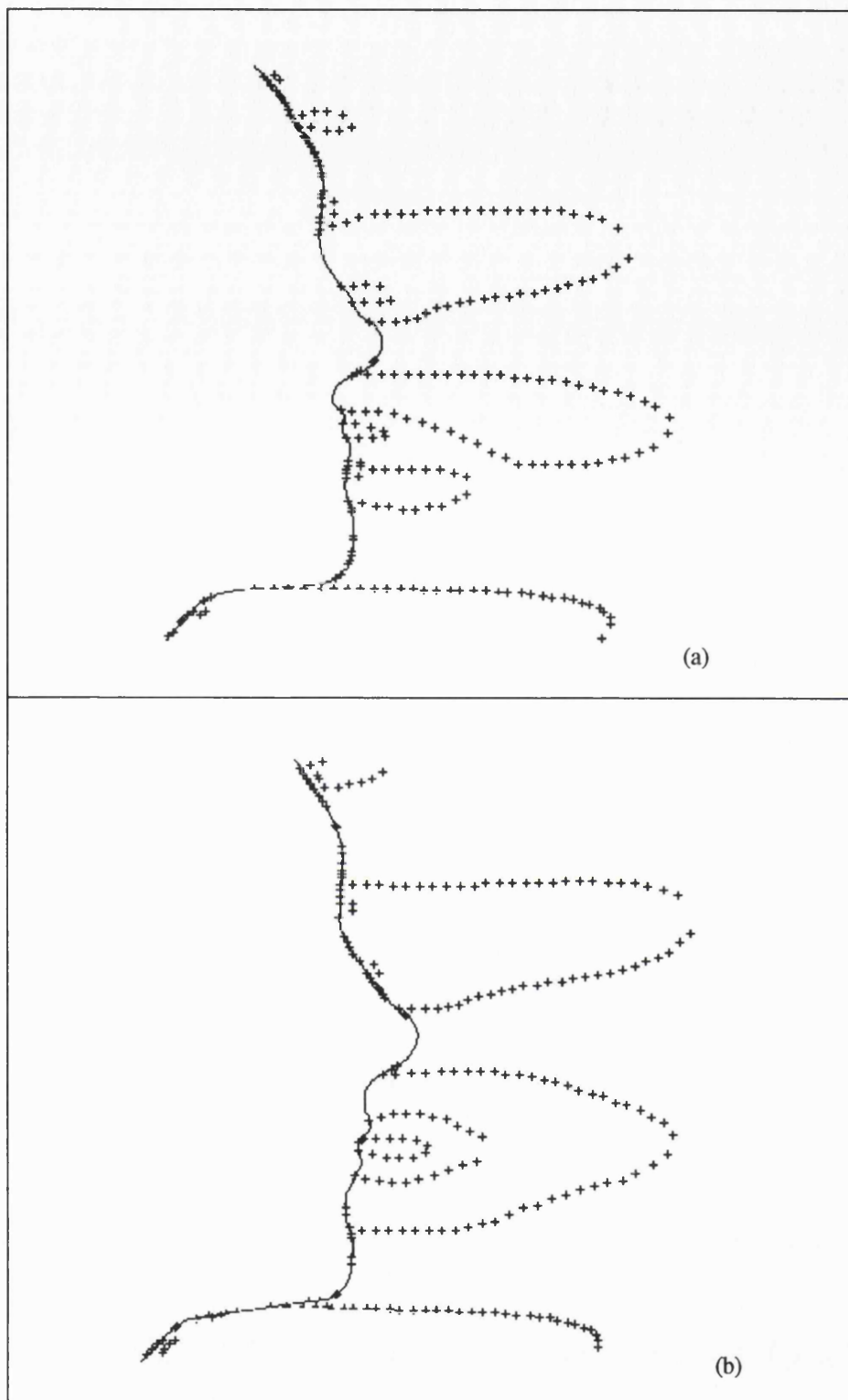


Figure 6-26 - Profiles and the zero crossing contours (skeletal III case).

The *alternative display* where the zero crossing contours can be related to the underlying facial features. (a) before treatment ; (b) after treatment.

Applications: Skeletal III


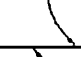

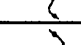
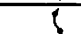

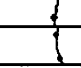

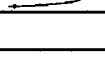
Segment no.	Segment shape	Start	End	no. points	Length (mm)	Average curvature	Average bending energy	Roundness	Compactness	Skew
0		0	24	25	25.51	0.006	5.7E-05	0.15	37.18	
1		24	61	38	41.80	0.011	4.1E-04	0.43	9.57	0.132
2		61	79	19	20.33	-0.026	8.4E-04	0.50	13.04	-0.016
3		79	116	38	39.90	0.039	3.7E-03	1.50	3.24	0.671
4		116	130	15	13.53	-0.086	8.8E-03	1.28	5.37	0.038
5		130	136	7	5.95	0.003	3.9E-04	0.02	34.71	2.39E-04
6		136	141	6	5.30	0.016	2.5E-04	0.10	17.03	-0.007
7		141	154	14	14.46	0.010	3.3E-04	0.14	39.51	-0.007
8		154	161	8	7.76	-0.022	5.0E-04	0.17	43.40	0.003
9		161	212	52	57.08	0.029	1.5E-03	1.53	2.85	-1.446
10		212	248	37	39.60	-0.023	6.1E-04	0.84	6.94	

Table 6-5- Table with the segment's shape and quantitative descriptive measures (*before surgery*).

These values refer to the segmented vertical profile outline of figure 6-24(c) (skeletal III case).




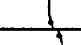
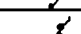


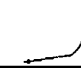
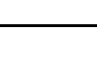
Segment no.	Segment shape	Start	End	no. points	Length (mm)	Average curvature	Average bending energy	Roundness	Compactness	Skew
0		0	10	11	9.14	-0.0002	1.7E-06	0.002	184.51	
1		10	42	33	33.58	0.0173	3.8E-04	0.571	10.64	0.106
2		42	67	26	25.94	-0.0225	6.4E-04	0.586	10.56	-0.005
3		67	111	45	43.81	0.0334	3.4E-03	1.502	3.57	0.593
4		111	126	16	14.28	-0.0482	3.0E-03	0.770	8.98	0.009
5		126	135	10	8.35	0.0140	2.5E-04	0.140	53.61	-0.011
6		135	137	3	1.83	-0.0004	1.7E-06	0.001	18.30	-1.74E-07
7		137	145	9	7.63	0.0065	6.5E-05	0.059	9.11	-1.85E-04
8		145	161	17	16.25	-0.0214	6.7E-04	0.363	16.87	0.002
9		161	203	43	42.74	0.0360	2.1E-03	1.546	3.26	-1.164
10		203	248	46	46.49	-0.0153	4.0E-04	0.706	7.92	

Table 6-6- Table with the segment's shape and quantitative descriptive measures (*after surgery*).

These values refer to the segmented vertical profile outline of figure 6-25(c) (skeletal III case).

6.3.1. Describing Curve Segments

The changes brought about by surgery are exposed by the qualitative and quantitative descriptions generated by this analysis.

6.3.1.1. Using the Qualitative Descriptions

The shape and relationship of the segments of the middle-third of the pre-operative profile are reflected by the zero crossing contours of the curvature scale space description seen in figure 6-24(a). They indicate, by the first two major arches, the relatively small nose, the marked concave subnasale segment, and the extremely flat upper lip (i.e. features typically caused by the retrognathic maxillary base - see also the cleft palate case). On a normal profile, the top of the first arch (or in some cases a single zero crossing contour) would be significantly higher (i.e. with a greater scale value) than the second one.

After the treatment, the same corresponding segments are now described by a distinctively different configuration of arches, particularly the set of three concentric arches (figure 6-25(a)). This is due to the fact that the group of segments composed by the subnasale, lips, mouth and labio-mental fold, has the overall shape of a large concave segment. Furthermore, this also indicates that the lips and mouth are still relatively small compared with the other facial features.

6.3.1.2. Using the Quantitative Descriptions

The local shape changes, as expressed by the curvature values of the profile points, is shown in figure 6-27. All the main facial features are represented in this plot, which shows that the most significant changes are localized between the subnasale segment and labio-mental fold.

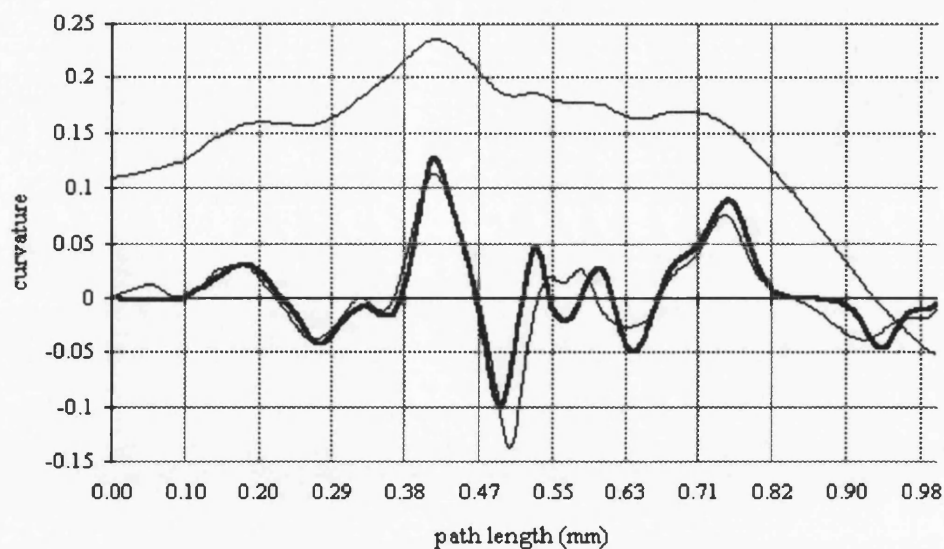


Figure 6-27 - Curvature plot (skeletal III case).

A scale value of 5 has been used in this analysis, indicating the local shape changes *before* (thin line) and *after* (thick dark line) surgical treatment.

From the diagrams of figure 6-28 it is possible to confirm these findings and also quantify the local curvature changes. They reveal a shorter and more concave brow ridge segment (1); that the nasion has become less concave and elongated (segment 2), and the nose less convex and elongated (segment 3). The subnasale segment has significantly reduced its concavity with a minor change in length (segment 4). Segment 5 shows a more convex upper lip, and segment 6 shows a surprisingly small mouth concavity, probably due to the marked reduction in its length. The lower lip (segment 7) has reduced in curvature and in length, whereas the labio-mental fold (segment 8) appears to only have been elongated without changing its concavity. The chin (segment 9) is shown with a slight increase in convexity and evidently shorter.

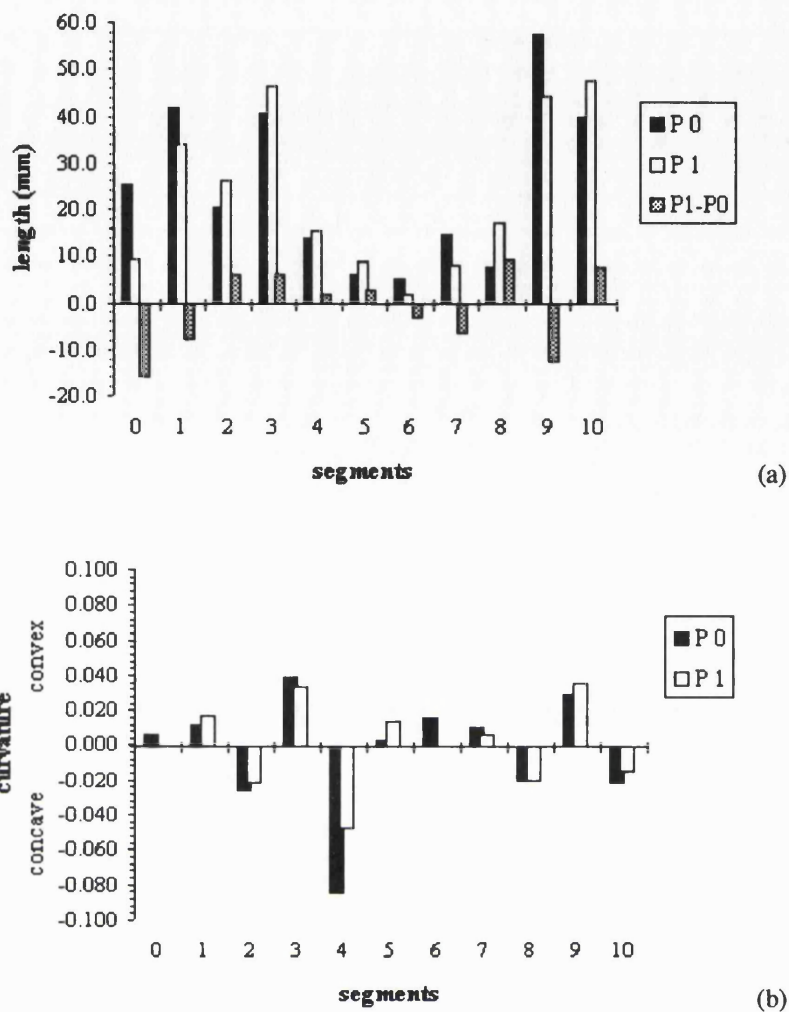


Figure 6-28 - Segment's quantitative measures.

On (a) the length of each segment is graphically illustrated. The dotted columns represents their difference. On (b) the mean curvature values are shown. **P0** and **P1** represent the *pre-* and *post-treatment conditions*, respectively.

6.3.1.3. Using the Bending Energy Concept

The bending energy plot, shown in the figure 6-29, reveals the shape changes as a result of the corrective surgical treatment. The scale value of three used in this plot identify the local shape changes, markedly in the segments four to seven.

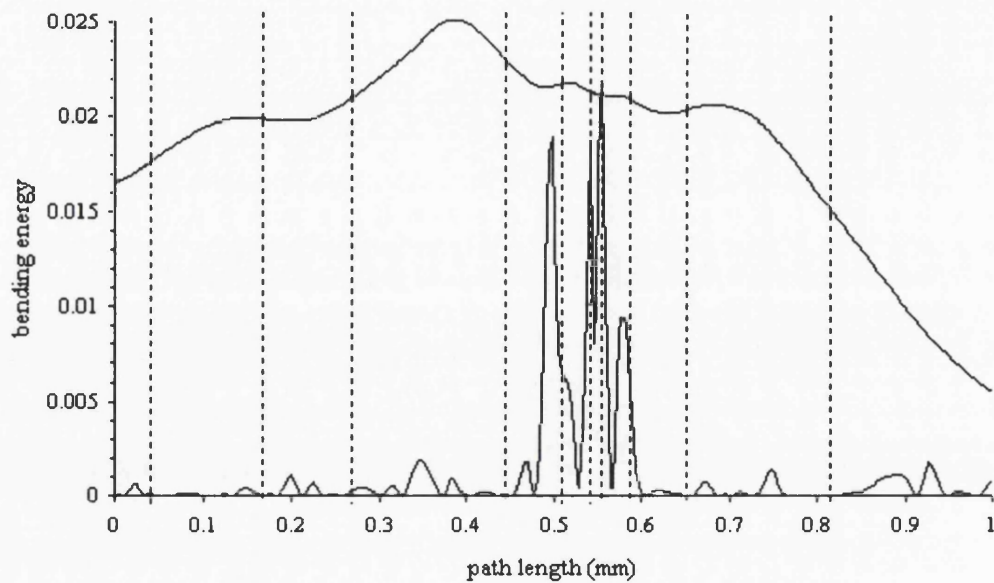


Figure 6-29 - Bending energy plot - Effects of surgical treatment (skeletal III case).

This plot shows the effects of the surgical treatment. A scale value of 3 has been used in this analysis, indicating the local shape changes on the *profile before treatment* when compared with the *profile after surgical treatment* (displayed on the diagram). The dashed vertical lines identify the bounds of the main segments.

Figures 6-30 and 6-31 show the bending energy analysis that represents the shape signatures for the skeletal III class of facial anomaly. This time, the mean facial profile was extracted from an mean face of a group of twenty normal male subjects (faces) of seventeen years old. Local shape changes are emphasized in the first plot, whereas the second plot emphasizes the global shape changes. They both describe the main shape deformation or the difference between the group of normal patients and this skeletal relationship class.

The results of the local analysis suggest that the major shape differences occurs in the region of the profile outline involving the subnasale segment and the labio-mental fold. The global analysis suggests that the primary areas of change involve segments four, five and nine, i.e. the subnasale segment, upper lip and chin.

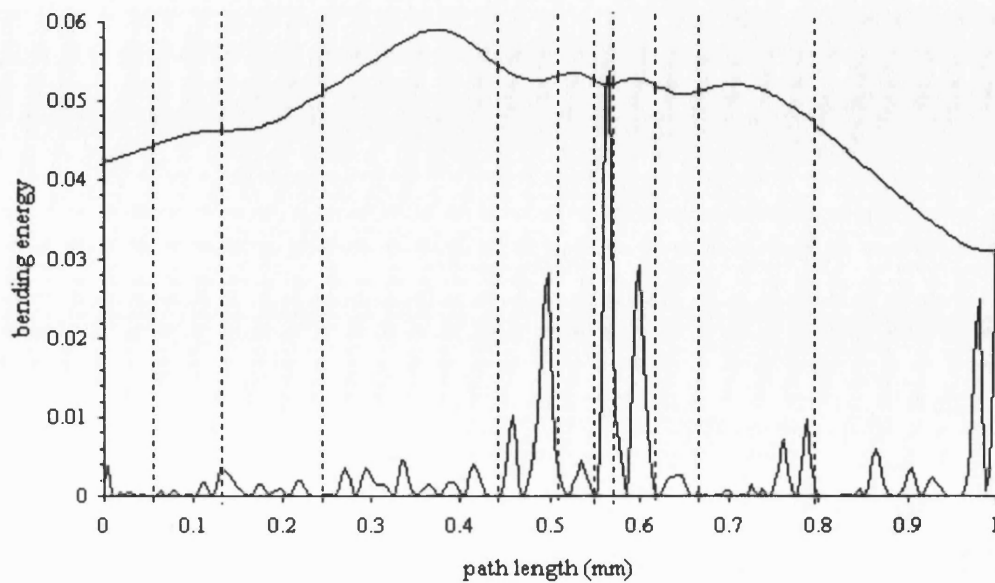


Figure 6-30 - Bending energy plot - Shape signatures for the skeletal III case.

A scale value of 2 has been used in this analysis, indicating the local shape changes on the *pre-operative profile* when compared with a *mean facial profile* (illustrated on the diagram). The dashed vertical lines identify the bounds of the main segments.

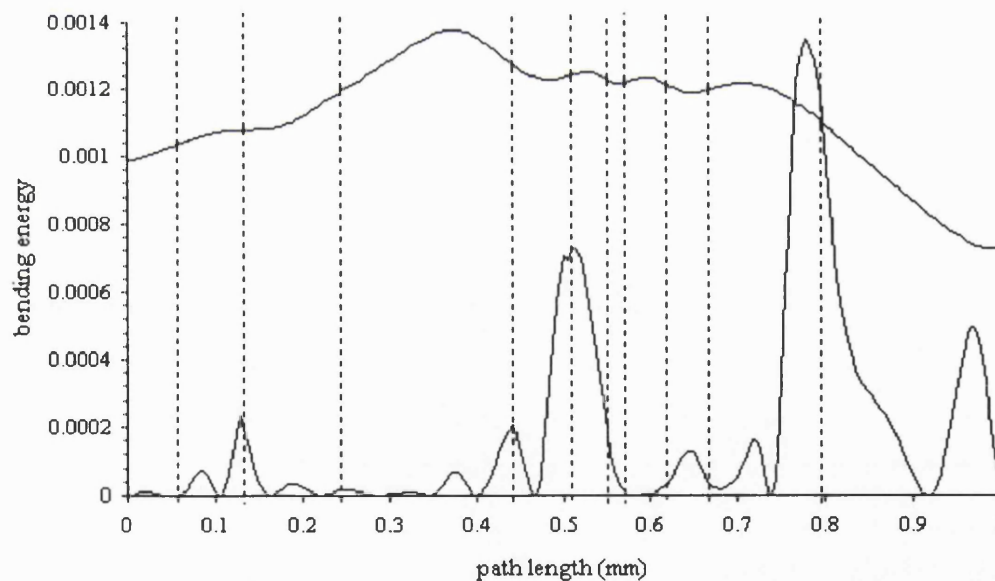


Figure 6-31 - Bending energy plot - Shape signatures for the skeletal III case.

A scale value of 10 has been used in this analysis, indicating the global shape changes on the *pre-treatment profile* when compared with a *mean facial profile* (illustrated on the diagram). The dashed vertical lines identify the bounds of the main segments.

Again, the bending energy analysis has been used to determine the main shape differences between the post-treatment profile and the mean facial profile (figure 6-32).

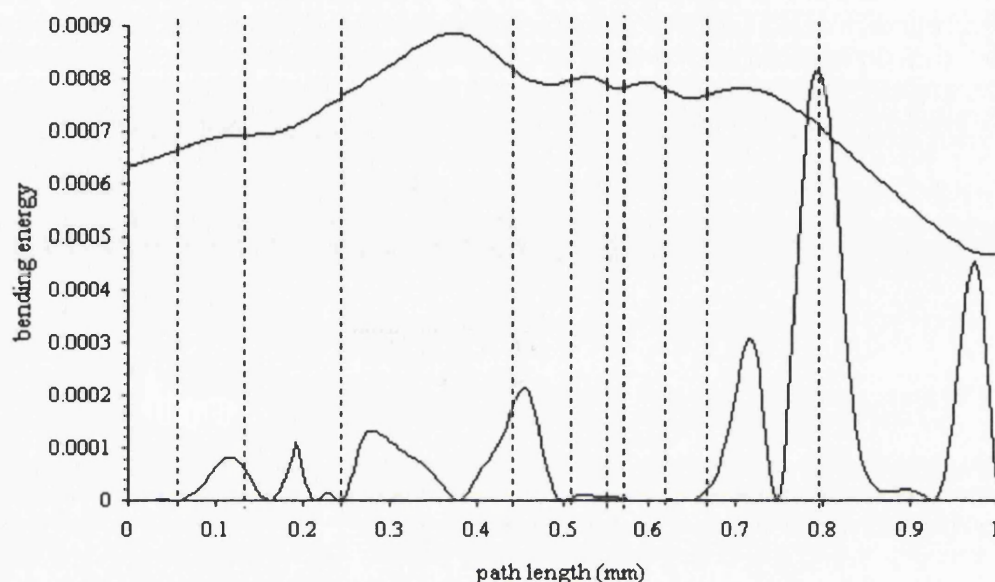


Figure 6-32 - Bending energy plot - closeness to the average (skeletal III case).

The scale value of 10 has been used in this analysis, indicating the global shape changes on the *pre-treatment* profile when compared with a *mean facial profile* (illustrated on the diagram). The dashed vertical lines identify the bounds of the main segments.

6.4. Growth Study

A growth study has been included in the scope of applications investigated here because of its fundamental importance on a number of scientific areas of research (e.g. orthodonty, anthropology and facial surgery). The number of investigations involving facial growth that have been made and reported in the literature is considerable. An interesting and broad review on facial growth, with an emphasis in orthodontics is given by Enlow (1990).

In many of these applications, a set of landmarks is defined and their location tracked down with time (see Farkas 1981, 1987). Although such methods do describe the changes of the landmarks, they provide no information about the changes of the segments in between those landmark points. Partially, this limitation was due to the

lack of methods which could deal with quantifying shape and shape changes, in a meaningful way, specially from a clinician's point of view.

That is precisely the focus of the investigation describe below. In fact, this growth study was part of a larger investigation made by J.P. Moss, myself and A.D. Linney (1992), when applying the methodology developed in this work. Therefore, the growth study consisted of representing the facial profiles as a sequence of convex and concave segments (anatomically meaningful) and then quantifying the changes in their shape observed over a period of time.

The group consisted of ten individuals at the ages of five, nine, thirteen, sixteen and twenty (also part of another growth study being conducted at King's College Hospital). The mid-line vertical profile of each patient was digitized from a lateral X-ray film, stored as a series of x- and y-coordinated points (approx. 300 points), from which the qualitative and quantitative descriptions were then generated.

Figure 6-33 illustrates the segments used in the analysis.

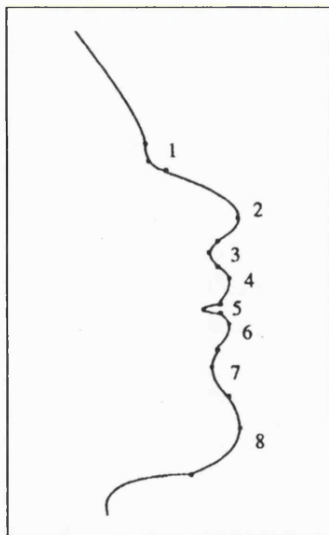


Figure 6-33 - Profile segmentation (growth study).

The segments are indicated by their bounding points, which represents the inflection points along the profile outline. They are : (1) soft tissue nasion ; (2) nose ; (3) subnasale area ; (4) upper lip ; (5) mouth ; (6) lower lip ; (7) labio-mental fold and (8) chin.

The curvature values are presented in the figure 6-34. The results for the soft tissue nasion (curve one), show little change over the period of observation. The nose (curve two) indicated some change in shape around puberty, and another at the age of twenty, at which point the shape characteristics become similar to those at the age of five. The curves of the upper and lower lips (numbers four and six)

Applications: Facial Recognition

showed some correlation at some ages, a possible indication that the growth pattern is similar at these points. Again, the same observation can be made with the curves representing the nose and the chin.

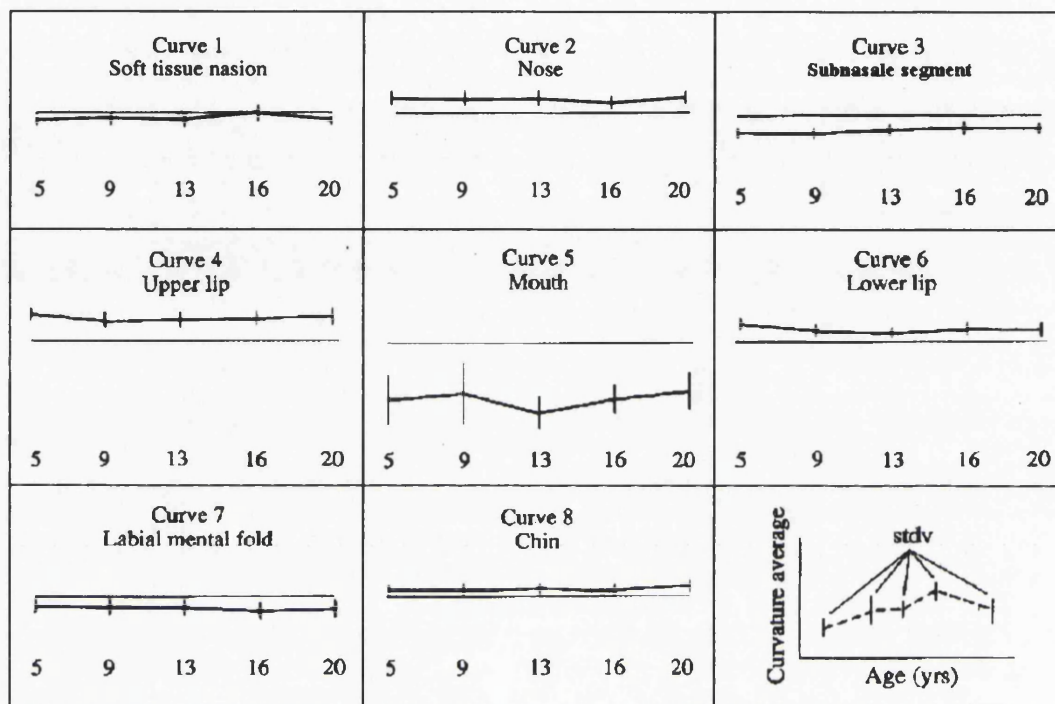


Figure 6-34 - Curvature diagrams (growth study).

The diagrams show the mean curvature value of each curve segment (see figure 6-33). The horizontal axis represents the age. The vertical line at each age represents the standard deviation of the group at that age. The vertical axis represents the curvature, with the continuous horizontal line indicating the zero value.

This analysis of the profiles of the growing individuals demonstrates the changes in the curves of the face with growth.

6.5. Facial Recognition

The last application to be considered is on facial recognition. Undoubtedly, the recognition of faces, in itself, constitutes a fascinating field of research, involving a large number of disciplines and different approaches. New technology and techniques have enabled researchers to considerably expand the human knowledge and understanding in this area of work (see Coombes 1993 for a survey). As reviewed in

chapter 3, facial profiles have been used for this purpose on a number of scientific publications, some of which dating as far back as the late 1800.

The aim of this pilot study was to explore and evaluate the use of the curvature scale space description on the identification of faces when represented by the mid-line vertical profile. The primary interest is to verify if a given face can be identified from a reference database, and whether more than one face would be pointed as a possible candidate for the match.

Following are the stages of the method employed to achieve this : the profiles are first segmented and a number of facial parameters calculated; a matching scheme based on these parameters is then used to measure the similarity of profiles.

6.5.1. Setting up the Data

The faces of ten subjects, male and female adults of a mixed age group and ethnic origin, were used in this trial investigation. Their faces were digitized using the UCL-MGI optical surface scanner (section 4.6.1) on two separate occasions. None of them had glasses or facial hair. From these data sets, twenty mid-line vertical profiles were extracted (section 5.3), one for each face, and then separated into two groups : the *reference* group, containing one profile for each individual, and the *test* group, containing the remaining profiles.

The CSS descriptions were used to identify and locate a set of ten inflection points along the profile, dividing them into nine curve segments (basically, the same ones used in the clinical applications as illustrated in figure 6-1(b)). Subsequently, to represent a profile for identification, a set of “facial parameters” consisting of inflection points and mean curvature values were used.

6.5.2. Matching Scheme

To compute the match between a given test profile against the reference database, the facial parameters were compared with each other. In cases where they would coincide or fall within a limited band defined around the tested parameter, the value of ‘1’ would be returned, otherwise, the value would be ‘0’. At the end, these ‘values’ were

Applications: Facial Recognition

yielding a score, one *for each profile* of the reference database. This score was then used as a measure of similarity of profiles, with the highest score indicating the identified profile. In addition to that, a second score was produced, this time by adding up the ‘values’ assigned *for each parameter* of the reference database. The new score was then used to determine the significance of each parameter within each set.

The band of the parameter mentioned above has been established with data from a previous study I have conducted on the reproducibility of identifying a set of landmark points (comparable to the one used here). A single mid-line vertical facial profile was used on which the same set of ten landmarks were identified on ten separate occasions, by one individual. The values of the standard deviation computed for landmarks 1 to 10 were: 0.0047, 0.0053, 0.0072, 0.0040, 0.0020, 0.0020, 0.0017, 0.0022, 0.0023 and 0.0118 . These values were adopted as a fixed increment, thus defining the band limits by being added to or subtracted from their corresponding test parameter (i.e. the inflection points).

At this point, a remark should be made regarding the landmarks located at the extremes of the profile, more specifically, the landmarks 1 and 10 which define the bounding points of the brow ridge and of the chin segments. Landmark 1 is located on a relatively large straight region of the profile outline which could lead to a number of closely defined inflection points at the finest scale value. On the other hand, landmark 10 is located under the chin, a part of the face which is critical to the optical surface scanner system, and where some loss of data could occur (see section 4.6.1). This is reflected in the facial profile outline and in the inflection points defined at the finest scale value. Consequently, some variation in the location of these landmarks could occur, with the greatest being on landmark 10 (this is graphically illustrated in figure 5-38, section 5.10.2.1, on landmarks 2 and 12).

6.5.3. Facial Parameters

In a first experiment, the normalized path length values given by the inflection points defined a set of ten facial parameters, used to represent the facial profile (denoted by p_1, p_2, \dots, p_{10}).

The results shown in table 6-7 are for the scores given by each reference profile (lines horizontally across the table) when identifying the test profiles (lines vertically across the table). Each score indicates the total number of parameters, belonging to the test profile, that were found in the reference group. For example, the first three values in the first column show ten on R1, one on R2 and zero on R3. Thus, indicating that all ten parameters could be found on R1, only one on R2 and none on R3.

Reference group	Test group										foreign
	T1	T2	T3	T4	T5	T6	T7	T8	T10	T11	
R1	10	2	0	1	0	0	0	1	0	1	1
R2	1	6	1	0	0	0	1	0	0	1	0
R3	0	0	6	0	0	1	1	0	0	0	0
R4	1	0	0	4	2	1	0	0	0	0	3
R5	1	0	0	2	5	2	0	2	2	3	2
R6	0	0	2	0	1	6	0	0	0	0	0
R7	0	1	0	0	1	1	3	0	1	0	0
R8	1	0	0	1	2	1	0	10	1	2	0
R10	0	2	0	1	1	4	0	1	7	1	0
R11	1	2	0	0	3	0	0	2	0	10	0

Table 6-7 - Scores used as a measure of similarity of profiles (*first experiment*).

Table of scores given by *each reference profile* (lines horizontally across the table) when identifying the test profiles (lines vertically across the table). The highest score indicates the identified profile.

The highest scores being on the diagonal of the table suggests that all profiles from the test group could be identified. However, if a threshold of five was added to the analysis (i.e. the minimum number of parameters necessary for a profile to be identified), T4 and T7 would be excluded from the group of identified profiles. Moreover, the scores show that not more than one candidate would be identified as the tested profile.

A 'foreign' profile (i.e. one not included in the database) was also tested, as shown on the right side of the table. The closest candidate for that 'unknown' profile would be profile R4.

Applications: Facial Recognition

Table 6-8, in the same way as with the previous table, show the scores given by each facial parameter (lines horizontally across the table). The value of 1 indicates the highest significance. The parameters p5, p6, p7 and p9 appears to be the most significant ones from the set.

Facial parameter	Test group										foreign
	T1	T2	T3	T4	T5	T6	T7	T8	T10	T11	
p1	2	2	1	1	3	2	1	3	0	3	0
p2	1	2	1	1	2	1	1	1	0	2	0
p3	2	1	1	1	1	3	0	5	3	5	0
p4	2	1	1	1	1	3	1	2	2	1	0
p5	1	1	1	0	1	1	0	1	0	1	0
p6	1	1	1	0	1	1	0	1	1	2	1
p7	1	1	1	1	1	1	0	1	1	1	0
p8	1	1	0	1	2	2	0	1	1	1	2
p9	1	1	0	1	1	0	0	1	1	1	0
p10	3	2	2	3	2	2	2	1	2	1	3

Table 6-8 - Scores used as a measure of significance of facial parameters (first experiment).

Table of scores given by *each facial parameter* (lines horizontally across the table) when identifying the test profiles (lines vertically across the table). The value of 1 indicates a significant parameter.

A second experiment was carried out, by adding four parameters to the set used to represent the facial profile. They were the mean curvature values of some pre-selected segments, judged to be highly characteristic features of the profile, including the brow ridge, soft tissue nasion, nose and subnasale segments (denoted by ku1, ku2, ku3 and ku4, respectively).

The results showing how well the profiles from the test group (and a foreign) were classified is given by the table 6-9. They indicate a notable increase on the scores which identified the test group (i.e. the diagonal), suggesting that the added parameters were useful in the analysis. Interestingly, T7 still remained with a low score value.

Reference group	Test group										
	T1	T2	T3	T4	T5	T6	T7	T8	T10	T11	foreign
R1	13	3	1	1	0	0	0	1	0	2	1
R2	3	8	2	0	0	0	1	1	0	3	0
R3	2	1	9	0	1	1	1	0	0	1	0
R4	1	0	0	6	2	2	0	0	0	0	3
R5	1	0	1	2	8	2	0	2	2	3	3
R6	0	0	2	1	1	7	1	0	1	0	1
R7	0	2	0	0	1	1	4	0	1	1	0
R8	1	1	0	1	2	1	0	12	2	3	0
R10	0	2	0	1	1	5	1	2	8	1	1
R11	2	4	1	0	3	0	0	3	0	13	0

Table 6-9 - Scores used as a measure of similarity of profiles (*second experiment*).

Table of scores given by *each reference profile* (lines horizontally across the table) when identifying the test profiles (lines vertically across the table). The highest score indicates the identified profile.

When looking at the performance of the new parameters (table 6-10), the mean curvature value of the brow ridge segment (ku1) seems to be the best one. This could be explained by the fact that the band limits need to be adjusted to more appropriate values (in this case they were computed based on 10% of the nominal value).

Facial parameter	Test group										
	T1	T2	T3	T4	T5	T6	T7	T8	T10	T11	foreign
p1	2	2	1	1	3	2	1	3	0	3	0
p2	1	2	1	1	2	1	1	1	0	2	0
p3	2	1	1	1	1	3	0	4	3	5	0
p4	2	1	1	0	1	3	1	2	2	1	0
p5	1	1	1	0	1	1	0	1	0	1	0
p6	1	1	1	0	1	1	0	1	1	2	1
p7	1	1	1	1	1	1	0	1	1	1	0
p8	1	1	0	1	2	2	0	1	1	1	2
p9	1	1	0	1	1	0	0	1	1	1	0
p10	3	2	2	3	2	2	2	1	2	1	3
ku1	3	0	1	0	1	0	1	0	0	1	0
ku2	4	4	4	2	1	1	0	1	0	4	1
ku3	0	0	0	0	0	0	0	0	0	0	0
ku4	1	4	2	1	2	2	2	4	3	4	2

Table 6-10 - Scores used as a measure of significance of facial parameters (*second experiment*).

Table of scores given by *each facial parameter* (lines horizontally across the table) when identifying the test profiles (lines vertically across the table). The value of 1 indicates a significant parameter.

6.6. Summary

The applications presented in this chapter have demonstrated the potential of the methodology proposed in this work.

In each clinical case, the qualitative and quantitative aspects of the analysis have clearly described the profile before the treatment and the overall effect of the surgical corrections shown in the profile after the treatment.

The qualitative descriptions, more specifically the curvature scale space, seems to provide a unique description of the facial profiles. The changes in shape of the main areas of the profile affected as a result of the treatment may be visually observed and assessed by the relative size and position of the zero crossing contours.

The segmentation using inflection points and the quantitative analysis have shown to produce a pattern of concavity and convexity corresponding to the clinical perception of the changes that occurred in the facial profiles due to surgical treatment. The curvature values, the bending energy and the complementary measures have allowed the changes in the shape of the various segments to be quantified and described in a repeatable and objective manner. More importantly, they enabled the results of the treatment to be quantitatively assessed (or audited) by establishing how close the post-operative profile was to the average.

In the last two applications, the analysis produced meaningful data on the growth of the face, and the use of the curvature scale space description have shown encouraging results on the identification of facial profiles. Certainly, some improvements could be achieved by incorporating the scale value in the matching scheme, and perhaps adding other curvature points (i.e. maxima and minima) to the facial parameter list.

Chapter Seven

7. Discussion and Conclusions

A methodology for the analysis of human facial profiles has been developed in this thesis. Qualitative and quantitative mathematical representations can be derived which describe the shape of the profile, and also the changes in the profile morphology, specially as a result of orthodontic treatment or reconstructive surgery.

From the review of the literature in shape analysis and of the study of the human face, it was possible to identify the notion of curvature as a powerful representation for contours, and also the importance attached to the use of landmarks, by the existing methods, in the overall analysis.

These led me to define the basic requirements for the description of the shape of facial profiles, later incorporated in the methodology here proposed. They are : (i) the importance of curvature variation along the outline; (ii) the concept of curvature as a result of processes acting on the shape; (iii) the use of metric information extracted from curvature analysis; (iv) the use of curve segments bounded by perceptually relevant points (i.e. inflection points); (v) the role played by the identification and location of landmarks in segmenting the profile as a pre-cursor for analysis; (vi) an automatic process of locating landmarks reducing the overall error by eliminating the subjectivity error; (vii) the emphasis given to the changes in shape of the segments between the landmarks rather than their relative movements; (viii) the flexibility in describing local and global facial features; (ix) robustness against noise; and (x) invariance under profile rotation, uniform scaling and translation.

In order to meet these requirements, I have used the technique of scale space filtering and its particular application to planar curves. Although such a technique has been used before in analyzing closed contours, it has not, to my knowledge, been applied to the analysis of changes in the morphology of facial profiles.

Discussion and Conclusion

Furthermore, this work has benefited from the use of data from the an optical surface scanner, which provided the means of producing accurate measurements of the surface of the face, from which a number of arbitrary profiles could be extracted for analysis.

Initially in the analysis, two main *qualitative descriptions* are derived from the analyzed facial profile : the *curvature scale space*, which fully describes the behavior of the inflection points (or zero crossings) along the outline over a continuum of scale values, and the *interval tree*, which also uses inflection points but this time organized by scale. From the latter, the exact location of inflection points along the profile may be obtained, thus dividing the profile into a number of convex and concave curve segments. It has been shown here that this automatic segmentation process is highly objective, which represents a great advantage over the existing methods based on an operator to located specific and often poorly defined points on the profile.

Then, the profile segments produced in this manner are quantified, based on the curvature approach. The curvature and bending energy plots are generated from this analysis. In addition, complementary measures such as length, compactness, roundness and skew are also computed for the individual segments. These *qualitative descriptions* allow the various curve segments to be classified in terms of their concavity.

The experiments carried out to evaluate the method have determined the stability of the curvature scale space description to noise, and its response to local and global shape variations along the profile. In addition, the repeatability and reliability of the segmentation process have been verified, even under circumstances in which the profile has being transformed by uniform scaling, translation and rotation. Although the patterns of the zero crossing contours in the curvature scale space description may vary, the segments can always be identified.

The potential of the methodology here proposed has been demonstrated when applied to some typical clinical cases. The curvature scale space description provides a unique description of the facial profiles, allowing the changes in shape, as a result

of the treatment, to be visually observed and assessed. On the one hand, the segmentation using inflection points and the quantitative analysis have been shown to produce a pattern of concavity and convexity corresponding to the clinical perception of the changes that occurs in the facial profiles due to surgical treatment. On the other hand, the quantitative measures have allowed the changes in the shape of the various segments to be quantified and described in a repeatable and objective manner. More importantly, the curvature and bending energy measures enable the results of the treatment to be quantitatively assessed by establishing how close the post-operative profile is to the average. This is of great significance to the improvement of the existing clinical methods through an audit scheme. Furthermore, these measures could be used on a pattern recognition system to automatically classify and identify the profiles on a clinical basis, according to the facial anomaly they represent (for example, skeletal pattern, cleft palate, first arch, etc.).

Meaningful data has been produced by the analysis on the growth of the face. Finally, as a pilot study, the method has shown encouraging results in the identification of facial profiles, based on a set of facial parameters consisting of inflection points and mean curvature values.

7.1. Conclusions

The following points may be draw from this work :

1. The multiscale approach allows qualitative descriptions to be derived, uniquely representing the facial profile.
2. Based on the notion of curvature, powerful and clinically meaningful quantitative descriptions may be achieved.
3. The ability of the method to equally analyse horizontal and vertical profiles, expanding the analysis to outlines other than the standard mid-line profile.
4. The idea of segmenting the profile using scale space techniques proved to be efficient as it avoids the problems of identification of landmarks by using mathematically constructed points.

Discussion and Conclusion

5. The established metric is sensitive to shape, rather than simply to the spatial relationship of landmark points.
6. The advantage of using inflection points is that they indicate where the curve changes from concave to convex and vice-versa. Thus, it is possible to naturally represent the profile as a number of convex and concave curve segments.
7. The method of analysis, using curvature values, produces a pattern of concavity and convexity corresponding to the clinical perception of the profile, and gives a valuable shape description as one is able to quantify whether the segment has altered its curvature.

7.2. Further Work

1. To explore the qualitative measures of the profile segments to present some parameters that would classify the different facial features. For example, within the segment that represents the nose one might be able to characterize two or three types by considering the length of the spine, or the curvature of the tip of the nose, or even its base.
2. To include statistical analysis in the study and classification of the profile segments.
3. To expand the growth study including the use of bending energy approach.
4. To expand the investigation on facial identification, by using different matching schemes, and also developing the use of the interval tree description.

Bibliographical References

- E.H. Albery, I.S. Hathorn and R.W. Pigott (1986), Cleft lip and palate : a team approach, published by John Wright & Sons Ltd.
- A.L. Allen (1950), Personal Descriptions, Butterworth & Co. Publishers, London.
- T.R. Alley (1988), Social and Applied Aspects of Perceiving Faces, Clemson University.
- F.L. Alt (1962), Digital Pattern Recognition by Moments, Journal Assoc. Comput. Machine vol.11, pp.24-258.
- H. Anton (1988), Calculus with analytic geometry, Drexel University, Edit. John Wiley & Sons.
- C.C. Archibald and S.R. Sternberg (1986), Mathematical Morphology applied to range image processing, Proc. Graphics Interface '86, Vision Interface '86, pp.293-299.
- S. Arridge, J.P. Moss, A.D. Linney and D. James (1985), Three dimensional digitisation of the face and skull, J. Max.-Fac. Surgery, vol.13, pp.136-143.
- H. Asada and M. Brady (1986), The curvature primal sketch, IEEE-PAMI, vol.8, no.1, pp.2-14.
- F. Atteneave (1954), Some Informational Aspects of Visual Perception, Psychol. Rev. vol.61, pp.183-193.
- F. Atteneave and M.D. Arnoult (1956), The Quantitative Study of Shape and Pattern Perception, Psychological Bulletin, vol.53, no.6, pp.452-471.
- J. Babaud, A. Witkin, M. Baudin and R.O. Duda (1983), Uniqueness of the gaussian kernel for scale-space filtering, IEEE - PAMI vol.8, no.1, pp.26-33.
- D.H. Ballard and C.M. Brown (1982), Computer Vision, Englewood Cliffs, N.J., Prentice-Hall.
- D.H. Ballard (1988), Strip Trees : A hierarchical representation for curves, Comm. Assoc. Comput. Mach. Vol.24, pp.310-321.
- S. Baumrind and R.C. Frantz (1971), The reliability of head film measurements - 1. Landmark identification, American Journal of Orthodontics, vol.60, no.2, pp.111-127.
- A. Bengtsson and J.O. Eklundh (1991), Shape representation by multiscale contour approximation, IEEE - PAMI, vol.13, pp.85-93.
- A. Bennett and I. Craw (1991), Finding Image Features using Deformable Templates and detailed prior Statistical Knowledge, Proc. British Machine Vision Conference.

References

- R.H. Benson, R.E. Chapman and A.F. Siegel (1982), On the Measurement of Morphology and its Change, *Paleobiology* vol.8, no.4, pp.328-339.
- A. Bertillon (1885), *Identification Antropometric - Instructions Signalétiques*, Ministere de L'Interieur, Melun Typographie.
- A. Bertillon (1890), *La Photographie Judiciaire*, Gauthier-Villars et Fils, Paris.
- P.J. Besl (1988), *Surfaces in Range Image Understanding*, Springer-Verlag, N.Y., USA.
- P.J. Besl and R.C. Jain (1988), Segmentation through variable-order surface fitting, *IEEE-PAMI*, vol.10, no.2, pp.167-192.
- S. Bhatia and J. Sowray (1984), A computer aided design for orthognathic surgery, *British Journal of Oral Maxillofacial Surgery*, pp.22-237.
- C.L. Bisson (1965), Location of some facial features by computer, Report PRI:20, Panasonic Research Inc., Palo Alto, Calif.
- A. Björk (1947), *The Face in Profile*, Svensk Tandlak - T40, suppl. 5B
- A. Blake (1986), Surface Reconstruction from Stereo and Shading, *Proc. Alvey Computer Vision and Image Interpretation Meeting*, University of Sussex, pp.15-18.
- C. Blakemore and R. Over (1974), Curvature Detectors in Human Vision, *Perception*, vol.3, pp.3-7.
- W.W. Bledsoe (1964), The model method in facial recognition, Report PRI:15, Panasonic Research Inc., Palo Alto, Calif.
- H. Blum (1973), Biological Shape and Visual Science, *Int. J. Theory Biol.*, pp.205-287.
- H. Blum and R.N. Nagel (1978), Shape description using Weighted Symmetric Axis Features, *Pattern Recogn.* vol.10, pp.167-180.
- J.D. Boissonnat (1985), Surface Reconstruction from Planar Cross-Sections, *Proc. IEEE*, pp.393-397.
- F.L. Bookstein (1978a), *The Measurement of Biological Shape and Shape Change*, Lecture Notes in Biomathematics 24, Springer - NY.
- F.L. Bookstein (1983), The Geometry of Craniofacial Growth Invariants, *Am.J.Orthod.* vol.83, no.3, pp.221-234.
- F.L. Bookstein (1984), A Statistical Method for Biological Shape Comparisons, *J.Theoret.Biol.* vol.107, pp.475-520.
- F.L. Bookstein (1986), Size and Shape Spaces for Landmark Data in Two-Dimension, *Statistical Science* vol.1, no.2, pp.181-242.
- F.L. Bookstein (1989), Princial Warps: Thin-plate Splines and the Dicomposition of Deformations, *IEEE-PAMI* vol.11, no.6, pp.567-585.
- F.L. Bookstein and F.J.Rohlf (1990), *Proceedings of the Michigan Morphometrics Workshop*, Special Publication No.2, The University of Michigan Museum of Zoology, Ann Arbor, Michigan.

References

- F.L. Bookstein (1991), *Morphometric Tools for Landmark Data*, Cambridge University Press, Cambridge.
- P. Boulanger, K.B. Evans, M. Rioux and P. Ruhlmann (1985), Object input for CAD/CAM using a 3D laser scanner, National Research Council of Canada Laboratory for Intelligent Systems, NRCC memo no.25446.
- F.D. Bower (1930), *Size and Form in Plants*, Macmillan, London.
- J.E. Bowie and I.T. Young (1977), An Analysis Technique for Biological Shape - II, *Acta Cytologica*, vol.21, no.3, pp.455-746.
- M. Brady (1982), Smoothed Local Symmetries and Frame Propagation, *Proc. Conf. Pattern Recognition Image Processing*, N.Y., IEEE Comp.Soc., pp.629-633.
- M. Brady (1983), Criteria for representations of shape, in *Human Machine Vision*, J.Beck, B.Hope and A.Rosenfeld ed., Academic Press, N.Y., pp.38-84.
- M. Brady and H. Asada (1984), Smoothed Local Symmetries and their Implementation, *Inter. Journal of Robotics Research*, vol.3, no.3, pp.36-61.
- M. Brady and A. Yuille (1984b), An Extremum Principle for Shape from Contour, *IEEE-PAMI*, vol.6, no.3, pp.288-301.
- B.H. Broadbent (1931), A New X-Ray Technique and Its Application to Orthodontia, *Angle Ortho.*, vol.1, pp.45-66 ; Reprinted on the *Angle Orthodontist*, vol.51, no.2, pp.93-114, 1981.
- B.H. Broadbent (1937), The Face of the Normal Child : Bolton Standards and Technique, *Angle Orthodontist*, vol.7, pp.183-233.
- A.G. Brodie (1941), On the Growth of the Human Head from the Third Month to the Eighth Year of Life, *Amer. J. Anat.* Vol.68, pp.209-262.
- E.S. Broadway, M.J.R. Healy and H.G. Poyton (1962), The accuracy of tracings from cephalometric lateral skull radiographs, *Trans. B.S.S.O., The Dental Practitioner*, pp.455-459.
- V. Bruce and P. Green (1990), *Visual Perception : Physiology, Psychology and Ecology*, 2nd edition, Published by Lawrence Erlbaum Assoc. Ltd.
- V. Bruce, A. Coombes and R. Richards (1993), Describing the shape of faces using surface primitives, *Image and Vision Computing*, vol.11, no.6, pp.353-363.
- J.C. Campos, A.D. Linney and J.P. Moss (1992), The Analysis of Facial Profiles using Scale Space Techniques, *Colloquium on Machine Storage and Recognition of Faces*, IEE Electronics Division, Digest no. 1992/017, 24th January, pp.10/1-10/3.
- J.C. Campos, A.D. Linney and J.P. Moss (1993), The Analysis of Facial Profiles using Scale Space Techniques, *Pattern Recognition*, vol.26, no.6, pp.819-824.
- J.W. Carl and C.F. Hall (1972), The applications of filtered transforms to the general classification problem, *IEEE Trans.Comput.* vol.C-21, no.7, pp.785-793.
- G.E. Carlson (1967), Error in X-ray cephalometry, *Odont. Tidskr.* Vol.75, pp.99-129.

References

S.J. Chaconas (1980), Orthodontics, Postgraduate dental handbook series, vol.10, PSG Publishing Co. Inc.

A.M. Cohen (1984), Uncertainty in Cephalometrics, British Journal of Orthodontics, vol.11, pp.44-48.

A.M. Cohen, H.H-S. Ip and A.D. Linney (1984), A preliminary study of computer recognition and identification of skeletal landmarks as a new method of cephalometric analysis, British Journal of Orthodontics, vol.11, no.3, pp.143-154.

W.M. Conway (1958), The Writings of Albrecht Dürer, P.Owen Ltd, London.

A.M. Coombes, A.D. Linney, S.R. Grindrod, C.A. Mosse and J.P. Moss (1990a), 3D Measurement of the face for the simulation of facial surgery, Proc. 5th International Symposium on Surface Tomography and Body Deformity, Edit. H. Neugebauer and G. Windischbauer, G.Fisher-Verlag, N.Y., pp.217-222.

A.M. Coombes, A.D. Linney, R. Richards and J.P. Moss (1990a), A method of the 3D shape of the face and changes in the shape brought about by facial surgery, Proc. SPIE, vol.1380, pp.180-189.

A.M. Coombes, J.P. Moss, A.D. Linney, R. Richards and D.R. James (1991), A mathematical method for the comparison of three-dimensional changes in the facial surface, European Journal of Orthodontics, vol.13, pp.95-110.

A.M. Coombes (1993), Shape Classification: Towards a Mathematical Description of the Face, Ph.D. Thesis, Department of Medical Physics and Bioengineering, University College London.

C. Cutting, B. Grayson, F. Bookstein, L. Fellingham and J.G. McCarthy (1986), Computer-Aided planning and evaluation of facial and orthodontic surgery, Computers in Plastic Surgery, vol.13, no.3, pp.449-462.

P.E. Danielsson (1978), A new shape factor, Computer Graphics and Image Processing, vol.7, pp.292-299.

K.L. Denis and M.T. Speidel (1987), Comparison of Three Methods of Profile Change Prediction in Adult Orthodontic Patients, Am.J.Orthod. Dentofacial Orthop. vol.92, pp.396-402.

V.P. Delfino, F. Potente, E. Vacca, T. Lettini and R. Lenoci (1985), Analytical Morphometry in Fronto-facial Profile Comparison of Taung 1 Plesianthropus Transvaalensis Homo Sapiens Infant and Homo Sapiens Adult, Proc. Int. Symp. On Biological Evolution, Bari-Italy, April, pp.151-188.

G. Doemens, R. Buerger, W.W. Geabel, G. Haas and R. Schnieder (1986), A Fast 3D Sensor with High Dinamic Range for Industrial Applicationos, Applications Proc. Of ROVISEC Conf.

L. Dorst and A.W.M. Smeulders (1987), Length Estimators for Digitized Contours, CVGIP, vol.40, pp.311-333.

W. Downs (1948), Variation in Facial Relationships : Their Significance in Treatment and Prognosis, Amer. J. Orthod. Vol.34, pp.812-840.

J.S. Duncan, F.A. Lee, A.W.M. Smeulders and B.L. Zaret (1991), A Bending Energy Model for Measurement of Cardiac Shape Deformity, IEEE Trans. On Medical Imaging, vol.10, no.3, pp.307-320.

References

- D.H. Enlow (1990), Facial Growth, 3rd edition, W.B. Saunders Co.
- G. Farin (1993), Curves and Surfaces for Computer Aided Geometric Design: A Practical Guide, Academic Press, pp.145-199.
- L.G. Farkas (1981), Anthropometry of the Head and Face in Medicine, Edit. Elsevier, N.Y.
- L.G. Farkas, T.A. Hreczko, J.C. Kolar and I.R. Munro (1985), Vertical and horizontal proportions of the face in young adult North American Caucasians : revision of neoclassical canons, Plastic Reconstructive Surgery, vol.75, pp.328-337.
- L.G. Farkas, I.R. Munro (1987), Anthropometric Facial Proportions in Medicine, Published by Charles C. Thomas, U.S.A.
- O.D. Faugeras, F. Germain, G. Kryze, J.D. Boissonnat, M. Hebert, J. Ponce, E. Pauchon and N. Ayache (1983), Towards a Flexible Vision System, Robot Vision, A. Pugh edit., Springer-Verlag, N.Y., pp.129-147.
- H. Freeman (1961), On the encoding of arbitrary geometric configurations, IEEE Trans. Electronic Computers vol.EC-10, pp.260-268.
- H. Freeman (1970), Boundary encoding and processing, in Picture Processing and Psychopictorics, B.S.Lipkin and A.Rosenfeld Ed., Academic Press, N.Y., pp.241-266.
- H. Freeman and R. Shapira (1975), Determining the minimum area encasting rectangle for an arbitrary closed curve, Comm. of the Assoc. Comput. Machinery, vol.18, no.7, pp.409-413.
- W.R. Fright and A.D. Linney (1993), Registration of 3-D Head Surfaces using Multiple Landmarks, IEEE Trans. Medical Imaging, vol.12, no.3, pp.515-520.
- H. Fuchs, Z.M. Kedem and S.P. Uselton (1977), Optimal surface reconstruction for planar contours, Commun. ACM, vol.20, pp.693-702.
- F. Galton (1888), Personal Identification and Description-I, Nature, vol.38, June 21, pp.173-177.
- F. Galton (1888a), Personal Identification and Description-II, Nature, vol.38, June 28, pp.201-202.
- F. Galton (1910), Numeralized Profiles for Classification and Description, Nature, vol.83, March 31, pp.127-130.
- O. Glasser (1934), William Conrad Röntgen and the Early History of the Roentgen Rays, Edit. C.C. Thomas, Baltimore, Md.
- G.G. Gordon (1991), Face Recognition from Depth and Curvature, Ph.D. thesis, Division of Applied Sciences, Harvard University, Cambridge, Massachusetts.
- H. Gouraud (1971), Continuous Shading of Curved Surfaces, IEEE Trans. on Computers, vol.C-20, no.6, pp.623-628.
- W.C. Grabb, S.W. Rosenstein and K.R. Bzoch (1971), Cleft lip and palate : surgical, dental and speech aspects.

References

- J.F. Gravely and P.M. Benzie (1974), The Clinical Significance of Tracing Error in Cephalometry, *British Journal of Orthodontics*, vol.1, no.3, pp.95-101.
- J.E. Green (1970), IEEE Conference records, Symposium on Feature Extraction and Selection in Pattern Recognition, Edit. Argonne, IL, N.Y., pp.100-109.
- R.A. Groeneveld (1979), An Introduction to probability and statistics using BASIC, Statistics: textbooks and monographs, vol.26, pp.108, Marcel Dekker Inc., N.Y., Basel.
- D.J. Halazonetis, E. Shapiro, R.K. Gheewalla and R.E. Clark (1991), Quantitative Description of the Shape of the Mandible, *Am. J. Orthod. Dentofac. Orthop.* vol.99, no.1, pp.49-56.
- R.M. Haralick, L.T. Watson and T.J. Laffey (1983), The topographic primal sketch, *International Journal of Robotics Research*, vol.2, no.1, pp.51-72.
- L.D. Harmon (1976), Automatic Recognition of Human Face Profiles, *Proc. 3rd Int. Joint Conf. Pattern Recognition*, pp.183-188.
- L.D. Harmon and W.F. Hunt (1977), Automatic Recognition of Human Face Profiles, *Computer Graphics and Image Processing*, vol.6, no.2, pp.135-156.
- L.D. Harmon, S.C. Kuo, P.F. Ramig and U. Raudkivi (1978), Identification of Human Face Profiles by Computer, *Pattern Recognition*, vol.10, pp.301-312.
- L.D. Harmon, M.K. Khan, R. Lasch and P.F. Ramig (1981), Machine Identification of Human Faces, *Pattern Recognition*, vol.13, pp.97-110.
- D.D. Hoffman and W.A. Richards (1982), Representing smooth plane curves for recognition, *Proc. AAAI*, pp.5-8.
- D.D. Hoffman and W.A. Richards (1984), Parts of Recognition, *Cognition* 18, pp.65-96.
- H. Hofrath (1931), Die Bedeutung der Roentgenfern- und Abstands aufnahme für die Diagnostik der kieferanomalien, *Fortschr. Orthodont.* vol.1, pp.232-258.
- B.K.P. Horn (1975), Obtaining shape from shading information, *The psychology of computer vision*, P.H. Winston editor, McGraw Hill, N.Y., pp.115-155.
- B.K.P. Horn (1986), *Robot Vision*, MIT Press, Cambridge, Massachusetts, USA.
- Z. Hussain (1988), Automatic Segmentation and Measurement of Cephalometric Landmarks on Lateral Skull Radiographs using Cellular Logic Image Processors, Ph.D. thesis, University College London.
- X. Jia and M. Nixon (1992), On Developing an Extended Feature Set for Automatic Face Recognition, *Colloquium on Machine Storage and Recognition of Faces*, IEE Electronics Division, Digest no. 1992/017, 24th January, pp.8/1-8/4.
- A.C. Kak (1976), *Digital Picture Processing*, N.Y., Academic Press.
- T. Kanade (1977), *Computer Recognition of Human Faces*, Interdisciplinary Systems Research, vol.47, Birkhauser.
- H.M. Karara (1989), *Non-Topographic Photogrammetry*, Published by the American Society for Photogrammetry and Remote Sensing.

References

- G.J. Kaufman and K.J. Breeding (1976), The Automatic Recognition of Human Faces from Profile Silhouettes, *IEEE Trans. Syst. Man Cybern.* vol.6, no.2, pp.113-121.
- K. Kaya and K. Kobayashi (1972), A Basis Study on Human Face Recognition, *Frontiers of Pattern Recognition*, Ed. S.Watanabe, Academic Press, pp.265-289.
- M.D. Kelly (1970), Visual Identification of People by Computer, Ph.D. thesis, Stanford University, CA.
- D.G. Kendall (1977), The Definition Of Shape, *Adv.in Appl.Probab.* 9, pp.428-430.
- D.G. Kendall (1984), Shape Manifolds, Procrustean Metrics and Complex Projective Spaces, *Bull. London, Math.Soc.* vol.16, pp.81-121.
- D.G. Kendall (1986), Comments, *Statistical Science* vol.1, pp.181-242
- D.G. Kendall (1989), A Survey of the Statistical Theory of Shape, *Statistical Science* vol.4, no.2, pp.87-120.
- J.J. Koenderink (1984), The Structure of Images, *Biological Cybernetics*, vol.50, pp.363-370.
- J.J. Koenderink and A.J. van Doorn (1986), Dynamic Shape, *Biological Cybernetics*, vol.53, pp.383-396.
- L.D. Landau and E.M. Lifshitz (1986), *Theory of Elasticity*, Oxford, Pergamon.
- R.S. Ledley (1964), High-Speed Automatic Analysis of Biomedical Pictures, *Science*, vol.146, no.9, pp.216-223.
- J.C. Lee and E. Milios (1991), Matching Range Images of Human Faces, *IEEE*, pp.722-726.
- S.R. Lele and Richtsmeier J.T. (1991), Euclidean Distance Matrix Analysis: A Coordinate-free Approach for Comparing Biological Shapes Using Landmark Data, *Am.J.of Physical Anthropol.* vol.86, pp.415-427.
- P.E. Lestrel (1978), A Quantitative approach to Skeletal Morphology : Fourier Analysis, *SPIE* vol.166, pp.80-93.
- P.E. Lestrel and A.F. Roche (1986), Cranial Base Shape Variation with Age: A Longitudinal Study of Shape using Fourier Analysis, *Human Biology*, vol.58, no.4, pp.527-540.
- M.D. Levine (1985), *Vision in Man and Machine*, Edit. McGraw-Hill, N.Y.
- F. Leymarie and M.D. Levine (1988), Curvature Morphology, Report TR-CIM-88-26, December, Computer Vision and Robotics Lab., McGill University, Montreal, Canada.
- F. Leymarie and M.D. Levine (1992), Simulating the Grassfire Transform using an Active Contour Model, *IEEE-PAMI* vol.14, no.1, pp.56-75.
- M. Leyton (1987), Symmetry-Curvature duality, *Computer Vision, Graphics and Image Processing* vol.38, pp.327-341.
- M. Leyton (1988), A Process-grammar for shape, *Artificial Intelligence* vol.34, pp.213-247.

References

- J. Liggett (1974), *The Human Face*, ed. Constable & Co.Ltd., London.
- T. Lindeberg (1990), Scale-space for discrete signals, *IEEE - PAMI* vol.12, no.3, pp.234-254.
- T. Lindeberg (1994), *Scale-Space Theory in Computer Vision*, Royal Institute of Technology, Stockholm, Sweden, Edit. Klumer Academic Publish.
- A.D. Linney, S.R. Grindrod, S.R. Arridge and J.P. Moss (1989), Three-dimensional Visualization of Computerized Tomography and Laser Scan Data for the Simulation of Maxillo-facial Surgery, *Medical Informatics*, vol.14, no.2, pp.109-121.
- A.D. Linney, J.P. Moss, R. Richards, C.A. Mosse, S.R. Grindrod and A.M. Coombes (1991), Use of 3-D Visualization Systems in the Planning and Evaluation of Facial Surgery, *Proc. SPIE, Conference on Biostereometrics technology & applications*, R.E.Herron editor, vol.1380, pp.190-199.
- A.D. Linney (1992), The Acquisition, Visualisation and Applications of Three Dimensional data on the Human Body, *CSERIAC workshop on 3-D electronic imaging of the human body*, Dayton, Ohio, March.
- A.D. Linney, A.C. Tan, R. Richards, J. Gardener, S. Grindrod and J.P. Moss (1993), Three-dimensional visualization of data on human anatomy: diagnosis and surgical planning, *Journal of Audiovisual Media in Medicine*, vol.16, no.1, pp. 4-10.
- M.M. Lipschutz (1969), *Differential Geometry*, McGraw-Hill, N.Y.
- D.G. Lowe (1988), Organization of smooth image curves at multiple scales, *Proc. 2nd International Conf. Computer Vision*, pp.558-567.
- K.H. Lu (1965), Harmonic Analysis of the Human Face, *Boimetrics*, vol.21, no.6, pp.491-505.
- N. MacLeod and J.A. Kitchell (1988), Morphometrics and Evolutionary Inference: A Case Study Involving Ontogenetic and Developmental Aspects of Foraminiferal Evolution, *Proc. Michigan Morphometrics Workshop*, Ann Arbor, Michigan, pp.283-299.
- McMahon (1956), *Treatise on Painting (Codex Urbinas Latinus 1270)* by Leonardo da Vinci, ed. A.P. McMahon, 2 vols., Princepton.
- K.V. Mardia (1989), Comment: Some Contributions to Shape Analysis, *Statistical Science* 4, pp. 108-111.
- K.V. Mardia (1989b), The Statistical Analysis of Shape Data, *Biometrika* 76, no.2, pp.271-281.
- K.V. Mardia (1991), Statistical Shape Models in Image Analysis, *Proc. Interface*, pp.550-557, Seattle.
- K.V. Mardia, S.Rabe and J.T.Kent (1993), *Statistics, Shape and Images*, Technical Report 93/16/C, Dept. Statistics, University of Leeds, Leeds, England.
- D. Marr (1976), Early Processing of Visual Information, *Phil.Trans.Royal Soc. London B275*, pp.483-524.

References

- D. Marr and T. Poggio (1979), A computational theory of human stereo vision, Proc. Royal Soc. London B204, pp.301-328.
- D. Marr and K. Nishihara (1978), Representation and Recognition of the Spatial Organisation of Three Dimensional Shapes, Philosophical Trans. Royal Society of London, vol.B200, pp.269-294.
- D. Marr and E.C. Hildreth (1979b), Theory of edge detection, M.I.T. Artificial Intelligence Memo no.518, Cambridge, Massachusetts.
- D. Marr (1982), Vision: A Computational Investigation into the Human Representation and Processing of Visual Information, Freeman, San Francisco.
- S. Marshall (1989), Review of Shape Coding Techniques, Image and Vision Computing 7, no.4, pp.281-294.
- A.D. Marshall and R.R. Martin (1992), Computer Vision, Models, and Inspection, World Scientific Series in Robotics and Automated Systems, vol.4, World Scientific Publishing Co.
- H.C. Marz and R.L. Nielsen (1993), Cameras, Scanners and Image Acquisition Systems, Proc. SPIE, vol.1901, San Jose.
- N. Masui, S. Akamatsu and Y. Suenaga (1990), A Preliminary study for recognition of human faces by 3D measurements, ICS 90-51, AIPS 90-43. (in Japanese).
- G. Matheron (1967), Elements pour une Theorie del Milieux Poreux, Masson, Paris. (in French).
- P. Meer, E.S. Baugher and A. Rosenfeld (1988), Extraction of trend lines and extrema from multiscale curves, Pattern Recognition vol.21, no.3, pp.217-226.
- P.A. Miller, B.S. Savara and I.J. Singh (1965), Analysis of Errors in Cephalometric Measurement of Three-dimensional Distances on the Maxilla, Angle Orthodo. Vol.36, no.2, pp.169-175.
- F. Mokhtarian and A. Mackworth (1986), Scale-Based Description and Recognition of Planar Curves and Two Dimensional Shapes, IEEE-PAMI vol.8, no.1, pp.34-43.
- F. Mokhtarian and A. Mackworth (1988), The Renormalized Curvature Scale Space and the Evolution of Planar Curves, Proc. IEEE Comp.Vision and Pattern Recog. Ann Arbor, MI, pp.318-326.
- F. Mokhtarian (1988b), Evolution Properties of Space Curves, Proc. IEEE-ICCV, 2nd International Conf. Computer Vision, pp.100-105.
- F. Mokhtarian and A. Mackworth (1992), A theory of multi-scale, curvature-based shape representation for planar curves, IEEE-PAMI vol.14, pp.789-805.
- J.P. Moss, A.D. Linney, S.R. Grindrod, S.R. Arridge and J.S. Clifton (1987), Three-dimensional Visualization of the Face and Skull using Computerized Tomography and Laser Scanning Techniques, European Journal of Orthodontics, vol.9, pp.247-253.

References

- J.P. Moss, A.D. Linney, S.R. Grindrod and C.A. Mosse (1989), A Laser Scanning System for the Measurement of Facial Surface Morphology, *Optics and Lasers in Engineering*, vol.10, pp.179-190.
- J.P. Moss, J.C. Campos and A.D. Linney (1992), The Analysis of Profiles using Curvature Analysis, *European Journal of Orthod.* Vol.14, no.6, pp.457-461.
- R.E. Moyers and F.L. Bookstein (1979), The Inappropriateness of Conventional Cephalometrics, *Am. Journal of Orthodontics* vol.75, pp.599-617.
- O. Nakamura, S. Mathur and T. Minami (1991), Identification of Human Faces based on Isodensity Maps, *Pattern Recognition*, vol.24, pp.262-272.
- M. Nixon (1985), Eye spacing measurement for facial recognition, *Proc. SPIE*, vol.575, pp.279-285.
- C.E. Oxnard (1973), *Form and Pattern in Human Evolution*, Univ. Chicago Press, Chicago.
- C.E. Oxnard (1978), One Biologists view of morphometrics, *Annu. Rev. Ecol. Syst.* Vol.9, pp. 219-241.
- Y. Park and C.J. Burstone (1986), Soft-tissue Profile - Fallacies of Hard-tissue Standards in Treatment Planning, *Am. Journal Orthod. Dentofac. Orthop.* vol.90, pp.52-62.
- T. Pavlidis (1977), *Structural Pattern Recognition*, Springer-Verlag, NY.
- T. Pavlidis (1977b), Polygonal Approximations by Newton's method, *IEEE Trans. Computing*, vol.C-26, no.8, pp.800-807.
- T. Pavlidis (1978), A Review of Algorithms for Shape Analysis, *CGVIP* vol.7, pp.243-258.
- T. Pavlidis (1980), Algorithms for Shape Analysis of Contours and Waveforms, *IEEE-PAMI* 2, no.4, pp.301-312.
- K. Pearson (1924), *The life, letters and labours of Francis Galton, Photographic Researches and Portrature*, Cambridge University Press, Cambridge, vol.II, chapter XII, pp.283-333.
- S.C. Pei and C.N. Lin (1992), The detection of dominant points on digital curves by scale-space filtering, *Pattern Recognition*, vol.25, no.11, pp.1307-1314.
- E. Persoon and K.S. Fu (1977), Shape discrimination using Fourier descriptors, *IEEE Trans. Systems Man and Cybernetics*, vol.7, pp.170-179.
- S.M. Pizer, W.R. Oliver and S.H. Bloomberg (1987), Hierarchical Shape Description via the Multiresolution Symmetric Axis Transform, *IEEE PAMI-9*, no.4, pp.505-511.
- J. Porril, S.B. Pollard, T.P. Pridmore, J.E.W. Mayhew and J.B. Frisby (1987), *TINA : The Sheffield AIVRU Vision System*, Sheffield University, AIVRU no.031.
- W.H. Press, B.P. Flannery, S.A. Teukolsky and W.T. Vetterling (1978), *Numerical Recipes*, Cambridge University Press.

References

- R.A. Reyment (1988), Reification of Classical Multivariate Statistical Analysis in Morphometry, Proc. Michigan Morphometrics Workshop, Ann Arbor, Michigan, pp.123-144.
- W. Richards and D.D. Hoffman (1985), Codon constraints on closed 2D shapes, CVGIP vol.31, pp.265-281.
- W. Richards, B. Dawson and D. Whittington (1986), Encoding contour shape by curvature extrema, J. Opt. Soc. Am. A, vol.3, no.9, pp.1483-1491.
- A. Richardson (1966), An investigation into the reproducibility of some points, planes and lines used in cephalometric analysis. American Journal of Orthodontics, vol.52, pp.637-651.
- J.P. Richter (1970), The Notebooks of Leonardo da Vinci, Compiled and edited from the original manuscripts, vol. I, Dover Public., N.Y.
- R.M. Ricketts (1957), Planning Treatment on the Basis of the Facial Pattern and an Estimate of its Growth, Angle Orthod., vol.27, no.1, pp.14-37.
- R.M. Ricketts (1961), Cephalometric Analysis and Synthesis, Angle Orthodo. Vol.31, no.3, pp.141-156.
- R.M. Ricketts (1981), Perspectives in the Clinical Application of Cephalometrics, Angle Orthodo., vol.51, no.2, pp.115-150.
- J.T. Richtsmeier (1989), Applications of Finite-Element Scaling Analysis in Primatology, Folia Primatol 53, pp.50-64.
- J.T. Richtsmeier, Grausz H.M., Morris G.R., Marsh J.L. and Vamuer M.W. (1991), Growth on the Cranial Base in Craniosynostosis, Cleft Palate-Craniofacial Journal 28, pp.55-67.
- R.A. Riedel (1950), Esthetics and Its Relation to Orthodontic Therapy, Angle Orthodontist, vol.20, no.3, pp.168-178.
- T.F. Rhodes (1956), Alphonse Bertillon - Father of Scientific Detection, G.G. Harrap & Co., London.
- H. Rom and G. Medioni (1991), Hierarchical Decomposition and Axila Representation of Shape, Proc. SPIE, vol.1570, San Diego.
- A. Rosenfeld and M. Thurston (1971), Edge and curve detection for visual scene analysis, IEEE Trans. On Computers, vol. C-20, pp.562-569.
- A. Rosenfeld and A.C. Kak (1976), Digital Picture Processing, Academic Press, N.Y.
- A. Rosenfeld (1986), Axial Representations of Shape, CVGIP no.33, pp.156-173.
- P.L. Rosin (1992), Representing curves at their natural scales, Pattern Recognition vol.25, no.11, pp.1315-1325.
- P.L. Rosin (1993), Multiscale Representation and Matching of Curves using Codons, CVGIP: Models and Image Processing, vol.55, no.4, pp.286-310.
- B. Shahraray and D.J. Anderson (1985), Uniform Resampling of Digitized Contours, IEEE - PAMI, vol.7, no.6, pp.674-681.

References

- T. Sakai, M. Nagao and T. Kanade (1972), Computer Analysis and Classification of Photographs of Human Faces, In. 1st USA-Japan Computer Conference, pp.55-62.
- M.A. Shakleton and W.J. Welsh (1991), Classification of Facial Features for Recognition, IEEE Conf. On Computer Vision and Pattern Recognition (CVIP'91).
- A. Samal and P.A. Iyengar (1992), Automatic Recognition and Analysis of Human Faces and Facial Expression: A Survey, Pattern Recognition, vol.25, no.1, pp.65-77.
- B.S. Savara (1965), A Method for measuring facial bone growth in three dimensions, Human Biology, vol.37, pp.245-255.
- B.S. Savara, W.E. Tracy and P.A. Miller (1966), Analysis of Errors in cephalometric measurements of three-dimensional distances on the human mandible, Archs. Oral Biol. Vol.11, pp.209-217.
- J. Serra (1982), Image Analysis and Mathematical Morphology, Academic Press, London.
- A.F. Siegel and R.H. Benson (1982), A Robust Comparison of Biological Shapes, Biometrics vol.38, no.6, pp.341-350.
- C.G. Small (1988), Techniques of Shape Analysis on Sets of Points, Int. Statist. Rev. 56, pp.243-257.
- A.W.M. Smeulders, A.M. Vossepoel, J. Vrolijk, J.S. Ploem and C.J. Cornelisse (1980), Some Shape Parameters for Cell Recognition, Pattern Recognition in Practice, Editors E.S. Gelema and L.N. Kanal, pp.131-142.
- J.L. Stansfield (1980), Conclusions from the commodity expert project, MIT Artificial Intelligence Lab Memo no. 601.
- J.D. Subtelny (1959), A Logitudinal Study in Soft-tissue Facial Structures and their Profile Characteristics defined in relation to Underlying Skeletal Structures, American Journal of Orthodontics, vol.45, pp.481-507.
- A.C. Tan, R.Richards and A.D.Linney (1988), 3D Medical Graphics - Using the T800 Transputer, Proc. of the 8th OCCAM User Group Technical Meeting, J.Kerridge editor, pp.83-89.
- A.C. Tan, R. Richards and A.D. Linney (1991), The MGI Workstation : An Interactive System for 3D Medical Graphics Applications, CAR'91 Computer Assisted Radiology, edited by H.Lemke, M.L.Rhodes, C.C.Jaffe and R.Felix, Springer-Verlag, Berlin, pp.705-710.
- Tektite (1989), Xtram User's Manual, Edit. Tektite Limited, U.K.
- C.H. Teh and R.T. Chin (1980), On image analysis by the methods of moments, IEEE-PAMI, vol.10, no.4, pp.496-513.
- C.H. Teh and R.T. Chin (1989), On the detection of dominant points on digital curves, IEEE-PAMI, vol.11, no.8, pp. 859-872.
- S.M. Thomas and Y.T. Chan (1989), A simple approach for the estimation of circular arc center and its radius, CVGIP vol.45, pp.
- D'Arcy W. Thompson (1917 [1942]), On Growth and Form, J.T.Bourner editor, Cambridge, Cambridge Univ. Press.

- W. Turton (1819), *A Conchological Dictionary of the British Islands*, Booth, London, frontispiece.
- F. Ulupinar and R. Nevatia (1990), Inferring shape from contour for curved surfaces, *Proc. Int. Conf. Pattern Recognition*, Atlantic City, N.J., pp.147-154.
- K.H. Veltman (1986), *Studies on Leonardo da Vinci I : Linear Perspective and the Visual Dimensions of Science and Art*, Deutscher Kunstverlag, pp.202-234.
- G.F. Walker and C.J. Kowalski (1971), A Two Dimensional Coordinate Model for the Quantification, Description, Analysis, Prediction and Simulation of Craniofacial Growth, *Growth* vol.35, pp.191-211.
- A.P. Witkin (1981), Recovering surface shape and orientation from texture, *Artificial Intelligence*, vol.17, pp.17-45.
- A.P. Witkin (1983), Scale Space Filtering, *Proc.8th.Int.Joint Conf. Artificial Intell.*, Karlsruhe, West Germany, pp.1019-1022.
- A.P. Witkin (1986), Scale Space Filtering, in *From pixels to predicates : recent advances in computational and robotic vision*, Edit. Alex P. Pentland, pp.5-19.
- P.J. Wisth and O.E. Bøe (1975), The Reliability of Cephalometric Soft tissue Measurements, *Archs. Oral Biol.* Vol.20, pp.595-599.
- T.C. White, J.H. Gardiner and B.C. Leighton (1976), *Orthodontics for dental students*, Publ. The Macmillan Press Ltd.
- R.J. Woodham (1981), Analysing Images of Curved Surfaces, *Artificial Intelligence*, vol.17, pp.117-140.
- M. Worring and A.W.M. Smeulders (1993), Digital Curvature Estimation, *CVGIP: Image Understanding*, vol.58, no.3, pp.366-382.
- C.J. Wu and J.S. Huang (1990), Human Face Profile Recognition by Computer, *Pattern Recognition* vol.23, no.3/4, pp.255-259.
- N. Yokoya and M.D. Levine (1987), Range Image Segmentation based on Differential Geometry : A Hybrid Approach, *IEEE-PAMI*, vol.11, no.6, pp.643-649.
- K.C. You and K.S. Fu (1979), A syntactic approach to shape recognition using attributed grammars, *IEEE Trans. Systems Man Cybernet.*, vol.9, no.6, pp.334-344.
- I.T. Young, J.E. Walker and J.E. Bowie (1974), An Analysis Technique for Biological Shape : I, *Information and Control*, vol.25, pp.357-370.
- A.L. Yuille and T. Poggio (1983), Scaling Theorems for Zero-Crossings, *MIT-AI Memo 722*, June.
- A.L. Yuille and T. Poggio (1983b), Fingerprints Theorems for Zero-Crossings, *MIT-AI Memo 730*, October.
- A.L. Yuille, D. Cohen and P. Hallinan (1989), Facial feature extraction by deformable templates, *Technical Report CICS-P-124*, Cambridge, MA 02139.
- C.T. Zahn and R.S. Roskies, Fourier descriptors for plane closed curves, *IEEE Trans. Comp.*, vol.C-21, no.3, pp.269-281.

References

B.M. Zide, B. Grayson and J.G. McCarthy (1981), Cephalometric Analysis and preoperative planning - parts I and II, *Plastic and Reconstructive Surgery*, pp.68-961.

B.M. Zide, B. Grayson and J.G. McCarthy (1982), Cephalometric Analysis and preoperative planning - part III, *Plastic and Reconstructive Surgery*, pp.69-155.